Bulletin
of
The Geological Society of America

VOLUME 67 May 1956 NUMBER 5

CONTENTS

	Pages
Physical limnology and sedimentation in a glacial lake. By W. H. Mathews	537–552
Geomorphology and glacial history of southernmost Baffin Island. By J. H. Mercer	553–570
Quantitative slope analysis. By A. N. Strahler	571–596
Evolution of drainage systems and slopes in badlands at Perth Amboy, New Jersey. By S. A. Schumm	597–646
Structures of porphyritic granite and associated metamorphic rocks of East Manbhum, Bihar, India. By S. Sen	647–670
Short Notes	
Unusual "pothole". By Charles G. Higgins	671–673
Carbon-14 date for a marine terrace at Santa Cruz, California. By William C. Bradley	675–677
Types of *Bathyuriscus howelli* var. *lodensis* Clark. By Alexander Stoyanow	679–681

Subscription $15.00 per year,

Printing Office: Mt. Royal & Guilford Aves., Baltimore 2, Md.

Communications for publications should be addressed to The Geological Society of America, Dr. H. R. Aldrich, Secretary, 419 West 117 Street, New York, N. Y.

Please give notice of change of address 4 weeks in advance. Claims for non-receipt of the Bulletin of a given month must be sent to the Secretary of the Society before the end of the second succeeding month.

Entered as second-class matter at the Post Office at Baltimore, Md.
under the Act of Congress of July 16, 1894.
Accepted for mailing at special rate of postage provided for in Section 1103
Act of October 3, 1917, authorized on July 8, 1918.

PAPERS IN PRESS FOR FORTHCOMING ISSUES

Coarse Conglomerates of the Middle Ordovician in the Southern Appalachian Valley. By J. M. Kellberg and L. F. Grant

Three-dimensional Applied Potential Studies at Austinville, Virginia. By H. V. McMurry and A. D. Hoagland

Hemphillian Mammalian Assemblage from Northeastern Oregon. By J. Arnold Shotwell

Classification of Patterned Ground and Review of Suggested Origins. By A. L. Washburn

Statistical Analysis of Low-level Radioactivity of Pennsylvanian Black Fissile Shale in Illinois. By W. C. Krumbein and H. A. Slack

Structure and Petrology of Enchanted Rock Batholith, Llano and Gillespie Counties, Texas. By Robert M. Hutchinson

BULLETIN OF THE GEOLOGICAL SOCIETY OF AMERICA
VOL. 67, PP. 537-552, 6 FIGS., 1 PL. MAY 1956

PHYSICAL LIMNOLOGY AND SEDIMENTATION IN A GLACIAL LAKE

By W. H. Mathews

Abstract

The following conclusions stem from a study of limnology and bottom sediment in Garibaldi Lake, a glacial lake in the southern Coast Mountains of British Columbia.

Meltwater streams entering the lake cause overflows or underflows depending on local conditions, notably stream temperature and sediment load, temperature distribution in the lake, and apparently the topography at the stream mouth. Conditions vary with season and time of day. Mixing of stream and lake waters at shallow (less than 35 feet) and moderate (65 to 100 feet) depths could be demonstrated; penetration of stream waters to greater depths could not be precluded. Sediment loads of the two glacial streams entering the lake are relatively low, and persistent underflows forming significant subaqueous channels probably do not occur.

The glacial streams, notwithstanding their low sediment content, provide most of the sediment reaching the lake; a minor amount of debris is apparently ice-rafted from nonglacial areas.

The bottom sediment consists of rock flour in which clay minerals are rare or absent.

Turbidity currents are considered responsible for the occurrence of graded laminae of fine sand and coarse silt in the deep, flat-bottomed part of the lake, up to 2½ miles from the source of this sediment. Subaqueous slumps probably caused the turbidity currents.

Absence of visible varves is attributed to (1) low rate of accumulation of suspended sediment, averaging a small fraction of a millimeter a year, (2) a lag of years, rather than months, between the introduction of much of the suspended sediment into the lake and its deposition on the lake floor, and (3) obliteration of any thin and inconspicuous varves by small-scale slumping on the steeper slopes of the lake basin and by the deposits from nonperiodic turbidity currents on the flat lake floor.

CONTENTS

TEXT

	Page
Introduction	538
Acknowledgments	538
Geologic setting	538
Lake-bottom topography	538
Stream discharges	540
Sediment loads of streams	541
Character of lake water	542
Movement of stream water into lake	544
Characteristics of bottom sediments	546
General statement	546
Distribution	547
Physical characteristics	547
Structure	547
Porosity and specific gravity	547
Size distribution	547
Atterburg limits	548
Composition	548
Discussion	550
Deposition of clays	550
Deposition of stratified clay, silt, and fine sand	550
Source of sediment	551
Rates of sedimentation	551
References cited	552

ILLUSTRATIONS

Figure	Page
1. Geologic map of Garibaldi Lake and vicinity	539
2. Bottom topography, Garibaldi Lake	539
3. Echo-sounder profiles	540
4. Bathythermograph records, bottom topography, and surface distribution of turbid water in Garibaldi Lake near Sphinx Creek	544
5. Bathythermograph records, bottom topography, and surface distribution of turbid water in Garibaldi Lake near Sentinel Creek	545
6. Particle-size distribution of lake-bottom sediments	549
Plate	**Facing page**
1. Core samples of lake-bottom sediments	548

TABLES

Table	Page
1. Estimated mean annual runoff into Garibaldi Lake	541
2. Temperatures of streams entering Garibaldi Lake	542
3. Temperatures of water in Garibaldi Lake	543
4. Porosities and specific gravities of lake-bottom sediments	547

Introduction

Physical conditions prevailing within a glacial lake and their influences on the distribution of sediment-laden meltwater has been the subject of recent papers (Antevs, 1951; Kuenen, 1951). Heretofore few glacial lakes have been investigated (Johnston, 1922; Kindle, 1930); little attention has been paid to temperatures and silt loads of inflowing glacial streams and their behavior on entering the lake. The present report provides additional information on this subject based on a study in Garibaldi Lake, a deep meltwater lake in the southern Coast Mountains of British Columbia.

Field work was carried on in Garibaldi Lake in late August 1952 and early September 1954. Though the lake lies only 45 miles north of the City of Vancouver, it is accessible only by air or pack trail, and lack of time and funds has precluded field work in other months. Seasonal changes of conditions in the lake have not been studied directly, but observations on water levels and stream flow at Garibaldi Lake (Dominion Water and Power Bureau, 1934a) and on surface turbidity provide some data on the annual cycle. Though the record is incomplete and some conclusions are tentative, it is hoped that this report will provide a better understanding of conditions in glacial lakes and stimulate research in this field of limnology and sedimentation.

Acknowledgments

The writer acknowledges assistance provided by the following organizations and individuals: the Penrose Bequest of the Geological Society of America, which supplied financial aid for field work and part of the laboratory equipment; the Consolidated Mining and Smelting Company Research Fund which contributed additional laboratory equipment; Dr. G. L. Pickard, who worked with the writer in the collection of samples and field data; my wife, who assisted both in the field work and in the editing of the report; Drs. R. M. Thompson and C. A. Rowles, Messrs. R. A. Spence, C. Ripley, L. Farstad, J. Day, H. Hortie, and J. Stewart, and Mrs. G. Knight for advice and laboratory work; the Physical and Crystal Chemistry Section, Department of Mines and Resources, Ottawa, for thermal analysis of a clay; and the Canadian and British Columbia Foundations for Poliomyelitis for electron photomicrography.

Geologic Setting

Garibaldi Lake lies in the upper part of a valley which has been carved partly by stream action and partly by Pleistocene glaciers. Metamorphosed sediments, including graywacke, conglomerate, quartzite, and slate, are exposed on the north wall of the valley (Fig. 1); biotite and hornblende-rich quartz diorite predominate at its head. The southwestern side is covered by Pleistocene dacitic lavas, some glaciated, some unglaciated, through which the plutonic basement rocks are locally exposed.

Garibaldi Lake basin originated in late Wisconsin time by the damming of Rubble Creek valley by the Clinker Mountain lava flow (Mathews, 1952, p. 554–555) (Fig. 1). At that time, a remnant of the Cordilleran ice sheet apparently blocked the mouth of the valley up to the 4000-foot level, and the mountain glaciers were almost certainly no larger than they are today; the area of the present lake was then probably free of both water and ice. Had the lava dam been impervious, the basin would have overflowed after about 15 years of normal runoff. However, leakage through the dam now amounts to about four-fifths of normal runoff, and greater leakage probably took place before sediment accumulated on the upstream slope of the dam, so that more than 75 years may have been required for filling. Though this body of water has probably been a "meltwater lake" throughout most of its history, for a time within the past 4 centuries the glaciers extended down to its shores and presumably discharged icebergs; during this brief period, it was an "ice lake" in the strict sense.

Lake-bottom Topography

Several dozen soundings throughout the lake and echo-sounder profiles in its shallower parts reveal the general shape of its bottom (Figs. 2, 3). The soundings indicate a deep central basin with a remarkably level floor sloping gently northwest; four wire-line soundings in an area 4000 feet by 2500 feet range from 837

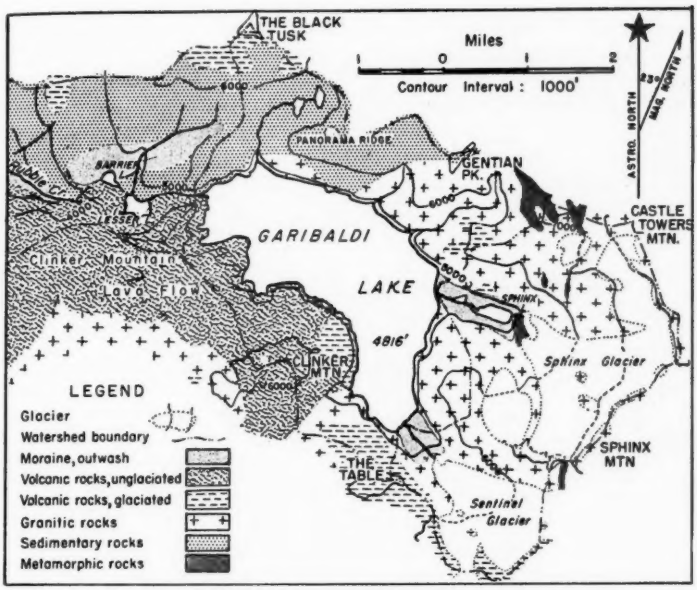

FIGURE 1.—GEOLOGIC MAP OF GARIBALDI LAKE AND VICINITY

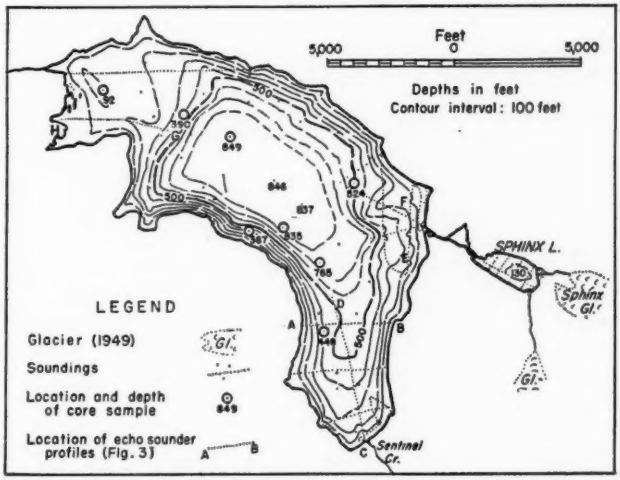

FIGURE 2.—BOTTOM TOPOGRAPHY, GARIBALDI LAKE

to 849 feet; 20 soundings taken in this same area along a northerly trending line at intervals of about 50 feet reveal a gentle slope with a relief of 15 feet; 10 successive soundings in the northern part of this line varied less than 1 foot. The southeastern part of the lake floor slopes irregularly (Fig. 3) northward toward the central deep; local flats evidently mark areas of recent sedimentation, and elsewhere hummocky profiles suggest a glaciated bedrock surface thinly, or not at all, covered by recent sediment. The walls of the basin are abrupt; they slope at angles rarely less than 20° and in places as much as 45° for vertical intervals of

several hundred feet. An irregular platform, most of which is less than 250 feet deep, underlies the western end of the lake and is evidently the submerged extension of the lava dam forming the western shore. Its surface is marked by spring and early summer snow melt. This storage, combined with a significant but variable leakage from Garibaldi and Lesser lakes, maintains a flow of at least 80 c.f.s. in Rubble Creek even during the coldest and driest winters.

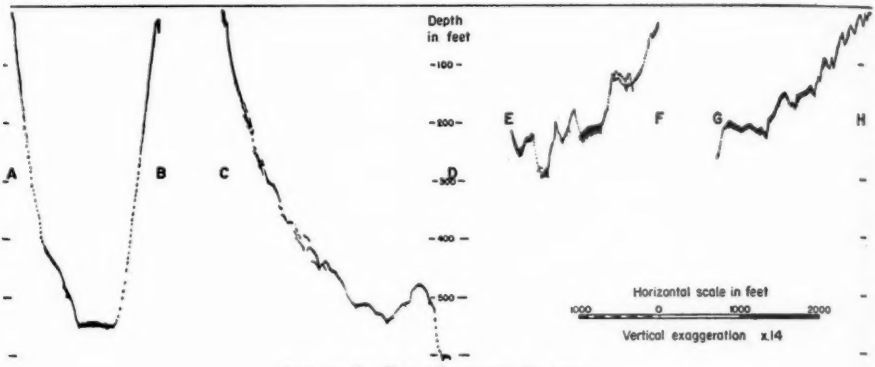

FIGURE 3.—ECHO-SOUNDER PROFILES

ridges 5 to 50 feet high, which form several parallel chains of islets close to the western shore.

STREAM DISCHARGES

Stream-flow measurements made at the mouth of Rubble Creek (Dominion Water and Power Bureau, 1924–1934), elevation 1100 feet, 4½ miles below the outlet of Garibaldi Lake, indicate an average annual runoff from the drainage basin of about 80 inches (176 cubic feet per second from 24 square miles). Water released from the shrinking glaciers has contributed annually the equivalent of 10 inches to this runoff (Mathews, 1951, p. 360). Normal runoff when glaciers were neither advancing nor retreating, would amount to about 70 inches. Meteorological data suggest that precipitation, hence runoff, increases from the mouth of Rubble Creek to the vicinity of Garibaldi Lake, but the extent of variation is not known.

The stream-flow records from the mouth of Rubble Creek are of limited use in estimating seasonal changes in the streams entering Garibaldi Lake. The large storage capacity of Garibaldi Lake with its 3.96 square-mile area and 10-foot seasonal fluctuation in level delays and obscures runoff resulting from the late

Some data are available from a detailed study made by the Dominion Water and Power Bureau (1934a) in 1932 and 1933 of Garibaldi and Lesser lakes and of the stream linking them. These data indicate that underground leakage from Garibaldi Lake directly to Rubble Creek below the barrier is about 65 c.f.s.[1] and to the stream entering Lesser Lake about 15 to 18 c.f.s. Allowing for this leakage, for surface outflow, and for changes in storage with rise and fall of the lake, it appears that influx declined irregularly from about 350 c.f.s. at the end of July 1932 until late October, after which it rarely exceeded 40 c.f.s. until the latter part of May 1933. After mid-June, the influx increased rapidly to highs of 400 c.f.s. in the first and third weeks of July; after falling to 250 c.f.s. about the first of August, it rose to another peak of more than 375 c.f.s. in mid-August 1933. The July peak flow in both years can be attributed to snow melt, for at this time of year rainfall is relatively light and the glaciers largely snow-covered. The August peak, on the other hand, can be attributed to melting of the glaciers, for by that time nearly all snow has disappeared

[1] The outflow from the lake, assuming a runoff of 80 inches a year from an area of 19.8 square miles, averages 117 c.f.s.

except from the névés. The maintenance of inflow, though at declining rates until October, can be assigned in part to springs, in part to melting of glaciers, and in part to early autumn rains. Low water from November through April is a result of cold weather; most precipitation is in the form of snow, and little melting takes place. No doubt the seasonal cycle of stream flow varies from year to year, both in rates of flow and precise timing, but except for exceptionally low water during the winter the period of 1932–1933 was not unusual.

TABLE 1.—ESTIMATED MEAN ANNUAL RUNOFF INTO GARIBALDI LAKE

Basin	Area (sq. mi.)				Runoff (c.f.s.)			
	Glacier	Ice-free	Total	Per cent	Glacier*	Ice-free†	Total	Per cent
1927								
Sphinx	3.6	2.0	5.6	35	37.6	10.3	47.9	44.3
Sentinel	1.4	0.8	2.2	14	14.6	4.1	18.7	17.3
Others	....	8.0	8.0	51	....	41.5	41.5	38.4
					52.2	55.9	108.1	....
1947								
Sphinx	2.8	2.8	5.6	35	29.3	14.4	43.7	42.5
Sentinel	1.2	1.0	2.2	14	12.5	5.1	17.6	17.1
Others	....	8.0	8.0	51	....	41.5	41.5	40.4
					41.8	61.0	102.8	....

* Assumed 70-inch contribution from annual precipitation plus 76-inch contribution from melting ice for the entire area of the glacier

† Assumed 70-inch contribution from annual precipitation alone

The approximate mean annual inflow into Garibaldi Lake and the discharge of the two meltwater streams draining Sphinx and Sentinel glaciers can be estimated from the measured watershed areas, the areas of the glaciers, and the estimates of mean annual runoff and glacier shrinkage. The results are given in Table 1.

These estimates indicate that, though the basins occupied in part by Sphinx and Sentinel glaciers make up only half the area tributary to Garibaldi Lake, they contribute about three-fifths of the inflow. Melting of glaciers, or of snow cover on glaciers, may provide more than two-fifths of the total inflow and about two-thirds of the flow of the two meltwater streams. Seasonal variation in these streams is probably at least as great as that for the influx into the lake; for example, Sphinx Creek, during warm periods in midsummer, may discharge an average of 200 c.f.s. Diurnal variations in stream flow from a glacier can be great, increasing as much as four times from early morning to mid-afternoon (*e.g.*, head of Sunwapta River at Athabasca Glacier, Alberta) (Unpublished data, Dominion Water and Power Bureau). Such variations may influence Sentinel Creek at its entrance to Garibaldi Lake, but flow at the mouth of Sphinx Creek is stabilized by the relatively large storage capacity of Sphinx Lake (approximately 2,000,000 square feet of surface area), and diurnal fluctuations are much less pronounced.

Measurements of Sphinx and Sentinel creeks, made in the afternoon of September 10, 1954, during an extended cool, cloudy, and moist period, indicate discharges of about 85 and 40 c.f.s. respectively.

SEDIMENT LOADS OF STREAMS

Little is known of the sediment loads of the streams entering Garibaldi Lake. The only extensive areas of flat ground along the shores of Garibaldi Lake are near Sphinx and Sentinel glaciers, and apparently most of the sediment, ice borne and stream borne, that has reached the lake has come from Sphinx and Sentinel basins. Characteristically the two meltwater streams are muddy, whereas the nonglacial streams are clear even during times of rapid snow melt or heavy rain; similarly the lakes fed by meltwater streams are cloudy, and the ponds fed from nonglacial sources are clear.

Samples of water were taken with an Anderson suspended-load sampler (Anderson, 1941), from rapidly flowing stretches of the two streams where it was hoped that nearly all sediment load would be in suspension. Sphinx Creek, on September 10, 1954, contained approximately 13 ppm (milligrams per liter) suspended matter, all of fine silt to clay size. Samples from Sentinel Creek on the same day contained from 140 to 265 ppm suspended

matter, nearly all of sand or coarse silt sizes. The weighted average load of this stream was about 175 ppm. The opacities of the stream waters, as indicated by the depth at which a white plate (Secchi disk) ceased to be visible,

TABLE 2.—TEMPERATURES OF STREAMS ENTERING GARIBALDI LAKE

Day	Time	Stream temperatures
Sentinel Creek at Garibaldi Lake		
Oct. 2, 1949	midday	4.15°C
Sept. 13, 1950	midafternoon	3.7
Aug. 28, 1952	late morning	3.3
Sept. 10, 1954	early afternoon	5.0°C
Sphinx Creek at Garibaldi Lake		
Oct. 2, 1949	midafternoon	7.6°C
Sept. 13, 1950	early afternoon	6.7
Aug. 27, 1952	late afternoon	7.0
Sept. 9, 1954	midday	3.8°C

2.1 feet for Sphinx Creek and 1.5 feet for Sentinel Creek, were similar and probably reflected similar concentrations of the finer fractions. Water from both streams was clear after being filtered through a No. 4 Whatman filter.

Almost nothing is known of the seasonal variation in sediment concentration of glacial streams. Presumably, this concentration is closely related to the sediment load of the glacial ice and this, in turn, to the size of the glacier and the rocks of its bed and walls. Concentration in meltwater reaches a maximum in mid and late summer (Greim, 1903), when contributions from ice melt are greatest, and is low in early summer when contributions to the meltwater streams come mainly from the melting of the relatively clean snow cover. In September 1954, after a remarkably cool summer, conditions at Garibaldi Lake were more nearly typical of July; snow still covered most of the glaciers and contributed most of the meltwater. Thus, the sediment concentrations noted at that time may be well below the maxima for normal years.

When Sentinel and Sphinx creeks leave the glaciers, their temperatures must be close to 0°C, but both streams become warmer downstream (Table 2), probably by conduction and condensation from the atmosphere and by accession of relatively warm water from nonglacial tributaries. The water of Sphinx Creek is retained for an average period of 1–2 weeks in Sphinx Lake where there is added opportunity for warming. The summer of 1954 was so cool that no part of this lake warmed above 4°C, but in the summers of 1949, 1950, and 1952 the surface layer at least reached 7°C, notwithstanding the accession of cold water from the glacier. Such elevated temperatures may never be reached by Sentinel Creek in which flow from glacier to lake requires about 1 hour.

Diurnal fluctuations are probably insignificant in lower Sphinx Creek because of the stabilizing influence of Sphinx Lake. On the other hand, the temperature of Sentinel Creek at its mouth may fluctuate from day to night as much as the glacial stream feeding Lake Louise, Alberta, where in July 1904 the temperature changed from 5.2°C in an average midday to 1.8°C in an average evening (Sherzer, 1907, p. 29).

Seasonal changes may also differ slightly in the two streams. Temperatures of both streams at the mouths must be near 0°C during winter and spring. Temperatures rise during the summer, presumably slowly at Sphinx Creek and more rapidly but more irregularly at Sentinel Creek. Both streams cool in the autumn, though Sphinx Creek may cool slowly until reserves of warm water held in Sphinx Lake become exhausted.

CHARACTER OF LAKE WATER

Density of lake water is influenced by temperature, suspended sediment, dissolved matter, and pressure. In considering the stability, instability, or movement of two or more water masses within a lake, densities can be compared at a standard depth and the effect of pressure thus eliminated. The concentration of dissolved matter in Garibaldi Lake is very low (one sample of surface water yielded 14 ppm total solids, and perhaps as much as 6 ppm was suspended matter) and probably uniformly distributed; hence this factor can be neglected. Temperature is generally the most significant

factor in determining density, but at temperatures close to 4°C the thermal coefficient of expansion approaches zero, and the influence of suspended matter may be dominant.

waters in the lake. Higher turbidity at greater depth appears both necessary and sufficient to maintain stability. Compared with pure water 552 feet deep at 3.68°C, the additional 24±

TABLE 3.—TEMPERATURES OF WATER IN GARIBALDI LAKE
Degrees Centigrade

Depth		Temperatures					Rel. turbidity Sept. 7/54
Meters	Feet	Oct. 2, 1949*	Sept. 13–14 1950*	Aug. 27–29 1952†	Sept. 7 1954**	Tmd Strøm	
0	0	+9.4	+13.3–14.5	+10.1–13.1	+8.5–9.5	+3.94	0.2
5	16	9.0	11.2–12.3	9.9–10.3	9.3–9.6	3.93	.....
10	33	7.85	7.2–8.5	7.5–7.6	6.9–7.6	3.93	.....
20	65	6.0	5.0–6.1	4.1–4.3	4.3–4.7	3.92	.....
30	98	4.5	4.2–6.0	.....	3.9–4.2	3.90	.....
40	131	4.2	.....	.....	3.9–4.0	3.89	.....
50	164	.....	4.0–4.9	3.93–3.96	3.8–4.0	3.88	.....
100	328	.....	4.0–4.7	3.78–3.89	3.8–3.9	3.82	.....
140	462	.....	.....	.....	3.8–3.9	3.77	.....
168	552	.....	.....	.....	3.68	3.74	0.2
213	699	.....	.....	.....	3.74	3.70	0.5
240	786	.....	.....	3.87	.....	3.67	.....
250	819	.....	.....	.....	3.95	3.66	1.0††
259	849	.....	.....	.....	4.00	3.65	1.0††
Secchi disk reading		2.3 m = 7.6′	2.8–3.1 m = 9.2–10.2′	.....	11–13′***	....	.....

* Records courtesy Research Division, British Columbia Game Department

† Ranges recorded on reversing thermometer

** Figures quoted to one decimal place based on bathythermograph trace; figures quoted to two places based on reversing thermometers

†† Combined water sample from these two depths yielded 30 ppm suspended sediment on flocculation

*** Secchi disk reading increased to 14 feet in October, 1954 and 22 feet on July 23, 1955, then decreased to 14 feet on August 9, and 12 feet on September 4 and September 11, 1955

The vertical distribution of temperature in the main body of the lake was determined on several occasions (Table 3) with reversing thermometers, supplemented in 1954 by a bathythermograph which provides a continuous record of temperature against depth. In 1952 and 1954 temperatures in the deep waters were less than 3.94°C, the temperature of maximum density at the surface. This is a condition rarely described in North America but known to be typical of those deep lakes that cool in winter below 3.94°C throughout their extent (Strøm, 1945). In 1954 the temperature 552 feet below the surface was 3.68°C, somewhat below the temperature of maximum density for that depth and colder than deeper

ppm of suspended matter in the bottom water added approximately 15×10^{-6} gms/cc to the density, and its higher temperature (4.00°C) reduced it by less than 2×10^{-6} gms/cc. Much of the sediment in the deep water was so fine that the water passing a No. 4 Whatman filter remained cloudy.

Seasonal changes in temperature distribution at Garibaldi Lake have not been investigated but can be inferred from those known in non-glacial temperate lakes, particularly Lake Eikeren in southern Norway (Strøm, 1944). Garibaldi Lake is normally ice-covered from December to June. Mixing of deep and surface water, the semiannual "overturn", can take place during the isothermal conditions follow-

ing breakup and preceding freeze-up. The direct thermal stratification, warm above and cold below, observed at Garibaldi Lake is typical only of summer and autumn.

extended on surface only about 20 feet into the lake. In August 1952, a sharply defined interface sloped downward and outward at about 15° from the mouth of the estuary. Wave stir-

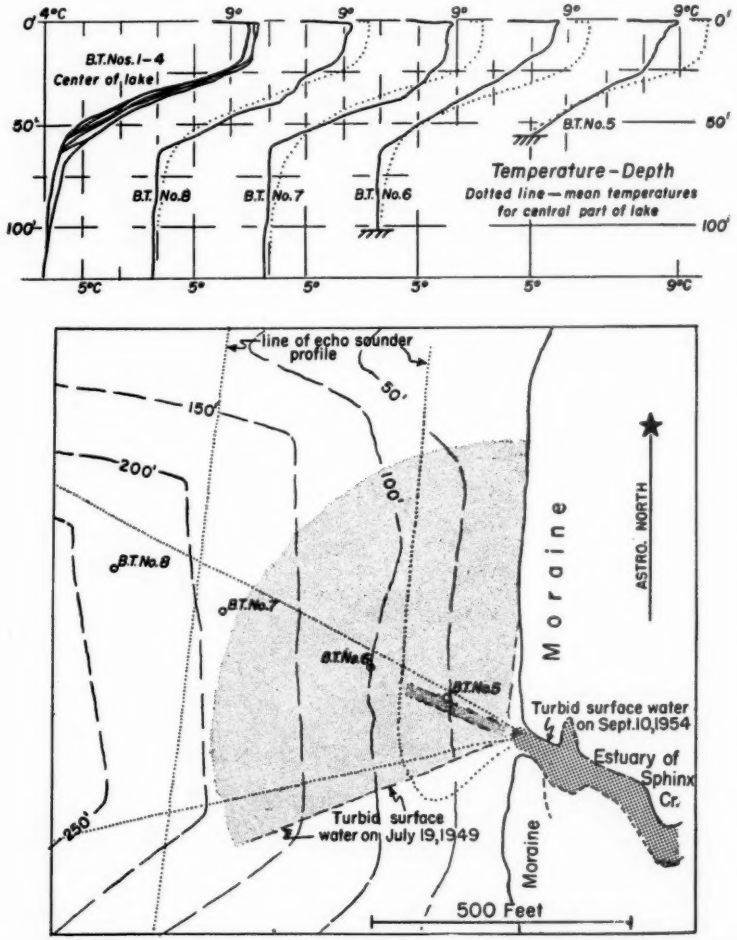

FIGURE 4.—BATHYTHERMOGRAPH RECORDS, BOTTOM TOPOGRAPHY, AND SURFACE DISTRIBUTION OF TURBID WATER IN GARIBALDI LAKE NEAR SPHINX CREEK

MOVEMENT OF STREAM WATER INTO LAKE

The movement of water from the two glacial streams into the lake is partly shown by the surface distribution of turbidity. The milky water of Sphinx Creek filled its estuary in September 1954 (Fig. 4), and August 1952, but

ring was then slight, and the stream water was denser than the surface water of the lake; hence Sphinx Creek discharged as an underflow. On the other hand, an air photograph taken July 19, 1949, shows milky water extending in a broad fan (Fig. 4) fully 700 feet into the lake. This was part of a surface layer, for the tur-

bidity of the lake is sufficient to mask all detail more than 10 or 20 feet below the surface. Sphinx Creek at this time was evidently discharging as an overflow.

near-surface lake waters was also taking place judging from the slight but significant decrease in its transparency near the turbid tongue. On July 19, 1949, the tongue of turbid water was

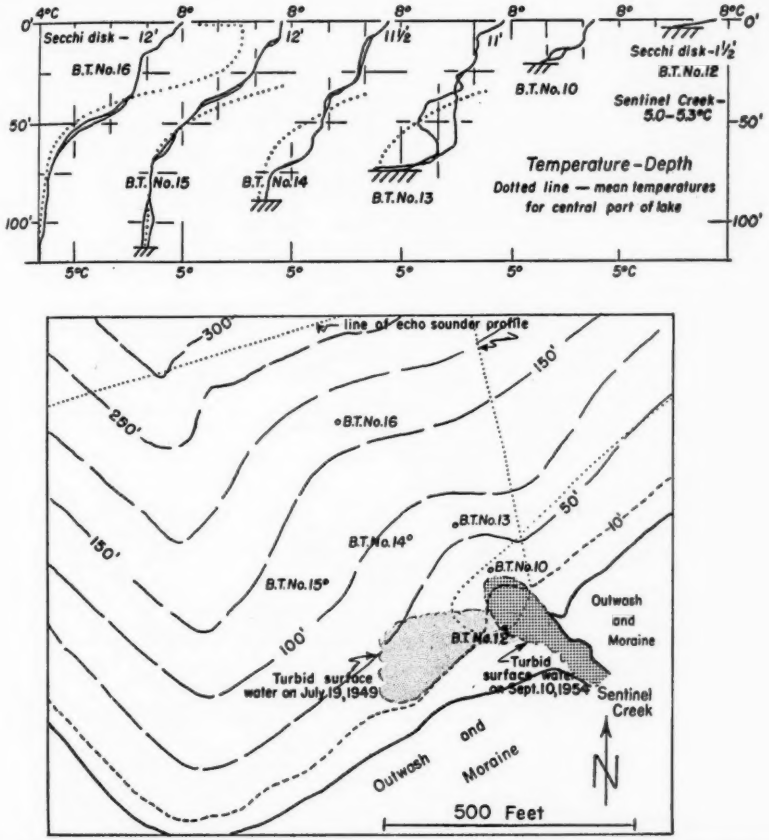

FIGURE 5.—BATHYTHERMOGRAPH RECORDS, BOTTOM TOPOGRAPHY, AND SURFACE DISTRIBUTION OF TURBID WATER IN GARIBALDI LAKE NEAR SENTINEL CREEK

Sentinel Creek in September 1954 discharged turbid water which extended at the lake surface as a tongue 150 feet long (Fig. 5), bounded sharply on the north from the clearer lake water along the line of a submerged shoal and limited on the south and west by a convoluted boundary extending over relatively deep water. The boundary remained essentially stationary; evidently the influx from the creek was compensated mainly by sinking of the cool, turbid water into the lake. Some mixing with the more extensive and deflected sharply to the left, possibly by the shoal noted above.

To determine the distribution of cool, turbid creek waters beyond visible limits, detailed bathythermograph records were made at several points (Figs. 4, 5). These differ from the records made in the central part of the lake in that: (1) temperatures in the uppermost 35 feet are lower by as much as 1 Centigrade degree off Sphinx Creek and 3 Centigrade degrees off Sentinel Creek; (2) off Sphinx Creek

the water 60 to 100 feet below the surface is cooler; (3) the curves, especially those recorded off Sentinel Creek, are more irregular, show sharp inflections, vary with position, and apparently change with time, judging from the discrepancies between the curves formed during the lowering and hoisting of the instrument at a single station (*e.g.*, B.T. No. 13. Fig. 5). The first difference may result from mixing, aided by wave action, of lake and stream waters in the near-surface layers. The second difference may result from stream water flowing between warm lake water above and cold dense lake water below. Irregularity of the curves could result from incomplete mixing of lake and stream waters and would testify to the recent development of the temperature distribution.

Some estimates are pertinent on the time required to produce the thermal anomalies off the creek mouths. In a 180-degree sector, 800 feet in radius and 38 feet deep, the 0.4 Centigrade degree average chilling from 9.0°C to 8.6°C, indicated at the four B.T. stations, could be produced by mixing 11 parts of lake water at 9°C with 1 part of stream water at 4°C in about 10 hours flow at 85 c.f.s. On the other hand, the 0.3 Centigrade degree average chilling, from 4.3°C to 4°C, in the water of the same sector 65 to 100 feet deep, would necessitate elimination of almost all lake water by stream water and would require fully 120 hours flow. In September not more than 8 per cent of Sphinx Creek water was mixing with the surface layers of the lake. The introduction of an unlimited supply of stream water at 4°C would have almost no effect on the temperature of the deeper lake waters, already at about 4°C, and could remain undetected. Since the stream water at this temperature can spread readily 65 to 100 feet below the surface, it may disperse in three dimensions and move gradually into the deeper part of the lake. Existence of this type of movement or of a rapidly moving and persistent underflow could be neither proved nor disproved with the conditions prevailing in September 1954. Though about 130 hours of flow from Sphinx Creek would be necessary to produce the observed effects within the 800-foot limit, much more time may have been involved.

Estimates for Sentinel Creek are not easy to make because of variable stream temperature. Assuming that the mean daily stream temperature was 4°C, mean discharge 40 c.f.s., and station 16 representative of a 180-degree sector 800 feet in radius about the mouth of Sentinel Creek, the 2 Centigrade degree chilling down to the 35-foot depth would require about 100 hours flow. No reliable figure can be obtained for the relative volume or duration of any interflow or underflow.

Sentinel Creek thus mixed readily with the near-surface water of the lake, but Sphinx Creek mixed hardly at all. Water densities, so similar in the two streams, cannot account for such differences in mixing. More probably the relatively great surface extent and perimeter of the intruding tongue of Sentinel Creek water favors mixing at shallow depth. Perhaps, too, the abrupt steepening of slope at the outer edge of Sentinel Creek delta permits cool stream water to flow out over warmer lake waters, creating inverted thermal gradients (*e.g.*, B.T. Nos. 13, 15) in which vertical mixing is favored.

The mingling of stream and lake waters is important in determining the level at which the entrained sediment is discharged into the lake. Sphinx Creek introduces little sediment into the uppermost 60 feet of the lake in September but may contribute much in July. Sentinel Creek evidently drops much of its coarser load at its mouth to form the submerged delta (Fig. 5), but some of the finer suspended matter is introduced into the uppermost 35 feet of the lake. The possibility of some sediment accompanying underflows along the bottom to great depths cannot be precluded. However, no significant subaqueous channel, such as those formed by persistent underflows at Lakes Geneva and Constance (Forel, 1885), was revealed by echo sounding off either Sentinel or Sphinx Creek.

Characteristics of Bottom Sediments

General Statement

Three types of sediment can be distinguished on the basis of structure, porosity, and size distribution:

(1) Obscurely stratified to massive clays[2] (cores 92[3], 390, 367)

(2) Distinctly stratified sediment including laminae of clay, silt, and fine sand (cores 849, 835, 448)

(3) Slumped sediment of mixed sizes (core 765)

One sample, core 524, a clay-rich silt, has characteristics of the first type but is coarser.

Distribution

The clays were found only on the steep slopes leading down to the central basin and on the western platform; the second and third types were found only on the basin floor and on the slope leading up to the southeast end of the lake. Judging from dregs on the coring tube and from dents in its cutting edge, the bottom near the southeast end is sandy to rocky. No cores were recovered there.

Physical Characteristics

Structure.—The structure is shown in Plate 1, but the following points are noteworthy:

(1) One relatively thick lamina of coarse silt and fine sand in core 448 terminates abruptly within the limits of the core sample (top of photo; 1 foot of overlying sediment has been removed). The silt and clay layers immediately beneath this lens, or ribbon, of sandy material are thinner than elsewhere, presumably because of differential compaction.

(2) Core 367, though composed throughout of clay, exhibits a marked, irregular disconformity cutting at 60° across the axis of the core and truncating an obscure lamination. Absence of coarser-grained material precludes the possibility that the disconformity records a temporarily lowered lake level. Downslope movement of the near-surface sediment, without marked disturbance of the bedding, may account for the relationship.

[2] The term "clay" is used here as a sediment consisting predominantly of particles finer than 0.002 mm irrespective of mineral composition. Clay minerals are almost or completely absent from these sediments.

[3] Cores are identified by the depth of the lake in feet at the point at which they were taken (Fig. 2).

(3) Core 524 consists of 3 inches of massive, clayey silt to the base of which adheres a layer of well-sorted, fine gravel which evidently prevented further penetration of the coring tube. The gravel resembles the granitic detritus on the present beaches and may mark a shore deposit formed during the initial flooding of the lake basin. If so, the 3 inches of overlying, clayey silt is all the sediment that has accumulated and remained in place since that time.

TABLE 4.—POROSITIES AND SPECIFIC GRAVITIES OF LAKE-BOTTOM SEDIMENTS

Sample	Type	Porosity (% by vol. of water in undist. sed.)	Specific gravity dry solids
92	clay	73%	2.76
390	clay	75½	2.70±
367	clay	69%	n.d.
524	clay-rich silt	59±	n.d.
849	stratif. clay	60½	2.80±
	silt, sand	61½	2.82
448	silt	63%	2.78
765	slumped sed.	63%	2.84±

(4) Core 92, which exhibits no stratification, is marked by abundant, nearly horizontal dark lenticles, a few tenths of a millimeter thick and a few millimeters long. A thin section shows parallelism of micaceous minerals within the lenticles, but no continuous laminae are distinguishable by either size or orientation of constituent grains.

Porosity and specific gravity.—Porosity determinations (Table 4) were made by drying measured volumes of the sediment shortly after they had been brought to the laboratory in sealed containers. Relatively high porosity of the clays is significant, as is the relatively high specific gravity of solids in all the sediments.

Size distribution.—Size analyses were made of weighed samples of wet sediment taken directly from the sealed containers. Duplicate samples were taken at the same time to be weighed, dried, and weighed again so that the equivalent dry weight of the analyzed sample could be determined. Each wet sample for analysis was stirred with fresh water in an

electric mixer and washed through a 325-mesh screen. Mechanical analyses were then made of the fine fraction, using a modification of the ASTM hydrometer method. Normally no dispersing agent was added in the preparation of the samples; however, a few samples tended to flocculate even in fresh water, possibly because of the relatively high concentrations used in the hydrometer analysis (Oden, 1916). As repeated stirring did not eliminate this flocculation, duplicate samples were run using either sodium carbonate or Calgon as a dispersing agent, with satisfactory results. The coarse fractions of the sediment, retained on the 325-mesh screen, were dried and analyzed by dry sieving.

The results of the mechanical analyses are presented in cumulative curves in Figure 6. These curves show the contrast between the obscurely bedded to massive clay (samples 390, 367, 92) and the slumped or clearly stratified silts (samples 765, 448, 849). Only sample 524 was anomalous, for although it lacks obvious stratification, it exhibits the relatively coarse median diameter and the poor sorting of the well-stratified and of the slumped material.

The analyzed samples of cores 448 and 849, which show the clear stratification, included many distinct but minute laminae of clay, silt, and fine sand, hence the poor sorting indicated by the curves. Only a few of the thicker and coarser laminae in the 1-inch diameter cores contained a sufficient weight of solid matter to be amenable to mechanical analysis. A remarkably high degree of sorting was revealed for the laminae (Fig. 6) though many graded from coarse below to fine above.

Atterburg limits.—Liquid and plastic limits of one sample of clay from core 367 are 72 and 35 respectively; the natural water content (water loss at 110°C divided by dry weight) was 90 per cent, corresponding to 71 per cent porosity. The clay is "sensitive", as is the clay of Steep Rock Lake (Legget and Bartley, 1953, p. 526), and with sufficient disturbance it may be converted to a semifluid.

Composition

Red dacite, typical of the volcanic rocks west of the lake, occurs as widely scattered discrete particles, mainly 0.045–8 mm in diameter, in the clays (cores 390, 367, 92). As much as 5 per cent of the sediment in core 390 is red dacite. The coarse fraction from core 367 consists largely of this volcanic detritus, but some quartz and granitic particles are present.

Quartz, plagioclase, and hornblende, all from granitic rocks, are conspicuous in the coarser fractions of the stratified sediment in the central part of the lake. No volcanic detritus was found; debris from a western source must have been lost in a flood of material from the opposite shore. Biotite is present in some bottom sediments (cores 445, 890, 765) and is abundant in the massive clayey silt from the eastern slope (core 524). Minute limonitic pellets of unknown source have been noted in the slumped sediment (core 765).

The composition of the finer sizes of the clays has been investigated in a minus 0.4-micron fraction from core 390. X-ray analysis indicates feldspar, quartz, biotite, and muscovite. The proportion of biotite is higher than in a sample of fine sand from core 445, and the proportion of quartz lower. No hornblende could be recognized in the x-ray analysis, but an electron photomicrograph showed at least one grain which, judging from its shape and opacity, might be hornblende. No clay minerals

PLATE 1.—CORE SAMPLES OF LAKE-BOTTOM SEDIMENTS

×1½

FIGURE 1.—CORE 367, FROM 20 TO 22 INCHES BELOW SEDIMENT INTERFACE; OBSCURELY STRATIFIED CLAY WITH LOCAL DISCONFORMITY

FIGURE 2.—CORE 849, FROM 1 TO 3 INCHES BELOW SEDIMENT INTERFACE; IRREGULARLY STRATIFIED CLAY, SILT, AND FINE SAND

FIGURE 3.—CORE 448, FROM 12 TO 14 INCHES BELOW SEDIMENT INTERFACE; IRREGULARLY STRATIFIED CLAY, SILT, AND FINE SAND, WITH A LENS OR RIBBON OF SAND NEAR THE TOP OF THE SAMPLE

FIGURE 4.—CORE 765, FROM 2 TO 4 INCHES BELOW SEDIMENT INTERFACE; SLUMPED AND BRECCIATED SILT AND CLAY

FIGURE 1

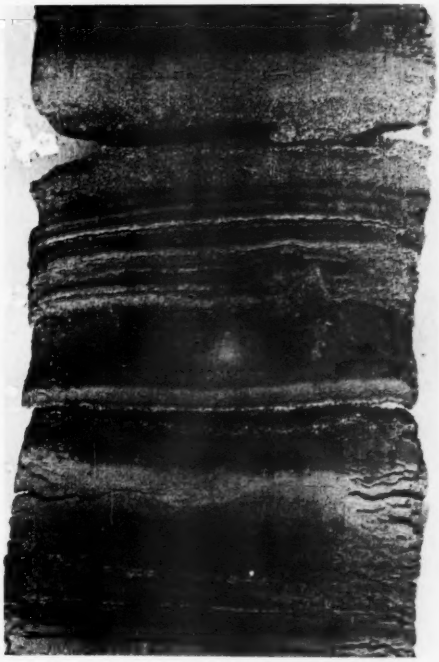

FIGURE 2

FIGURE 3

FIGURE 4

CORE SAMPLES OF LAKE-BOTTOM SEDIMENTS

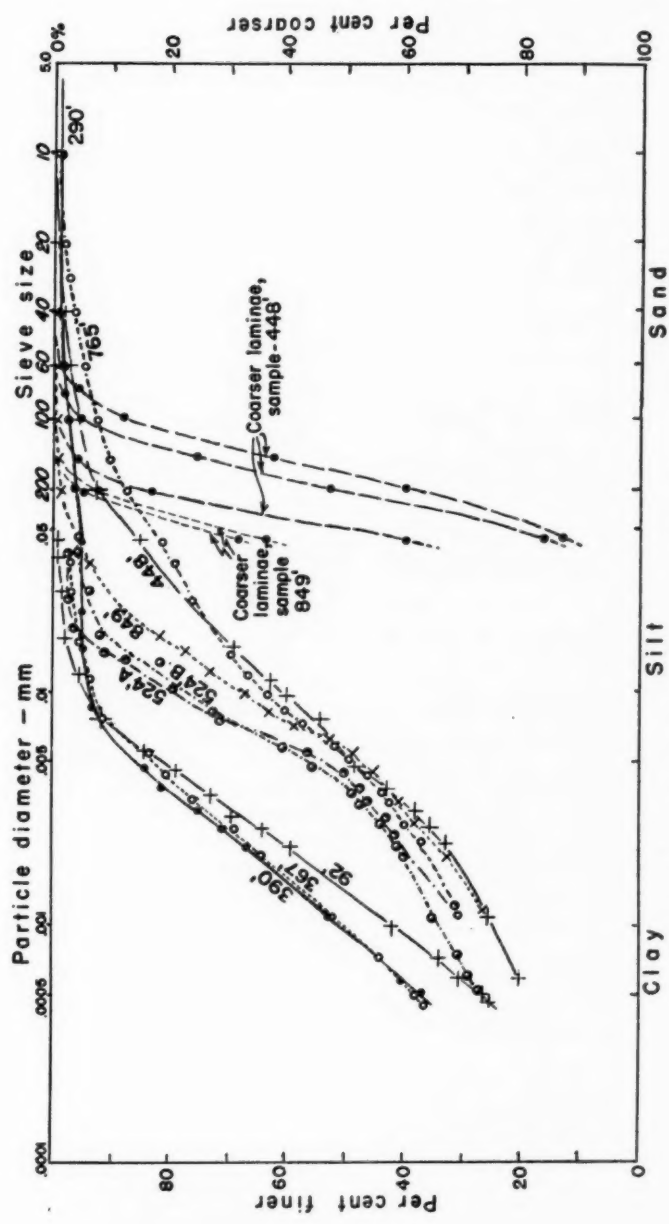

FIGURE 6.—PARTICLE SIZE DISTRIBUTION OF LAKE-BOTTOM SEDIMENTS

were detected by x-ray or thermal analysis, and no grains with the hexagonal or tubular shape of many of the clay minerals were seen in the electron photomicrograph. Even the finest fraction of the lake sediment must consist of essentially unweathered rock flour.

The base-exchange capacity of a sample from core 92 was about 19 milliequivalents per gram, low for clays of either the montmorillonite or illite groups, though seemingly high for a mixture of quartz, feldspar, and mica, unless very large surface area is responsible.

Discussion

Deposition of Clays

The clays found at the western end of the lake and on the slopes of the central basin differ from typical glaciolacustrine sediment only in the poorly defined lamination and lack of obvious varves. Well-defined, rhythmic bedding may be absent because: (1) relatively slow rate of deposition may lead to inconspicuous varves of microscopic thickness; (2) slow transport to the deeper part of the lake, and perhaps also to its more distal portions, may cause such a time lag between the entrance of sediment into the lake and its accumulation on the bottom that the effect of its intermittent introduction is effectively lost; (3) bedding, particularly if thin, may be obliterated by small-scale slump after deposition.

Slow rate of deposition can be inferred. Assuming that the concentration of fine, suspended sediment in the two glacial streams has a mean annual value of 15 ppm (approximately the amount carried by Sphinx Creek in early September 1954), the average thickness of this sediment accumulating in a single year would be only 0.15 mm over the entire basin; undoubtedly the distal, western part of the lake would receive less.

Slow transport to the site of deposition is also indicated. The middle 50 per cent of the clays, for example, is made up mainly of particles (between the first quartile, 0.0035 mm diameter, and the third quartile, 0.00035 mm diameter) which settle in still water at 4°C at rates of from 10 hours to 37 days per foot. From 15 weeks to 30 years might be required for such particles to sink 300 feet below the level at which they were introduced, if the water were free from vertical currents. Probably most of these settling particles would be involved in and redistributed by the semiannual overturn of lake waters, and actual time for deposition in the deeper parts of the lake can only be conjecture. The rate of horizontal movement of the particles is also uncertain. An average, westerly drift of about a quarter of a mile per year is needed to compensate for influx and outflow of water. Wind-driven currents are much more vigorous: driftwood has moved across the lake, about 3 miles, in less than 2 days under a strong and continuing wind, and surface water must move at comparable rates. Rate of dispersal of sediment-laden waters from the eastern end of the lake, particularly if they are tens of feet below the surface, remains unknown. This hypothesis for the lack of bedding requires much more investigation before its full importance is established.

Slumping is at least of local importance: the disconformity of core 367 and the slump structure of core 765 show that subaqueous transfer does take place. The dark lenticles of core 92 may be the remains of bedding disrupted by downslope movement of the sediment.

The coarse fraction, 0.045 to 8 mm in diameter, in the clays is distinct both in source and mode of deposition from the more abundant fine fraction. Though red dacite probably underlies the slopes from which the clay cores were recovered, it probably did not work into the sediment during downslope movement; the coarse, granitic detritus in core 367 cannot have been incorporated in this way. The dacite grains probably dropped from melting lake ice, perhaps after being blown onto it from the near-by shores.

Deposition of Stratified Clay, Silt, and Fine Sand

The coarseness of sediment on the flat bottom of the central basin is striking, compared with the fine texture of sediment resting on, or slumped from, its flanks. A mechanism of transport, other than sedimentation from dilute suspensions, is indicated. Stream velocity

of 1 cm/sec (Hjulstrom, 1939) would be necessary to transport and deposit fine sand, such as occurs in core 448, and lake-bottom currents of about this velocity can be inferred. Such currents cannot be credited to surface winds or thermal overturns. Turbidity currents could transport such sediments at the velocities indicated, judging from laboratory and field experience (Kuenen and Migliorini, 1950, p. 101–108; Bell, 1942, p. 522–523). Graded bedding, restriction of sandy layers to topographic lows, and association with a gently sloping bottom characterize deposits attributed to turbidity currents.

The source of turbidity currents may lie in (1) the glacial streams, at times when their temperatures and sediment loads give rise to densities sufficiently high to cause continuous bottom flows, or (2) slumping of previously deposited sediment from the steep basin walls and particularly from the steep delta fronts. Some doubt exists that the water of Sentinel Creek could maintain its identity as a continuous bottom flow for a distance of 2½ miles, but conceivably conditions may permit this on rare occasions.

Some data suggest that slump-generated turbidity currents can develop in the lake. Sediments partly disrupted by slump do occur (core 765). The clays are "sensitive", containing sufficient water to exceed the "liquid limit" at which flow can be induced by disturbance. Slopes are steep; even sandy sediment from Sentinel Creek is spilled onto a subaqueous delta front inclined at 20°–25°. The concentration of filterable sediment found in the water below a depth of 550 feet in September 1954 was far in excess of concentrations in the inflowing streams. Both the volume of water below this level and the amount of filterable sediment within it were well in excess of the annual supply from the two streams. A large, slump-generated turbidity current some time between August 1952 and September 1954, offers the best explanation for presence of this muddy and relatively warm water at depth. Finally, the irregular distribution of coarser laminae is more in keeping with intermittent, slump-generated currents than with stream-generated bottom currents which might be expected to exhibit a seasonal rhythm.

Source of Sediment

The granitic area east of the lake, where the tributary glaciers now exist, has provided nearly all sediment accumulating in the lake, judging from its mineral content. The red dacite lava outcropping along about 40 per cent of the lake shore has contributed but a few per cent of the detritus in the clays and has not been detected in the stratified silts, sands, and clays of the central basin. No fragments of chloritic graywacke or slate exposed north of the lake have been observed in the coarser detritus, and no chlorite has been detected by x-ray analysis of the clays. Thus mineralogy confirms the visual impression that the glacierized areas now contribute most of the sediment.

Sediment sampling of the two streams indicates that only Sentinel Creek now contributes sand-size particles to the lake; Sphinx Lake effectively traps all coarse debris from Sphinx Glacier.

Rates of Sedimentation

Enough coarse and fine sediment was transported by the two glacial streams in September 1954 to deposit a uniform layer on the lake floor at the rate of 0.65 mm per year. Of this, more than half consisted of sand and coarse silt and would be deposited either in the delta of Sentinel Creek or on the lake floor as far down as the central basin. Fine suspended sediment would be distributed on floor and slopes alike, according to distance from the source and perhaps also depth of water. Some suspended sediment settling on the slopes evidently avalanches periodically and comes to rest on the basin floor. As a result, a high proportion of the incoming sediment is concentrated in the half-square-mile floor of the central basin, where accumulation may go on at a rate of millimeters or even centimeters per year. Sedimentation on the slopes, particularly at the western end of the lake, may go on at only a small fraction of a millimeter a year, and over a period of years, parts of this may

be lost by sliding. For example, the 4 cm of clay in core 524 may be all that remains of sediment accumulating at this point since the lake first inundated it. Marked difference in rates of sedimentation can also account for the high concentration of ice-rafted(?), dacite debris in the clays and its scarcity in deposits of the central basin.

References Cited

Anderson, A. G., 1941, A combination suspended-load sampler and velocity meter for small streams: U.S. Dept. Agriculture Circ. 599, 21 p.

Antevs, E., 1951, Glacial clays in Steep Rock Lake, Ontario, Canada: Geol. Soc. America Bull., v. 62, p. 1223–1262

Bell, H. S., 1942, Density currents as agents for transporting sediments: Jour. Geology, v. 50, p. 512–547

Dominion Water and Power Bureau, 1924–1934, Surface water supply of Canada, Pacific drainage: Water Resources Papers 47, 53, 61, 65, 67, 72, 78, and 86

—— 1934, Final report on Garibaldi Lake study, July, 1932 to November, 1933: Rept. 362

Forel, F. A., 1885, Les ravins sous-lacustres des fleuves glaciares: Comptes Rendus, Acad. Sci. Paris, v. 101, p. 725–730

Greim, G., 1903, Studien aus dem Panzaun: Gerlands Beitrag z. Geophys., v. 5, p. 567–662

Hjulstrom, F., 1939, Transportation of detritus by moving water: Recent marine sediments, Am. Assoc. Petroleum Geologists, p. 5–31

Johnston, W. A., 1922, Sedimentation in Lake Louise, Alberta, Canada: Am. Jour. Sci., 5th ser., v. 4, p. 376–386

Kindle, E. M., 1930, Sedimentation in a glacial lake: Jour. Geology, v. 38, p. 81–87

Kuenen, Ph. H., 1951, Mechanics of varve formation and the action of turbidity currents: Geol. Fören Förhandl., v. 73, p. 69–84

Kuenen, Ph. H., and Migliorini, C. I., 1950, Turbidity currents as a cause of graded bedding: Jour. Geology, v. 58, p. 91–127

Legget, R. F., and Bartley, M. W., 1953, An engineering study of glacial deposits in Steep Rock Lake, Ontario, Canada: Econ. Geology, v. 48, p. 513–540

Mathews, W. H., 1951, Historic and prehistoric fluctuations of alpine glaciers in the Mount Garibaldi map-area, southwestern British Columbia: Jour. Geology, v. 59, p. 357–380

—— 1952, Ice-dammed lavas from Clinker Mountain southwestern British Columbia: Am. Jour. Sci., v. 250, p. 553–565

Oden, S., 1916, Allgemeine Einleitung zur Chemie und physikalischen Chemie der Tone: Bull. Geol. Inst. Upsala, v. 15, p. 175–194

Strøm, K. M., 1944, Heat in a south Norwegian lake: Geofys. Pub. v. 16, no. 3, 23 p.

—— 1945, The temperature of maximum density in fresh waters: Geofys. Pub., v. 16, no. 8, 14 p.

Sherzer, W. H., 1907, Glaciers of the Canadian Rockies and Selkirks: Smithson. Contr. Knowledge, v. 34, no. 1692, 135 p.

The University of British Columbia, Vancouver 8, B. C.

Manuscript Received by the Secretary of the Society May 23, 1955

BULLETIN OF THE GEOLOGICAL SOCIETY OF AMERICA
VOL. 67, PP. 553–570, 4 FIGS., 4 PLS. MAY 1956

GEOMORPHOLOGY AND GLACIAL HISTORY OF SOUTHERNMOST BAFFIN ISLAND

BY J. H. MERCER

ABSTRACT

The southernmost peninsula of Baffin Island is a tilted peneplane, with an escarpment along Frobisher Bay. During most of the Wisconsin age, precipitation in the area must have been low, and there is evidence that the higher parts of the escarpment remained above the ice. Cirques with submerged floors show that during a considerable part of the glacial ages sea level was lower than today. Strand lines up to 1425 feet A.T. indicate very great depression of the land in the late Wisconsin, possibly connected with an increase of ice in the Hudson Strait area as precipitation increased after the disappearance of the topographic barrier of the main Laurentide Ice Sheet. When the sea level was between 210 and 180 feet the overflow from an ice-dammed lake cut two great gorges and formed a large bay-head delta. The dam may have been the northern margin of an ice sheet centered in the Quebec-Labrador Peninsula. There is evidence of a warmer period in the recent past, and the present small icecaps are probably the rejuvenated relics of a larger icecap.

CONTENTS

TEXT

	Page
Introduction	553
Geomorphology of the peneplane	554
Geomorphology of the Frobisher Bay coast	555
General characteristics	555
Head of Frobisher Bay to Egglestone Bay	556
Egglestone Bay to Cape Lawrence	556
Cape Lawrence to Watts Bay	556
Watts Bay to York Sound	557
Southeast of York Sound	558
Drainage of Kingaite Peninsula	558
Raised strand lines	558
Previous observations in neighboring regions	558
General statement on Kingaite Peninsula strand lines	559
Jackman Sound to York Sound	560
York Sound to Watts Bay	561
Watts Bay to Cape Lawrence	561
Cape Lawrence to Egglestone Bay	561
Egglestone Bay to the head of Frobisher Bay	561
Kingaite Peninsula during the Pleistocene Epoch	562
Introduction	562
Onset of glaciation	562
Wisconsin Maximum	563
Late Wisconsin time	567
Recent changes in the ice cover	568
Summary of the physiographic history	569
References cited	569

ILLUSTRATIONS

Figure	Page
1. Location map	554
2. Kingaite Peninsula	555
3. York Valley area	559
4. Changes in sea level and hypothetical changes in ice cover in the Kingaite Peninsula vicinity	564

Plate	Following page
1. Coastal views and a partly submerged cirque	556
2. Aerial view of coast, felsenmeere on erosion surface, and inland margin of icecap	556
3. York Valley, and a gorge at its head	556
4. High-level strand lines and a fiord-head gorge	556

TABLES

Table	Page
1. Raised strand lines on the west coast of Frobisher Bay	560

INTRODUCTION

The southernmost peninsula of Baffin Island (Fig. 1) is not named on the latest maps. Hall (1865, p. 188) called it Kingaite, and this name is used throughout the present paper. The peninsula is part of the Canadian Shield and, except for one known outlier of Ordovician limestone near the head of Frobisher Bay, is composed of igneous and metamorphic Pre-

cambrian rocks. Essentially it is a tilted peneplane with a drowned coast along Hudson Strait and an abrupt northwest-southeast escarpment facing Frobisher Bay. On the plateau behind the southeastern end there are two small icecaps, the Grinnell and the Terra Nivea (Fig. 2). Field work during the summers of 1952–1953, under a McGill University-Arctic Institute-Carnegie grant, was concentrated on the escarpment and the narrow strip of the peninsula behind it which drains into Frobisher Bay, since this was readily accessible by water. Information about the rest of the peninsula was obtained largely from air photographs. This paper presents a reconnaissance account of the geomorphology of the peninsula and a preliminary conception of the Pleistocene history.

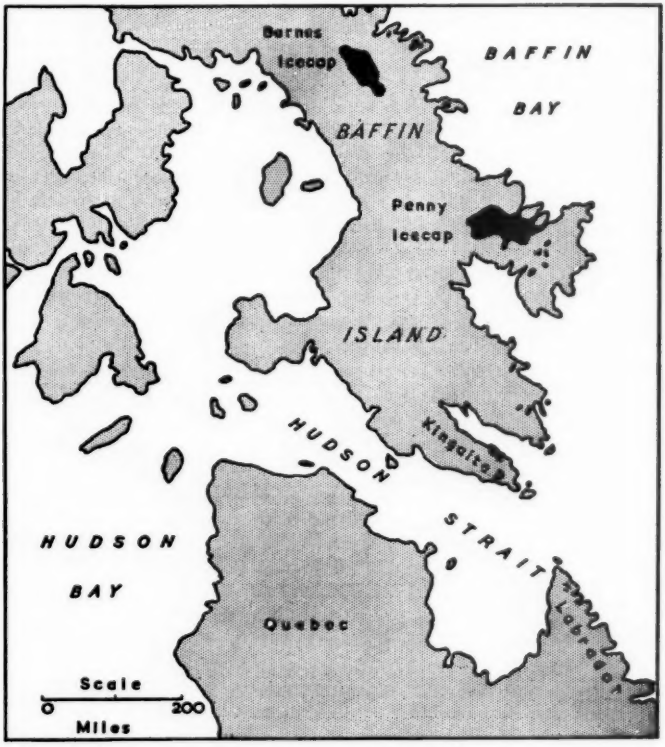

FIGURE 1.—LOCATION MAP

GEOMORPHOLOGY OF THE PENEPLANE

The peninsula is not a simple tilted peneplane since toward the southeast it narrows but the escarpment becomes higher. Air photographs show that an ill-defined escarpment approximately parallel to Hudson Strait separates a high-level plateau from a lower one, both rising to the northeast. The high-level plateau narrows to the southeast. The structure of the bedrock shows clearly from the air; the relief is low (Pl. 1, fig. 2; Pl. 2, fig. 3), and there are many rock-basin lakes. The low-level plateau has greater relief and fewer lakes. Bell (1901, p. 9M) described it as rough, mountainous country, which rises gradually to the north and has been half submerged.

Odell (1933, p. 208) considered that the pene-

plane in northern Labrador had been sufficiently modified by continental glaciation to be a glacial peneplane. This view appears extreme; certainly in the Kingaite Peninsula there is no evidence that the ice profoundly modified the preglacial surface. Its activity was restricted to roughening the surface by selective erosion so that the ridges and valleys now coincide with outcrops of different erodibility. Some of the lakes are along lineations, some are along soft bands of rock, and others have no obvious relation to the structure. The lineations may run in any direction, but the best developed run northeast at right angles to the coast.

FIGURE 2.—KINGAITE PENINSULA

GEOMORPHOLOGY OF THE FROBISHER BAY COAST

General Characteristics

It is uncertain when the peneplane was uplifted, but Cooke (1930, p. 71) considered from the evidence of the rivers that the Shield was uplifted in the late Pliocene. The significance of the abrupt escarpment along Frobisher Bay

is not known, but the linear character of the coast suggests that it is a fault-line scarp. Southeast of the archipelago the water is 2000 feet deep in places within a mile of the shore (Grainger, 1954).

The coast (Fig. 2) can be divided into five sections northwest to southeast.

Head of Frobisher Bay to Egglestone Bay

From the head of Frobisher Bay to Egglestone Bay, the coast line has no marked embayments. The height of the escarpment near Egglestone Bay is about 2200 feet, and the whole section shows evidence of ice-sheet action, but with none of the results of alpine glaciation that appear farther down the coast.

Egglestone Bay to Cape Lawrence

From Egglestone Bay to Cape Lawrence, the coast is cut by deep glaciated valleys which open into Hidden, Newell, Leach, and Kneeland bays. These valleys and the cirques on their flanks have been modified by ice-sheet action.

Cape Lawrence to Watts Bay

The coast line from Cape Lawrence to Watts Bay is very straight except for several short fiords (Pl. 1, fig. 2). The fiords have developed in the same directions as lineations. Most cut the coast line at right angles, opening to the northeast, but a few open nearly eastward. The largest are Ney Harbour, and Griffin, Minturn, Delano, and Watts bays, all about 5 miles long. Streams flowing to the heads of the fiords through broad, glaciated valleys have cut narrow gorges up to 50 feet deep (Pl. 4, fig. 3). There are also several low-level cirques, a few still containing small glaciers, and some short valleys with submerged mouths that are incipient fiords. Some of these valleys are wide at the mouth and taper to a point within a short distance. Such a valley is seen in Figure 1 of Plate 2 next to a normal cirque. The genesis of these valleys is not clear. In the Rondane area of Norway many of the cirques are at the heads of finger valleys. Strøm (1945, p. 366) concluded that this elongation is due to the fact that the rocks shatter so easily that backwall recession is very rapid. If the rock is resistant but has vertical lines of weakness, stream erosion along one of these lines of weakness behind a cirque glacier might result in leaf-shaped valleys.

The walls of all these valleys are steep, and some are precipitous. In a few places the walls of adjacent valleys have intersected to form ridges, but in most places long strips of the old

---

PLATE 1.—COASTAL VIEWS AND A PARTLY SUBMERGED CIRQUE

FIGURE 1.—VIEW SOUTHEAST FROM THE SUMMIT OF THE PRESIDENT'S SEAT; GRINNELL ICECAP ON THE RIGHT, OUTLET GLACIERS FLOWING THROUGH HIGHLY DISSECTED ESCARPMENT TO FROBISHER BAY

FIGURE 2.—VIEW NORTHWEST FROM THE SUMMIT OF THE PRESIDENT'S SEAT (2980 FEET)

Foreground: left, erosion surface remnant terminated by cirque backwall; right, another small erosion surface remnant isolated by cirque erosion. Background: left, the low relief of the inland plateau; right, the dissected escarpment

FIGURE 3.—CIRQUE WITH SUBMERGED FLOOR, PRESIDENT'S SEAT PENINSULA

The peak behind is about 2500 feet high

PLATE 2.—AERIAL VIEW OF COAST, FELSENMEERE ON EROSION SURFACE, AND INLAND MARGIN OF ICECAP

FIGURE 1.—COAST NEAR CAPE LAWRENCE; LOWER LEFT, PART OF NEY HARBOUR; UPPER RIGHT, CAPE LAWRENCE

In valley marked X, the seaward part has gullied walls and felsenmeere on the erosion surface remnants above. The upper part has walls free from gullies, and the structure of the plateau above is plainly visible. (R.C.A.F. photo)

FIGURE 2.—FELSENMEERE ON EROSION SURFACE REMNANT; ALTITUDE 2150 FEET

Above right-hand wall of valley X in Figure 1 of Plate 2

FIGURE 3.—INLAND MARGIN OF GRINNELL ICECAP AT 1800 FEET; SHOWS LOW RELIEF OF HIGH-LEVEL PLATEAU, AND DEAD ICE SLOPING IN OPPOSITE DIRECTION TO ICECAP; 1 AUGUST, 1952

FIGURE 1

FIGURE 2

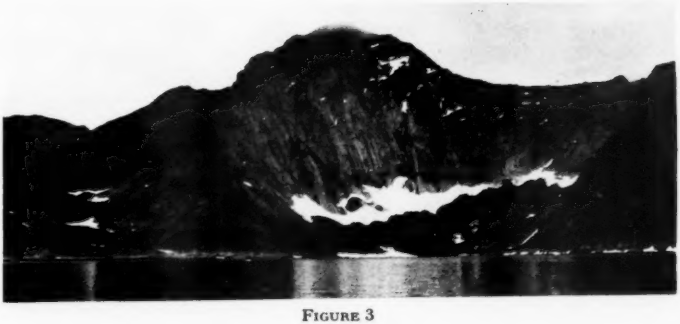

FIGURE 3

COASTAL VIEWS AND A PARTLY SUBMERGED CIRQUE

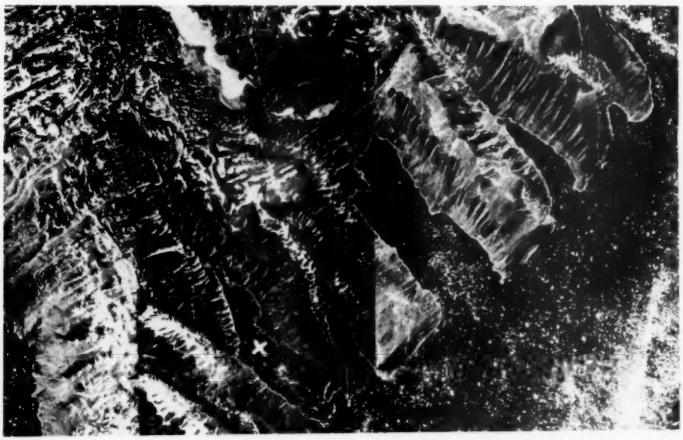

FIGURE 1

FIGURE 2

FIGURE 3

AERIAL VIEW OF COAST, FELSENMEERE ON EROSION SURFACE, AND INLAND MARGIN OF ICE CAP

FIGURE 1

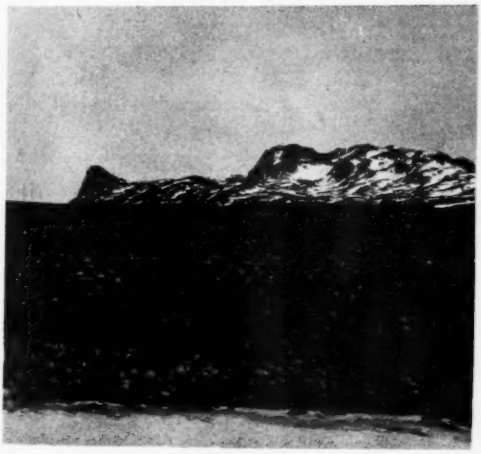

FIGURE 2

FIGURE 3

YORK VALLEY AND A GORGE AT ITS HEAD

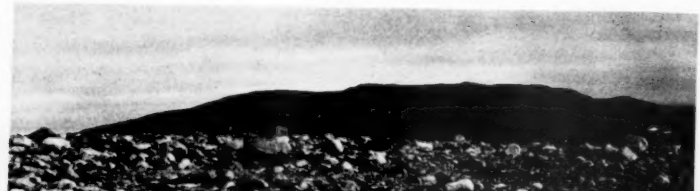

FIGURE 1

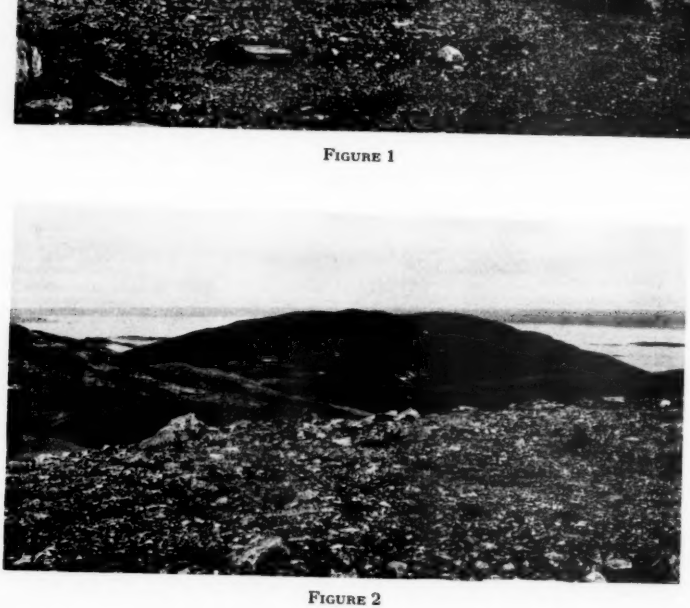

FIGURE 2

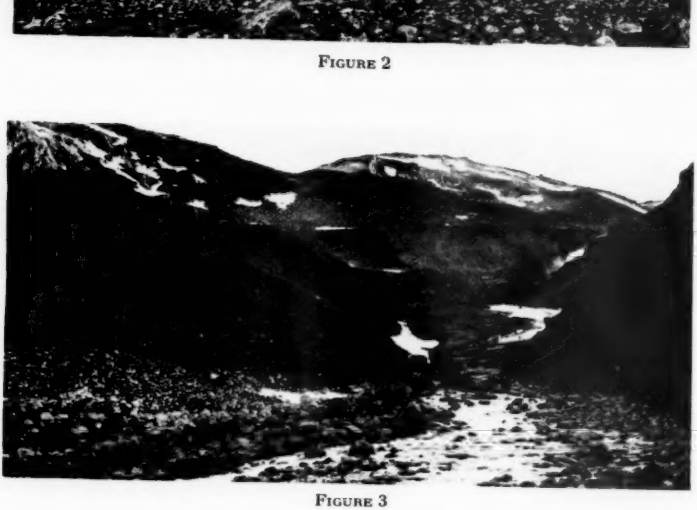

FIGURE 3

HIGH-LEVEL STRAND LINES AND A FIORD-HEAD GORGE

erosion surface have been preserved between adjacent valleys (Pl. 2, fig. 1). These undissected strips are almost parallel in profile, and the height of land is about 2 miles from the outer coast. Inland, there is a gradual descent of about 300 feet to the plateau, which then slopes more gently southwestward (Pl. 1, fig. 2). Seen from the air, these strips appear very different from the inland plateau, since the structure of the underlying rocks is not apparent. Examination on the ground shows a smooth surface almost completely covered with stones; exposures of bedrock are rare (Pl. 2, fig. 2).

One of the most striking features of this part of the coast is the gullying of the valley sides (Pl. 2, fig. 1). As seen clearly from the air, the shorter valleys are gullied throughout, the longer ones in the seaward section only. The valley marked X is severely gullied for about a mile from the outer coast, and the walls meet the old erosion surface sharply. Just above the head of the fiord the gullying is only incipient, and half a mile farther inland the valley sides are almost devoid of gullying.

Above the gullied section of the valley the plateau surface is smooth, and the bedrock is covered with stones; above the slightly gullied section the surface is rougher; above the section without gullies and inland from there, the plateau surface has considerable relief, the stony covering is absent, and the grain of the underlying rock has been sharply etched. The difference is not lithological, for throughout there are steeply dipping, highly metamorphosed rocks which, although varying from band to band, are similar in the mass. Reasons given below show that the extreme coastal section was ice free during the last glaciation.

In this section, initial differences in the size of the drainage areas, and differences in erodibility of the lines of weakness that the streams follow have resulted in great differences in valley size. Subsequent modification of the valleys by cirque glaciers and by outlet glaciers from the former icecap has accentuated the differences.

Watts Bay to York Sound

Southeast of Watts Bay the straight southeasterly course of the coast line is interrupted by the President's Seat peninsula, which projects eastward for 4 miles. Beyond this the coast again runs southeastward, interrupted by short fiords, to York Sound[1]. The dominant rock in the peninsula is a charnockitic adamellite[2]. Alpine glaciers have dissected the peninsula, and the character of the rock has enabled cirque backwalls nearly 3000 feet high to develop. Four cirques still contain glaciers, and several empty cirques have floors below sea level (Pl. 1, fig. 3). Only fragments of the old erosion surface are found, such as the summit

[1] Neither York Sound nor Jackman Sound is a sound in the modern sense of the word, but a bay. They were named in the sixteenth century by Sir Martin Frobisher.

[2] Identified by W. B. Dallwitz, Bureau of Mineral Resources, Canberra, Australia.

PLATE 3.—YORK VALLEY AND A GORGE AT ITS HEAD

FIGURE 1.—YORK VALLEY FROM ABOUT 20,000 FEET; VIEW EAST

Lower right, mouth of one of the gorges, and delta built by tributary almost across the York River; upper left, York Sound; upper right, Jackman Sound, one outlet glacier of the Terra Nivea visible; maturely dissected coastal mountains. (R.C.A.F. photo)

FIGURE 2.—SURFACE OF YORK VALLEY, 4 MILES FROM THE COAST; VIEW EAST FROM NEAR LEFT-HAND BEND IN RIVER (CF. PL. 3, FIG. 1.)

FIG. 3.—SOUTHERN GORGE ENTERING YORK VALLEY; VIEW SOUTHWEST; HUDSON STRAIT IN BACKGROUND

Lake at head of gorge drains into Hudson Strait; stream in gorge, now ponded by screes, flows toward camera. (R.C.A.F. photo)

PLATE 4.—HIGH-LEVEL STRAND LINES AND A FIORD-HEAD GORGE

FIGURE 1.—STRAND LINE AT 1140 FEET NEAR CAPE RAMMELSBERG; VIEW EAST; SHINGLE SURFACE IN FOREGROUND, BOULDERS INCREASING TO FORESLOPE 80 YARDS AWAY WHICH IS ENTIRELY OF BOULDERS

FIGURE 2.—STRAND LINE AT 1425 FEET NEAR CAPE RAMMELSBERG; VIEW NORTHEAST; FROBISHER BAY IN BACKGROUND

FIGURE 3.—HEAD OF DELANO BAY. GORGE CUT THROUGH RAISED STRAND LINES AND BEDROCK

platform of the President's Seat. Fragments preserved near by at considerably lower altitudes show that the surface, though smooth, was not flat (Pl 1, fig. 2).

In contrast to the coast northwest of Watts Bay, very little of the old erosion surface is preserved between the fiords (Pl. 1, fig. 1). The valleys leading to the fiords contain outlet glaciers of the Grinnell Icecap, some of which reach sea level; otherwise this section is very similar to the coast of northern Labrador, as described by Odell (1933, p. 208) and Tanner (1944, p. 66).

Southeast of York Sound

At York Sound the escarpment, hitherto continuous from the head of Frobisher Bay, is interrupted by the flat alluvial plain of the York Valley and its associated gorges (Pl. 3, fig. 1). Southeastward, the coastal escarpment is broken into isolated groups of mountains. As in the section of the coast northwest of Watts Bay, cirque erosion is confined to the coastal mountains, where it has advanced to maturity. There are no inlets corresponding to the fiords to the northwest. Jackman Sound is a T-shaped bay; the stem of the T passes between two groups of mountains and is at right angles to the coast. Overlooking the bay is the Terra Nivea Icecap, whose outlet glaciers flow in shallow valleys; this subdued landscape is in marked contrast to the spectacularly sculptured country through which the Grinnell outlet glaciers flow to the sea.

Drainage of Kingaite Peninsula

As in northern Labrador (Tanner, 1944, p. 160), the drainage of Kingaite Peninsula is mainly structurally controlled, and the streams flow along lineations. Where lineations intersect, a stream may abandon one for another, or it may follow the same one for a long way. This is well illustrated by the streams that have cut the two gorges opening into the York Valley. One of these has a very straight course (Pl. 3, fig. 3); the other takes several right-angled bends.

The streams flowing northeastward into Frobisher Bay are short, except for the two engorged rivers. The watershed separating the Hudson Strait and Frobisher Bay drainage areas is not far inland from the height of land, but it is difficult to know where it is because of the profusion of lakes on the plateau. The two gorges begin in comparatively low country to the southwest and cut through the highest part of the plateau (Fig. 3; Pl. 3, fig. 3). The northern gorge begins at a pronounced nick point, and half a mile upstream there is a corrom watershed: a tributary has built a fan, and the rivulets on one half flow into Frobisher Bay, on the other half into Hudson Strait (Fig. 3A).

The present streams could not have excavated these gorges. The impotence of the streams is shown by the screes ponding them in the gorges, and by the delta built by a tributary almost across the channel of the combined river (Fig. 3B; Pl. 3, fig. 1). Gorges up to 50 feet deep with actively eroding streams are found at the heads of most of the bays and ice-free fiords (Pl. 4, fig. 3), but those entering the York Valley are 1000 feet deep in places and probably result from headward erosion along lines of weakness. Tanner (1944, p. 133) expressed a similar opinion about the Fraser River gorge in Labrador. The absence of comparable gorges elsewhere in the peninsula indicates that the York Valley gorges contained exceptionally powerful rivers at the time of their formation.

Raised Strand Lines

Previous Observations in Neighboring Regions

In Frobisher Bay, Wengerd (1951, p. 635) described a series of strand lines up to 912 feet that he had seen from sea level near Cape Rammelsberg. He claimed that, when standing at 1000 feet at another point, he had seen strand lines some distance away and several hundred feet higher.

In northern Baffin Island, Freuchen and Mathiassen (1925, p. 554) claimed to have found "well-defined shore terraces" up to 660 feet at Pond Inlet, and at 1320 feet west of Milne Inlet. The highest undoubted marine beach found by Nichols (1936, p. 6) in the Eastern Arctic was at 550 feet near Wolstenholme. Above it were forms that might have been either true beaches or solifluction terraces.

According to Coleman (1921, p. 27) and

Daly (1902, p. 258), the marine limit in northern Labrador is between 220 and 265 feet. Bell (1890, p. 308), however, claimed, "At Nachvak . . . raised beaches show with great distinctness 1500 feet above the sea."

marily upon their composition, and only secondarily upon their age. Solifluction has had little effect upon boulder terraces and terraces with foreslopes of boulders, and these remain well preserved. Gravel strand lines

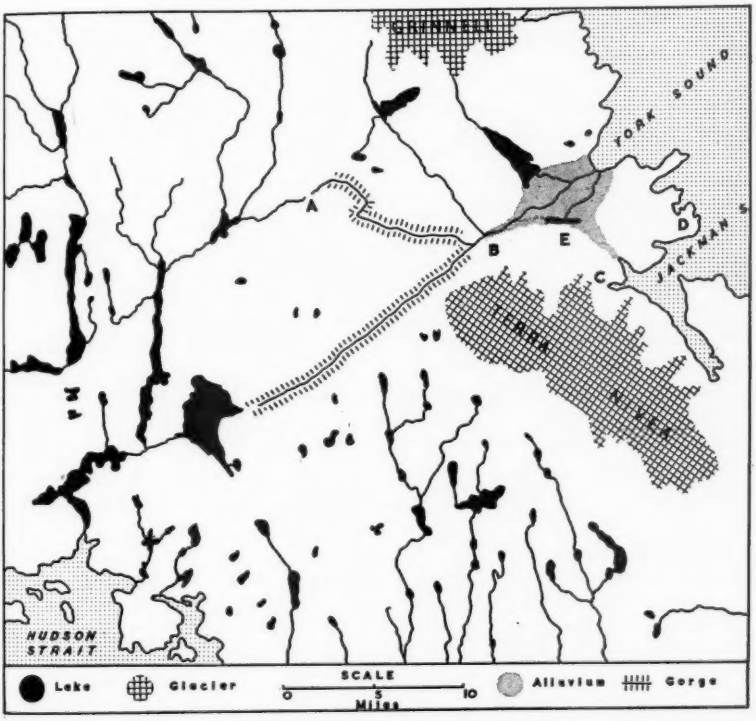

FIGURE 3.—YORK VALLEY AREA

Since it is sometimes difficult to distinguish raised beaches from solifluction terraces, lateral moraines, and kame terraces, it is hard to evaluate these observations without further investigation. Wengerd's claim was found to be essentially correct, which lends credibility to the other observations.

General Statement on Kingaite Peninsula Strand Lines

Elevated strand lines were found along the entire coast between Jackman Sound and the head of Frobisher Bay, from 10 to 1425 feet above sea level (Table 1). The state of preservation of these strand lines has depended pri-

have suffered more, and recognizable strand lines of clay are found only at the lowest altitudes. A few shells were found in the strand lines at 140 and 65 feet only. This is not surprising, however, since shells are rare in the modern beach. Shells on the surface are soon destroyed and those below the surface in permeable deposits are subjected to solution by percolating water, whose solvent powers are greatest at low temperatures. Thus only in beach material largely of clay can shells reasonably be expected.

The strand lines are described from southeast to northwest as they were seen in the field. The coast was not visited southeast of Jackman Sound.

Jackman Sound to York Sound

Around Jackman Sound, strand lines at 65 and 140 feet are widespread. In the northwestern arm of the bay, there is a series at 90, 120, 140, and 175 feet, and an outlet glacier of the Terra Nivea Icecap is retiring from a recent advance into the 90-foot terrace (Fig. 3C). Above 140 feet, patches of gravel similar to that composing the lower terraces and the present beach occur up to 1200 feet. From sea level to about 1200 feet, pebbles of whitish fossiliferous limestone of unknown origin distinguish the surface deposits from those above, which consist of frost-shattered bedrock. In places, such as the southeastern end of the bay, there is a continuous covering of this material with no terraces. Elsewhere, there are some well-marked terraces. Although many look like marine terraces, none are very extensive, and they may be the result of solifluction. On the north side of the entrance to Jackman Sound there is a flat area of limestone-bearing gravel in a col above the backwall of a cirque at an altitude of 1030 feet (Fig. 3D).

The cliffs at the head of York Sound are of alluvium. Behind them stretches a plain, 5 miles long and up to 3 miles wide, bounded by steep, rocky hillsides (Pl. 3, fig. 1). Through this plain flows the entrenched York River. On the north side of the river mouth the alluvial cliffs are 65 feet high, but the flat area above them is small. On the south side the cliffs are 120 feet high, and the surface of the plain rises gradually to 210 feet 5 miles inland. The whole feature appears to be an elevated bay-head delta. The cliffs show marked deltaic bedding and are composed of fine gravel and sand with a few bands of shells. Across the mouth of the river is a bar, and a short distance behind the cliffs is a fossil bar 140 feet above sea level.

The composition of the plain is revealed to a depth of about 100 feet by the entrenched river. The material coarsens progressively until, 2 miles inland at a height of 180 feet, it is of rounded boulders 6–12 inches in diameter (Pl. 3, fig. 2); farther inland the composition remains the same. At the head of the plain where the surface is at 210 feet, terraces on the hillside at 270 and 360 feet are also of rounded boulders. A short distance above this point two streams of approximately equal size combine to form the York River. Just above the confluence the streams emerge from the gorges previously described; these are evidently the source of the material in the alluvial plain (Pl. 3, fig. 1).

Above the York Plain at its widest point

TABLE 1.—RAISED STRAND LINES ON THE WEST COAST OF FROBISHER BAY
Height in feet. Parentheses denote a doubtful strand line

Jackman Sound					120												
		65	90		140	175									(1030)	(1120)	
York Sound		65			140					460		640	(725)	(830)			
President's Seat Peninsula		65			140	180		330									
Watts Bay	15 to	65			130			330	370	450							
Delano Bay					120												
		65	to		130	180	220	330		450	530						
Minturn Bay	30	65	85		130					450	540						
Griffin Bay											540						
Ney Harbour		65			140												
2 miles north of Ney Harbour															(920)		
Leach Bay		65	(several intermediate)							450							
Egglestone Bay							210, 270, 290	320									
Cape Rammelsberg		65			140		210 235		390	(460)		(675)	740 to 840			1140	1425

are limestone-bearing gravels at 640, 725, and 830 feet; the deposit at 640 feet is especially well developed (Fig. 3E).

York Sound to Watts Bay

Between York Sound and Watts Bay there are many cirques, some with submerged floors, and steep-walled fiords with glaciers of the Grinnell Icecap at their heads. In most of the cirques there are strand lines at 65 and 140 feet. Most of the higher slopes are too steep for the preservation of high strand lines, but one is found at about 180 feet in three cirques and at 330 feet in one. The steep-walled fiords, their heads occupied by glaciers, have only fragments of the 65-foot strand line.

Watts Bay to Cape Lawrence

The heads of the fiords between Watts Bay and Cape Lawrence are not occupied by glaciers, and many strand lines are preserved in the valleys leading to them. At the head of Watts Bay is a terrace at 130 feet. Above this, scree has covered any strand lines that may have existed. In a cirque on the south side of the fiord, however, there are strand lines at 330, 370, and 450 feet. On a small peninsula at the entrance to the fiord there is an uninterrupted series of strand lines, at intervals of about 1 foot, from 15 to 65 feet.

On a large island at the entrance to Delano Bay there is a similar series of strand lines from 65 to 130 feet. At the head of the fiord there is a striking series of terraces at 120, 180, 220, 330, 450, and 530 feet. The two lowest terraces are of shingle, the rest of boulders (Pl. 4, fig. 3).

At the head of Minturn Bay are six strand lines at 30, 65, 85, 130, 450, and 540 feet. The lower four are of shingle, and the others of boulders.

In Griffin Bay there is a shingle strand line at 540 feet, unusually well preserved for one of this composition at this altitude.

In Ney Harbour only two strand lines at 65 and 140 feet were found, but in a valley 2 miles north was an expanse of shingle at 920 feet.

Cape Lawrence to Egglestone Bay

Between Cape Lawrence and Egglestone Bay there is a series of strand lines from 65 to 450 feet in Leach Bay. In Egglestone Bay there is a massive deposit of sand and shingle 320 feet high, terraced at 210, 270, and 290 feet.

Egglestone Bay to the Head of Frobisher Bay

There was not time to investigate the entire coast between Egglestone Bay and the head of Frobisher Bay. It was decided, therefore, to concentrate on the Cape Rammelsberg area, to examine closely the strand lines that Wengerd had reported.

Cape Rammelsberg is a low-lying peninsula. Much of it is covered with the clay forming the 65-foot strand line, which is being rapidly destroyed by mass movement. Along the coast to the northwest are terraces of sand and gravel at 140, 210, and 235 feet. In the first stream valley northwest of the Cape there is a terrace at 390 feet with a foreslope of boulders. Above this there is gravel on the valley sides with a number of terraces. Those found on one side of the valley only may have been caused by solifluction, but those at 460, 675, and 840 feet, found on both sides of the valley, are probably strand lines. On the south side there is an ill-defined gravel terrace at 1140 feet. Below this the hillside is covered with similar material in which solifluction is very active.

The head of the valley is a col slightly above the 840-foot terrace. On the other side of the col there is another valley running at right angles, parallel to the coast. The inland side of this valley rises to about 2000 feet and has several horizontal terraces upon it; the most extensive lies at 1140 feet and there is a very well-preserved series between 740 and 840 feet. The foreslope of the 1140-foot terrace and the surface just behind it are composed of sub-rounded boulders mostly 6 to 18 inches in diameter but with a considerable number of much larger ones up to 4 feet in diameter. The terrace ranges in width from a few yards to about 300 yards where there is an embayment in the hillside. Where it is narrow the terrace is composed entirely of boulders; where it is widest the surface is of boulders alone at the top of the foreslope and grades through scattered boulders to fine shingle 100 yards back (Pl. 4, fig. 1). There is a less well-preserved terrace at 1425 feet, the highest that was found (Pl. 4, fig. 2).

Since the terraces are evidently shore line deposits but no shells were found, it may be suggested that they are not of marine origin but were lake-formed. They face Frobisher Bay, however, and thus could not have been formed by a lake confined to the valley they are in (Pl. 4, fig. 2). The land on the opposite side of the Bay is below 1400 feet for a considerable distance inland, and the height of land between Frobisher Bay and Amadjuak Lake to the northwest is also lower, so that it is difficult to account for an ice-dammed lake with waters at this altitude. Furthermore, the lower members of this series are almost certainly of marine origin.

Kingaite Peninsula during the Pleistocene Epoch

Introduction

Most of the larger landforms of Kingaite Pensinula were probably forming throughout the Pleistocene; successive generations of glaciers enlarged the cirques and lengthened and deepened the fiords. (*Cf.* Flint, 1947, p. 96.) When the fiords were small the drainage facilities they afforded the plateau ice may have been inadequate, so that the entire escarpment was covered by ice. There is evidence, however, that the higher parts of the escarpment were not glaciated during the Wisconsin age, at least by moving ice, probably because of improved drainage into the fiords. A similar view was expressed by Bretz (1935, p. 225) about the coast of East Greenland.

Onset of Glaciation

There is no evidence that the climatological causes and accompaniments of glaciation changed during the Pleistocene. At the beginning of glacial ages, according to Flint (1952, p. 142):

"Glaciers descending the western slopes of the mountains of Ellesmere and Baffin Islands and of Labrador and Quebec formed a piedmont apron of ice that chilled the air above it and thus drew snowfall from the comparatively moist air masses that approached it from the south and southwest. The added snowfall increased the thickness of the ice, which thereby gradually became a topographic barrier to the southerly and southwesterly winds. . . . The high cold front of the combined glacier crept slowly westward and southward, fed by moisture brought to it by the winds it intercepted. At the same time the ice thickened until it buried or nearly buried the highlands along the northeast coast on which the earliest glaciers had formed".

According to Flint's description, the mountains of Labrador and Baffin Island are mountain ranges, that is, high ground of relatively small summit area with moderate to steep slopes on both flanks. In mountains of this kind, cirque glaciers could lengthen into valley glaciers and debouch onto plains to form piedmont glaciers. The mountains of Baffin Island and northern Labrador, however, are eastward-facing escarpments terminating tilted peneplanes. The western slopes are gentle, and the valleys very shallow, in contrast to the eastern slopes. Ice must have flowed westward on a broad front; presumably a plateau icecap expanded, and its margin moved progressively westward. Gradients and relief were insufficient to allow the ice to advance as individual tongues.

A valley glacier represents the excess accumulation of a large area concentrated into a narrow and relatively fast-moving stream. It can thus extend far below the equilibrium line,[3] and when it reaches the lowlands it may form a piedmont apron of ice. The margin of a plateau icecap can never be far below the equilibrium line, or the ratio of the ablation area to the accumulation area will be too high. The Grinnell Icecap, for example, has steep and narrow tongues descending to sea level on the Bay side, but on the plateau its edge is close to the equilibrium line. The lesser activity on the landward side is partly caused by greater exposure to the sun, but mainly by the topography.

For these reasons the land being covered by the advancing ice to the west of the high land in Baffin Island and Labrador probably was not very far below the equilibrium line.

[3] The equilibrium line on a glacier or icecap separates the area of net ablation below from the area of net accumulation above. On 'temperate' glaciers this coincides with the firn line. On many glaciers in the arctic, however, refrozen meltwater is important in the economy, and a wide band of this superimposed ice may separate the equilibrium line from the firn line. On the Barnes Icecap in northern Baffin Island there is no firn, and nourishment is entirely by superimposed ice (Baird, 1952, p. 9); on the Grinnell Icecap the equilibrium line is at about 1800 feet and the firn line at 2200 feet.

Wisconsin Maximum

As the ice sheet moved westward and southwestward from the Quebec-Labrador Peninsula, it intercepted precipitation that would otherwise have fallen on Baffin Island. Cyclones continued to cross it at first, dropping an increasing proportion of their precipitation upon the western and southwestern sides as it grew thicker. Eventually the ice became thick enough to act as a topographic barrier, tending to deflect the cyclones along the southern margins. Some cyclones may have passed over the icecap as high-level perturbations, as they do over Greenland today (Dorsey, 1945, p. 140), but they did not bring much precipitation to Baffin Island. The northern parts of the ice sheet may thus have become reduced. This opinion was expressed by Flint (1943, p. 353) who also gives the following description of the character of the Pleistocene ice sheets (1947, p. 52):

"The vast former ice sheets of North America, Europe and Western Siberia were climatically more like the Greenland Icesheet than like its larger Antarctic counterpart. None of them were in regions of extreme cold; all of them lay in the paths of traveling cyclonic air masses; they tended to receive abundant precipitation and to be affected, at times at least, by strong ablation. If analogies with present conditions are to be pressed, we must look to Greenland rather than to Antarctica for them."

Flint is apparently referring to the southern part of the Greenland Ice Sheet. Ablation on the high and on the more northerly parts of the Laurentide Ice Sheet must have been small, and these parts of the ice sheet were probably of polar and not of temperate type. (*Cf.* Ahlmann, 1953, p. 5.) This also applies to the higher and to the more northerly parts of the Greenland Ice Sheet; in the north of Greenland, however, there is a considerable area of ice-free land which allows summer temperatures to rise well above freezing point. In the south of Baffin Island during the height of a glacial age, conditions must have been much more severe, since only a few nunataks projected above the ice. The region was separated from warm air sources by thousands of miles of ice and snow, and even southeastward the sea may have been covered with floating shelf ice for a considerable distance (Flint, 1947, p. 235). Today, such conditions prevail only in coastal Antarctica, and comparisons should be made with this region to understand conditions in Baffin Island at the glacial maxima.

The small amount of erosion being accomplished by Antarctic glaciers today, noted by Taylor (1914, p. 369), Priestley (1923, p. 46), and Gould (1940, p. 847), is shown by the scarcity of moraines, the clearness of the glacier streams, and the minor modification of cirques which have been buried by the ice and subsequently exhumed. Thus erosion by ice on the Kingaite Peninsula at the height of the glacial ages was probably slight. Cirques and fiords probably were not formed in the opening stages or they would have developed along the entire escarpment. Northwest of Egglestone Bay, however, there are none. This section has been covered by an ice sheet and cirques had not developed before this buried the escarpment. Cirques were formed down the coast because the escarpment was ice-free much longer. Between Egglestone Bay and Cape Lawrence the cirques have subdued outlines; they were apparently modified by ice after their formation, and not reoccupied. Southeast of Cape Lawrence the cirques have maximum development and are fresh in appearance. They must have been formed mainly after the escarpment to the northwest was buried in ice. They were not occupied in the closing stages of the Wisconsin, since they were then below sea level; strand lines up to 450 feet occur in them. If erosion was slight because of intense cold at the time of maximum extension of the ice sheets, the cirques must have been formed between the time the escarpment to the northwest was buried and the onset of conditions of antarctic severity. The size of the cirques indicates that this period was long. The absence of even highly modified cirques northwest of Egglestone Bay points to a similar sequence of events in each glacial age.

Many of the largest cirques have floors below sea level. When they were formed sea level must have been lower than it is today, since a cirque glacier probably could not excavate below sea level in the presence of sea water. A valley glacier can end in the sea only if there is sufficient movement of ice from behind to replace the wastage at the terminus.

Cirques with floors below sea level are also known in northern Labrador, the Lofoten Islands, and in Antarctica. Taylor (1914, p. 554), writing of such a cirque in East Antarctica, concluded that it was formed at the beginning of the advancing hemicycle of glaciation. On Moskenaesö, in the Lofoten Islands, there are many partly submerged cirques. According to Vogt (1913, quoted by Linton, 1949, p. 26) and Ahlmann (1919, p. 236), the islands were not covered by the continental ice sheet during the last ice age. Ahlmann does not suggest when these cirques were excavated, but he says that cirque erosion on the island as a whole proceeded throughout the last glacial period. This is also the opinion of Undås (1939, quoted by Linton, 1949, p. 28). The islands were not isostatically depressed during the last ice age (Gutenberg, 1941, p. 738) and were affected only by the eustatic fall in sea level. Cirque erosion could thus proceed to about 300 feet below present sea level.

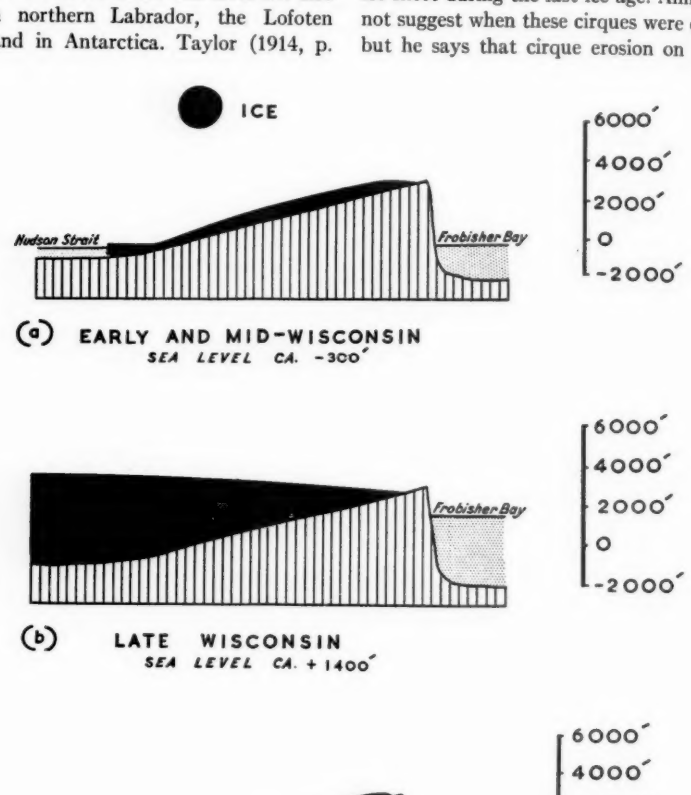

FIGURE 4.—CHANGES IN SEA LEVEL AND HYPOTHETICAL CHANGES IN ICE COVER IN THE KINGAITE PENINSULA VICINITY

Sections from Hudson Strait northeast to Frobisher Bay: (a) Early to mid-Wisconsin (b) Late Wisconsin (c) Present. All heights relative to present sea level

At the height of general glaciation the eustatic fall of sea level was between 230 and 330 feet (Flint, 1947, p. 427). The evidence of the partially submerged cirques shows that the eustatic fall of sea level affected south Baffin Island long before the region was isostatically depressed. This supports the supposition that ice on the Kingaite Peninsula was thin because of starvation while the main Laurentide Ice Sheet existed (Fig. 4a). The land may have stood higher, however, before the Wisconsin. Cooke (1930, p. 86) estimated that at the beginning of the Pleistocene the southwest coast of the peninsula stood 400 feet higher than today. Whether it fully recovered in each interglacial is not known, but the only cliffing apparent today is associated with the sea at its present level, suggesting that emergence of the land is virtually complete.

The sharp topography of the coast southeast of Cape Lawrence suggests freedom from ice-sheet action. Conflicting views have been held on this subject. Taylor (1914, p. 554) and Wright and Priestley (1922, p. 149) noted the small amount of modification in cirques buried and subsequently exhumed by the Antarctic Ice Sheet. T. C. Chamberlin (1895, p. 219), with first-hand knowledge of about 1000 miles of the west coast of Greenland, noted that stretches of angular, unsubdued topography alternated with stretches of rounded, flowing contours. He concluded that the ice did not reach the coast along its entire length. Tarr (1897, p. 254) found transported blocks and patches of boulder clay on the highest summits in the Upper Nugssuak Peninsula of West Greenland. Nevertheless, he said (1897, p. 258), "The ruggedness of the hills was such that from the topography alone no one would infer glaciation." He concluded (p. 267), "It is evident that rugged, angular topography does not necessarily indicate freedom from ice invasion." On the same peninsula, however, Demorest (1937, p. 55) reported:

> "... some unoccupied cirques ... show evidence of having been eroded by the continental glacier. Their sides have been smoothed and polished by the overriding ice and grooves and striae are cut high in the walls where recent cirques should show only the effects of plucking and frost-action."

Thus an overriding ice sheet may produce little alteration in the large-scale appearance of a jagged landscape, but close examination will reveal evidence of its passage. At the least, loose shattered rock will be removed, and an ice sheet flowing over a steep escarpment would do more. By these criteria the Frobisher Bay coast of the Kingaite Peninsula southeast of Cape Lawrence has not been covered by an ice sheet since the cirques and fiords were occupied by ice.

Differing views regarding the ice coverage have been held about the Torngat Mountains in northern Labrador, 250 miles to the south. Bell (1895, p. 335) considered that throughout the glacial period the coastal range was above the ice and the average elevation of the valley glaciers was about 2000 feet. Low (1896, p. 310L), Daly (1902, p. 205), and Coleman (1920, p. 319; 1941, p. 117) held the same view. Coleman (1941, p. 117) said, "... I was much impressed by the wilderness of loose residual blocks covering the tableland, all composed of the immediately underlying bedrock and evidently undisturbed for many thousands of years."

Odell, however, believed that at some stage the Torngats were submerged beneath the ice sheet. Since his view has won wide acceptance (Flint, 1947, p. 237; Tanner, 1944, p. 184), and since the problem is similar to that in the Kingaite Peninsula, it is worth examining carefully. Firstly (1938, p. 204), he discounted the significance of the felsenmeere on the uplands:

> "In the mountains of Spitsbergen and East Greenland high terrain near the sea with ample moisture-laden winds in a region of intense frost action has been observed to produce thick coverings of frost-riven stony soil. This has happened entirely since these terrains have been freed of ice by recent withdrawals of the ice sheets into the interior."

Secondly (1938, p. 205), he asserted that he had positive evidence of high-level ice action:

> "... the writer found actual evidence of ice-polished rocks at about 4700 feet ... that is, nearly 3000 feet higher than the elevation others have thought to be the maximum ice level. However, the somewhat weathered condition of this rock surface at the time showed that it might possibly be due to an ice advance earlier than the ... Wisconsin."

It is hard to judge the significance of this observation in view of the difficulty of recognizing a weathered, ice-polished surface with certainty. Dahl (1947, p. 233) declared that

total ice cover is impossible where high mountains are near a deep ocean, since ice extending beyond the border of the ocean will break and float away. He specifically disagreed with Tanner (1944, p. 184) about the Torngats. If the slope of the ice is 1 in 100 (which he considered the maximum) all mountains with sharp relief higher than 1000 m will protrude as nunataks for a distance of 100 km from the ice edge (Dahl, 1946, p. 232; 1947, p. 234). These figures would be slightly less if a belt of shelf ice existed off the coast, but Dahl's objection appears well founded.

In the Kingaite Peninsula, the comparative morphology of the coast and the hinterland shows that the higher coastal mountains were above the ice for a long time during the Wisconsin. A section of the coast a short distance southeast of Cape Lawrence (Pl. 2, fig. 1) shows the contrast between the plateau surface with evident signs of ice-sheet erosion, and the coastal mountains which have been subjected to very different processes. Precipitous gullied valley sides, flat hilltops thickly covered with stones, and, in places, fretted upland topography with unmodified cirques point to a combination of alpine glaciation and subaerial erosion over a long period. The valley walls have undergone more subaerial erosion in their coastal sections than further inland. The gullies are typical of the weathering of steep bare slopes. The lithology and structure of the valley walls are the same throughout, so that the absence of gullies in the upper parts of the valleys indicates that these were ice-covered. The intermediate zone of incipient gullying indicates two stages in the withdrawal of the ice. Apparently ice flowed from the plateau over the heads of the valleys for a considerable period. Lower down, the glacier tongues occupied the present fiords and valleys bottoms, leaving the walls bare. No lateral moraines were seen in the valleys, but, if the firn line was at sea level, probably none would have been formed (Dahl, 1946, p. 228). Furthermore, the subsequent marine transgression would have removed much loose material from the valley sides.

These conditions would account for the undisturbed stony covering of the erosion-surface remnants above the gullied walls, which would have had no moving ice upon them. They may have had a protective capping of immobile ice, such as is found today in similar positions in the Cumberland Peninsula, 250 miles to the north. Here also, in places recently bared by the shrinkage of an immobile ice capping, the surface has a stony covering (H. R. Thompson, Personal communication). The plateau remnants may have remained largely ice free, however, for in the Antarctic, Wright and Priestley (1922, p. 176) reported that many mountains fringing the continental ice in the Ross Sea sector were fairly free of snow, showing that locally, at least, ablation on a rock surface exceeded precipitation. Under these conditions, the agents of ablation were solar radiation and wind. In Baffin Island, without the present summer conditions of frequent fogs and much frontal cloud, solar radiation must have been more effective during the Wisconsin age than it is today.

There has been wide disagreement about the time necessary for the formation of a felsenmeere. Odell (1938, p. 204) believed the Torngat felsenmeere could have formed rapidly; Coleman (1941, p. 117) considered that it must have taken thousands of years to form; Linton (1949, p. 30) believed that similar features in the Lofoten Islands and northern Norway must be at least interglacial and possibly preglacial. Dahl (1947, p. 235) noted that above 1700 m in central Norway felsenmeere are abundant, whereas below 1700 m only single blocks are weathered out. If the felsenmeere are postglacial, he declared, frost action must be of a very different nature above 1700 m than below it. In the Kingaite Peninsula the very restricted occurrence of felsenmeere indicates that it is of great age. It occurs only on the coastal plateau remnants which stand slightly above the level of the main plateau surface. The remainder of the high plateau has much frost-shattered rock, but nothing approaching a complete debris covering. This shows clearly from the air (Pl. 2, fig. 1). It is reasonable to conclude that the coastal belt has been free from moving ice much longer than the inland plateau and the valleys leading down to the fiords. Since the valleys became ice-free, sufficient time has passed for the sea level to fall at least 530 feet, and for the streams at the heads of many of

them to cut deep gorges. Furthermore, the bay-head delta at the head of York Sound extending from 210 to 120 feet above sea level was formed while only a fraction of this change of level was taking place. Therefore the time since the fiord-head valleys became deglaciated probably must be measured in thousands of years, in which case the coastal strip has been ice-free for at least tens of thousands of years. This shows that the felsenmeeres are not post-glacial in origin, and that the coastal strip southeast of Cape Lawrence was not covered by moving ice during the Wisconsin age. It is difficult to know whether the felsenmeeres are interglacial and were protected during the Wisconsin by stagnant ice or whether they were formed on ice-free terrain during the Wisconsin.

The sea level cirques and the intensely weathered cliffs extending almost down to sea level at the mouths of the fiords indicate that during much of the Wisconsin age the land stood at least as high relative to the sea as it does today. This implies that the ice in the area was not very thick. Precipitation was so slight that a locally generated icecap could not have buried the escarpment. The main Laurentide Ice Sheet was starved in its northern parts, and ice would have flowed sluggishly northward from the Quebec-Labrador Peninsula. It would not have overwhelmed the 3000-foot high Kingaite Peninsula since it could flow eastward along Hudson Strait, which averages 1000 feet in depth (Cooke, 1930, p. 71).

When equilibrium between snowfall and outflow of ice on the Kingaite Peninsula had been reached, a long period of comparative stability probably followed. Whatever occurred at the southern margin of the Laurentide Ice Sheet, precipitation and ablation in southern Baffin Island must have been very small while the main ice sheet existed.

Late Wisconsin Time

The latter part of the Wisconsin age in middle latitudes was a time of rising temperatures and general deglaciation. It is unlikely, however, that deglaciation of southern Baffin Island progressed far until very late Wisconsin time, since the decaying Laurentide Ice Sheet to the south and southwest would have kept the summers cool. When this ice sheet had shrunk to about half its maximum extent, it covered the Hudson Bay region and most of Quebec and Labrador, according to Flint (1947, p. 244). As the Hudson Bay ice decreased, more nourishment came to the Quebec ice on its high platform. Hence the Quebec ice may have increased despite the general shrinkage.

Ice in the Hudson Strait area may have increased also in late Wisconsin time for the same reason; otherwise it is hard to account for the great depression of the land shown by the highest strand lines of Frobisher Bay. The partly submerged cirques show that sea level during much of Wisconsin time was lower than it is today. In late Wisconsin time the land was greatly depressed, and when the sea was more than 1400 feet above its present level deglaciation of the Kingaite Peninsula had already begun. It is not certain that these changes of level were isostatic, but the fact that the sea level has now returned approximately to the level it held during much of Wisconsin time suggests that no independent earth movements were responsible. It is hard to account for so large a depression of the earth's crust if the ice on the peninsula was not thick enough to bury the coastal mountains. If the ice stretched southwestward from near the crest of these mountains, however, it would have been about 4000 feet thick in the center of Hudson Strait if the surface was level and 7000 feet thick if there was an average slope of 1° (Fig. 4b). A. L. Washburn (1947, p. 55) estimates the amount of downwarping at about two-sevenths of the thickness of the ice causing it, so that 5000 feet of ice could cause 1400 feet of downwarping directly beneath it. How much ice would be necessary to cause 1400 feet of downwarping 100 miles away is not known, and the problem is further complicated by the fact that the 1425-foot strand line is on land that was formerly ice-covered, showing that the ice cover of the Kingaite Peninsula had already decreased considerably when the sea level was 1400 feet. The response of the crust probably lags about 2000 years behind the unloading (Flint, 1953, p. 916), so that the 1425-foot strand line may have been caused by the Hudson Strait ice at its maximum (Fig. 4b). Explaining the highest strand lines of Frobisher

Bay by postulating a great increase in the Hudson Strait ice in later Wisconsin time is, however, only a hypothesis based on indirect evidence.

The sea level fell intermittently from its greatest height and strand lines at lower altitudes were formed. When the sea stood at 640 feet, a shingle strand line was formed above the York Valley, showing that gorge cutting had not yet begun. When the sea level had fallen to about 360 feet (the height of the highest boulder terrace at the head of the valley) excavation of the York Valley gorges began. At 270 feet another boulder terrace points to similar conditions of moderate gorge cutting. Below this, starting at 210 feet at the head of the plain and falling to 120 feet at the present shore line 5 miles distant, is the alluvial expanse of the York Valley, formed during a period of rapid gorge cutting.

In the Platen Peninsula of North East Land, Glen (1941, p. 74) found similar though smaller gorges occupied by underfit streams, and concluded that they were excavated during a period of excessive summer ablation preceding the present conditions of approximate balance. In southern Baffin Island there is some evidence that temperatures have been higher and glacier ice more abundant than today (see below), but runoff was not much greater when the sea level was 140 to 210 feet above today's level. This is shown by the engorged steam that has cut through the strand lines at the head of Delano Bay (Pl. 4, fig. 3). Had the runoff been much greater than it is today, the stream would have removed more material than it has. The present drainage basins of the York Valley rivers therefore could not have provided the increased volume of water necessary to excavate the gorges. These gorges and the expanse of alluvium between them and the sea indicate that a much greater river once flowed into York Sound.

The water that once flowed down the gorges into Frobisher Bay now probably flows into Hudson Strait. The southern gorge has a large lake at its head (Fig. 3; Pl. 3, fig. 3). The watershed, however, lies in the gorge a short distance from the lake, whose overflow now runs into Hudson Strait. The gorge could not have been formed when the watershed was in this position; the overflow from the lake must have flowed down it. The present overflow stream is not much incised, so that the lake level was not lowered in this manner. There must have been an ice-dammed lake or lakes at the heads of these gorges at the time of their formation. The dam may have been an icecap of small area, similar to the Barnes Icecap in northern Baffin Island, but this is unlikely. The Barnes Icecap is on comparatively low ground west of the main watershed of the island, and along its eastern edge are many ice-dammed lakes, all spilling eastward (Baird, 1952, p. 3). In the Kingaite Peninsula, however, the head of the southern gorge is so close to Hudson Strait that an icecap of this type would have had to be very small. The ice may have been the northern margin of an ice sheet centered the other side of Hudson Strait in the Quebec-Labrador Peninsula.

The surface of the country between the heads of the gorges and the coast appears from air photographs to have a considerable cover of material, either alluvium or ground moraine, and in places the bedrock is hidden by what looks like hummocky moraine. There are also features which may be structural or may be shore line terraces or moraines; without examination on the ground it is impossible to know.

The excavation of the material now filling the York Valley began when the sea level was at 210 feet. Great quantities of boulders were delivered by the rivers until the sea level had fallen to about 180 feet. The plain below this level has a surface of shingle with scattered boulders, grading to sand near the present shore. This part of the delta was probably formed below sea level. After the sea had fallen to about 180 feet gorge cutting stopped, for no more boulders were deposited. This implies that the ice-dammed lake or lakes at the heads of the gorges no longer existed.

Recent Changes in the Ice Cover

Conditions differ greatly on the coastal and inland sides of the icecaps. The coastal glaciers have retreated slightly from a recent maximum extension that elevated strand lines and the scarcity of old moraines show was the greatest for a long time. One of the Terra Nivea outlet

glaciers is retreating from a recent advance into an elevated strand line at 90 feet, with strand lines up to 175 feet near by. A strand line at 640 feet occurs within 3 miles of the icecap, and deposits, probably marine, are found up to 1200 feet. On the western side of the Grinnell Icecap are found the last stages of a dying glaciation. The margin of the icecap is at about 1800 feet. Inland, the land rises again in a series of low ridges to about 2300 feet, and in the hollows of this terrain are several small masses of glacier ice, one of which is in contact with the icecap (Pl. 2, fig. 3). They have no accumulation areas and are thus dead ice, although they are above the level of the equilibrium line on the icecap. In the Platen Peninsula of North East Land, Glen (1941, p. 74) found similar ice bodies which he concluded were the relics of a much more extensive icecap.

Since the sluggish or motionless ice on the plateau could not have adjusted to changing climatic conditions more rapidly than the steep, relatively fast-moving outlet glaciers, the shrinkage of the plateau ice cannot have been caused by the recent slight amelioration. This shrinkage is evidence of an earlier warmer period, during which a climatically dead icecap wasted away on the plateau while the coastal outlet glaciers were small or nonexistent. At the end of the warm period, only the larger remnants of the icecap on the higher parts of the plateau were able to re-establish themselves, and became the Grinnell and Terra Nivea Icecaps. Smaller bodies of ice continued to waste away, more slowly than before, although they were above the level of the equilibrium line on the icecap. It is therefore probable that if the iceaps did not exist today they would not reform. Judging by the size of the dead ice masses and the relief of the country, the warmer period causing their isolation must have been hundreds rather than thousands of years ago and was therefore not contemporaneous with the Thermal Maximum of lower latitudes.

Summary of the Physiographic History

The Kingaite Peninsula is a tilted peneplane that was elevated, probably in the Pliocene, resulting in an escarpment along Frobisher Bay. In each glacial age, the sequence of events was similar. The northwestern part of the escarpment was buried by an ice sheet before cirques could form; in the southeast cirque erosion advanced to maturity. In the Wisconsin age, the southeastern part of the escarpment remained above the ice, and there is no evidence that in the earlier glacial ages it was otherwise.

In the late Wisconsin, the peninsula was greatly depressed, possibly because of a great increase in ice thickness in the Hudson Strait area. The sea was at one time at least 1425 feet above its present level. It fell intermittently, resulting in the formation of raised strand lines. When it was between 210 and 180 feet an ice-dammed lake drained through the divide from the west. The ice damming this lake may have been centered in the Quebec-Labrador Peninsula.

The sea has remained at its present level longer than it remained at higher levels.

The present icecaps and glaciers are retreating slightly from a recent maximum extension on their seaward sides. Preceding this extension, there was a period of unknown duration when temperatures were higher than today and the climatically dead icecaps extended farther inland.

References Cited

Ahlmann, H. W., 1919, Geomorphological studies in Norway: Geog. Annaler, v. 1, p. 1–149, 193–244

—— 1953, Glacier variations and climatic fluctuations: Am. Geog. Soc. Bowman Mem. Lect., ser. 3, 51 p.

Baird, P. D., 1952, Method of nourishment of the Barnes Icecap: Jour. Glaciology, v. 2, no. 11, p. 2–9

Bell, R., 1890, Glacial phenomena in Canada: Geol. Soc. America Bull., v. 1, p. 287–310

—— 1895, The Labrador Peninsula: Scottish Geog. Mag., v. 11, p. 335–361

—— 1901, Report of an exploration on the northern side of Hudson Strait: Geol. Survey Canada, Ann. Rept., new ser., v. 11, p. 5M–33M

Bretz, J H., 1935, Physiographic studies in East Greenland, *in* Boyd, L. A., The fjord region of East Greenland: Am. Geog. Soc. Special Pub. 18, 357 p.

Chamberlin, T. C., 1895, Recent glacial studies in Greenland: Geol. Soc. America Bull., v. 6, p. 199–220

Coleman, A. P., 1920, Extent and thickness of the Labrador ice-sheet: Geol. Soc. America Bull., v. 31, p. 319–328

—— 1921, Northeastern part of Labrador and New Quebec: Geol. Survey Canada Mem. 124, 68 p.

Coleman, A. P., 1941, The last million years. A history of the Pleistocene in North America: Toronto Univ. Press, 216 p.

Cooke, H. C., 1930, Studies of the physiography of the Canadian Shield, Pt. 11: Glacial depression and postglacial uplift: Royal Soc. Canada Trans., ser. 3, v. 24, sec. 4, p. 51–87.

Dahl, E., 1946, On different types of glaciated areas during the ice ages and their significance to phytogeography: New Phytologist, v. 45, p. 225–242

—— 1947, A reply to an address by V. Tanner: Norsk Geologisk Tidsskrift, v. 26, p. 233–235

Daly, R. A., 1902, The geology of the northeast coast of Labrador: Harvard Coll. Mus. Comp. Zoology Bull., v. 38, p. 205–270

Demorest, M., 1937, Glaciation of the Upper Nugssuak Peninsula, West Greenland: Zeitschr. Gletscherk., v. 25, p. 36–56

Dorsey, H. G., Jr., 1945, Some meteorological aspects of the Greenland Icecap: Jour. Meteorology, v. 2, p. 135–142

Flint, R. F., 1943, Growth of the North American ice sheet during the Wisconsin Age: Geol. Soc. America Bull., v. 54, p. 325–362

—— 1947, Glacial geology and the Pleistocene Epoch: N. Y., John Wiley and Sons, 589 p.

—— 1952, The Ice Age in the North American Arctic: Arctic, v. 5, p. 135–153

—— 1953, Probable Wisconsin substages and Late-Wisconsin events in northeastern United States and southeastern Canada: Geol. Soc. America Bull., v. 64, p. 897–920

Freuchen, P., and Matthiassen, T., 1925, Contributions to the physical geography of the region north of Hudson Bay: Geog. Rev., v. 54, p. 549–562

Glen, A. R., 1941, A sub-arctic glacier cap: the West Ice of North East Land: Geog. Jour., v. 98, p. 65–76

Gould, L. M., 1940, Glaciers of Antarctica: Am. Philos. Soc. Proc., v. 82, p. 835–877

Grainger, E. H., 1954, Station list of the "Calanus" Expeditions, 1951–52, together with Frobisher Bay stations, 1948, 1950 and 1951, and Resolution Island Stations, 1950: Jour. Fisheries Research Board Canada, v. 11, no. 1

Gutenberg, B., 1941, Changes in sea level, postglacial uplift, and mobility of the earth's interior: Geol. Soc. America Bull., v. 52, p. 721–772

Hall, C. F., 1865, Arctic researches and life among the Esquimaux: N. Y., Harper and Bros. 595 p.

Linton, D. L., 1949, Unglaciated areas in Scandinavia and Great Britain: Irish Geography, v. 3, p. 25–33

Low, A. P., 1896, Reports on explorations in the Labrador Peninsula, in 1892–5: Geol. Survey Canada Ann. Rept., new ser., v. 8, pt. 2, p. 1L-387L

Nichols, D. A., 1936, Physiographic studies in the eastern arctic: Canadian Surveyor, v. 5, no. 10, p. 2–7

Odell, N. E., 1933, The mountains of Northern Labrador: Geog. Jour., v. 82, p. 193–211, 315–326

—— 1938, The Great Ice Age and its effects, *in* Forbes, A., Northernmost Labrador mapped from the air: Am. Geog. Soc. Special Pub. 22, p. 204–215

Priestley, R. E., 1923, Physiography (Robertson Bay and Terra Nova Bay regions): *in* British Antarctic (Terra Nova) Expedition, 1910–13: London, Harrison and Sons, 84 p.

Strøm, K. M., 1945, Geomorphology of the Rondane area: Norsk Geologisk Tidsskrift, v. 25, p. 360–379

Tanner, V., 1944, Newfoundland-Labrador: Acta Geographica, v. 8, 906 p.

Tarr, R. S., 1897, Former extension of Cornell Glacier near the southern end of Melville Bay: Geol. Soc. America Bull., v. 8, p. 251–268

Taylor, G., 1914, Physiography and glaciology of east Antarctica: Geog. Jour., v. 44, p. 365–382, 452–467, 553–571

Undås, I., 1939, Kvartaerstudier i Vestfinmark og Vesteralen: Norsk Geologisk Tidsskrift, v. 18, p. 81

Vogt, T., 1913, Landskapsformene i det ytterste Lofoten: Norsk Geografiske Selskab, Aarbok, v. 23, p. 1–50

Washburn, A. L., 1947, Geology of Victoria Island and adjacent regions: Geol. Soc. America Mem. 22, 142 p.

Wengerd, S. A., 1951, Elevated strandlines of Frobisher Bay, Baffin Island: Geog. Rev., v. 41, p. 622–638

Wright, C. S., and Priestley, R. E., 1922, Glaciology, *in* British Antarctic (Terra Nova) Expedition, 1910–13: London, Harrison and Sons, 581 p.

AUSTRALIAN NATIONAL UNIVERSITY, CANBERRA, AUSTRALIA

MANUSCRIPT RECEIVED BY THE SECRETARY OF THE SOCIETY MAY 18, 1955

BULLETIN OF THE GEOLOGICAL SOCIETY OF AMERICA
VOL. 67, PP. 571-596, 20 FIGS. MAY 1956

QUANTITATIVE SLOPE ANALYSIS

BY ARTHUR N. STRAHLER

ABSTRACT

Statistics describing ground surface slope have geomorphic, hydrologic, engineering, and military applications, because slope steepness influences rates of runoff, soil creep, and soil flowage and the ease of cross-country movement of men and vehicles. Slope maps can be drawn to show the areal distribution of (1) degree of slope and (2) magnitude of the downslope component of gravitational acceleration. The first uses lines of equal slope tangent (isotangents) and is therefore a form of first-derivative map. Isotangents are drawn from a large number of slope readings determined from a large-scale contour map or by field measurement with surveying instruments. Planimeter measurement of areas between successive isotangents yields a percentage-frequency distribution from which slope-tangent mean, variance, and standard deviation are computed as population parameters.

The second type of map uses lines of equal sine of slope (isosines) and shows the distribution of the downslope component of gravitational acceleration, which determines the intensity of shear stresses acting upon soil, surface water, and any surface objects. Measurement of areas between successive isosines yields a frequency distribution from which sine mean, variance, and standard deviation are computed as population parameters.

Isotangent and isosine maps were drawn and associated frequency distributions computed for drainage basins in three areas unlike in size and stage of erosional development: (1) a small, youthful basin in weak clays of badlands at Perth Amboy, New Jersey; (2) two mature basins strongly controlled by massive sandstones of the Catskill plateau; (3) two basins with smooth slopes in the vicinity of Emporium, Pennsylvania, where Carboniferous strata are maturely dissected. Frequency distribution of sine of slope is strongly skewed and has a high mean in the Perth Amboy locality because of immaturity of stage of basin development. It is bimodal in the Catskill locality, where structural benching is pronounced, but is smoothly symmetrical with almost normal form in the Emporium locality, which may be representative of typical mature erosional topography developed on a homogeneous rock mass.

Because of time and labor needed to prepare slope maps and measure frequency distributions by planimeter, two methods of rapid point sampling of slope were tested for reliability: (1) location of sampling points by drawing random pairs of rectangular co-ordinates; (2) use of sampling points uniformly spaced on a rectangular grid. A test area of about 1 square mile was selected near the center of the Emporium, Pennsylvania, topographic quadrangle. Population parameters of tangent of slope were computed by planimeter measurements of a detailed isotangent map of the test square. Samples of 100 points each were then taken directly from the topographic map of the test square by both random co-ordinate and grid methods and compared with the slope population. In tests using the statistic χ^2/d.f. and the statistic z the hypotheses that random co-ordinate sample and population variances are equal and that sample and population means are equal were accepted at the 5 per cent level. Confidence limits based on population variance were determined for distribution of means for samples of various sizes. A chi-square test of goodness of fit required acceptance of the hypothesis that random-coordinate sample distribution is similar to the population distribution.

Operator variance was tested by means of a t-test of paired differences in tangent values read by two operators at the same points. A low mean of differences, not significantly different from zero, established that variations introduced by operator judgment are small compared with natural slope differences. It is concluded that the random-coordinate method of point sampling can be applied to determine slope mean, variance, standard deviation, and general form of slope distribution within predictable small limits.

CONTENTS

TEXT

	Page
Introduction	572
Acknowledgments	573
Slope maps	573
Previous mapping methods	573
Slope envelopes and slope segments	574
Use of topographic maps and choice of localities	574
Technique of slope estimation	575
Isotangent and isosine maps	576
Practical uses of slope maps	577
Appearance of slope maps	578
Frequency distribution of slope	578
Planimeter measurement of areas	578
Frequency-distribution histogram and statistical parameters	578
Correction of observed areas for slope of surface	579
Practical applications of slope-frequency distributions	579
Forms of the slope-frequency distribution	579
Perth Amboy locality	579
Catskill locality	582
Emporium, Pennsylvania, locality	586
Comparison of the three localities	588
Simplified point-sampling methods	589
Selection of sampling test area	589
Population parameters in statistical testing	589
Random-co-ordinate sampling method	589
Drawing random numbers	591
Measurement of slope at co-ordinate points	591
Comparison of sample and population distributions	592
Test of sample variance	592
Test of sample mean	592
Confidence limits of sample means	593
Chi-square test of goodness of fit	593
Evaluation of sampling methods	594
Operator variance	594
Conclusion	595
References cited	596

ILLUSTRATIONS

Figure	Page
1. Subdivision of slope profile into short line segments	574
2. Steps in construction of isotangent map and slope frequency-distribution histogram	575
3. Measurement of slope at a point on topographic map	575
4. Theorem of mean value applied to slope measurement	576
5. Relation of downslope shear force to force of gravity	577
6. Relation of true slope areas to projected slope areas	579
7. Contour topographic map of drainage basin in Perth Amboy, N. J., badlands	580
8. Isotangent, or first-derivative, slope map of Perth Amboy drainage basin	581
9. Isosinal, or shear-stress intensity, slope map of Perth Amboy drainage basin	581
10. Histogram and cumulative frequency diagram of tangent of slope, Perth Amboy drainage basin	582
11. Histogram and cumulative frequency diagram of sine of slope, Perth Amboy drainage basin	583
12. Contour topographic map of Si Meade and Turk hollows, Westkill, N. Y., quadrangle	583
13. Isosinal map of Si Meade and Turk hollows	584
14. Histograms and cumulative frequency diagrams of Si Meade and Turk hollows	585
15. Contour topographic map of Lucore and Russell hollows and test sampling square, center of Emporium, Pa., quadrangle	586
16. Histograms and cumulative frequency diagrams of Lucore and Russell hollows	587
17. Cumulative frequency curves of three drainage basins	588
18. Isotangent map of Emporium, Pa., locality	590
19. Methods of point sampling	591
20. Histograms of random-co-ordinate sample, grid sample, and population compared	592

TABLES

Table	Page
1. Comparison of populations parameters of Si Meade and Turk hollows	585
2. Comparison of population parameters of Lucore and Russell hollows	588
3. Test of variance	592
4. Test of mean	593
5. Confidence intervals	593
6. Chi-square test of goodness of fit	594
7. Test of paired differences in slope readings	595

Introduction

In one usage slope means an actual unit of ground surface. All landforms consist of assemblages of such slope elements. In a second sense, intended throughout the present paper, slope is the property of inclination of the ground surface or of a profile line from the horizontal—*i.e.* an angular measure, or dip. Commonly these meanings are combined in expressions such as "steep slopes" or "gentle slopes", where the actual land surface and its orientation in space are referred to simultaneously.

Voluminous as is the literature on evolution of slope forms under the action of geologic processes upon various structures, it is only in recent years that attempts have been made to express slope properties in quantitative terms.

Inevitably, geomorphology must become a modern analytical science in which both the empirical data measured directly from the natural phenomena and the rational principles deduced by reflection and intuition have quantitative, or mathematical expression. Each geometric property of a landscape must be viewed as a function of a combination of controlling variables. To quantify such relationships both the geometrical forms and the controlling forces must be reduced to quantitative terms.

The present paper is concerned with the technique of measurement of only one of many form elements comprising the total landform geometry: the property of slope. The problem is to quantify the slope properties of a complex land surface taken in its entirety instead of measuring slope at one point on the surface, or along a single profile line. Two means of analysis of surface slope are available. One, the geographical, shows by a suitable map the distribution in plan of the degree of slope. The other is a statistical treatment in which the relative frequencies of occurrence of slopes of given magnitudes, or classes of magnitudes, are determined for an entire tract of ground, or estimated by means of a small rapidly measured sample. Both treatments have distinctive uses, and the second can be derived from the first, but by means of mathematical statistics the frequency-distribution treatment provides the more flexible and widely applicable form of slope analysis for scientific inference and verification of hypotheses.

Acknowledgments

The research for this paper was carried out under support and sponsorship of the Geography Branch of the Office of Naval Research as Project NR 389-042, under Contract N6 ONR 271, Task Order 30, with Columbia University. The writer is indebted to several specialists in the field of mathematical statistics for advice and encouragement: Professors Robert H. Bechhofer and Allan Birnbaum, through the Statistical Consulting Service of the Department of Mathematical Statistics of Columbia University aided in planning and reviewing the statistical analysis. Professor Howard Levene of that same Department generously gave advice on certain theoretical problems. Members of the Earth Sciences Panel of the American Statistical Association who made helpful suggestions concerning sampling methods are Professor William C. Krumbein of Northwestern University, Dr. Felix Chayes of the Geophysical Laboratory, Professor John C. Griffiths of Pennsylvania State University, Dr. Paul E. Potter of the Illinois Geological Survey, and Dr. Churchill Eisenhart of the National Bureau of Standards. Professor William G. Madow of the Department of Mathematics of the University of Illinois called attention to certain pitfalls connected with grid sampling. Although the statistical treatment was greatly facilitated and improved through the advice and criticism of these men they are in no way responsible for such mistakes and misconceptions as may be in the text.

Graduate students of the Geology Department of Columbia University who assisted greatly with the slope measurement and statistical computation are John P. Crawford, George F. Collins, and Marie E. Morisawa.

Slope Maps

Previous Mapping Methods

Maps which depict the steepness of slope over an entire ground surface have previously been prepared on a small scale to show broad classes of slope values. Raisz and Henry (1937) prepared an average-slope map of New England using six classes of average slopes ranging from 50 feet per mile to 500 feet or more per mile. Determinations were based on contour density. Calef and Newcomb (1953) prepared an average-slope map of Illinois using four classes: less than 1%, 1–5%, 5–9%, and over 9%. Average slopes were determined by counting contour crossings along various intersecting lines and calculating average slope by means of the Wentworth equation (1930). These maps have been used chiefly in making qualitative generalizations about the relation of average slope to land usage and to other geographical elements.

Slope Envelopes and Slope Segments

If quantitative slope analysis is to increase understanding of the geometry and formative processes of individual landform types, surface-slope conditions must be mapped on a large scale. Slope measurements must be made on unit lengths of line or unit areas of ground surface which are small fractional parts of the linear or areal dimensions of individual landforms. In this way we can avoid the use of a generalized line or surface applied as an envelope over essential elements of the landscape. Carried to an opposite extreme, the scale of slope mapping could be enlarged to depict microrelief features of the soil surface or of rock outcroppings. Such minutiae, produced by chance variations in soil-forming and weathering processes, would be best excluded where interest centers on the form of an entire hillside or drainage basin.

In the present study the surface envelope is imagined to pass smoothly over microirregularities. To quantify this statement is difficult because no rigorous rules have been set up to govern map and field measurements. In practice, on a slope which extends continuously from drainage divide to the nearest stream channel over a length of 500 to 2000 feet and through a vertical descent of 250 to 750 feet, surface irregularities on the order of 5 feet amplitude and 20 feet wave length have been disregarded (Fig. 1). Valley walls of the above dimensions are characteristic of parts of the Appalachian Plateau in north-central Pennsylvania, where many hillsides are covered with soil pits, 10 to 15 feet across, each rimmed on the downslope side by a soil mound or ridge, giving a microrelief of 2 to 5 feet. By measuring the ground slope along a straight 100-foot line orthogonal to the contour—by hand-level sight in the field or by a short line drawn on the topographic contour map—the soil pits and mounds are disregarded. The 100-foot segment of sight line represents only a fraction ($\frac{1}{5}$ to $\frac{1}{20}$) of the length of the slope profile and therefore reflects characteristic convexities and concavities of valley-side slopes.

In badlands, slopes may be no more than 10, 20, or 30 feet long from a divide to the nearest channel. Here the micro-relief is formed by individual clay nodules or pebbles and by thin beds of more resistant material. A board 20 to 30 inches long laid on the slope forms a satisfactory envelope to mask these irregularities and gives slope segments short enough to reflect the curvature of the entire slope profile.

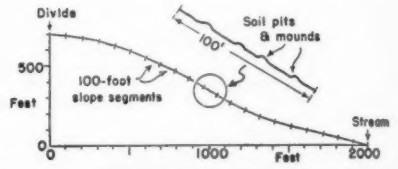

FIGURE 1.—SUBDIVISION OF SLOPE PROFILE INTO SHORT LINE SEGMENTS

Use of Topographic Maps and Choice of Localities

When slope is read from a contour map the problem is further complicated by the degree of generalization introduced by mapping. Where individual landforms are small in relation to the contour interval, countless surface inflections are not mapped, and the map becomes a uselessly generalized envelope. Where map scale is small and landform elements are small, plan of the contours is oversimplified and becomes generalized. The writer has discussed suitability of U. S. Geological Survey and Army Map Service topographic maps for direct slope measurement (Strahler, 1950, p. 679, 690-692). It is concluded that only modern maps on scales of 1:24,000 or 1:25,000 or larger, made by photogrammetric methods, can be safely used for direct measurement of slope, and only where slopes are long and relief is strong, so that a large number of contours is intercepted by a single valley side.

In the three examples of slope mapping used below, the first map is taken from badlands at Perth Amboy, New Jersey, where a special large-scale map was surveyed in the field with plane table and alidade by the writer and Donald R. Coates (Fig. 7). In the second and third areas, (the Catskill Mountains and Appalachian Plateau of north-central Pennsylvania), Army Map Service and U. S. Geological Survey topographic maps on the scale of 1:25,000 and 1:24,000 were used. Both areas have strong relief and long slopes (Figs. 12, 15). Field use of both map series in these

areas showed that minor details of topography are faithfully shown. A statistical test (Strahler, 1950, p. 690–692) between field and map slope samples in a near-by quadrangle in the Catskills had previously shown no significant difference in sample means or variances.

Interest was also centered upon the distribution of slope within a normal drainage basin. The example chosen from the Perth Amboy locality represents a youthful, or inequilibrium, stage of basin development in which great contrast of slope steepness exists between lower and upper parts of the basin (Fig. 7). In the Catskill locality two simple, pear-shaped drainage basins of low stream order were selected (Fig. 12). It was anticipated that the influence of structural benching on slope distribution would be evident. In the Emporium locality of north-central Pennsylvania slopes are exceptionally smooth, and the topography might be taken to represent the mature, or equilibrium, stage of development with little or no structural modification (Fig. 15). Here two adjoining similar drainage basins of third order of magnitude were selected and an additional area included to form a square superimposed over the two basins.

Technique of Slope Estimation

After an area is selected the map is photostatically enlarged two or more times. Enlargement permits the subsequent steps to be carried out with less eye strain and facilitates planimeter measurements; it does not change available information on slope configuration. The map scale is then recomputed to make certain no distortions have been made. On a tracing paper overlay the amount of slope is then determined for a large number of points over the contour map and these quantities inscribed directly on the tracing paper (Fig. 2, step 2). Slope determination is made with the aid of a pair of dividers whose points are set to a fixed opening, equivalent to a specified horizontal ground distance (Fig. 3, distance *ab*). At a particular point, *P*, where slope is to be determined, the divider points are set down on the map to lie on a line orthogonal to the contour passing through the point and with approximately equal distances falling upslope and downslope from the point (Fig. 3). The drop in elevation is then estimated by counting the contour intervals intercepted and adding proportionate parts of incomplete intervals.

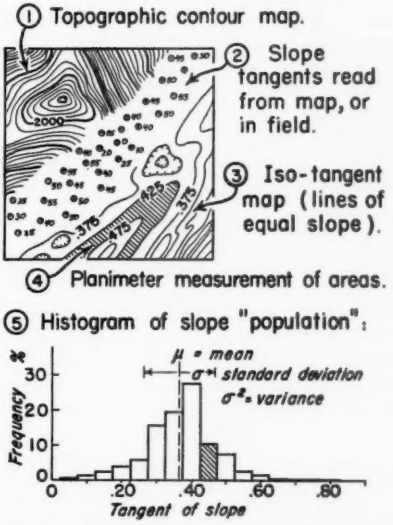

FIGURE 2.—STEPS IN CONSTRUCTION OF ISOTANGENT MAP AND SLOPE FREQUENCY DISTRIBUTION HISTOGRAM

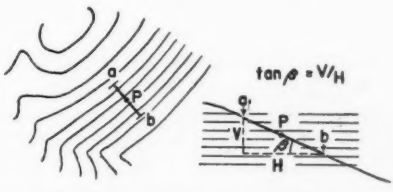

FIGURE 3.—MEASUREMENT OF SLOPE AT A POINT ON TOPOGRAPHIC MAP

Slope of the line is first calculated as the tangent of the angle of slope, angle β, where $\tan \beta = V/H$. If the map is to show the tangent function, these tangent values are inscribed on the map, beside their respective points (Fig. 2, step 2). If the map is to show sine of slope angle, tangent values are converted into sines from trigonometric tables and the sine values inscribed.

The same procedure can be carried out in the field. When a particular point on the ground is selected, a line orthogonal to the contour is formed by two persons holding a tape measure

between them. One person sights to the partner with an Abney hand level, on which slope can be read directly as a tangent (per cent scale). The only assurance one has that the line is a true downslope, or orthogonal, line comes from trying out alternate positions. The sight line of maximum slope is chosen. On steep, smooth slopes pebbles can be rolled down to determine the best line. The field method of slope determination has been used by Strahler (1950, p. 677–679) in sampling maximum valley-side slopes but was not used in the present slope-mapping study.

On the Perth Amboy map the divider points were set to 2 feet, on the Catskill map to 300 feet, on the Emporium, Pennsylvania, map to 100 feet. These distances represent a small part of the total length of a line from divide to adjacent channel and usually include only a few contours. A serious difficulty arises in estimating slope where the surface has low inclination and is convex or concave, as on broadly rounded divides or in valley floors. Wide spacing of contours in such places makes estimation of vertical drop highly uncertain. Such problems are few in the selected areas, which have high relief and steep slopes, but the method might prove inapplicable to areas of low relief or large contour interval. In such cases direct field mapping is required.

Selection of points at which to take slope readings is governed by the same considerations as topographical mapping with plane table and alidade. Use of a grid to obtain equidistant spacing of points is not so efficient as selection of those points where the quality being contoured is changing. Thus the topographer places his rod stations on ridge lines, drainage lines, and wherever the slope changes conspicuously in steepness or azimuth. Similarly, by moving the dividers over the contours one can easily see where contour parallelism exists and where contour spacing changes. Where slope changes, points are concentrated to limit the position of the new slope lines. As in topographic mapping, the number of points determined per unit area depends on the detail desired and is limited by the space on which numbers can be written legibly. On the Perth Amboy slope maps, about 300 points were used in contouring and on the Emporium, Pennsylvania, map about 2500.

Isotangent and Isosine Maps

The next step is the drawing of a new system of contours to depict those lines on which slope angle is constant (Fig. 2, step 3). Two trigonometric functions of the slope angle have been used: *tangent* and *sine*. Where tangent

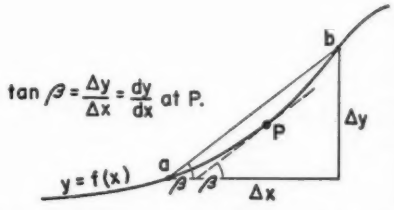

FIGURE 4.—THEOREM OF MEAN VALUE APPLIED TO SLOPE MEASUREMENT

of the angle of slope is contoured there results an *isoclinal* or *isotangent map* (Fig. 2, step 2; Figs. 8, 18). Because the tangent of the slope angle is the ratio of vertical to horizontal distance, it is identical with the first derivative of that function which relates vertical to horizontal distance and defines the slope profile line (Fig. 4). The theorem of mean value of the calculus tells us that if points a and b on the curve of a continuous function $y = f(x)$ relating y and x are connected by a straight line ab, whose slope is $\Delta y/\Delta x$, then there will be at least one point, P, on the curve between a and b whose slope, dy/dx, is identical to the slope of the straight line ab. In determining ground slope with the dividers on the map, or with hand level and tape in the field, we have applied the theorem of mean value. We assume that, if the slope profile has a uniform curvature, the point P lies midway along the line ab. Consequently the isotangent map may also be termed a *first-derivative map*, depicting the value of the first derivative of the slope function over the entire ground surface. We might describe this map as a *rate-of-change* map. Because engineers treat slope in terms of per cent of grade, which is identical with the tangent of the slope angle, the isotangent map can be applied to civil engineering problems.

The sine function may also be used for slope maps. Examples are *isosinal* maps (Figs. 9, 13). The sine of the angle of slope has an important connotation in dynamics of slope-form-

ing processes. Consider a particle of soil or rock on the slope at point P, in Figure 5. The force of gravity, F_g, tending to draw the particle vertically downward, is equal to the mass of the particle, m, times the acceleration of gravity, g, and is represented as a force vector

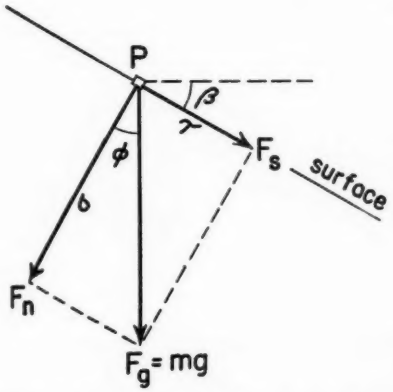

FIGURE 5.—RELATION OF DOWN SLOPE SHEAR FORCE TO FORCE OF GRAVITY

by a vertical arrow of unit length. This force may be resolved into two components normal to one another: a force, F_s, acting downslope parallel with the surface, and another, F_n, normal to the slope. The force F_s tends to move the particle along the slope, *i.e.*, to produce shear between the particle and the surface upon which it rests. This force is also designated as τ in conventional mechanical analysis. The force F_n, which tends to hold the particle to the slope and has a directly proportionate effect upon friction of the particle with the surface, is also designated as σ. There may be forces of cohesion not related to the gravitation field, but we are not concerned with them here. From the geometry of angles, and the trigonometric relations, it is evident that the angle β of the ground surface is equal to the angle ϕ, and that

$$\sin \phi = F_s/F_g$$

or

$$F_s = F_g \sin \phi = F_g \sin \beta.$$

Thus the sine of angle of ground slope represents that part of the total gravitational force which tends to produce downhill sliding or flowage of rock particles or fluids on the surface. Where gravitational force is considered for a unit mass the downslope force is equal to $g \sin \beta$. Our slope map, consisting of lines of equal sine of slope angle, tells the distribution of the part of gravitational acceleration, g, contributing to the downslope force at any given point on the surface. We may, therefore, also designate the isosinal map as a "*g map*".

Practical Uses of Slope Maps

Where viscous fluids or plastic solids flow downslope the isosinal map may supply the relative value of the shearing force to which the rate of shear is directly proportional. In the case of the plastic solids following Bingham's Law (Strahler, 1952a, p. 926)

$$du/dy = \frac{F_s - f}{\eta}$$

where du/dy is rate of shear (rate of change of velocity u, with respect to depth y), F_s is shearing force, f is Bingham's yield stress, and η is consistency of the plastic solid (analogous to viscosity in a fluid), the critical value, f, might be shown by an isosinal line on the map, and values in excess of f by special shading of areas of greater sine of slope. Such a map might indicate the portions of slope on which soil flowage could be expected when consistency of the plastic solid attained a certain value dependent upon soil moisture content.

It is possible to delineate on a slope map any area whose slope lies above or below a critical value, or between two critical values. In military science, the critical value might refer to the maximum slope a vehicle or foot soldier can climb. The critical value would depend on vegetative and soil properties and would fluctuate with soil-moisture changes. Nevertheless, the critical slope value could be applied to the slope map and the extent and shapes of impassable areas marked out.

In soil erosion and sediment-production studies the slope maps could show those areas of steep slope on which accelerated soil erosion takes place and from which the principal sediment yield of the drainage basin is obtained. In planning land management to reduce erosion to a practical minimum the slope map provides the base for designating areas to be used for specific types of cultivation or permanent cover.

Appearance of Slope Maps

Isotangent and isosinal maps differ only slightly in appearance from one another, but seem strange to one accustomed to dealing only with conventional topographical contour maps. Setting aside all preconceived mental images of the actual surface form of a drainage basin and considering only the abstract surface depicted by isotangents and isosines, the most striking feature is a crescentic trough or depression coinciding with the drainage divide. The bottom points of the depression coincide with topographic peaks or saddles of zero slope. Nesting within the arc of the trough is an arcuate zone of steep ground slopes which takes the form of a positive belt or ridge on the slope map. An example is seen in the head of Si Meade Hollow (Fig. 13). From this region to the center of the drainage basin slope contours are widely spaced and often aimless in the azimuths of their broad curves. Shallow, equidimensional depressions of the slope surface are characteristic (Fig. 18), indicating that the central part of the basin is a region of long, smooth slopes. In most small basins the axial drainage channel is difficult to locate. If the stream occupies a narrow channel between smooth valley sides of equal slope, the channel is only a thin line across which the isotangents and isosines pass without deviation, because these forms of contours do not register azimuthal orientation of a surface and therefore take no account of a dihedral angle formed by two planes of equal slope. Where the valley sides are of unequal slope, one or more isotangents or isosines will run along the channel (Fig. 13, near the words "Turk Hollow").

Frequency Distribution of Slope

Planimeter Measurement of Areas

Slope maps also provide information on slope distribution over an entire area. *Frequency distribution* of slope is the proportion of the total surface falling within each class of slope into which the total angular range of slope can be subdivided. To obtain the frequency distribution from an isotangent or isosine map, the polar planimeter is used to measure areas between successive isotangents or isosines (Fig. 2, step 4). Within one drainage basin there may be as many as 10 or 20 discrete areas belonging to the same slope class. Each is measured, and the areas summed to give the total surface area within that class. The planimeter operation is tedious, especially for a complex map such as that of the Emporium, Pennsylvania, area (Fig. 18). To avoid errors of omission or repetition, a tracing sheet is overlaid on the map, and each area colored when it is measured. A color code system and serial number on each area makes possible its recovery and remeasurement. The sum of the small parts should equal the entire area. Agreement to within 1 per cent is acceptable for complex maps with many extremely narrow strips between closely spaced isotangents, but may be within 0.2 per cent for simple maps.

Frequency Distribution Histogram and Statistical Parameters

Areas read with planimeter are in conventional units of measure, such as square inches or square centimeters. These can be reduced to map-scale units, but for comparative statistical operations the planimeter totals should be reduced directly to per cent of total area. Percentage frequency is thus dimensionless and forms a basis for comparisons of distributions among areas of different size. A frequency-distribution histogram can be drawn for visual appraisal of the slope properties of the entire map area (Fig. 2, step 5). Class limits coincide with the values of isotangent or isosinal lines.

The mean, variance, and standard deviation (Dixon and Massey, 1951, p. 20–22) of the distribution can be computed, although there is no body of individual variates, or raw data. For reasons stated in a later section, the symbols for population parameters, μ, σ^2, and σ are assigned to the mean, variance, and standard deviation respectively, rather than the corresponding sample statistics: $\bar{x}$, s^2, and s. In calculating variance and standard deviation the sum of the squared deviations is divided by 100, representing N, the total number of variates, rather than by $N - 1$.

Correction of Observed Areas for Slope of Surface

The frequency distribution of surface slope as calculated from the isotangent and isosine maps by planimeter measurement treats the ground surface as a plane. By projection of an

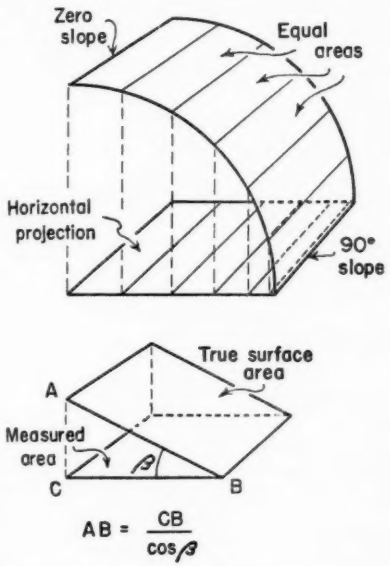

FIGURE 6.—RELATION OF TRUE SLOPE AREAS TO PROJECTED SLOPE AREAS

undulating surface to a plane the true surface areas are altered so that steeply sloping surfaces are reduced in area. Figure 6a shows a 90-degree portion of a cylinder projected upon a horizontal plane. Although the areas on the cylindrical surface are equal, they are reduced in projected area in direct relation to the steepness of slope. Cliff surfaces would be reduced to almost nothing; areas in gentle slope would be greater. Figure 6b shows that for a plane sloping surface the true surface area will be equal to the projected surface area divided by the cosine of the angle of slope, β. For a land surface made up of plane facets an accurate correction of area could be made for slope variations, but in the case of continuously changing slope of an actual landform surface the correction can only be estimated from grouped data of the frequency distribution. If the measured surface area for a given slope class is divided by the cosine of the angle of the class mid-value (or multiplied by the secant of that angle) an approximate correction is made on the assumption that areas are uniformly distributed within the class.

Correction for surface inclination has been made in all frequency distributions in this paper except those of tangents in the Emporium area, which are used directly for statistical test of sampling methods. In Figure 10 the tangent distribution for the Perth Amboy map is shown for the measured areas (dashed line) and for adjusted, or true, areas (solid line). The difference is considerable in this distribution because of the prevalence of steep slopes. Mean, standard deviation, and variance are computed from adjusted frequencies.

Practical Applications of Slope Frequency Distributions

Slope-frequency distributions have the same applications in engineering, military science, soil conservation, and hydrology as do slope maps, except that the use is more general. Given a characteristic frequency distribution obtained rapidly by simplified point-sampling methods described below a slope value critical to the given application can be located on the frequency distribution. The cumulative distribution in Figure 10, for example, shows that about 88% of the total ground surface has a slope of less than 150% (tangent = 1.5), or that 12% of the total surface has slopes steeper than 150%. Such information may be important in decisions concerning the composition of military forces and weapons to be used in a given terrain, or the suitability of land for cultivation.

FORMS OF THE SLOPE-FREQUENCY DISTRIBUTION

Perth Amboy Locality

The three regions selected for slope mapping differ in scale, stage of development, and rock type, permitting observation of the effect of geometrical differences upon frequency distribution.

The small drainage basin in the Perth Amboy badlands (Figs. 7–9) was selected because it is in a youthful, or inequilibrium, stage of development (Strahler, 1952b, p. 1128–1129). The central and lower part of the basin has one place a cliff upheld by resistant clay has slopes between 65° and 72°. Here a single .90 isosine encloses the entire cliff area, whereas the isotangents are closely crowded and exceed 3.0.

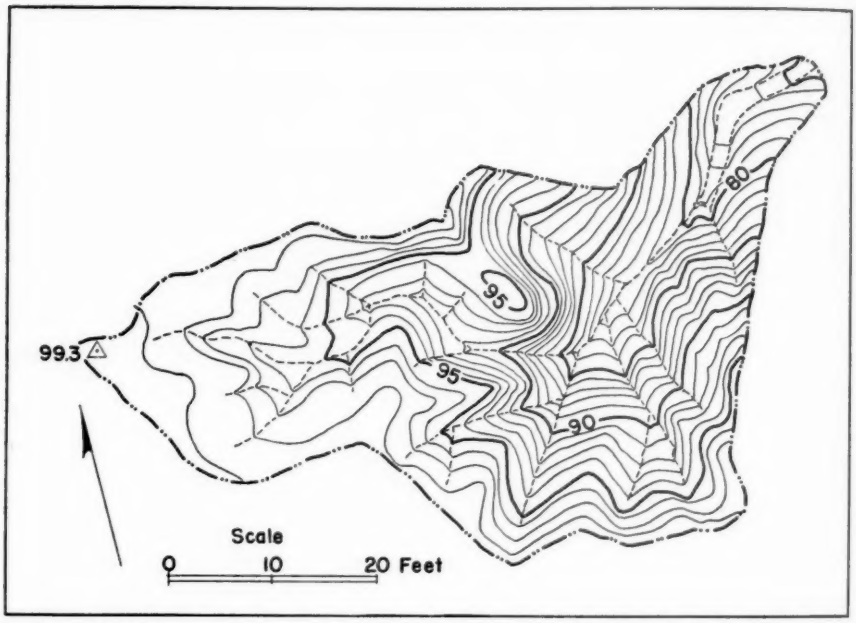

FIGURE 7.—CONTOUR TOPOGRAPHIC MAP OF DRAINAGE BASIN IN PERTH AMBOY, N. J., BADLANDS
Contour interval 1 foot. From a special field survey by A. N. Strahler and D. R. Coates, 1948.

been transformed into steep slopes, as the gully system of which this basin is a part has been deepened and enlarged. The upper, or headward, part of the basin remains undissected and has gentle slopes, only slightly modified from the original flat terrace surface into which the gully is developing. On a large scale this upper surface might represent an initial land surface or a peneplain uplifted and incised by the youthful valleys of a stream system. The isotangent and isosine maps (Figs. 8, 9) show differences in spacing of lines; those on the isosinal map are more uniformly distributed because the tangent function shows a rapid increase in value with angles over 60°, approaching infinity as the angle approaches 90°. The sines by contrast are more nearly uniformly distributed with respect to degrees of arc and range only between 0 and 1.0. In

Because of the composite nature of this drainage basin the frequency distributions should be strongly skewed, perhaps even bimodal, and this is actually the case (Figs. 10, 11). Ordinary and cumulative distributions are shown for tangents and sines. The smoothly curved dashed lines in the cumulative distributions were drawn by inspection through the class midpoints. Ordinarily a smooth curve signifies a population of an infinite number of variates conforming to a theoretical function, but this is not intended here. Measured areas and adjusted (true) areas are shown for both distributions.

The tangent histogram is skewed to the right, compressing the low slope values on the left but expanding the high values on the right. The sine histogram has left skewness and a secondary mode in the low-slope side. This

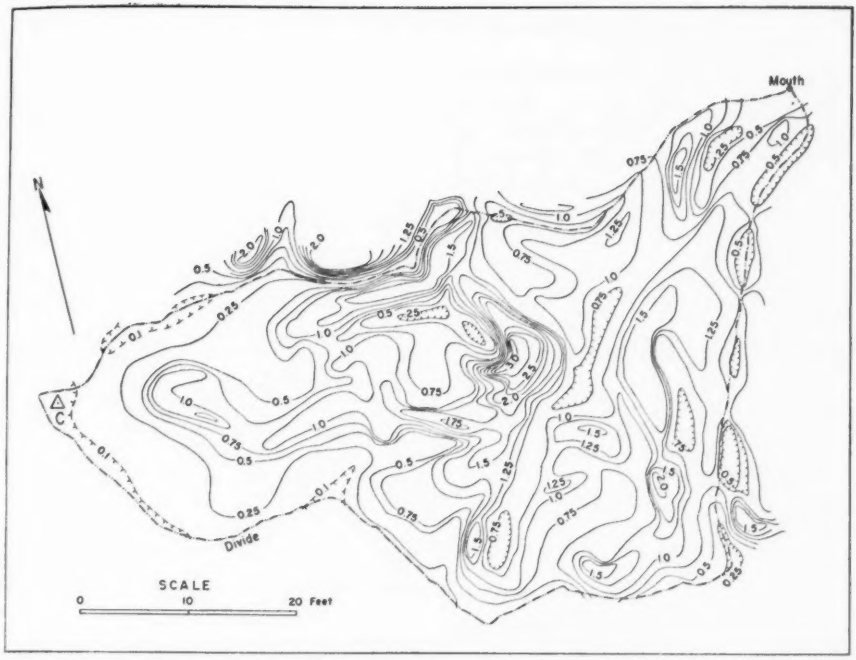

FIGURE 8.—ISOTANGENT, OR FIRST-DERIVATIVE, SLOPE MAP OF PERTH AMBOY DRAINAGE BASIN
In this and other slope maps hachured lines show negative areas, or closed depressions on the slope.

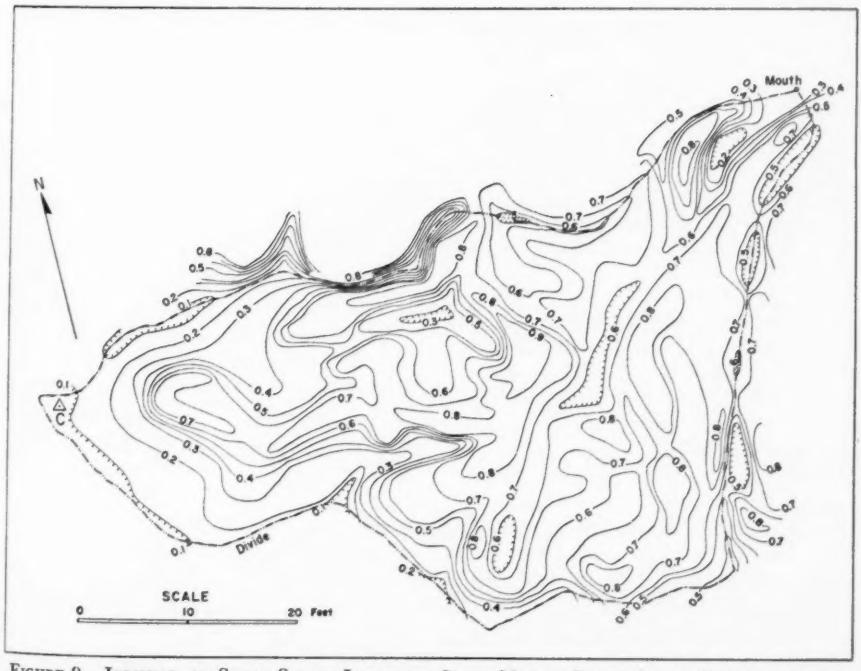

FIGURE 9.—ISOSINAL, OR SHEAR-STRESS INTENSITY, SLOPE MAP OF PERTH AMBOY DRAINAGE BASIN

mode is obscured in the tangent distribution by compression of low-slope classes. The means of the two distributions are not identical when reduced to degrees. The tangent mean of 0.95

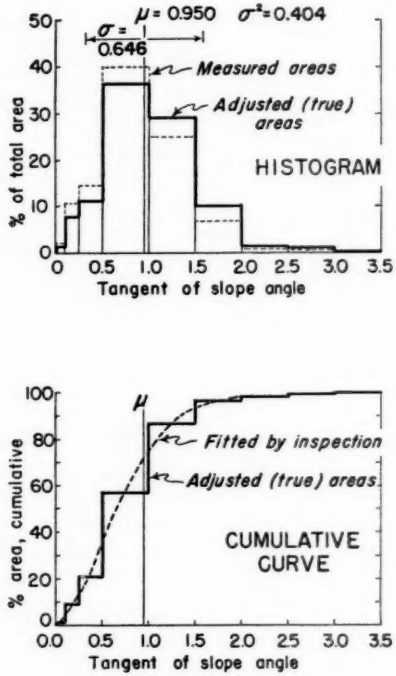

FIGURE 10.—HISTOGRAM AND CUMULATIVE FREQUENCY DIAGRAM OF TANGENT OF SLOPE, PERTH AMBOY DRAINAGE BASIN

Areas measured by planimeter from isotangent map (Fig. 8).

is equivalent to an angle of about 43°; the sine mean of 0.61 is equivalent to an angle of about 38°. This is expected in the computation of means from data organized into classes according to two measurement scales.

Standard deviations also differ when both are reduced to degrees. Standard deviation of tangents is 0.64, equivalent to about 32½°; that of the sines is 0.20, equivalent to about 12°. This is expected because the deviations of tangents are measured with respect to a larger mean and include high tangent values in the upper tail of the distribution.

Catskill Locality

The Catskill locality lies near the northern edge of the West Kill, New York, quadrangle, mapped by the U. S. Army Map Service on a scale of 1:25,000. Figures 12, 13, and 14 show the topographic map, isosinal map, and frequency distributions of two similar drainage basins: Si Meade Hollow and Turk Hollow. Each basin is about 1 mile wide and 2 miles long; total relief is about 1400 feet. Drainage density is extremely low, and streams are widely separated by long slopes. The structure is one of near-horizontal sedimentary strata of Devonian age. Strata near the summits include highly resistant, massive beds of conglomeratic sandstone which produce flattened divides and conspicuous structural benches in the upper basin slopes. Strata underlying the lower elevations are less resistant and include much red weak shale. Consequently the lower parts of the drainage basins are open with gentle slopes.

Only the sine of slope was mapped for this area (Fig. 13). Frequency distributions of sine of slope were derived for Si Meade and Turk hollows (Fig. 14). Similarity of the distributions is striking. Population parameters (interpreting each drainage basin as a population within itself) are surprisingly similar (Table 1).

Because both distributions represent the entire slope population, standard statistical tests of difference in means and variances cannot be applied. Even if these data were regarded as samples instead of populations, such tests would be impossible because, without a finite number of variates, the number of degrees of freedom is not defined. If, in test of variances, we compute the statistic F, the ratio of the two variances, and enter the F-distribution tables for infinite number of degrees of freedom for both numerator and denominator, a critical rejection value of 1.00 is found (Dixon and Massey, 1951, p. 310–312). This means that any difference in variances is significant, a logical conclusion because no two populations can be identical unless they agree perfectly in all parameters.

In any region of horizontal strata the development of structural benching might be

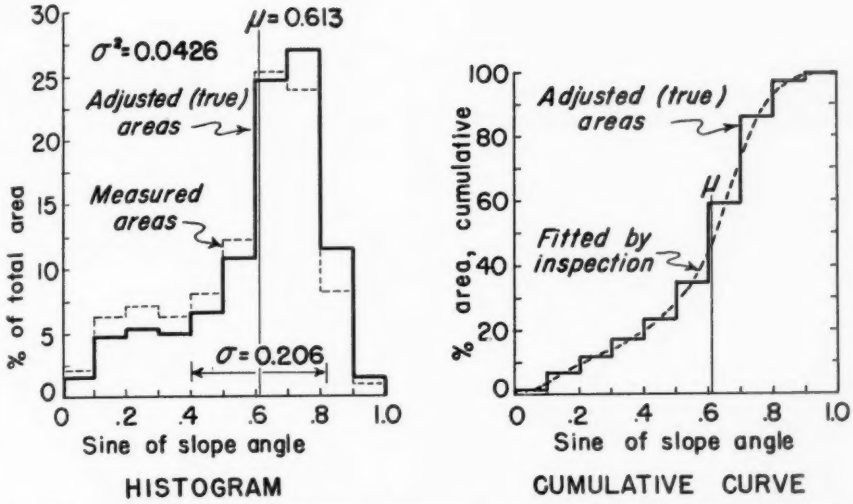

FIGURE 11.—HISTOGRAM AND CUMULATIVE FREQUENCY DIAGRAM OF SINE OF SLOPE, PERTH AMBOY DRAINAGE BASIN

Areas measured by planimeter from isosinal map (Fig. 9).

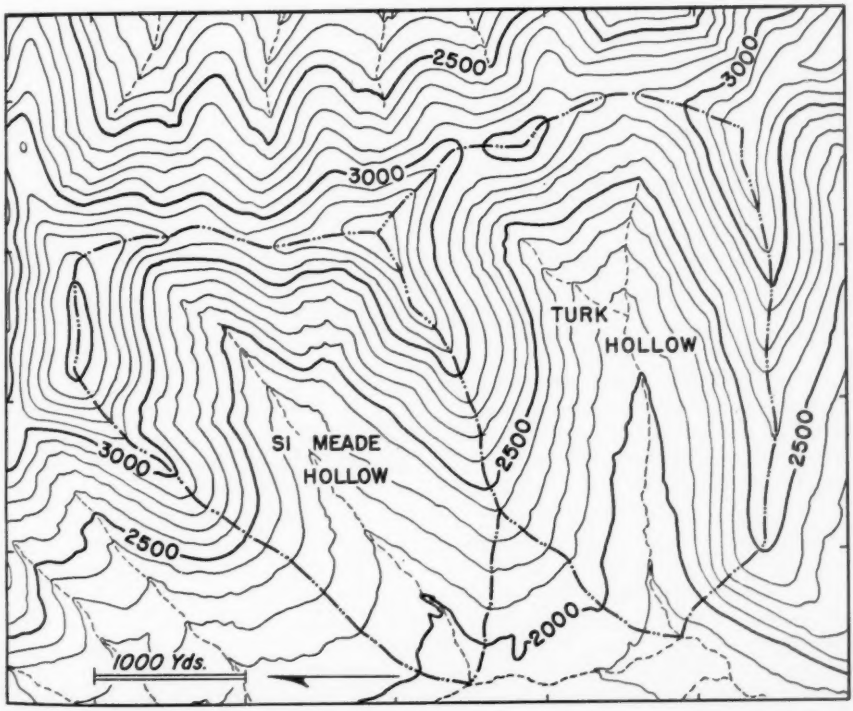

FIGURE 12.—CONTOUR TOPOGRAPHIC MAP OF SI MEADE AND TURK HOLLOWS, WESTKILL, N. Y. QUADRANGLE

Map simplified from Army Map Service Sheet 6168 III NW, scale 1:25,000, compiled from air photographs in 1945.

expected to produce a bimodal distribution because each bench consists of a step, or platform of less-than-average slope bounded on the outer edge by a scarp of steeper-than-average slope. The presence of many such benches

observed frequencies are compared with expected frequencies of a normal distribution having the same mean and variance through a χ^2 test of goodness of fit some information may be obtained on the question of whether the

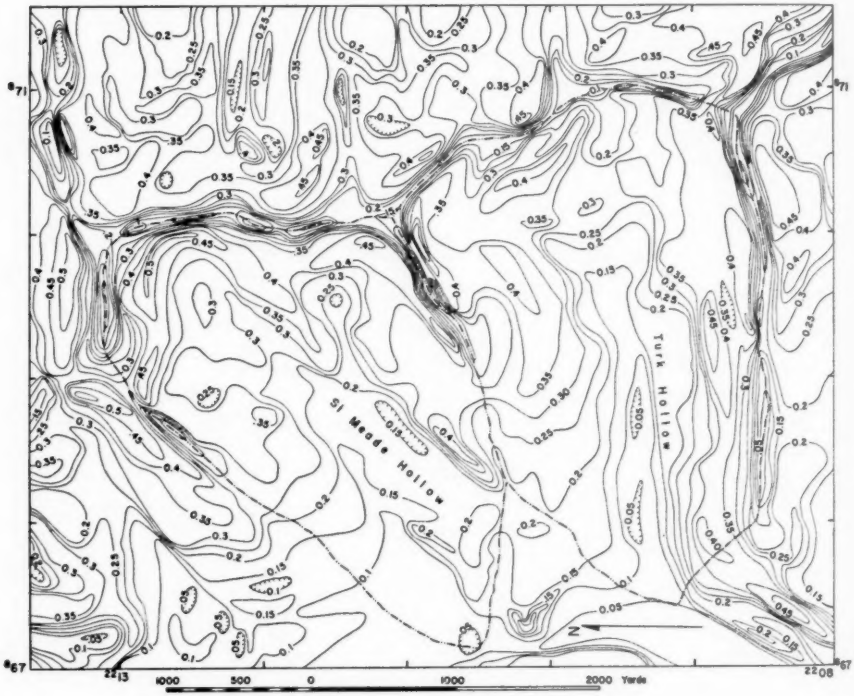

FIGURE 13.—ISOSINAL MAP OF SI MEADE AND TURK HOLLOWS
Hachured lines are applied only to slope depressions on side walls of valleys.

gives abnormally large surface areas of slope both higher and lower than the mean. In an idealized geometrical case benching will produce a topography resembling a flight of stairs and consisting wholly of horizontal and vertical surfaces. This would yield a frequency distribution of two end classes only. The normal landform with benching will have a distribution intermediate between this extreme and the unimodal form of a region of smooth slopes.

A statistical test may be used with grouped data to test the hypothesis that the observed frequency distribution conforms to some previously specified theoretical distribution. If the bimodal form could be expected by chance sampling from a normal population, or whether bimodality is actually inherent in the nature of the distribution of slope sines in this area.

The Turk Hollow sine data were reduced to 8 classes (Dixon and Massey, 1951, p. 190–191) by combining end classes so that no class has less than 5 per cent. This is a conservative measure in the light of a null hypothesis that the observed data are drawn from a normal population, inasmuch as it tends to minimize discrepancies in end classes where chance variability is great. Turk Hollow was chosen for this test because its distribution has less pro-

nounced bimodality. If the hypothesis of normal distribution is rejected for the Turk Hollow, it may also be rejected for Si Meade Hollow. Si Meade Hollow frequency distribution and is explained by the geometry of structural benching.

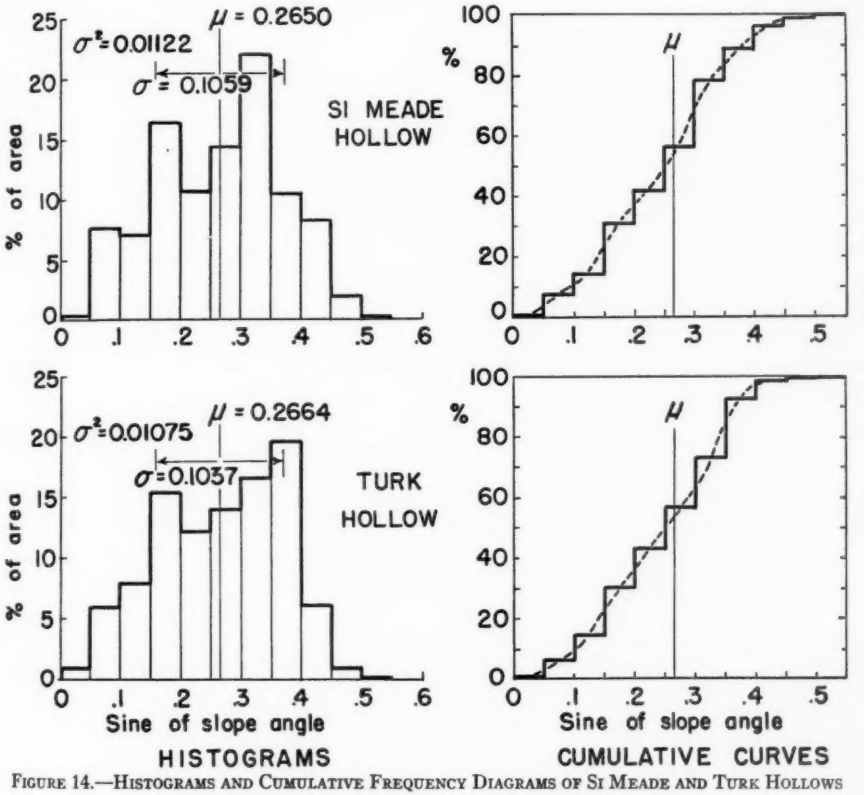

FIGURE 14.—HISTOGRAMS AND CUMULATIVE FREQUENCY DIAGRAMS OF SI MEADE AND TURK HOLLOWS
Areas measured by planimeter from isosinal map (Fig. 13).

The value of χ^2 in this test is approximately 10.9 with a probability of about 6 per cent for five degrees of freedom. For P of 0.10, χ^2 is 9.24; for P of .05, χ^2 is 11.1. We would be led to accept the hypothesis by a scant margin at the 5 per cent level, but to reject it at 10 per cent. Whatever choice one might make on acceptance or rejection it is clear that the fit is rather poor and that we should not expect this poor a fit or worse to occur readily through chance variations alone if the sine distributions are normal. The existence of inherent bimodality, if not strongly supported by the statistical test, is endorsed by similarity of the

TABLE 1.—COMPARISON OF POPULATION PARAMETERS OF SI MEADE AND TURK HOLLOWS

	Mean μ	Variance σ^2	Standard deviation σ
Si Meade Hollow....	0.2650	0.01122	0.1059
Turk Hollow.....	0.2664	0.01075	0.1037

The bimodal frequency distribution also appears strikingly in samples of 100 points located at random within the area.

Emporium, Pennsylvania, Locality

The third test area, near the center of the Emporium quadrangle in north-central Pennsylvania, was selected because it appears to be a typical fully mature topography in which slopes are smooth and structural benching unimportant. It was anticipated that this example might show the characteristically normal slope frequency distribution inferred for small drainage basins carved in homogeneous rock masses. Figure 15 is a generalized topographic contour map of the area, redrawn and simplified from the U. S. Geological Survey map. Two small drainage basins, Lucore and Russell hollows, each about 1 mile long and three quarters of a mile wide, were outlined for study. A superimposed square about 2200 yards across including large parts of these two basins and some parts of the adjoining basins, wsa mapped and measured separately for use as a control population in simplified sampling methods described below.

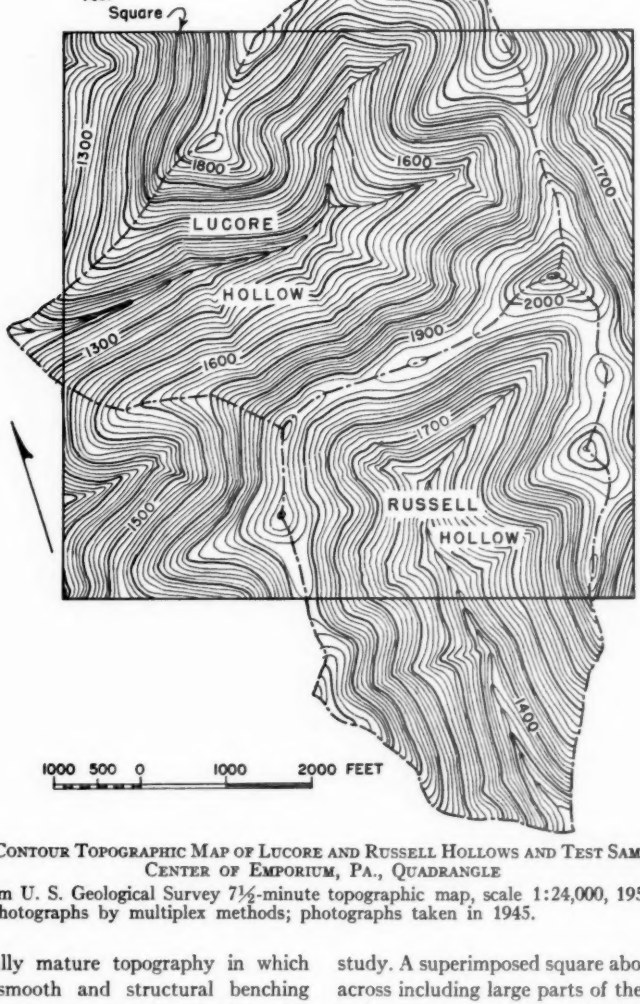

FIGURE 15.—CONTOUR TOPOGRAPHIC MAP OF LUCORE AND RUSSELL HOLLOWS AND TEST SAMPLING SQUARE, CENTER OF EMPORIUM, PA., QUADRANGLE

Copied from U. S. Geological Survey 7½-minute topographic map, scale 1:24,000, 1950; topography from aerial photographs by multiplex methods; photographs taken in 1945.

The Emporium area is a part of the unglaci-

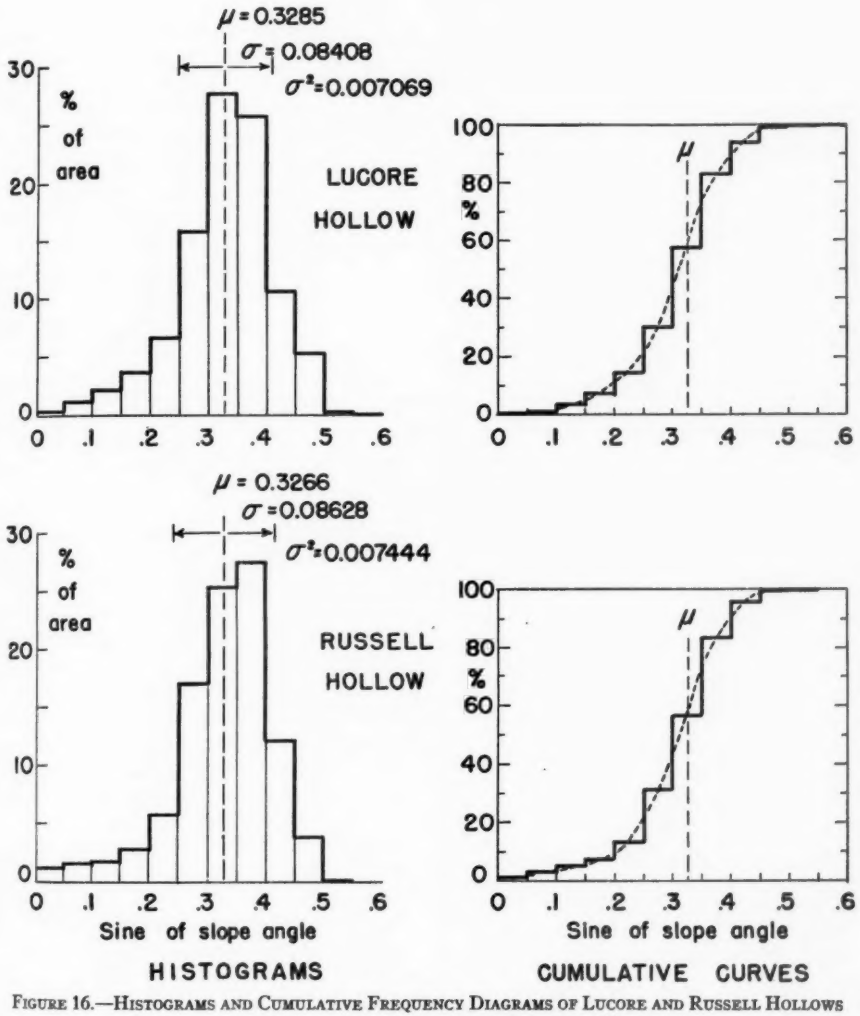

FIGURE 16.—HISTOGRAMS AND CUMULATIVE FREQUENCY DIAGRAMS OF LUCORE AND RUSSELL HOLLOWS
Areas measured by planimeter from isosinal map not illustrated.

ated Appalachian Plateau Province and lies in the northeastern part of the unglaciated Kanawha section. The region is underlain by resistant Pocono and Pottsville formations, deformed into broad, shallow folds. Within the area of the map the strata are essentially horizontal. Structural benching is evident in the broad divides at the 1940-foot elevation, but the valley slopes are smooth. Surrounding the central area of the Emporium quadrangle are broad interstream areas of low slope where the Pottsville sandstone forms a cap rock, but in the area chosen for slope mapping this surface is almost entirely dissected.

Figure 18 is an isotangent map of the Emporium area. Figure 16 shows frequency distributions of sine of slope for Lucore and Russell hollows, measured from an isosinal map made independently of the tangent map shown in Figure 18. Both distributions are similar in form

and agree closely in population parameters (Table 2).

These distributions are unimodal and have lower relative and absolute dispersion than the previous examples. Left skewness is evident in both histograms. Possibly the benching along divides at about 1940 feet accounts for the excessive development of classes under 0.2. Comparison of the Lucore Hollow distribution with a normal distribution of the same mean and variance was made by the χ^2 test of goodness of fit. Seven classes remained after combining end classes into groups containing 5 per cent or more. This yielded a value of 7.14 for χ^2, which with four degrees of freedom has an associated probability of 0.15. Thus the hypothesis that the Russell Hollow sine data are drawn from a normal population is accepted. Because we have defined the sine distributions of these basins as representing the total population within the boundaries of the watershed, the normal population referred to in this test is a theoretical, infinite, superpopulation of innumerable drainage basins imagined to be developed under similar conditions. We are justified in saying that the fit of the observed sine data to a normal distribution is not a poor one.

TABLE 2.—COMPARISON OF POPULATION PARAMETERS OF LUCORE AND RUSSELL HOLLOWS

	Mean μ	Variance σ^2	Standard deviation σ
Lucore Hollow.....	0.3285	.007069	.08408
Russell Hollow.....	0.3266	.007444	.08628

Comparison of the Three Localities

Characteristics of the three sine-frequency distributions can be compared on a cumulative frequency diagram (Fig. 17). Step graphs show observed frequencies by classes. Inasmuch as these sine data represent entire populations, the drawing of smooth curves by inspection only is justified as a crude representation of actual population curves. The Perth Amboy drainage basins shows great range (almost covering the entire slope quadrant), a broad dispersion, and a high mean slope. Lack of symmetry is evident in the long slope of the left side of the curve. Youthfulness of development explains the broad dispersion and wide range. The high mean is attributable to steep slopes in cohesive clays. The Lucore Hollow distribution is symmetrical, with a low dispersion. The distribution for Si Meade Hollow has an intermediate dispersion and is bimodal. These curves and general considerations of landform evolution suggest that the slope distribution in the inequilibrium stage of drainage-basin development has the broadest dispersion and shows strong left skewness. As the available mass is transformed by incision of the streams and lengthening of steep valley-side slopes, dispersion is reduced by an increasing proportion of steep surfaces and a decreasing importance of low-slope classes. When slope transformation is accomplished, leaving only narrow divides, dispersion is reduced to the minimum. A region of steep straight slopes with sharp divides and narrow canyon bottoms would yield an extremely narrow frequency distribution. Such a topography corresponds to W. Penck's "uniform development".

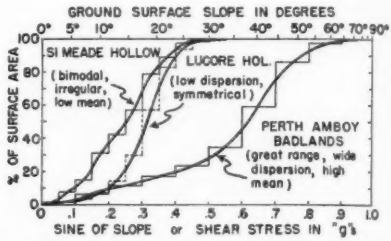

FIGURE 17.—CUMULATIVE FREQUENCY CURVES OF THREE DRAINAGE BASINS

Further change in form of frequency distribution may be steady reduction in mean slope value, if relief is reduced and slope steepness diminished. If, instead, the theory of slope evolution requires parallel slope retreat, accompanied by the development of widening basal slopes of low gradient (*Haldenhang* or pediments), the low-slope classes would be expected again to become important, increasing the dispersion and destroying the symmetry of the distribution.

Simplified Point-Sampling Methods

Selection of Sampling Test Area

Rapid methods of statistical analysis of slope must be devised if large areas or many localities are to be analyzed. Preparation of a slope map and its planimeter measurement may take an experienced operator 1–4 weeks, an unjustified time expenditure if we wish to know only the mean, variance, standard deviation, general shape, and range of the slope distribution. Rapid methods of obtaining this information by sampling slope at a limited number of points on the surface were investigated and their reliability determined by comparison with population data from the slope maps.

The area chosen for tests of sampling methods is a square, 2200 yards across, superimposed on parts of both Lucore and Russell hollows (Fig. 15). A detailed isotangent map was prepared, using about 2000 slope readings (Fig. 18). Divider points were set at an opening representing 100 feet horizontal distance; the same distance was used in point sampling. Planimeter measurement yielded a frequency distribution (Figs. 2, 20A). Correction of observed class frequencies to estimated (true) surface area was not made in this investigation. The percentage frequencies (Figs. 2, 20A) are taken directly from the map.

Population Parameters in Statistical Testing

An important assumption in the tests is that the frequency distribution measured from the isotangent map represents the actual slope population within the area mapped. This assumption seems justified because no part of the ground surface has been omitted. Although the isotangent lines were drawn from information consisting of point measurements, the drawing of lines constitutes an interpolation or estimate of the state of the ground slope at all points between the selected points. If two successive isotangents were drawn with perfect accuracy they would represent the boundares of an area in which all the surface is within the slope range of the given class. Perfect accuracy cannot be achieved, but with improvements in technique the observed lines will approach the true lines. Statistically, the frequency distribution measured from a slope map is an approximation of the entire slope population, rather than a sample drawn from the population. Consequently the symbols for population parameters—μ for mean, σ^2 for variance, and σ for standard deviation—have been used instead of corresponding sample statistic symbols, $\bar{X}$, s^2, and s, to describe all frequency distribution measured by planimeter from isotangent and isosinal maps.

The distinction between population parameters and sample statistics is important in selection of statistical hypotheses, because certain tests require that the population mean or population variance be known. The number of degrees of freedom cannot be determined, or is considered infinite, for the slope-frequency distribution measured from the slope maps; no finite number of variates contributes to each class in the distribution. Even the actual number of points (hundreds or thousands) from which the slope contours were drawn in preparation of the slope map is equivalent to an infinite number in statistical tests.

Random-co-ordinate Sampling Method

A method of drawing a sample of any desired number of points at random from the surface of a square area was developed through application of a rectangular co-ordinate system; it is designated as the "*random-co-ordinate method*" (Fig. 19A). The square is divided into 100 units on a side. On both abscissa and ordinate the units are designated by two-digit numbers from 00 through 99. Used in pairs, the first two-digit number representing the value of X, the second number of value of Y, a total of 10,000 points may be located within the square, as points are located by a military grid system. The population of points available for sampling is thus not infinite but is extremely large in terms of samples of sizes from 10 to 200 points each. To yield a sampling population of 1,000,000 points, we need only three digits, each series ranging from 000 to 999. This is not practical in a small square, because it is not possible to read scale subdivisions of one thousandth part of the side of the square, but if a much larger sampling square were used the degree of subdivision

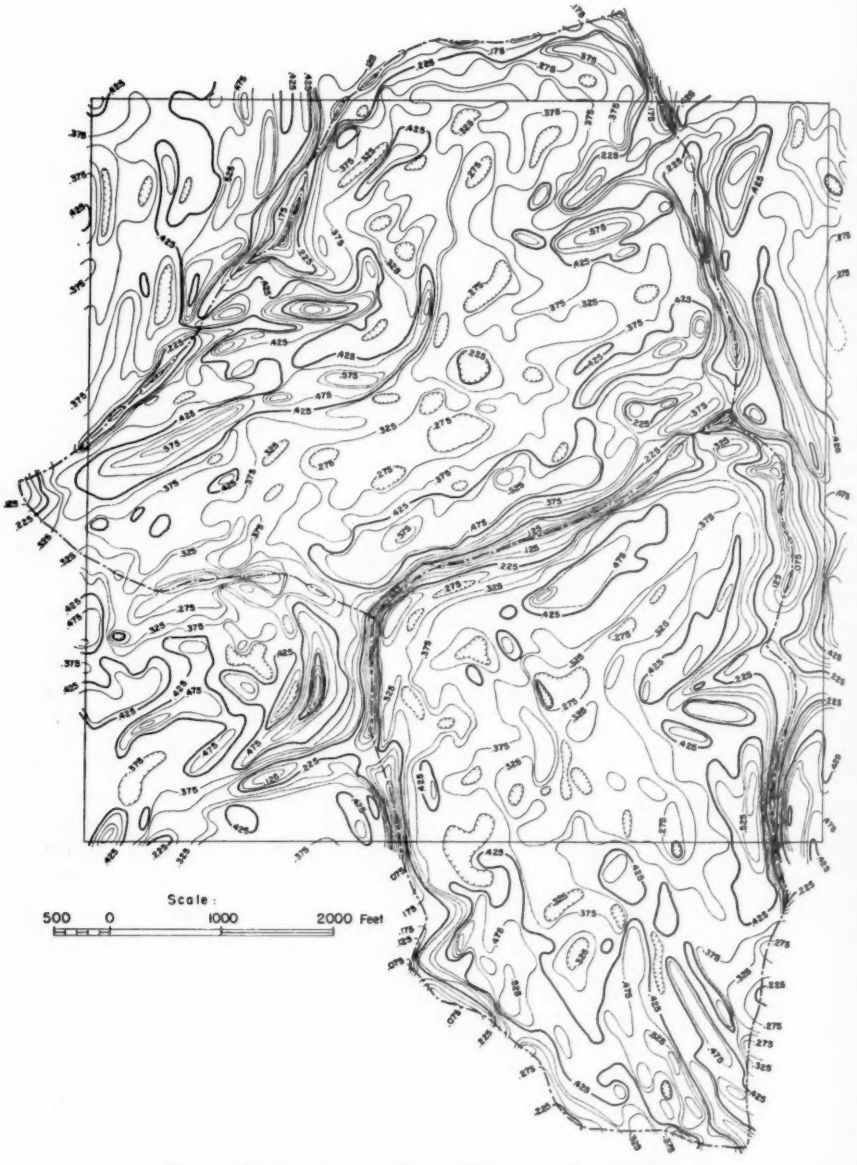

FIGURE 18.—ISOTANGENT MAP OF EMPORIUM, PA., LOCALITY

Numbers on lines tell tangent of angle of slope; hachured lines show only depressions in slope surface on valley side positions.

might be increased to 1000 or 10,000 units per side.

Drawing Random Numbers

The next step is to draw a random sample from the available points. Size of sample can be selected to meet the standards of probable

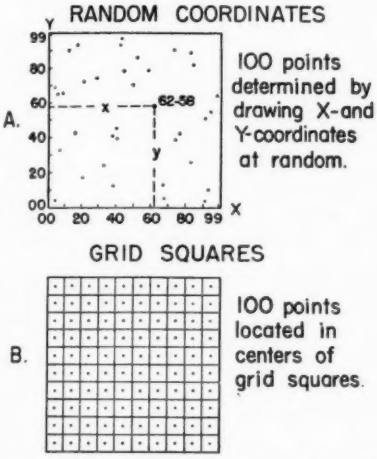

FIGURE 19.—METHODS OF POINT SAMPLING

error in the mean, as explained below. Here, a sample size of 100 is used. Thus it is necessary to draw 100 pairs of co-ordinates in a random series, i.e., to draw co-ordinate values so that every one of the 10,000 co-ordinate points in the square has an equal chance of being drawn on each draw.

This might be accomplished by taking 10,000 plastic discs of equal physical properties and inscribing on each a different co-ordinate pair. To obtain a random sample of 100 one would shake the discs in a bowl, draw one out, record the numbers, and return the disc to the bowl, repeating this process until the desired sample number is obtained. A simpler way is available through the table of random numbers, available in books of statistical tables, and in the appendices of most introductory statistical textbooks. Tables published by Dixon and Massey (1951, p. 290–294) were used; they consist of blocks of 25 two-digit numbers. We may begin at any number in the tables and record the consecutive pairs of digits until the desired sample number is drawn. Selection of the point of starting can be made by bringing down a pencil point to some chance point on the page. First a series of 100 two-digit numbers is listed, forming the X co-ordinates. A second series of 100 numbers is drawn and listed opposite the X list to form corresponding values of Y.

Measurement of Slope at Co-ordinate Points

A T-square and right triangle facilitate finding of the sample point, which may be marked by a needle prick. The divider points, set at a fixed distance (in this case equivalent to 100 feet horizontal distance), are then applied to the orthogonal passing through the sample point and the drop in elevation estimated from number of contour intervals and fractions of intervals intercepted. This operation is the same as that used in preparing the slope map (Fig. 3). The tangent of slope is recorded opposite the corresponding co-ordinate pair of the list, and the next sample point located. In this way the operator can relocate any sample point to check his determination, and other operators can find the same point and compare their results to determine operator variance.

A second method of rapid point sampling commonly encountered in geologic work uses grid squares (Fig. 19B) to secure uniform rectangular spacing of 100 points located in the centers of the squares. It might be supposed that a regularly distributed sample would give coverage more uniformly representative of the entire area and would be superior to the random-co-ordinate method. According to statistical principles, however, this grid sample is unsatisfactory because variance cannot be computed simply. Furthermore, the large size of the grid distance in relation to size of landform units makes it possible that, if the topographic units are elongated in one azimuth, some bias may be introduced by the fact that grid points are not spaced the same distance apart with respect to possible parallel sets of reference lines. An advantage of the random-co-ordinate method is that additional samples may be taken from the same square by drawing more pairs of random numbers; with a fixed

grid additional samples can be taken only by shifting the entire grid horizontally, changing the area covered.

Comparison of Sample and Population Distributions

After the random-co-ordinate sample is taken, the individual variates are grouped into classes, and the mean, $\bar{X}$, variance, s^2, and

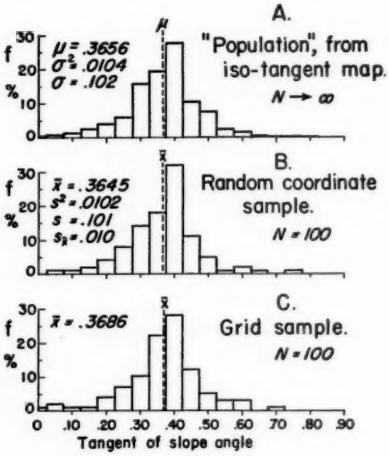

FIGURE 20.—HISTOGRAMS OF RANDOM-CO-ORDINATE SAMPLE, GRID SAMPLE, AND POPULATION COMPARED

Population histogram measured from isotangent map (Fig. 18)

standard deviation s, computed. In computation of variance the sum of squared deviations is divided by $(N - 1)$, which in this case equals 99. A histogram can be constructed, and the form of the distribution compared with the population histogram based on the slope map. Figure 20 shows three frequency distributions compared: (A) population distribution based on the slope map; (B) random-co-ordinate sample of 100 points; (C) the fixed grid-square sample of 100 points. Variance and standard deviation are given for the first two distributions but omitted from the grid-sample data for which the mean only was computed.

The close similarity in all three histograms is apparent. Means and variances differ only in the third decimal place. Slight left skewness is noticeable in all three distributions.

To evaluate the reliability of the random-co-ordinate sampling method statistical tests are available which tell the probability that the observed differences in means and variances are solely due to chance. In the present case

TABLE 3.—TEST OF VARIANCE

Random-co-ordinate sample vs. *Population*
$s^2 = 0.0102$ $N = 100$ $\sigma^2 = 0.0104$
Hypothesis: $\sigma^2 = \sigma_0^2$
Let $\alpha = .05$
Use statistic $\chi^2/\text{d.f.} = s^2/\sigma^2 = 0.98$
Critical region: $0.756 < s^2/\sigma^2 < 1.28$
Accept hypothesis.

such tests might seem superfluous, but they give additional support to the intuitive conclusions. The tests would be essential in cases where differences are marked.

Test of Sample Variance

To test sample variance the statistical hypothesis is proposed (Table 3) that the variance of the population from which the sample is drawn, σ_0^2, is identical with the known population variance, σ^2, derived from the slope map (Dixon and Massey, 1951, p. 86–87). We set the critical probability, α, equal to 5 per cent. The ratio of sample variance to population variance, s^2/σ^2, which has the distribution of $\chi^2/d.f.$ is used. If this ratio of variances is very large or very small, differing greatly from unity, the probability of the sample being drawn from the population is also small. At the 5 per cent level of significance, divided into two parts of 2½ per cent each to contend with values both excessively small and large, the hypothesis will be rejected if the ratio is less than 0.756 or greater than 1.28. In this instance the ratio is close to 1, and the hypothesis is accepted.

Test of Sample Mean

To test sample mean (Dixon and Massey, 1951, p. 94–97) the statistical hypothesis is proposed that the mean, μ_0, of the population from which the sample was drawn is identical with the slope-population mean, μ (Table 4). The critical level of significance is set at 5 per cent. This means that with repeated sampling,

for 1 in 20 such tests on the average, we will reject the hypothesis when it is actually true. The statistic, z, used for the test, is the ratio of the observed difference between sample mean and population mean to the standard error of the mean. Values of z will be almost normal in distribution in this case because the population distribution is not greatly different from normal. The hypothesis is to be rejected if values of z larger than $+1.96$ or smaller than -1.96 are found. The observed value of z in this test is 0.106. The hypothesis is therefore accepted.

TABLE 4.—TEST OF MEAN

Random-co-ordinate sample vs. *Population*

$\bar{x} = 0.36450 \quad \mu = 0.36580 \quad \sigma = 0.1022$

Hypothesis: $\mu = \mu_0$

Let $\alpha = .05$

Use statistic $z = \dfrac{\bar{x} - \mu}{\sigma/\sqrt{N}} = +0.106$

Critical region: $+1.96 > z > -1.96$

Accept hypothesis.

Confidence Limits of Sample Means

Where the population parameters are known, the behavior of sample means of any given sample size can be predicted on a strict probability basis. For a normally distributed population with variance σ^2 and sample size N, the sampling distribution of means will be normal and will have a standard deviation, $\sigma_{\bar{x}}$, which equals the standard deviation of the population, σ, divided by the square root of the number of variates, N. Thus we write the equation $\sigma_{\bar{x}} = \sigma/\sqrt{N}$. The statistic $\sigma_{\bar{x}}$ is commonly termed the "standard error of the mean". Table 5 shows use of this statistic to predict the expectable range in sample means of various sizes. The value of standard deviation found in the slope population based on the isotangent map is 0.1022. The standard error of the mean $\sigma_{\bar{x}}$ for a given sample size is obtained by dividing 0.1022 by the square root of the sample number N. Row A of the table gives these values for samples of 10, 50, 100, and 1000 slope readings drawn by the random-co-ordinate method. The number ± 0.0323 under sample size 10 can be interpreted to mean that about 68 per cent of the time, with repeated sampling, the sample mean will fall in a range not higher than 0.0323 more than the population mean of 0.3656 or lower than 0.0323 less than this population mean. Thus the interval, or spread of expected sample means, is from 0.3333 to 0.3979. For larger samples this spread is reduced inversely as the square root of the sample number. For samples of 100 variates the standard error is about 0.1, or about one-fifth of the width of the class interval used in the histograms (Fig. 20).

TABLE 5.—CONFIDENCE INTERVALS BASED ON POPULATION PARAMETERS, $\mu = 0.36558$, $\sigma = 0.1022$

Confidence level:	Statistic used:	Sample size:			
		10	50	100	1000
(A) 68%	$\sigma_{\bar{x}} = \sigma/\sqrt{N}$	$\pm.0323$	$\pm.0145$	$\pm.0102$	$\pm.0032$
(B) 95%	$\dfrac{1.96\,\sigma}{\sqrt{N}}$	$\pm.0633$	$\pm.0284$	$\pm.0200$	$\pm.0063$
(C) 95%	% of μ	$\pm 17.3\%$	$\pm 7.8\%$	$\pm 5.5\%$	$\pm 1.7\%$

Row B of Table 5 shows the probable range in sample means at the 95 per cent confidence level. The range to be expected 95 per cent of the time is $1.96\,\sigma_{\bar{x}}$, almost twice the standard error. The figures in row B tell the range above or below the population mean to be expected 95 per cent of the time with samples of 10, 50, 100, and 1000. For samples of 100, the size used here, 95 per cent of the sample means will fall not more than .02 above or below the population mean, if we are sampling from this population. The figures in row B are converted into percentage of the population mean in row C and tell us that our percentage error will not on the average exceed the values shown 95 per cent of the times samples of the given size are drawn at random. The percentage figures apply only to the population mean of 0.36558; the ranges in rows A and B are valid for any normal population with a standard deviation of 0.1022.

Chi-Square Test of Goodness of Fit

Another means of testing the sample for conformity with the known population is the χ^2 test of goodness of fit, commonly used to compare an observed distribution with a hypo-

thetical normal distribution assumed to have the same mean and variance (Dixon and Massey, 1951, p. 190–191). In this case the population is known in terms of classes and their frequencies. The hypothesis is that the sample distribution represents a population identical

TABLE 6.—CHI-SQUARE TEST OF GOODNESS OF FIT

Random-co-ordinate sample vs. *Population*
Hypothesis: Sample distribution conforms to population distribution.
Let $\alpha = .05$
Use statistic $\chi^2 = \Sigma\frac{(f - F)^2}{F}$
(F = expected freq.; f = observed freq.)
$\chi^2 = 2.72$; d.f. (9 classes) = 6; $\chi^2_{.95} = 12.6$
Accept hypothesis.

to the known population measured from the slope map (Table 6). We again set the level of significance at 5 per cent. The statistic used has the χ^2 distribution and is the sum of the ratios of the squared differences between observed and expected frequencies in each class to the observed frequencies in those classes. Expected frequency is the frequency measured from the slope map; observed frequency is the sample frequency. With six degrees of freedom (three less than the number of classes used) the critical value of σ^2, above which the hypothesis will be rejected, is 12.6. The observed value of χ^2 is, however, only 2.72, so we accept the hypothesis. The fit is a good one.

Evaluation of Sampling Method

The tests thus far have cast no doubt upon the hypothesis that the random-co-ordinate sample is drawn from the same population as represented by the slope map. The labor saved in the random sampling method testifies to its desirability in future slope studies. A similar random-sampling technique, based on surveying methods with plane table and alidade, could be applied in the field if adequate maps are not available. Because standard error of the mean can be estimated closely from sample data alone, the operator can judge the size of sample needed. Measuring a sample of even 1000 points takes far less time than preparing an isotangent or isosinal map and brings the probable error of the mean to very narrow limits (Table 5, row B.)

Operator Variance

In any sampling operation involving a series of measurements requiring some estimation the problem of operator variance is important. Given the same maps or field areas, the same instruments, and the same instructions, would there be differences in sample results? Would different operators produce significantly different means or variances from the same sample area? Although this question has not been fully studied for slope-sampling methods, a preliminary study of two operators' results suggests that operator differences are small (Table 7), and do not constitute a weakness in the sampling method.

Operator B took the list of 100 random co-ordinates used by the writer, Operator A (Fig. 20B; Tables 3, 4). At each sample point Operator B determined the tangent of ground slope independently, but used the same map and instruments. This yielded a second sample of 100 tangents, in which each variate is paired to a corresponding variate in Operator A's sample. The two samples are designated as 1A and 1B; the sample statistics are shown in the first row of Table 7. The mean of the paired differences, $\bar{x}_d$, is $-.00150$; the standard deviation of the differences, s_d, is 0.02508. The value of t is -0.598, which for $\alpha = .05$, is far less than the critical value above which rejection would be required under the hypothesis that the mean of the population of differences is zero and therefore that both samples are drawn from one population.

A second test was performed with a corresponding set of data (Table 7, second row). A random co-ordinate sample of 100 was drawn from a table of random numbers; each operator independently determined the slope tangent at each point. This yielded samples 2A and 2B in which variates are also paired. The mean of the differences was $+.0030$, which is twice as large as in the previous case and of opposite sign. The variance of the differences is larger in the second case. The value of t is again much less than the

critical value for $\alpha = .05$, and the hypothesis that mean of differences is equal to zero is again accepted.

These tests suggest that operator variance induces no significant differences in sample means. In Table 7 the two values of mean differences are comparable and are very small parts (only 10 to 20 per cent) of the differences in means of samples from the two sets of co-ordinates. The latter difference in means, averaging about .027 for both operators, would fall outside the 95 per cent confidence limits already set for sample means of size 100 (Table 5). This is not surprising because we expect that one sample in 20, on the average, will be rejected when the hypothesis is actually true. A t test between samples 1A and 2B (two sets of points, two operators) yields a value of t almost exactly coinciding with the critical value of t for $\alpha = .05$. In this test the variates are not paired. A two-way analysis of variance was not applied to the sample data (Table 7) because strong dependence exists between samples of each row.

TABLE 7.—TEST OF PAIRED DIFFERENCES IN SLOPE READINGS

	Operator A	Operator B	Statistics of paired differences	t Test
	1A	1B		
Samples 1A & 1B, $N = 100$				
$\bar{X}$	0.36450	0.36550	$\bar{X}_d - 0.001500$	$t = -0.598$
s^2	0.010167	0.010136	s^2_d 0.0006292	$t_{.025} = 1.99$
s	0.10083	0.10068	s_d 0.02508	Accept hyp. $\mu = 0$
	2A	2B		
Samples 2A & 2B, $N = 100$				
$\bar{X}$	0.39450	0.39150	$\bar{X}_d$ 0.00300	$t = 0.815$
s^2	0.006373	0.008185	s^2_d 0.001354	$t_{.025} = 1.99$
s	0.07983	0.09047	s_d 0.03680	Accept hyp. $\mu = 0$

CONCLUSION

Preparation of slope maps showing variations in amount of surface slope has served two purposes: (1) the slope map has potential value in engineering and military applications; (2) the slope map provides an approximation of the frequency distribution of a statistical population of slope and has value in testing the reliability of rapid methods of sampling.

Frequency distribution of slope tangents or slope sines provides a generalized picture of slope of an entire land surface. The study of slope-frequency distributions would be impractical on a large scale because of the time and labor involved, were it not for rapid point sampling methods. The random-co-ordinate method allows samples of any size to be drawn from square regions of any size in a minimum of time. Through statistical principles of sampling distribution of means, confidence limits can be set up and the sample size adjusted so that sample means will fall within specified limits in a given percentage of trials.

Statistics, such as the mean, variance, standard deviation, and measures of skewness, can be applied to slope-frequency distributions, enabling the geomorphologist to describe the slope properties of a region quantitatively and to compare two regions through objective tests of differences in variances and means. This should lead to the objective, systematic delineation of geographical regions according to slope properties. Slope-frequency distributions will differ with differences of stage in the geomorphic cycle of erosion of a region. Studies may reveal the systematic progression of values of slope-population parameters associated with the developmental cycle, thus making possible further quantification of landform stages.

References Cited

Calef, Wesley, and Newcomb, Robert, 1953, An average slope map of Illinois: Assoc. Am. Geographers Annals, v. 43, p. 305–316

Dixon, W., and Massey, F. J., Jr., 1951, Introduction to statistical analysis: N. Y., McGraw-Hill Book Co., 370 p.

Raisz, Irwin, and Henry, Joyce, 1937, An average slope map of New England: Geog. Rev., v. 27, p. 467–472

Strahler, A. N., 1950, Equilibrium theory of erosional slopes approached by frequency distribution analysis: Am. Jour. Sci., v. 248, p. 673–696, 800–814

Strahler, A. N., 1952a, Dynamic basis of geomorphology: Geol. Soc. America Bull., v. 63, p. 923–938

—— 1952b, Hypsometric (area-altitude) analysis of erosional topography: Geol. Soc. America Bull., v. 63, p. 1117–1142

Wentworth, C. K., 1930, A simplified method of determining the average slope of land surfaces: Am. Jour. Sci. 5th ser., v. 20, p. 184–194

Columbia University, New York 27, N. Y.

Project NR 389-042, Technical Report No. 9

Manuscript Received by the Secretary of the Society, January 19, 1955

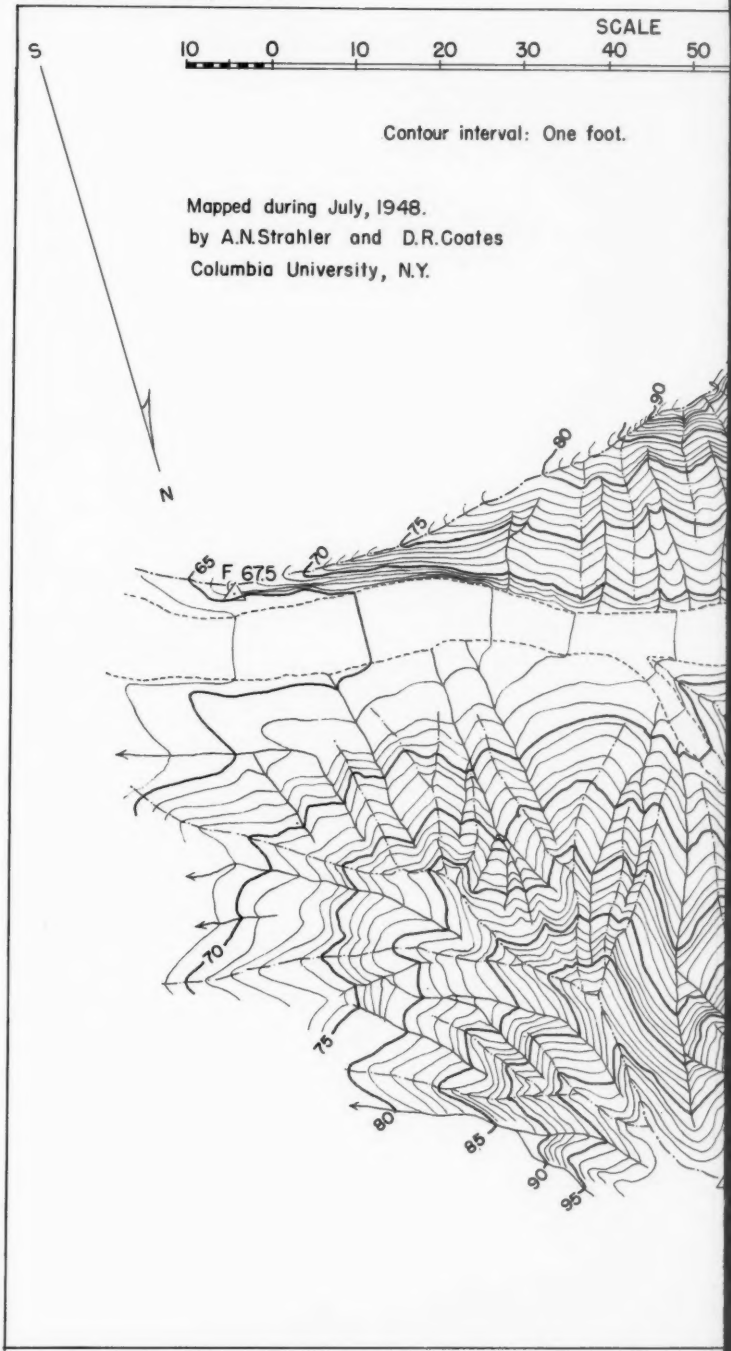
SCALE
10 0 10 20 30 40 50
S
N
Contour interval: One foot.
Mapped during July, 1948.
by A.N.Strahler and D.R.Coates
Columbia University, N.Y.
F 675
65
70
75
80
85
90
95

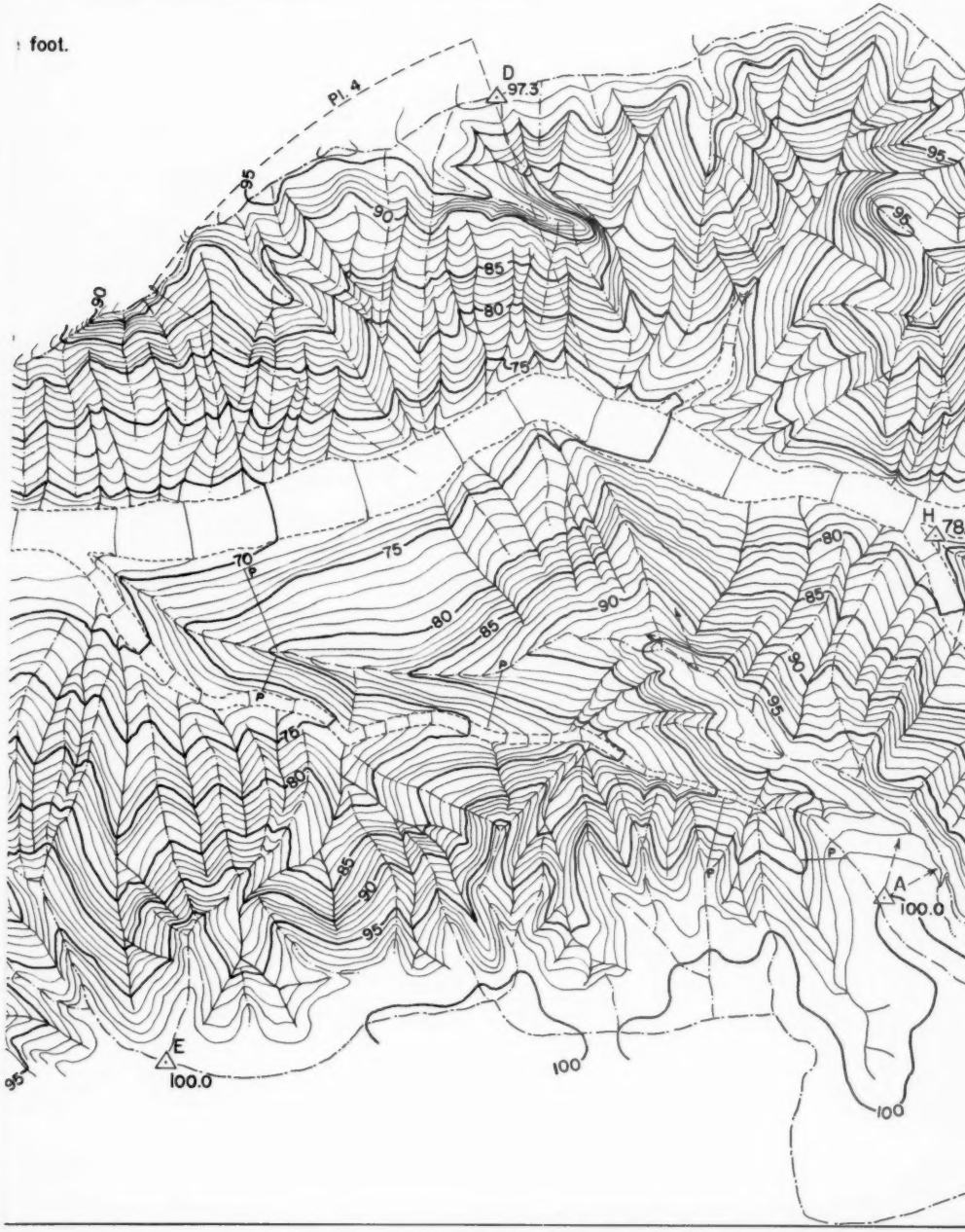

TOPOGRAPHIC MAP OF THE P

THE PERTH AMBOY BADLANDS

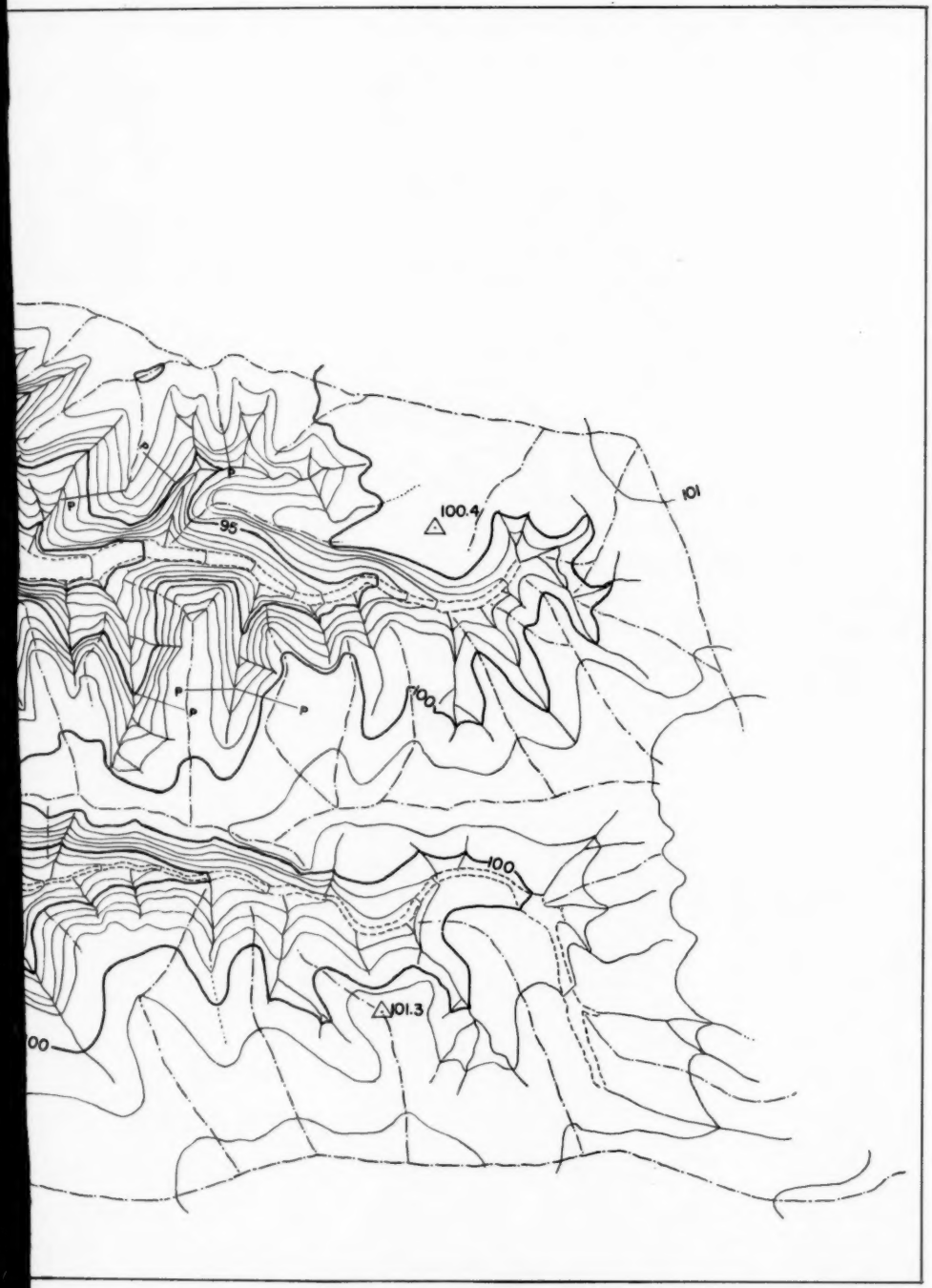
100.4
101
95
100
100
101.3
00

BULLETIN OF THE GEOLOGICAL SOCIETY OF AMERICA
VOL. 67, PP. 597-646, 43 FIGS., 6 PLS. MAY 1956

EVOLUTION OF DRAINAGE SYSTEMS AND SLOPES IN BADLANDS AT PERTH AMBOY, NEW JERSEY

BY STANLEY A. SCHUMM

ABSTRACT

To analyze the development of erosional topography the writer studied geomorphic processes and landforms in a small badlands area at Perth Amboy, New Jersey. The badlands developed on a clay-sand fill and were morphologically similar to badlands and areas of high relief in semiarid and arid regions. A fifth-order drainage system was selected for detailed study.

Composition of this drainage network conforms to Horton's laws. Within an area of homogeneous lithology and simple structure the drainage network develops in direct relation to a fixed value for the minimum area required for channel maintenance. Observed relationships between channel length, drainage-basin area, and stream-order number are dependent on this *constant of channel maintenance* which is in turn dependent on relative relief, lithology, and climate of any area.

Other characteristics of the drainage network and topography such as texture, maximum slope angles, stream gradients, drainage-basin shape, annual sediment loss per unit area, infiltration rate, drainage pattern, and even the morphologic evolution of the area appear related to relative relief expressed as a *relief ratio*, the height of the drainage basin divided by the length. Within one topographic unit or between areas of dissimilar but homogeneous lithology the relief ratio is a valuable means of comparing geomorphic characteristics.

Hypsometric curves are available for a series of 11 second-order drainage basins ranging in stage of development from initial to mature. Relief ratio and stream gradients attain a constant value when approximately 25 per cent of the mass of the basin has been eroded. Basin shape becomes essentially constant at 40 per cent of mass removed in accord with Strahler's hypothesis of time-independent forms of the steady state.

Comparison of the drainage pattern as mapped in 1948 with that of 1952 reveals a systematic change in angles of junction and a shift of the entire drainage pattern accompanying changes in the ratio between ground and channel slope.

Field observations and experimental studies suggest that badland slopes may retreat in parallel planes and that the rate of erosion on a slope is a function of the slope angle. The retreat of slopes may not conform to accepted concepts of runoff action as a function of depth and distance downslope. Runoff occurs as surge and subdivided flow which may be closely analogous to surficial creep.

Rills follow a definite cycle of destruction and reappearance throughout the year under the action of runoff and frost heaving.

At Perth Amboy, slopes are initiated by channel degradation and maintained by runoff and by creep induced through frost heaving. Runoff or creep may form convex divides, and both parallel and declining slope retreat are important in the evolution of stream-carved topography.

Hypsometric curves reveal that the point of maximum erosion within a drainage basin migrates upchannel and that the mass-distribution curve of any basin has a similar evolution to that of the longitudinal stream profile.

Comparative studies in badland areas of South Dakota and Arizona confirm conclusions drawn at Perth Amboy and show the importance of infiltration of runoff on topographic development and of subsurface flow in slope retreat and miniature pediment formation.

CONTENTS

TEXT

	Page
Introduction	599
Acknowledgments	600
General description of the Perth Amboy locality	600
Characteristics of the drainage network	602
Components of the drainage network	602
Limiting values of drainage components	607
Form of the drainage basins	612
Basin form related to geomorphic stage of development	614
Evolution of the drainage network	617
Effect of stage on angles of junction	617
Evolution of the Perth Amboy drainage pattern	620
Field observations and experimental studies on the development of badland topography	622
Field-erosion measurements	622
Experimental erosion measurements and study of runoff	627
Seasonal effects on erosion; the rill cycle	632
Cycle of development of erosional topography	634
Relation of stream profiles to slopes	634
Available relief and the development of landforms	636
Hypsometric study of geomorphic stages of development	638
Comparative studies in badland regions of the West	641
Topographic forms and erosion processes	641
Influence of regional upland slope on topography	644
Summary and conclusions	645
References cited	646

ILLUSTRATIONS

Figure	Page
1. Grain-size distribution of Perth Amboy fill	601
2. Relation of number of streams of each order to order number	603
3. Relation of mean basin area, mean stream length, mean stream gradient, to stream order	604
4. Comparison of shape of basin and main drainage elements of three areas	605
5. Relation of mean basin area and mean stream length to stream order	605
6. Relation of mean stream length of each order to mean basin area of each order	606
7. Frequency-distribution histograms of the logs of drainage-basin area	607
8. Frequency-distribution histograms of logs of stream-channel lengths	607
9. Position of interbasin area and method of classifying streams by order number	608
10. Frequency-distribution histograms of first- and second-order basin areas and interbasin areas	609
11. Frequency-distribution histograms of first- and second-order channel lengths and maximum interbasin lengths	610
12. Relation of drainage density to relief ratio	613
13. Relation of drainage density to relief ratio of third-order basins	613
14. Relation of mean stream gradients to relief ratio	613
15. Relation of mean maximum-slope angles to relief ratio	613
16. Relation of elongation ratio to relief ratio	614
17. Relation of mean estimated sediment loss to relief ratio	615
18. Sequence of second-order hypsometric curves	615
19. Sequence of second-order hypsometric curves	615
20. Relation of mass removed within a basin to relief ratio, gradient, elongation ratio, and drainage density	617
21. Frequency-distribution histograms of young, mature and combines angles of junction	618
22. Drainage-pattern changes in selected basins between 1948 and 1952 at Perth Amboy	620
23. Possible development of angles of bifurcation	621
24. Suggested evolution of the Perth Amboy drainage pattern	621
25. Frequency-distribution histogram of angles between tributaries and segments of the main channel	622
26. Typical Perth Amboy slope profiles	623
27. Regression fitted to scatter diagram of depth of erosion on per cent of distance from top of the straight slope segment	624
28. Regression line fitted to adjusted values of Figure 27	625
29. Frequency-distribution histograms of angles between stakes measured in September superimposed on histogram of angles measured in June	625
30. Frequency-distribution histograms of maximum-slope angles measured in 1949 and 1952	626
31. Relation of erosion to sine of slope angle	627
32. Relation of the largest particle moved on a slope to sine of slope angle	629
33. Depth of erosion measured on slope profile D during the summer of 1952	630
34. Slope profile D in June and September 1952	631
35. Depth of erosion measured on an initially straight slope during the summer of 1952	632
36. Development of valley-side slopes	635
37. Effect of direction of drainage of upland slopes on slope-profile form	636
38. Development of topography in areas of high, moderate, and low relief	637
39. Possible topographic differences, at a late stage of development, between areas of originally high, moderate, and low relative relief	638
40. Changes in longitudinal stream profiles at Perth Amboy	639
41. Method of dividing a drainage basin into five equal areas and the system of numbering each 20 per cent area	639
42. Relation of erosion within each 20 per cent area of a basin to total erosion during a complete geomorphic cycle	640
43. Two longitudinal stream profiles surveyed in Badlands National Monument, South Dakota	644

Plate — Facing page
1. Topographic map of the Perth Amboy badlands ... 597
2. Perth Amboy badlands ... 632
3. Rill cycle ... 633
Following page
4. Rill cycle
5. Badland slopes at Perth Amboy and Badlands National Monument, South Dakota ... 642
6. Badland slopes and drainage channels, South Dakota and Arizona

Table — Page
1. Method of deriving weighted mean bifurcation ratio ... 603
2. Drainage-network characteristics ... 606
3. Frequency distribution of logs of channel lengths ... 608
4. Frequency distributions of logs of drainage-basin areas ... 608
5. Frequency distributions of first- and second-order drainage-basin areas and interbasin areas ... 609
6. Frequency distributions of first- and second-order channel lengths and interbasin lengths ... 611
7. Drainage-basin characteristics ... 612
8. Drainage-basin characteristics of the second-order sequence ... 616
9. Frequency distributions of angles of junction ... 618
10. Angles of bifurcation and angles of junction ... 619
11. Frequency distributions of angles between tributaries and main channel ... 622
12. Erosion measured along the slope profiles ... 624
13. Frequency distributions of slope angles ... 626
14. Per cent by weight of eroded sediment greater than 2 mm ... 628

Introduction

The factor of time has been a major difficulty in investigations of the evolution of landforms. Laboratory scale models which operate rapidly are unsatisfactory because scale ratios cannot be suitably maintained. An alternative exists, however, in studies of badland regions of the western United States, where detailed investigations (Smith, In press) within small areas undergoing rapid erosion have led to inferences concerning processes operating on morphologically similar but larger erosional landforms.

Small badland areas developing in clay pits on the Coastal Plain of New Jersey were also suitable for study and could be observed during an annual cycle of climatic changes. A. N. Strahler and D. R. Coates of Columbia University had selected one area at Perth Amboy, New Jersey for detailed study and mapping in 1948. In 1951 the writer began his investigation of the area using Strahler's map as a basis for morphometric studies.

Several methods were used to evaluate the effectiveness of the erosive processes and to study the evolutionary development of badland topography: (1) Topographic and drainage maps, made with plane table and telescopic alidade, were sufficiently detailed for measurement of all components of the drainage net with planimeter and chartometer. A statistical analysis of the data followed. (2) Stakes placed along stream and slope profiles permitted repeated measurements of erosion within selected basins. (3) Photography from selected stations, combined with remapping, gave information on changes within the system. (4) Experiments made upon samples of fill from the Perth Amboy area showed the effect of slope angle on sediment loss and upon size of entrained particles of the eroded material. (5) Comparative field studies were made in selected badland areas of the western United States.

Landforms are functions of structure, process, and stage; all differences in landforms can be explained through combinations of these factors. Geomorphologists have emphasized striking form differences but have neglected the importance of persistent similarities among forms of geologically and climatically diverse areas. The morphology of the small badland areas is remarkably similar to youthfully dissected areas of high relief such as the recently uplifted mountains of the West, or any region of recent uplift that has not been severely glaciated. Scale of topography may have less influence than other factors in the creation of distinctive features of the landforms.

The project's primary objective was to study the development and modification of badlands, but it may also be considered a type of large-scale model study, with the hope that some of the conclusions reached at Perth Amboy may be extended in a tentative way to larger areas.

Fenneman (1922, p. 126) suggested the value of such studies in developing an understanding of the development of erosional landforms:

"The physiographer's conception of the progressive dissection of peneplains, as of other plains, is based mainly on the growth of gullies. Rapid downcutting,

steep sides, V-shaped cross section, and branching enter most abundantly into his mental pictures of an upland of homogeneous material or horizontal rocks that is undergoing dissection, especially when erosion is vigorous."

Acknowledgments

This investigation formed part of a quantitative study of erosional landforms sponsored by the Geography Branch of the Office of Naval Research as Project Number NR 389-042 under Contract N6 ONR 271, Task Order 30, with Columbia University.

The writer wishes to thank Prof. A. N. Strahler, who sponsored the project, for the use of data collected at Perth Amboy before 1951, and for the topographic map of the area (Pl. 1). Professor Strahler and members of the Seminar in Geomorphology at Columbia University during the years 1952 and 1953 gave much valuable criticism and advice. Messrs. J. T. Hack, L. B. Leopold, H. V. Peterson, and M. G. Wolman of the U. S. Geological Survey, Prof. John Miller of Harvard University, and Professor Strahler read and offered valuable suggestions for improvement of the manuscript.

During the field season of 1952 Mr. Iven Bennett of Rutgers University acted as field assistant. M. Rossics and A. H. Schumm also helped in the field. Mr. A. Broscoe kindly furnished the drainage map of the Chileno Canyon drainage basin.

General Description of the Perth Amboy Locality

The Perth Amboy badlands, where most of the investigation was made, were located on the western boundary of Perth Amboy, New Jersey, on the north bank of the Raritan River between the two highway bridges over the river. The area was conspicuous because it was anomalous in the humid climate of New Jersey and resembled larger badlands of the more arid West (Pl. 2, figs. 1, 2, 3). The Perth Amboy badlands are not unique, however; badlands have developed elsewhere in humid climates. Rapid badland erosion is occurring in the Ducktown Copper Basin of Tennessee where 10½ square miles are devoid of vegetation because of destruction by smelter fumes. It is considered the largest bare area in any humid region of the United States (Hursh, 1948, p. 2). Similar erosion occurs where volcanic ash covers the surface sufficiently to destroy vegetation (Segerstrom, 1950).

All the erosion forms in this badlands area were developed after 1929 when waste and overburden from other pits backfilled the abandoned clay pit at this site, producing a bench or terracelike deposit 40 feet high whose steep front and gently sloping upper surface rapidly gullied. The terrace as a whole was still in a youthful stage at the beginning of this study. Alluvial fans had been built along its base (Pl. 2, fig. 1, 2). The easily eroded terrace might be considered the initial stage of landform development of the theoretical Davisian cycle, with the elevated flat-terrace surface representing a rapidly elevated peneplain. Similar small badlands have developed elsewhere in the area where removal of vegetation and Pleistocene deposits have exposed the soft Cretaceous Raritan clays.

Plans for continued field studies to observe the cycle of development were unfortunately concluded when the area was leveled for construction purposes in the summer of 1953.

Reports of the nearest weather station at New Brunswick, New Jersey, 8½ miles northwest, reveal that erosion up to 1948 was accomplished by a total of 844 inches of precipitation and that mean yearly precipitation was 43 inches (U. S. Weather Bureau, 1929–1948). These figures contribute to a statement of general climatic conditions but not to a quantitative evaluation of the effect of rainfall, because there are no data on the local intensities of precipitation during this period. Intensities here are not low, however, compared with storms in the badland regions of the West. The maximum intensities of precipitation of any storm over periods of time ranging from 2 to 100 years may be expected in the eastern portion of the humid regions of the United States (Yarnell, 1935). Undoubtedly the erroneous impression of higher intensities in the arid West is due to the destructive nature of runoff on sparsely vegetated slopes.

Temperatures during this period ranged from 0° to 95°F., indicating that frost heaving was probably important during the 5½ months between the first and last severe frosts. The east-

west orientation of the major drainage channels affects the microclimatic environment, subjecting the north- and south-facing slopes to different frequencies of freeze and thaw.

In spite of high precipitation the sterility of the fill and the rapidity of erosion prevented the growth of vegetation within the basin studied, except for one wild cherry tree and a small patch of poison ivy on the western drainage divide.

It may be suspected that frost heaving probably modifies the topography somewhat because the soil has moderate to objectionable frost-heaving characteristics and the low temperatures at Perth Amboy cause frequent freezing during the winter months.

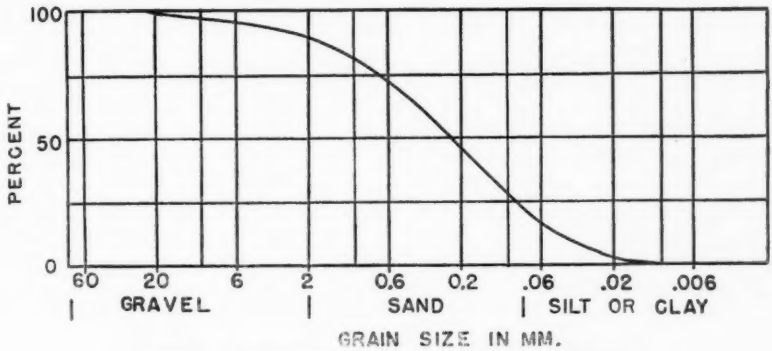

FIGURE 1.—GRAIN-SIZE DISTRIBUTION OF PERTH AMBOY FILL

The fill forming the terrace at Perth Amboy is essentially homogeneous and the topography shows no persistent control by structure or lithology. Mr. Richard Chorley of Columbia University made a grain-size analysis of the fill, showing that it is 67 per cent sand, 22 per cent silt and clay, and 11 per cent gravel. The almost equal amounts of silt and clay were determined by the low plasticity of the finer fraction of the sediment (Burmister, 1952, p. 102). A cumulative percentage curve was plotted for the sample (Fig. 1) and from this Hazen's "effective size", designated D_{10} by Burmister, was obtained. The quantity D_{10} is the grain size in millimeters for which 10 per cent of the material is finer. For the Perth Amboy fill D_{10} is 0.04 mm. Using this value the fill characteristics important to this study can easily be determined using Burmister's charts: (1) the drainage of the fill is fair with a coefficient of permeability approximately 0.004 cm/sec.; (2) the capillarity is moderate with an approximate rise of 5.0 feet; (3) the frost-heaving characteristics are moderate to objectionable.

The importance of the values for capillarity and permeability are apparent from Burmister's (1952, p. 83) statement that, during excavation, slopes seldom need to be cut flatter than 45° "in soils containing more than about 5% silt except where surface erosion of the slopes by the rapid runoff of rainwater is excessive." The 5 per cent silt causes enough capillary cohesion in the soil to maintain steep slope angles, and the permeability is low enough to aid runoff. Thus, steep slopes are maintained, but erosion is rapid.

The effect of capillary cohesion within the Perth Amboy fill makes the mean maximum slope angle for the area 48.8°, and thus the slopes are classified by Strahler (1950, p. 693) as high-cohesion slopes.

The drainage basin selected for intensive study was mapped in 1948 by Strahler and Coates of Columbia University on a scale of 1 inch equals 10 feet (Pl. 1). The contour interval is 1 foot. The drainage pattern was mapped with particular care so that all drainage-basin characteristics could be measured; all channels possessing recognizable drainage areas were considered permanent drainage features and mapped as such.

The drainage basin mapped was that of a fifth-order stream network. Streams are desig-

nated on the basis of orders; all unit or fingertip stream channels without tributaries are first-order streams (Horton, 1945, p. 281); the junction of two streams of the same order forms a stream of the next higher order.

In all the drainage basins studied the streams are assigned order numbers following the method outlined by Strahler (1952b, p. 1120) whereby the higher stream-order numbers are not extended headward to include smaller tributaries, but refer to segments of the main channel (Fig. 9). With the Horton classification, the higher stream-order numbers include the smallest headward extension of the main stream. Using Strahler's method, the two major channels joining at point H (Pl. 1) are third-order; using Horton's method, the south tributary would be the extension of the fifth-order channel and would be eliminated from studies involving third-order channels. This method will be referred to again in a discussion of channel lengths.

The fifth-order basin mapped includes 3531 feet of drainage channels within an area of 31,027 square feet. The drainage density (Horton, 1945, p. 283), equal to the sum of the channel lengths in miles divided by the area of the drainage basin in square miles, is 602, indicating that within an area of this type 602 miles of drainage channels occur for every square mile of drainage basin. This value is indicative of the fine texture of the area. Although the density is high compared to a typical value of 5 to 20 for humid regions, it is not high for badland topography.

Within the mapped area the first-, second-, and third-order stream basins show a transition from maturely developed topography near the mouth of the main stream, where the main channel has widened the valley until small segments of flood plain have developed, to progressively more youthful basins toward its head, where the tributaries are eroding into portions of the undissected surface of the fill.

The mean length of the first-order channels is 10.1 feet, and the mean drainage area is 85.0 square feet, indicating the small scale of the topography. The hypsometric integral (Strahler, 1952b) for the entire fifth-order network is 70 per cent, indicating that erosion has removed a minimum of 30 per cent of the total mass of the basin. This figure is reasonably accurate because the upper surface of the terrace into which the system developed is still preserved in the headwater areas. Although the terrace is not a natural deposit and the drainage is developing on a small scale, investigation of principles of drainage-network development is aided by knowledge of several factors not available in the study of the geomorphic evolution of other areas.

The homogeneity of the fill aided development of an insequent drainage pattern on the terrace. The rapid erosion developed youthful V-valleys with steep straight slopes descending from convex or sharp-crested divides. The longitudinal profile of the main channel, typical of streams growing headward into an upland surface, had a concave lower segment and an upper convexity where degradation was most rapid. Tributary profiles varied with stage from convex-up, where the streams were unable to maintain themselves against the rapid degradation of the main channel in the headwater areas, to concave-up where the main channel appeared to be at grade.

Stream-channel erosion with sheet and rill erosion on the slopes were the dominant geomorphic processes observed. Wind erosion was negligible, but frost action became important during the winter months.

Characteristics of the Drainage Network

Components of the Drainage Network

Morphometric studies of drainage-network components at Perth Amboy included measurements of all stream-channel lengths and drainage-basin areas for all stream orders, so that each component could be studied independently. Stream-order analysis permits comparison of the drainage network developed on the Perth Amboy terrace with patterns originating under natural conditions. Horton (1945) proposed certain laws of drainage composition which assume an orderly development of the geometrical qualities of an insequent drainage system. These laws were applied to data obtained from morphometric measurements on the Perth Amboy map (Pl. 1) to determine whether they conformed; if they did, conclusions from the Perth Amboy study might apply

to other larger areas. Geometry of two other fifth-order basins was measured for comparison with Perth Amboy basin (Table 2): Chileno Canyon basin (Chileno Canyon, California, quadrangle) and Mill Dam Run basin (Hughesville, Maryland, quadrangle).

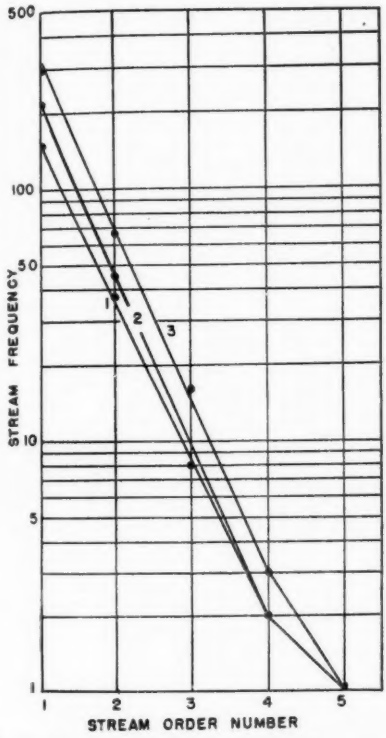

FIGURE 2.—RELATION OF NUMBER OF STREAMS OF EACH ORDER TO ORDER NUMBER
(1) Perth Amboy, (2) Chileno Canyon, (3) Hughesville area

The law of stream numbers, first of Horton's laws of drainage composition, is stated as follows (Horton, 1945, p. 291): "The numbers of streams of different orders in a given drainage basin tend closely to approximate an inverse geometric series in which the first term is unity and the ratio is the bifurcation ratio." If a geometric series exists, a straight-line series of points results where the numbers of streams of each order are plotted on a logarithmic scale on the ordinate against order numbers on an arithmetic scale on the abscissa. This has been done in Figure 2, in the manner of Horton's graphs. All three sets of points show a marked up-concavity at the lower end, suggesting that the geometric progression is not closely observed in the higher orders, but the Perth Amboy data show general similarity with the rest and there is no reason to believe that any fundamental dissimilarity exists.

TABLE 1.—METHOD OF DERIVING WEIGHTED MEAN BIFURCATION RATIO

1 Stream order	2 Number of streams	3 Bifurcation ratio	4 No. of streams involved in ratio	5 Products of columns 3 and 4
1	214			
		4.78	259	1238.0
2	45			
		5.63	53	298.4
3	8			
		4.00	10	40.0
4	2			
		2.00	3	6.0
5	1			

Total number of streams used in Col. 4 = 325.
Sum of products of Col. 5 = 1582.4.

Weighted mean bifurcation ratio = $\frac{1582.4}{325}$ = 4.87.

The weighted mean of the Perth Amboy bifurcation ratio is 4.87. Bifurcation ratio is the ratio of the total number of streams of one order to that of the next higher order (Horton, 1945, p. 280), *e.g.*, a basin with 20 second-order channels and 60 first-order channels would have a bifurcation ratio between these two orders of 3. Because of chance irregularities, bifurcation ratio between successive pairs of orders differs within the same basin even if a general observance of a geometric series exists. To arrive at a more representative bifurcation number Strahler (1953) used a weighted-mean bifurcation ratio obtained by multiplying the bifurcation ratio for each successive pair of orders by the total number of streams involved in the ratio and taking the mean of the sum of these values (Table 1).

The second law stated by Horton (1945, p. 291) concerns stream lengths: "The average lengths of streams of each of the different orders

in a drainage basin tend closely to approximate a direct geometric series in which the first term is the average length of streams of the first order."

lengths although the value of the length of the fifth-order stream is low in two cases Because integer values only are used for order numbers continued channel development might be ex-

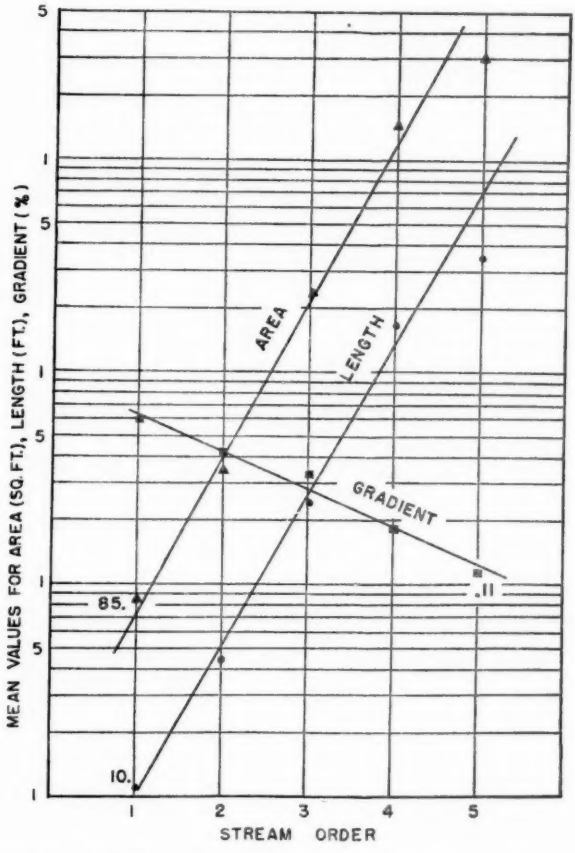

FIGURE 3.—RELATION OF MEAN BASIN AREA, MEAN STREAM LENGTH, AND MEAN STREAM GRADIENT TO STREAM ORDER

The length of streams of each order was obtained by measuring all the drainage channels within a basin of a given order; the length of the fifth-order stream at Perth Amboy is the total length of all the channels within the basin. This method differs from Horton's, but the total channel lengths may be more meaningful when considered within the area of each drainage basin. Using this method, however, the mean stream-length plots (Figs. 3, 5) for the Perth Amboy, Chileno Canyon, and Mill Dam Run systems adhere to Horton's law of stream

pected to raise the value of the fifth-order length, bringing it closer to the fitted regression line. The shortness of the fifth-order segment at Perth Amboy may be due to the truncation of the drainage pattern at the front of the terrace. In Figure 4 both the Hughesville and Perth Amboy drainage patterns have short fifth-order segments in comparison to that of the Chileno Canyon area. This may explain the low fifth-order channel lengths and areas for those two basins (Figs. 3, 5).

Horton's third law (1945, p. 295) states:

"There is a fairly definite relationship between slope of the streams and stream order, which can be expressed by an inverse geometric series law." The Perth Amboy stream slopes appear to conform (Fig. 3). In this case the gradient is obtained by dividing stream length measured from mouth to headwaters by the elevation difference.

Horton's laws may require revision because he obtained his data from old maps of small scale on which he measured as stream channels only the blue drainage symbols, thus omitting a large part of the first- and second-order channet network. His statements are sound, however, in the light of investigations made on modern topographic maps, either mapped for the purpose (Perth Amboy basin) or selected because of their large scale and detailed representation of topography (Hughesville and Chileno Canyons quadrangles). These undoubtedly afford data more precisely representative of the natural development of drainage systems than the old maps.

The writer compared the Hughesville and

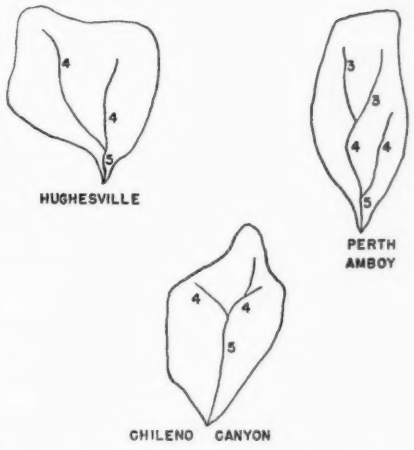

FIGURE 4.—COMPARISON OF SHAPE OF BASIN AND MAIN DRAINAGE ELEMENTS OF THREE AREAS
Numbers indicate order of main drainage channels

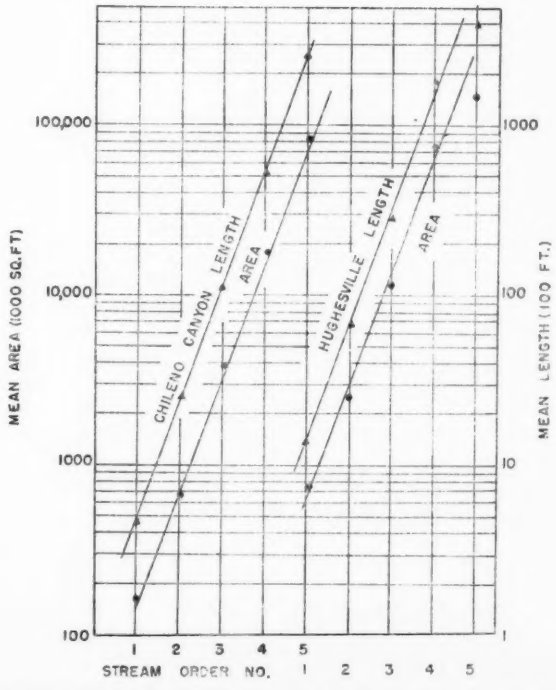

FIGURE 5.—RELATION OF MEAN BASIN AREA AND MEAN STREAM LENGTH TO STREAM ORDER

TABLE 2.—DRAINAGE-NETWORK CHARACTERISTICS

Basin	Order number	Number of streams	Mean length (ft.)	Mean area (sq. ft.)	Mean gradient (%)
Perth Amboy	1	214	10.1	85.0	59.9
	2	45	40.4	343	40.6
	3	8	242	2360	33.7
	4	2	1660	14600	18.2
	5	1	3530	31000	11.1
Chileno Canyon	1	296	482	167000	....
	2	66	2560	872000	....
	3	16	11400	3890000	....
	4	3	51100	18100000	....
	5	1	254000	86100000	....
Hughesville	1	150	1420	781000	....
	2	37	6860	2540000	....
	3	8	28400	12000000	....
	4	2	180000	78800000	....
	5	1	397000	154000000	....

length of channels close to the maximum value, perhaps obtainable only by detailed remapping in the field.

Further investigations included map measurement by polar planimeter of all drainage-basin areas. Horton (1945, p. 294) inferred that mean drainage-basin areas of each order should form a geometric series. A plot of the mean areas of stream basins of each order for the three basins compared above (Figs. 3, 5) reveals this relationship. A fourth law of drainage composition may therefore be formulated in the style set by Horton: the mean drainage-basin areas of streams of each order tend to approximate closely a direct geometric series in which the first term is the mean area of the first-order tasins. It could be assumed that such a relationship would exist if there were any connection between the length of a stream and the size of its drainage basin.

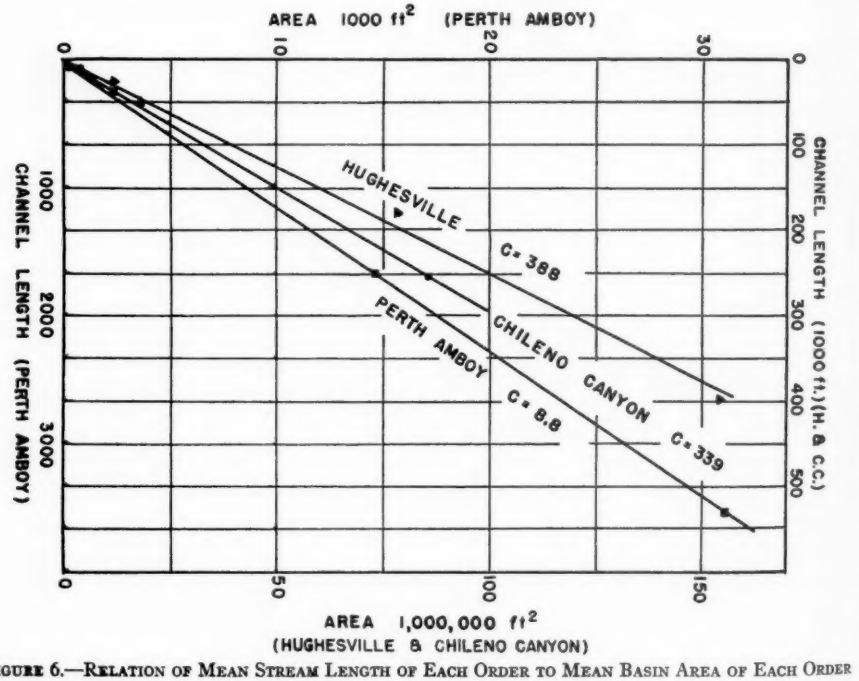

FIGURE 6.—RELATION OF MEAN STREAM LENGTH OF EACH ORDER TO MEAN BASIN AREA OF EACH ORDER

Chileno Canyon maps with aerial photographs so that the blue drainage lines could be extended to what appeared to be the correct length and small tributaries were also added to the drainage pattern. This method brought the

In Figures 3 and 5 the parallelism of the plots of mean stream length and mean drainage-basin area is striking and suggests a directly proportional relationship between the two. Figure 6 shows a plot of the mean drainage-basin areas

and mean stream-channel lengths for the three areas. The scatter of the Perth Amboy data is slight around a regression line fitted by the method of least squares and is described by the regression equation $Yc = 56.8 + 8.77X$. The ratio between mean area and length values is thus approximately 9. The calculated ratio for the Chileno Canyon basin is 339 and for the Mill Dam Run basin 388.

The significance of the ratio is that it represents in square feet the area required to maintain 1 foot of drainage channel. It is the quantitative expression of one of the most important numerical values characteristic of a drainage system: the minimum limiting area required for the development of a drainage channel. This value, *the constant of channel maintenance*, is a measure of texture similar to drainage density; it is in fact, equal to the reciprocal of drainage density multiplied by 5280 (because the channel-maintenance ratio is expressed in square feet while drainage density is expressed in miles). Along with drainage density this constant is of value as a means of comparing the surface erodibility or other factors affecting surface erosion and drainage-network development. A related texture measure is Horton's (1945) length of overland flow, the distance over which runoff will flow before concentrating into permanent drainage channels. The length of overland flow equals the reciprocal of twice the drainage density.

The discovery of the above relationship permits statement of a fifth law of drainage composition: the relationship between mean drainage-basin areas of each order and mean channel lengths of each order of any drainage network is a linear function whose slope (regression coefficient) is equivalent to the area in square feet necessary on the average for the maintenance of 1 foot of drainage channel. This law requires an orderly development of any drainage network, for the extension of any drainage system can occur only if an area equal to the constant of channel maintenance is available for each foot of lengthening drainage channel.

Limiting Values of Drainage Components

In addition to a lower limiting area necessary for channel maintenance there may be expected upper limits to basin areas and stream lengths of each order beyond which new tributaries or bifurcation occurs, forming new basins. These

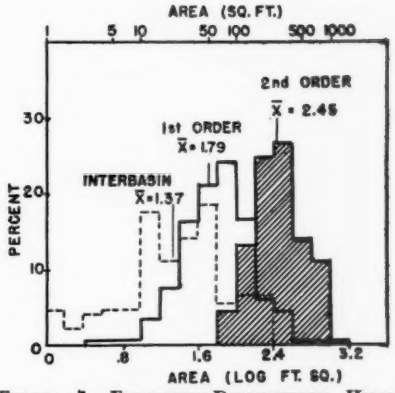

FIGURE 7.—FREQUENCY-DISTRIBUTION HISTOGRAMS OF THE LOGS OF DRAINAGE-BASIN AREA

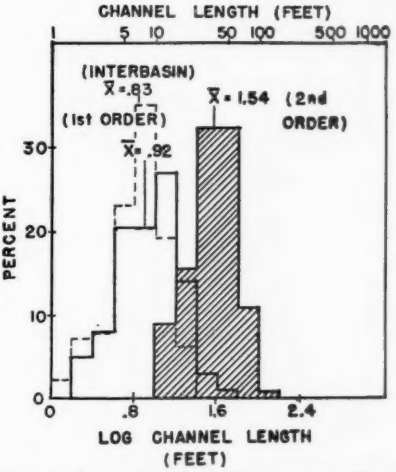

FIGURE 8.—FREQUENCY-DISTRIBUTION HISTOGRAMS OF THE LOGS OF STREAM-CHANNEL LENGTHS

relationships would appear in frequency-distribution histograms of the basin areas and stream lengths of each order and further confirm the principle of a channel-maintenance constant.

Frequency-distribution histograms of the stream lengths and basin areas show a marked right skewness, which appears to be corrected by plotting log values on the abscissa (Figs. 7, 8; Tables 3, 4). All measurements are made on a topographic map and are therefore taken from the horizontal projection of the drainage-basin elements rather than from true lengths and surface areas. Frequency-distribution study is limited to the first two orders by the small

number of streams in the third and higher orders. A study of the first- and second-order basin areas and interbasin areas may be adequate, however, to determine if a transition phase exists between orders.

TABLE 3.—FREQUENCY DISTRIBUTIONS OF LOGS OF CHANNEL LENGTHS*

Sample	Class mid-values in logs of lengths in feet										$\bar{X}$	s	N
	0.3	0.5	0.7	0.9	1.1	1.3	1.5	1.7	1.9	2.1			
First order channels	11	17	45	45	58	30	6	2	...	...	.92	.302	214
Second-order channels	...	...	...	...	4	7	14	14	5	1	1.54	.21	45

* In this and all following tables and figures, $\bar{X}$ is the arithmetic mean, s is the standard deviation, and N is the number of items in each sample.

Between adjacent drainage basins are *interbasin areas*, those roughly triangular areas which have not developed a drainage channel (Fig. 9), but which drain directly into a higher-order channel. The histograms of first- and second-order basin areas and interbasin triangular areas are superimposed in Figure 10 (Table 5); the histograms of first- and second-order stream lengths are compared with maximum interbasin-slope lengths in Figure 11 (Table 6). Figures 7 and 8 compare the histograms of the logarithms of basin area, channel length, interbasin areas, and interbasin maximum lengths. The discussion of limiting values of drainage components may be followed on either set of figures.

An overlap between the areas of each histogram suggests that transformation from first to second order takes place within a wide range of values. In Figure 10 interbasin areas show a sharp decrease in frequency for areas above 50 square feet, which is well below the mean of the first-order areas. Of the 27 interbasin areas over 50 square feet, 12 seemed capable of developing a channel at any time; the remaining 15 were irregular, wider than long, or were on rounded spurs where the divergence of orthogonals downslope prevents the concentration of runoff. From this investigation alone it is difficult to set limiting area above which channel development may be expected on the interbasin areas, especially since the comparison of triangular interbasin areas with elliptical first-order basins is questionable.

Areas of first-order basins rise sharply at the 10-square-foot class limit. Two first-order basins of less than 10 square feet were mapped by Strahler and Coates, but a field check revealed that these did not contain permanent drainage channels. The fact that areas of less than 10 square feet are remarkably free of drainage channels coincides with the concept of a constant of channel maintenance of about 9 (8.77). Thus, no permanent channel will develop without a drainage area of about 10 square feet, while the channel can lengthen only with the average increment of 9 square feet of area for each additional foot of length.

TABLE 4.—FREQUENCY DISTRIBUTIONS OF LOGS OF DRAINAGE-BASIN AREAS

Sample	Class mid-values in logs of area in square feet															$\bar{X}$	s	N
	0.3	0.5	0.7	0.9	1.1	1.3	1.5	1.7	1.9	2.1	2.3	2.5	2.7	2.9	3.1			
First-order areas	...	2	2	6	17	34	45	50	34	12	8	1	1	1	...	1.79	.19	214
Second-order areas	...	...	...	...	..	..	..	..	2	7	11	12	7	5	1	2.45	.284	45

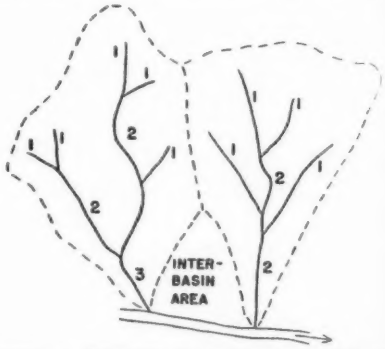

FIGURE 9.—POSITION OF INTERBASIN AREA AND METHOD OF CLASSIFYING STREAMS BY ORDER NUMBER

Most of the overlap between the first- and second-order areas falls between 50 and 150 square feet, although some first-order areas range up to 650 square feet. Again an inspection

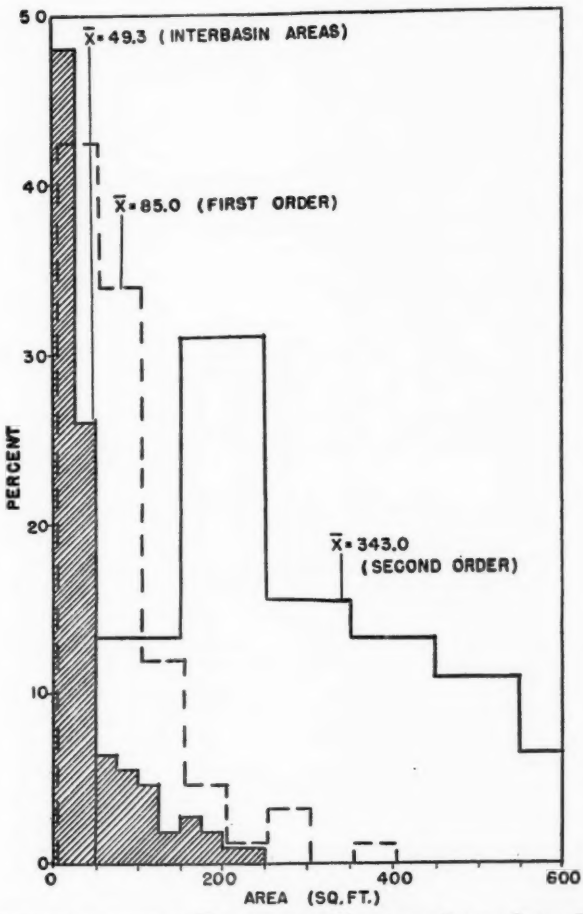

FIGURE 10.—FREQUENCY-DISTRIBUTION HISTOGRAMS OF FIRST- AND SECOND-ORDER BASIN AREAS AND INTERBASIN AREAS

TABLE 5.—FREQUENCY DISTRIBUTIONS OF FIRST- AND SECOND-ORDER DRAINAGE-BASIN AREAS AND INTERBASIN AREAS

Sample	Class mid-values in square feet															
Mid-values	30	80	130	180	230	280	330	380	430	480	530	580	630	$\bar{X}$	s	N
First-order areas	91	73	26	10	3	7	0	2	0	0	0	1	1	85	80	214
Mid-values	100	200	300	400	500	600	700	800	900	1000	1100	...	...	...	...	...
Second-order areas	6	14	7	6	5	3	2	0	1	0	1	...	...	343	218	45
Mid-values	12.5	37.5	62.5	87.5	112.5	137.5	162.5	187.5	212.5	237.5	..	...	...	...	...	...
Interbasin areas	51	28	7	5	5	3	4	3	1	1	..	...	...	49.3	49	108

of individual basin characterstics within the zone of histogram overlap is profitable. Of the 46 first-order areas greater than 110 square feet, 29 are of very youthful basins including basins it seems a fair generalization that first-order channels with areas greater than 100 square feet are unstable and ready for subdivision.

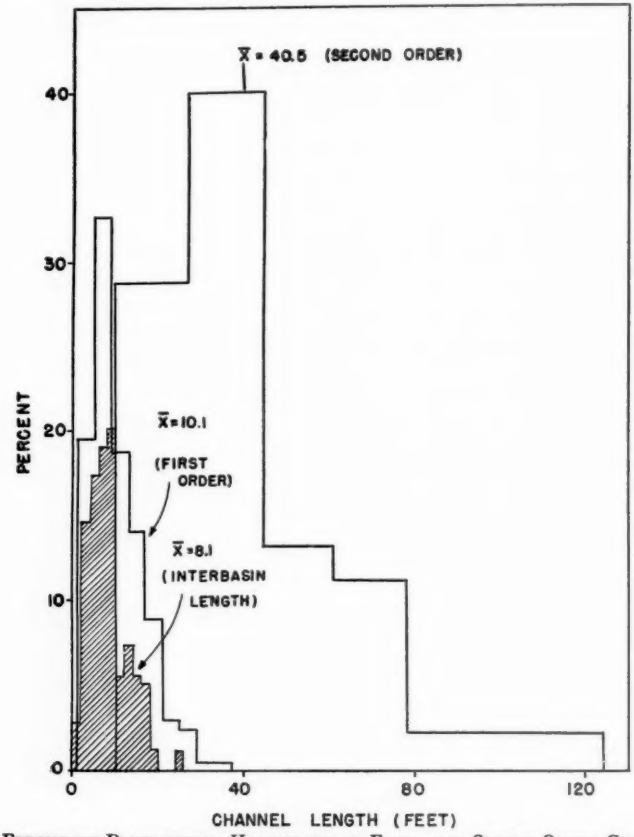

FIGURE 11.—FREQUENCY-DISTRIBUTION HISTOGRAMS OF FIRST- AND SECOND-ORDER CHANNEL LENGTHS AND MAXIMUM INTERBASIN LENGTHS

broad, gently sloping surfaces with only traces of channels on the flat undissected divide areas. With further development these would evolve to a higher order, for their longitudinal profiles are still essentially convex-up, retarding rapid tributary extension into their headwater areas. Thirteen of the 46 are narrow almost rill-like basins unable to broaden because of adjacent more aggressive basins. The remaining 4 of the 46 first-order basins larger than 110 square feet have no obvious reason for not developing into second-order channels. Although it is difficult to explain peculiarities of individual drainage

The smallest second-order channel area is 65 square feet. The class limits of the second-order areas within the overlap are 50 and 150 square feet (Fig. 10). Within this size range are six second-order basins which have developed tributaries recently and are capable of enlarging by headward extension so that the lowest-frequency class of the second-order area histogram would disappear unless replaced by new units created by bifurcation of first-order channels. Youthfulness of the entire system at Perth Amboy prevents the recognition of narrow transition zones between orders. A similar study in a

fully extended mature drainage system might show sharper distinctions.

In accordance with the fifth law of drainage composition, stream-length frequency distributions are similar to the area distributions. Maximum interbasin-slope lengths cannot be directly compared to actual stream lengths because a channel developing on the interbasin surface will not extend the entire length of the slope. Nevertheless, a sharp drop in frequency at 10 feet suggests that at lengths above this runoff surfaces are unstable in form and will tend to develop channels (Fig. 11). Twenty-six interbasin areas with lengths greater than 10 feet had no channels. Seven were very narrow with little drainage area. The remaining 19, as previously noted under the discussion of interbasin areas, are irregular or on rounded spurs, while 4 seem capable of developing channels.

The lower values for first-order stream lengths are not significant because all channels must originate from a point and then lengthen. The region of transition between first- and second-order stream lengths lies between 9 and 17 feet, but 17 feet is not the upper limit of first-order lengths. Of 27 streams longer than 17 feet, 20, within basins considered previously under the discussion of areas, were in very youthful or narrow basins; the remaining 7 seemed capable of change. All but 1 of the 12 second-order channels between 10 and 17 feet will continue to develop, eliminating these streams from the frequency class. Youthfulness of the area probably masks a more distinct transition zone.

Within the Perth Amboy drainage network there are recognizable limits to the areas and lengths of streams of each order. First-order streams have an upper limiting length between 9 and 17 feet and an upper limiting area between 65 and 110 square feet. The limited number of stream orders considered and the subjective evaluation of parts of the data make it more appropriate to set a lower limit below which higher orders cannot exist. The first-order streams require more than 10 square feet for development; second-order streams will not normally evolve from first orders until the drainage area is equal to 65 square feet and the first-order channel is longer than 10 feet.

The writer remapped the drainage pattern in 1952 and compared it with the pattern mapped in 1948, aiding the study of channel alterations within the zones of transition. In all cases the addition of channels occurred only in basins above the size limits set from the frequency-distribution analysis. No channels developed on areas less than 10 square feet. Four new channels developed on interbasin areas, all but one (46.5 sq. ft.) greater than 50 square feet. Twelve new tributaries developed on first-order channels, forming several new second-order basins. Each new basin was youthful (developing headward into the as yet undissected fills), and almost all exceeded 110 square feet. Four were within the transition zone between first- and second-order areas. The newer field study, therefore, seems to confirm the existence of the zones of transition and upper limiting values of development related to the constant of channel maintenance. The constant of channel maintanence, therefore, may be applied to the as yet undissected portions of a drainage system to aid in the prediction of areas of future sediment loss.

TABLE 6.—FREQUENCY DISTRIBUTIONS OF FIRST- AND SECOND-ORDER CHANNEL LENGTHS AND INTERBASIN LENGTHS

| Sample | Class mid-values in feet | | |

Form of the Drainage Basins

In addition to indices of drainage-network composition based on stream orders other important geomorphic characteristics are shape of the basins, relief, surface slope, drainage density, and stage of geomorphic development. Geomorphic development can be evaluated by means of the hypsometric integral (Strahler, 1952b). If each characteristic had a numerical value, comparisons could be made between topographic units. It may be appropriate to set up standards of comparison from the available information which can be modified later or rejected if unacceptable.

Relief is analyzed by a *relief ratio*, defined as the ratio between the total relief of a basin (elevation difference of lowest and highest points of a basin) and the longest dimension of the basin parallel to the principal drainage line. This relief ratio is a dimensionless height-length ratio equal to the tangent of the angle formed by two planes intersecting at the mouth of the basin, one representing the horizontal, the other passing through the highest point of the basin. Relief ratio allows comparison of the relative relief of any basins regardless of differences in scale of topography. Recent field studies, however, reveal that residuals or abnormally high points on the divide should be ignored when obtaining the total relief of a basin (Hadley and Schumm, In preparation).

The shape of any drainage basin is expressed by an *elongation ratio*, the ratio between the diameter of a circle with the same area as the basin and the maximum length of the basin as measured for the relief ratio. This ratio is the same as the Wadell sphericity ratio used in petrology (Krumbein and Pettijohn, 1938, p. 284), where the ratio approaches 1 as the sediment grain, or in this case the shape of the drainage basin, approaches a circle. Miller (1953, Ph.D. dissertation, Columbia University) used a similar measure, the *circularity ratio*, which is the ratio of circumference of a circle of same area as the basin to the basin perimeter.

Table 7 compares Strahler's data (1952b, p. 1134) on five mature drainage basins with the writer's data obtained from the more youthful Perth Amboy and Hughesville areas and the Chileno Canyon area.

The writer compared relief ratio and drainage density for fourth- and fifth-order channels (Fig. 12, Table 7) and found a definite positive trend in the mature basins. Points for the youthful Hughesville and Perth Amboy basins displace upward to positions well above the trend line. When the values for the individual third-order basins of each of the two youthful areas are plotted (Fig. 13), the points show a positive trend similar to the plot of the mature basins. Thus, within homogeneous areas of similar development the drainage density is a power function of the relief ratio.

TABLE 7.—DRAINAGE-BASIN CHARACTERISTICS

Area	Drainage density (miles/sq. mi.)	Relief ratio	Elongation ratio	Gradient (%)	Mean maximum slope angles (%)
1. Gulf Coastal Plain	4.6	.008	.975	0.33	5.9
2. Piedmont	6.9	.025	.935	1.13	17.5
3. Ozark Plateau	13.8	.062	.692	3.52	53.7
4. Verdugo Hills	26.2	.245	.594	22.46	99.0
5. Great Smoky Mts.	14.2	.267	.760	12.33	86.7
6. San Gabriel Mts.	15.6	.220	.675	17.2	73.4
7. Hughesville	13.6	.006	.730	0.22	7.0
8. Perth Amboy	602.0	.117	.602	11.1	110.8

In Figure 14 the relief ratio shows a close correlation with stream gradient. The gradient values are means for the entire stream length and thus would approach the value of the relief ratio if the stream length was measured to the drainage divide. In general, the gradient so measured will be less than the relief ratio, for meandering or the usual lack of straightness of a channel will increase the stream length beyond the drainage-basin length.

Valley-side slope angles are also clearly related to the relief ratio. In Figure 15 three values would lie well to the right of a line fitted to the other points. This may be the result of obtaining the mean slope values from topographic maps in these cases; all the data were not measured in the field, and slopes measured on maps usually are lower than field measurements (Strahler, 1950, p. 692).

In Figure 16 the shape of the drainage basin is plotted against relief. The trend is negative

and may indicate that as the relief ratio increases the drainage basin becomes more elongate. The data are not conclusive, but the steeper the slope on which small basins develop the more closely spaced are the drainage channels, resulting in more elongate basin shapes.

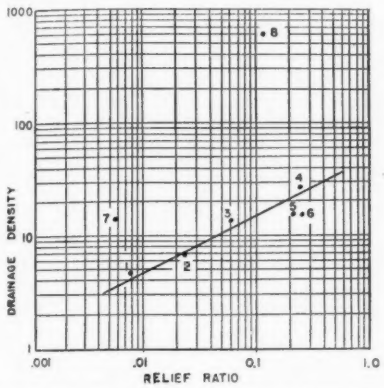

FIGURE 12.—RELATION OF DRAINAGE DENSITY TO RELIEF RATIO
Numbers refer to basins described in Table 7

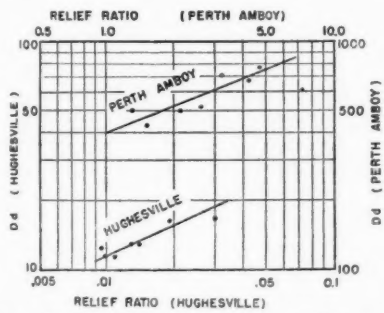

FIGURE 13.—RELATION OF DRAINAGE DENSITY TO RELIEF RATIO OF THIRD-ORDER BASINS

One practical application of the relief ratio is in estimation of sediment loss. Figure 17 shows the direct relation between mean relief ratio for several areas in Utah, New Mexico, and Arizona and mean annual sediment loss as estimated from sedimentation in small stock reservoirs. Once the characteristic regression trend has been established for a region the investigator may select areas of high potential sediment production from topographic maps (Schumm, 1955).

Various interrelationships among drainage-basin characteristics have been previously determined. Langbein (1947, p. 125) states that steep land slopes are generally associated with steep channel slopes and fine texture, and that

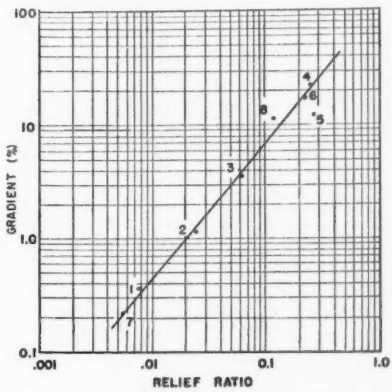

FIGURE 14.—RELATION OF MEAN STREAM GRADIENTS TO RELIEF RATIO
Numbers refer to drainage basins described in Table 7

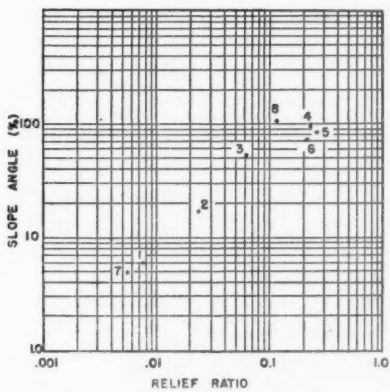

FIGURE 15.—RELATION OF MEAN MAXIMUM-SLOPE ANGLES TO RELIEF RATIO
Numbers refer to drainage basins described in Table 7

altitude of a basin above its outlet increases with steepening land and channel slopes. Paulsen (1940, p. 440) found that infiltration increases with decrease in mean land slope, explaining in part the increase of sediment loss with the relief ratio. Strahler (1952b, p. 1136) observed that the hypsometric integral de-

creased as basin height, slope steepness, gradient, and drainage density increased.

Although more data are desirable the relationships observed suggest that the geomorphic character and even rates of erosion may be predicted from the relief ratio, although it is only a geometrical element which is probably related to lithology, structure, stage, vegetation, and climate.

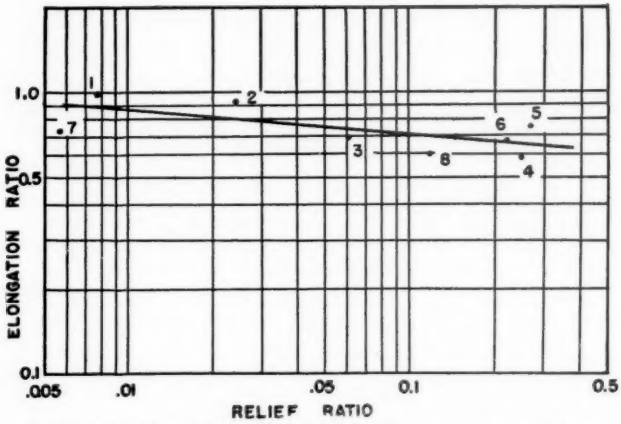

FIGURE 16.—RELATION OF ELONGATION RATIO TO RELIEF RATIO
Numbers refer to drainage basins described in Table 7.

The above relationships when considered in the light of recent discussions of the quasi equilibrium between the hydraulic and geomorphic characteristics of stream channels (Leopold and Maddock, 1953; Wolman, 1955; Leopold and Miller, in press) suggest that when more information becomes available this concept of quasi equilibrium in graded and ungraded stream channels may extend to the landforms adjacent to the stream channels, and close interrelationships may be found among the geomorphic, hydrologic, and hydraulic characteristics of a topographic type.

Basin Form Related to Geomorphic Stage of Development

During geomorphic development basin forms change with time. According to the classic Davisian analysis, relief, slope of valley walls, stream gradients, and drainage density increase rapidly during youth to a maximum in early maturity, then decline slowly throughout later maturity and old age. A unique opportunity to study stage changes was afforded by the developmental sequence of drainage basins tributary to the main channel at Perth Amboy. Eleven second-order drainage basins forming a sequence from earliest youth to late maturity were selected for map study and a comparison of hypsometric integrals. The hypsometric integral is a measure of stage (Strahler, 1952b) because it expresses as a percentage the mass of the drainage basin remaining above a basal plane of reference.

Figure 18 shows hypsometric curves plotted for each basin in the sequence. Data are obtained from the topographic map by measuring the total area of each basin with a planimeter, then measuring the area between each contour and the basin perimeter above it. Each area is converted into a percentage of total basin area, so that a cumulative percentage curve can be plotted, each area value corresponding to a percentage of the total height of the basin. Using this hypsometric curve it is possible to read the percentage of total basin area above any percentage of total height. The area-altitude relations of the basin are thus revealed by a curve illustrating in dimensionless co-ordinates the distribution of mass within the drainage basin (Langbein, 1947, p. 140; Strahler, 1952b). Area under the hypsometric curve is the hypsometric integral, expressed as per cent.

An integral of 60 per cent indicates that erosion has removed 40 per cent of the mass of the basin between reference planes passing through summit and base. Strahler (1952b) discussed in more detail the hypsometric curve and its use in geomorphic research.

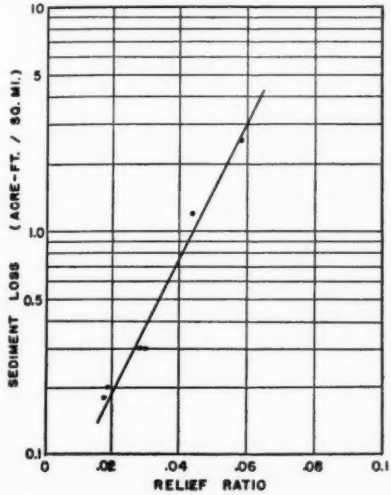

FIGURE 17.—RELATION OF MEAN ESTIMATED ANNUAL SEDIMENT LOSS TO RELIEF RATIO

From the U. S. Geological Survey studies of reservoir sedimentation in New Mexico, Arizona, and Utah

The 11 second-order basins selected for this study were of approximately the same area so that the series of hypsometric curves illustrate basin development with time accompanying lowering of the main channel through 40 feet of total relief. The convex curves with high integrals (Fig. 18) reveal youthful inequilibrium; the curves of more mature basins show the beginning of the typically mature sigmoid curve. The percentage curves cannot show continued down-wasting of the basin, because when maturity is reached curves tend to stabilize between integrals of 40 and 60 per cent. Strahler uses this stable integral as the point of onset of the equilibrium stage of drainage-basin development. Only basins containing monadnocks of resistant rock develop integrals markedly less than 40 per cent.

A better picture of the sequence of natural basin changes in terms of total erosional reduction may be obtained by plotting percentage of area against percentage of total elevation of the terrace at Perth Amboy rather than against

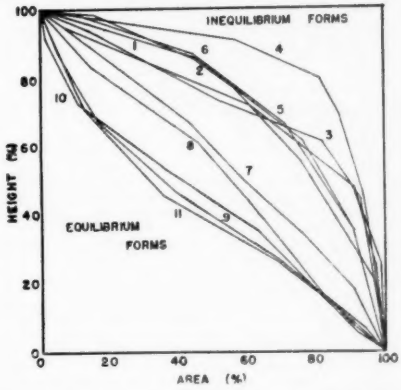

FIGURE 18.—SEQUENCE OF SECOND-ORDER HYPSOMETRIC CURVES

From Perth Amboy.

Numbers increase from youthful to mature basins

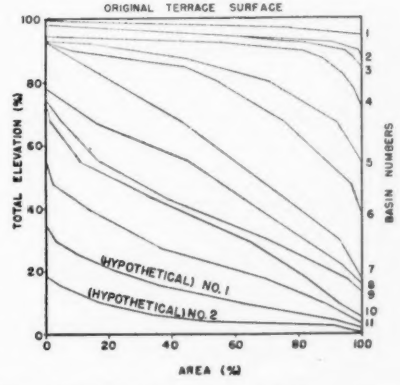

FIGURE 19.—SEQUENCE OF SECOND-ORDER HYPSOMETRIC CURVES

Per cent area is plotted against per cent of total relief at Perth Amboy. Numbers increase from youthful to mature basins and are the same areas as shown in Figure 18.

total relief within each basin. This method (Fig. 19) is more satisfactory because the square in which the curves are plotted may be visualized as a vertical section through the entire terrace at Perth Amboy. Each curve occupies its true relative vertical position within that mass and reveals the degradational history of

the basin. The 100 per cent elevation line should be visualized as the upper surface of the terrace, the base as the level of the main stream's mouth. The right edge of the chart is the locus of points of junction of second-order tributaries with some higher-order stream. Each line represents the distribution of mass within a second-order basin at a different stage of development, the position of its mouth controlled by the degrading stream to which it is tributary.

TABLE 8.—DRAINAGE-BASIN CHARACTERISTICS OF THE SECOND-ORDER SEQUENCE

Basin number	Per cent mass removed	Relief ratio	Elongation ratio	Gradient (%)	Drainage density (mi./sq. mi.)
1	2.4	.049	.993	4.0	553
2	4.9	.121	.648	14.4	504
3	5.6	.158	.595	18.6	270
4	9.5	.156	.645	21.8	241
5	17.2	.330	.783	42.0	672
6	23.5	.575	.725	52.0	560
7	39.8	.590	.507	58.3	610
8	50.8	.660	.473	67.5	895
9	60.8	.710	.474	65.5	1230
10	64.6	.620	.478	51.5	1150
11	77.0	.690	.530	50.7	1320

To determine the nature of basin-form changes with time, or stage of evolution, an important index is the percentage of mass removed at each position in the sequence of basins. This value, obtained by measuring the area above each curve and comparing it to the total area of the diagram, is a measure of the mass removed in relation to the total available for removal.

Percentage of mass removed, relief ratio, stream gradient, basin shape, and drainage density were determined for each of the 11 basins whose curves are drawn in Figure 19. The data for each basin in the sequence (Table 8) are plotted against corresponding per cent of mass removed (Fig. 20). The plot of relief ratio with per cent removed (A) reveals that with initial dissection the relative relief rapidly increases. A sharp break in the continuity of the plot occurs when approximately 25 per cent of the mass of the basin is removed, after which the relief ratio remains almost constant to 80 per cent of mass removed; beyond 80 per cent, data are lacking.

The stream-gradient plot (B) shows a similar form. The rapid increase in gradient is checked at approximately 25 per cent of mass removed; a decrease in gradient sets in at the upper part of the plot after a maximum value reached at 50 per cent removal. This agrees with the typical descriptive concept of stream development, but, in comparison to the rapid early increase in gradient, the portion of the plot above 25 per cent is essentially constant.

Maximum slope angles were not obtained for each basin, but, because these values cluster closely about a mean value for any homogeneous area (Strahler, 1950, p. 685), and because the close relationship between stream gradients and maximum slope angles has been established (Strahler, 1950, p. 689), any plot of slope angles and mass removed would be expected to approximate the gradient curve.

The relationships of basin shape and drainage density to stage (Fig. 20C, D) are less clear, but after early variations in which the basin is close to a circular shape the influence of increased relief is felt and the elongation ratio decreases to a constant of about 0.5 at 40 per cent mass removal, indicating that the basin maximum length is twice the diameter of a circle of the same area. The drainage-density plot is not regular, probably because of a high degree of length variability in the low order of the streams used. Nevertheless, the plot suggests rapid early increase in drainage density, followed by a decreasing increment. Probably continued headward development of the drainage channels continues until late in the erosion cycle, lagging behind the early stability of other basin characteristics. If other series of basins could be studied similarly, the additional data might lead to the establishment of a general system of basin evolution.

In summary, the form of the typical basin at Perth Amboy changes most rapidly in the earliest stage of development. Relief and stream gradient increase rapidly to the point at which about 25 per cent of the mass of the basin has been removed, then remains essentially constant. Because relief ratio elsehwere has shown a close positive correlation with stream gradient, drainage density, and ground-slope angles, stage of development might be expected

to have little effect on any of these values once the relief ratio has become constant.

The Perth Amboy data thus support the concept of a steady state of drainage-basin development as outlined by Strahler (1950, p. 676)

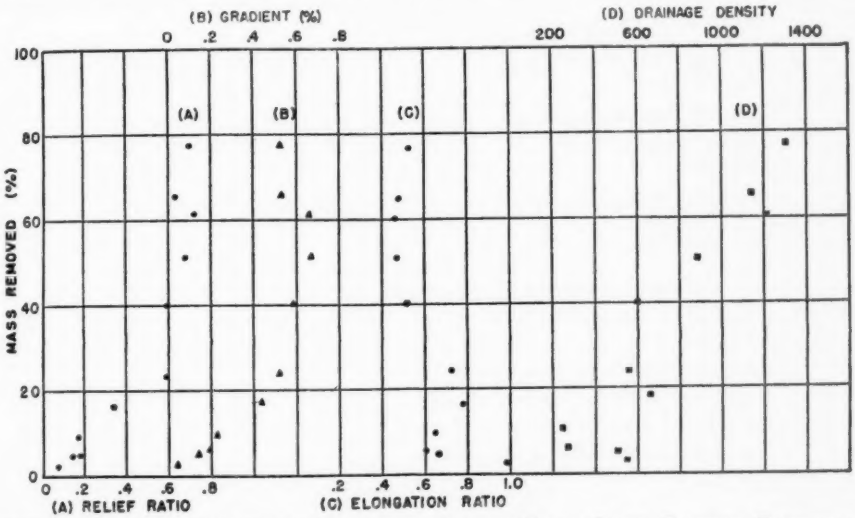

FIGURE 20.—RELATION OF MASS REMOVED WITHIN A BASIN TO RELIEF RATIO, GRADIENT, ELONGATION RATIO, AND DRAINAGE DENSITY

who compares a graded drainage system with an open dynamic system in a steady state:

"In a graded drainage system the steady state manifests itself in the development of certain topographic form characteristics which achieve a time-independent condition. (The forms may be described as "equilibrium forms"). Erosional and transportational processes meanwhile produce a steady flow (averaged over periods of years or tens of years) of water and waste from and through the landform system. . . . Over the long span of the erosion cycle continual readjustment of the components in the steady state is required as relief lowers and available energy diminishes. The forms will likewise show a slow evolution."

This hypothesis of time-independent forms and basin characteristics is supported by the constancy of the values of the basin parameters in the Perth Amboy sequence of second-order basins, once the amount of mass removed has exceeded 25 per cent.

EVOLUTION OF THE DRAINAGE NETWORK

Effect of Stage on Angles of Junction

In the early stage of basin development stream channels grow headward until they establish major drainage divides; the relief ratio then reaches a fixed value, but changes in channel network continue until a large portion of the basin mass is removed. Thus, the relief ratio becomes fixed before other network characteristics become constant. This is especially true of drainage density in the Perth Amboy area.

Angles of junction of tributaries, resurveyed in 1952, showed some marked differences from corresponding angles in the 1948 map. The writer reasoned that systematic changes were occurring in the drainage pattern as a normal part of the erosional development of the basins. Horton (1945, p. 349) recognized that the course followed by a new tributary is governed by both the slope of the ground over which it flows and the gradient of the channel to which it is tributary. Where the ground slope is great in relation to the gradient of the master stream a tributary joins at almost right angles; where master-stream gradient and valley-side slope are almost the same the tributary almost parallels the main channel, joining it at a small angle. Horton expresses this as follows:

$$\cos Zc = \tan Sc / \tan Sg$$

where the cosine of the entrance angle or angle of junction, measured between the tributary and main channel above the point of junction,

equals the ratio of the tangent of the main channel gradient to the tangent of the gradient of the tributary stream or of the ground slope over which the tributary flows. It follows that during the early part of basin development, stream-entrance angles change with stream gradients.

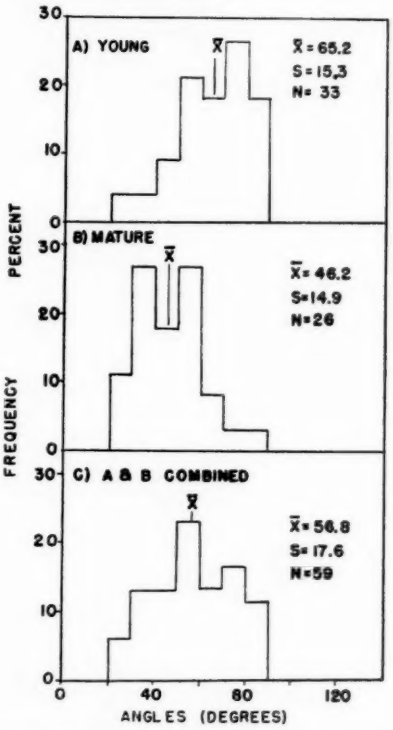

FIGURE 21.—FREQUENCY-DISTRIBUTION HISTOGRAMS OF YOUNG, MATURE, AND COMBINED ANGLES OF JUNCTION

Thus, a tributary will develop with an initially large angle of junction; then as the ratio between the two gradients increases the angle of junction decreases. Horton notes that as the ratio increases from 0.3 to 0.9 angles decrease from 72.3° to 25.5°. The decrease is accomplished by lateral migration of the tributary toward the main channel and down-valley shift of the junction.

The writer measured 61 entrance angles on the 1948 Perth Amboy map. The frequency-distribution histogram is broad and flat-topped with angles ranging from 24° to 90° (Fig. 21C; Table 9).

If the assumed changes occur, then by classifying all entrance angles according to stage of development of their tributary drainage basins a significant difference should occur between the means of youthful and more mature basins. The basins were separated into two groups on the basis of the existence of flat, undissected areas within the drainage areas, classifying as young basins capable of headward extension or having undissected areas within their drainage areas. The frequency-distribution histograms of each group (Fig. 21) show an expected overlap, but the means of the two groups are significantly different as judged by a *t*-test. The mean of the youthful class is 65°, that of the older group 46°. The probability that such a difference or greater would occur by chance alone is about 1 in 10,000. A reasonable explanation of the observed difference in angles is the shifting of tributary channels in response to changes in the gradient ratio.

TABLE 9.—FREQUENCY DISTRIBUTIONS OF ANGLES OF JUNCTION

Sample	Class mid-values in degrees							$\bar{X}$	s	N
	25	35	45	55	65	75	85			
Combined angles	4	8	8	14	8	10	7	56.8	17.6	59
Mature angles	3	7	5	7	2	1	1	65.2	15.3	26
Young angles	1	1	3	7	6	9	6	46.2	14.9	33

A similar test was applied to angles of bifurcation, defined as the angles between two approximately equal first-order branches. In this case, the stream has bifurcated at its upper end, whereas in the tributary junction referred to above a branch has grown from the trunk of an existing major drainage line. Twenty angles of bifurcation were measured from youthful drainage basins having undissected areas. The mean is 62.1°, compared with the mean of the youthful angles of tributary junction, 65.2°. The frequency distributions of both samples have such great dispersions that this observed difference in means is not significant.

Remapping of the drainage pattern revealed changes in the values of tributary entrance angles and angles of bifurcation. Table 10 shows data for mean entrance angles and angles of bifurcation measured from the 1948 and 1952 drainage maps. There is a decrease of 5.3° in the

TABLE 10.—ANGLES OF BIFURCATION AND ANGLES OF JUNCTION

	Mean angles (degrees)		Standard deviation (s)		Number in sample (N)	
	1948	1952	1948	1952	1948	1952
Angles of bifurcation	62.1	53.3	13.4	17.5	20	12
Angles of junction:						
Total	56.8	53.6	17.6	18.5	59	46
Young	65.2	59.9	15.3	17.1	33	29
Mature	46.2	43.0	14.9	14.9	26	17

mean of the youthful tributary-junction angles, but the standard deviation of each distribution is so large that a statistical test of the significance of difference between the means shows that such a difference would be expected through chance alone 20 per cent of the time and is not significant. This is true also of the difference between the mature angles, 3.2°.

The means of the young angles in both 1948 and 1952 are significantly different from those of the mature angles. It is interesting to note that the means for the total, youthful and mature angles decreased by several degrees during the 4-year period. The difference in each case is not statistically significant but suggests that with more time a significant change might occur.

Only the angles of bifurcation showed a significant reduction, 8.8°, between 1948 and 1952. Only 12 of the 20 original angles could be recognized and measured in 1952. The extreme youthfulness of the newly formed drainage basins, with rapid lowering of channel gradients in progress, is the cause of the great change in bifurcation angle.

A comparison of the drainage patterns showed marked drainage changes. Twelve new tributaries were added to the drainage system between mappings. Coincidentally, 12 others were eliminated, 6 by abstraction or lateral expansion of a more competent neighbor, 2 by angle reduction to the minimum with collapse of the divide and union of the streams, while the remaining 4 were in small, shrinking basins surrounded by headward-growing channels. Two of these channels were originally near the lower limiting area of channel formation, 11.8 and 15.3 square feet. It is interesting to note that both stages of Glock's (1931) drainage-development series are represented here: extension and integration, with abstraction as the major process of integration. Capture occurred in two other instances. Examples of the straightening of the stream channels were numerous.

One other change of pattern noted is the lateral shift of the major tributaries toward the center of the basin. This migration toward a common axis within the system is gradual, but the asymmetry of all high-order transverse-valley profiles testifies to its presence.

A series of drainage patterns traced from the 1948 and 1952 maps (Fig. 22) illustrates some of the changes during that period. The basins illustrated have steep channel gradients, and erosion would be rapid. In addition, the fill is easily eroded and presents few structural obstacles to drainage-channel modifications.

The following generalizations summarize changes in the drainage network at Perth Amboy: A tributary to a channel of higher order develops with an entrance angle dependent on the ratio between channel and ground slope. Because of relatively slower degradation of the main channel, a downstream migration of the point of junction occurs with lessening of the entrance angle. If the ratio between main-channel gradient and tributary gradient remains constant (steady state), no changes in junction will occur except those caused by chance structural irregularities in the fill. As channel gradation spreads throughout the entire system the main-channel gradient will first reach an essentially constant value, but the tributary gradient will continue to lower, with a lessening of the junction angle. When the junction angle becomes very small, lateral planation removes the intervening divide, and the junction migrates upstream. Comparable evolution of stream-entrance

angles and drainage patterns in other regions may occur only in youthful areas with a high relief ratio, but similarities between Perth Amboy and other areas in other aspects of drainage-basin morphology suggest that similar

In the initial stage the steep front of the terrace was probably strongly rilled. Because the upper surface of the terrace drained toward the front the rills quickiy advanced across the lip of the terrace onto the essentially flat upper

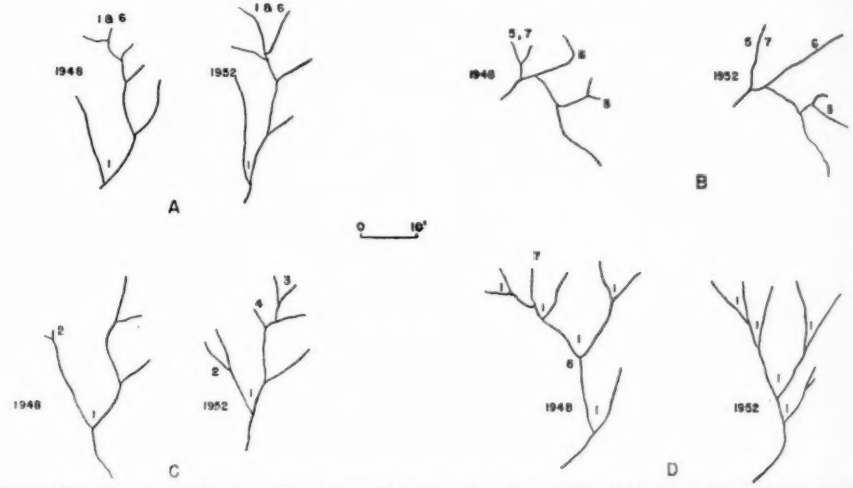

FIGURE 22.—DRAINAGE-PATTERN CHANGES IN SELECTED BASINS BETWEEN 1948 AND 1952 AT PERTH AMBOY

Basins A, C, and D are steep gradient streams. Basin B is a youthful basin on the upper surface of the terrace. Drainage changes are indicated by numbers on the figures:

1 Angle of junction change
2 Migration of junction
3 Bifurcation
4 Addition of tributary
5 Angle of bifurcation change
6 Channel straightening
7 Elimination of tributary

changes although perhaps less obvious, are nevertheless slowly occurring in all expanding drainage systems.

Because the observed drainage-pattern changes were occurring mainly as the stream channels were rapidly downcutting, any uplift of a land surface might initiate the same changes. Studies of drainage patterns on the Pleistocene terraces of the Atlantic Coast, for example, might indicate that height above base level and stage are correlatable with angles of junction.

Evolution of the Perth Amboy Drainage Pattern

From the observed systematic drainage changes at Perth Amboy and the known development of a network within the limiting values of basin area, it may be possible to deduce from the existing pattern the initial and future patterns.

surface. The channels most favored by chance encounter with weak patches of fill deepened and grew rapidly toward the divides of the individual small watersheds. These deeply cut permanent channels followed the path of initial drainage concentration manifested as faint channel traces on the upper surface. Channel traces of this type were observed at Perth Amboy in areas of headward channel development. The permanent channels follow these faint swales on the original surface because there the discharge of runoff is concentrated from the entire watershed. A headward developing incised channel is hydrophilic, advancing always toward maximum water supply.

The most vigorously developing initial rill channel thus dominated its less effective neighbors and established itself as the axis of a broadening ovate drainage basin. Its permanence was decided initially by a favored po-

sition in line with the axis of a shallow watershed on the terrace surface from which it was supplied with more runoff than its competitors. It may also have struck zones of weaker material in its bed. The added runoff allowed

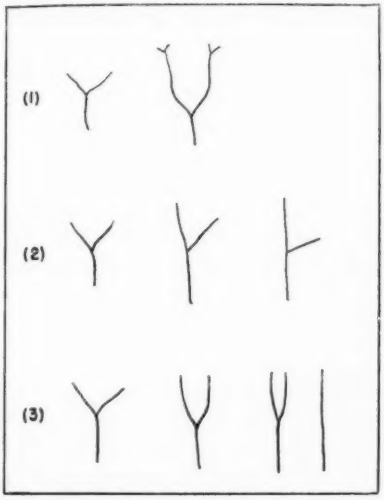

FIGURE 23.—POSSIBLE DEVELOPMENT OF ANGLES OF BIFURCATION

(1) Angle remains unchanged; (2) One channel becomes dominant; (3) On steepest slopes angles decrease and channels unite.

deepening of the drainage channel with corresponding oversteepening and collapse of its valley-side slopes. As soon as lateral expansion of the drainage basin produced sufficiently long slopes, tributary development set in on these slopes.

As the channel outstripped its neighbors the expanding drainage area permitted its bifurcation. The comparison of angles of bifurcation on the 1948 and 1952 maps suggests three predictions of possible future development of a bifurcated channel: (1) both segments of the bifurcated channel continue to grow headward unchanged in angle (Fig. 23, 1); (2) one segment becomes dominant and straightens its channel, while the other segment becomes tributary (Fig. 23, 2); (3) on steep slopes the angle of bifurcation reduces in accordance with the *Sc/Sg* ratio, and the two segments become one (Fig. 23, 3).

It is postulated that (2) occurred in the early stages of the Perth Amboy development, thus forming the first major tributary (Fig. 24, 1, 2). The tributary end grew normal to the main channel until it came under the influence of the forward slope of the terrace when its growth

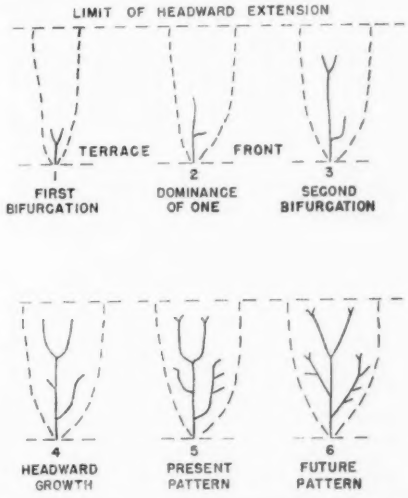

FIGURE 24.—SUGGESTED EVOLUTION OF THE PERTH AMBOY DRAINAGE PATTERN

direction altered and its upper segment developed parallel to the main channel (Fig. 24, 3). Perhaps the next permanent bifurcation was as indicated in Figure 24, 3, followed by headward growth (Fig. 24, 4) and other branches and bifurcations to yield the major elements of the present pattern (Fig. 24, 5; Pl. 1).

As these streams incised their channels secondary tributaries formed on the slopes of the valley walls. These tributaries were under the influence of the rapidly degrading main channels; many still are in the youthful headwater areas. Figure 25 is a frequency-distribution histogram of the angles measured between tributaries and the segments of the main channel (Table 11). The modal class lies between limits of 90° and 100°, indicating a right-angle pattern in accordance with a low *Sc/Sg* ratio. The earliest-formed of these tributaries became the most important and hindered the development of younger neighbors on adjoining slopes. This is borne out by the fact that the mean distance separating first-order streams along the

main channel (4.3 feet) is smaller than the mean distance separating first- and second-order stream channels (7.6 feet). Order number thus provides a rough means of classifying channels according to age; the oldest tributary channels have the higher order number.

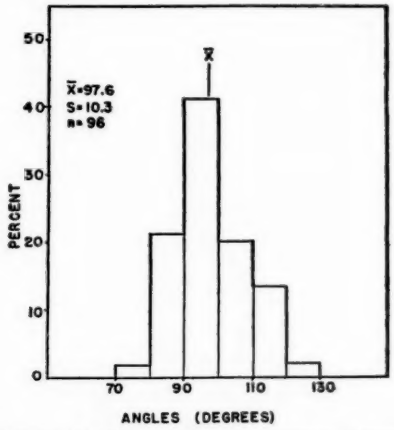

FIGURE 25.—FREQUENCY-DISTRIBUTION HISTOGRAMS OF ANGLES BETWEEN TRIBUTARIES AND SEGMENTS OF THE MAIN CHANNEL

TABLE 11.—FREQUENCY DISTRIBUTION OF ANGLES BETWEEN TRIBUTARIES AND MAIN CHANNEL

Sample	Mid-values in degrees						$\bar{X}$	s	N
	75	85	95	105	115	125			
Angles of junction	2	20	40	19	13	2	97.6	10.3	96

The present faintly trellised pattern of the principal large-order channels (Fig. 24, 5; Pl. 1) is not considered permanent. It is supposed that the angles of junction become smaller with the increased *Sc/Sg* ratio, and the lateral shifting of the larger tributaries toward the main channel would result in the acute-angled dendritic drainage pattern that is typical of mature areas of simple structure. This change would involve considerable lateral planation and channel straightening, with a modified final pattern perhaps like that in Figure 24, 6.

If, as previously noted, a positive relationship exists between stream gradients, maximum slopes, and relative relief (expressed as the relief ratio), it follows that the *Sc/Sg* ratio should vary as the relief ratio. Because entrance angles, and therefore the total drainage pattern, are dependent on this *Sc/Sg* ratio, similar areas differing only in relative relief probably have recognizable differences in drainage pattern, at least in the early stages of development.

FIELD OBSERVATIONS AND EXPERIMENTAL STUDIES ON THE DEVELOPMENT OF BADLAND TOPOGRAPHY

Field-Erosion Measurements

Field and experimental work at Perth Amboy was designed both to verify conclusions derived from map analysis and to obtain new insight into processes operative in the development of erosional landforms of the badland type.

Many recent geomorphic studies have been strongly influenced by the work of W. M. Davis and Walther Penck. Each approached the study of landforms with a separate purpose. Davis considered description of landforms for geographical purposes the aim of the geomorphologist, whereas Penck attempted to use the development of landforms as a key to the Earth's recent structural history and the nature of the diastrophic forces.

A chief point of controversy between Davis and Penck is the manner of retreat of slopes. Penck (1953) maintained that on a stable mass initial stream incision produces steep, straight slopes which retreat at a constant angle, that upwardly convex slopes indicate accelerated uplift, and upwardly concave slopes decreasing rate of uplift. Davis (1909, p. 268) imagined that the angle of valley-side slopes normally declines with time and reduction of relief.

Erosion on slopes at Perth Amboy was measured to clarify the basic geomorphic problem of slope retreat under the limited conditions of badland erosion.

The measurement of erosion on the badland slopes was accomplished by simple and inexpensive means. Wooden dowels ¼ inch thick and 1½ feet long were driven into the slopes at 1-foot intervals on downslope profile lines, orthogonal to the contours from crest to base of each slope (Fig. 26), and normal to the slope until flush with the surface.

Stake profiles were placed on 16 diversely oriented slopes, some with sharp crests and others with convex divides. On Plate 1, short lines labeled "P" locate profile lines. All slopes were composed of similar material; all had a measurable exposure of the stakes. The length of stake exposed, measured to the nearest tenth of an inch, indicated the depth of erosion at that point on the slope. The last measurement was made on September 10, 1952, when

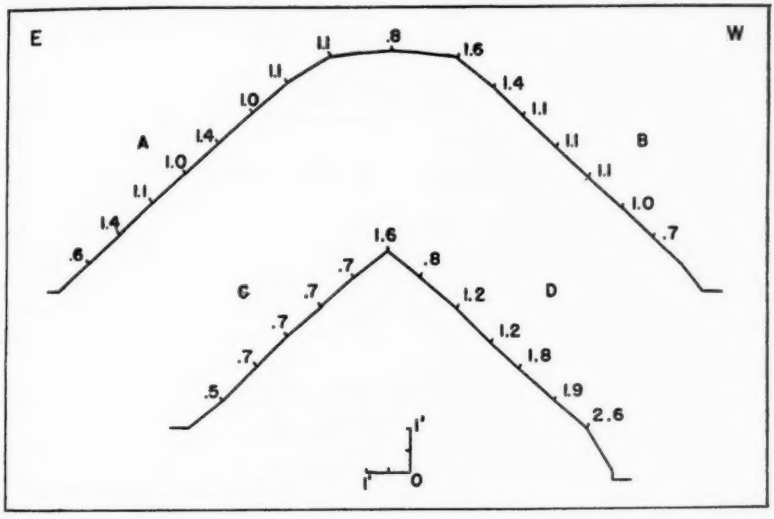

FIGURE 26.—TYPICAL PERTH AMBOY SLOPE PROFILES

Ticks on profiles show position of stakes; numbers indicate depth of erosion in inches. Profiles A, B, and C are typical of the area; profile D shows a basal convexity.

youthful, degrading, intermittent gully channel at the base. Slopes were selected, however, that showed no severe effects of rilling and offered no problem in the determination of a straight, downslope profile line. Slopes ranged from 6 to 14 feet long. The 16 profiles were installed on June 15 and July 1, 1952, but because a negligible amount of erosion occurred between those dates, they are treated as a group.

Slope angle and distance between successive stakes were measured at the time of installation, and the original slope profiles thus plotted. All profiles are remarkably straight except for those segments forming convex divides or where minor irregularities occur (Fig. 26). The straightness of profiles is characteristic of maturely dissected regions of steep slopes of widely differing scales of length, formed under various climatic and geologic conditions (Lawson, 1932, p. 711; Strahler, 1950, p. 681).

Measurement of erosion on the slopes began after the first runoff sufficient to produce a the measurement of slope angle and distance between successive stakes was repeated. During the 10 weeks of observation the depth of erosion differed both from slope to slope and from point to point on each slope. Erosion depth was greatest on sharp-crested divides and least on convex divides, but seemed to be essentially uniform along the straight segments of each slope, where a mean of 0.9 inch of material was removed.

Only two of the slopes investigated showed a measurable change of angle. Both had steepened, but neither had a simple, straight profile at the starting date in June. Slight convexities initially existing at the slope base caused increased erosion at those points so that, by the end of the observation period, the characteristic straight profile had been restored. Slope D (Fig. 26) shows this steeper basal segment caused by rapid channel undercutting. To determine significant increase or decrease of slope angle, only the straight parts of the profiles were used.

Erosion depth obtained from stakes on the convex divides, on sharp-crested divides, and in channel bottoms were eliminated by discarding all values of stakes at the crest or base of the

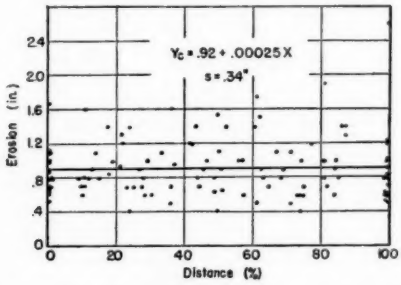

FIGURE 27.—REGRESSION FITTED TO A SCATTER DIAGRAM OF DEPTH OF EROSION ON PER CENT OF DISTANCE FROM TOP OF THE STRAIGHT SLOPE SEGMENT

erosion depths fall between 0.4 and 1.6 inches. On a given profile the depth of erosion was generally highly uniform for all stakes, whereas the mean depth differed considerably from one profile to another. Because absolute values for erosion are plotted on the ordinate the broad scatter zone produced (Fig. 27) fails to reveal the uniformity of erosion depth on a single slope. The marked differences in average from one profile to the next may be explained by variations in microclimatic environment, degree of compaction and permeability of the clay fill, or by slight compositional variations from slope to slope. For example, mean erosion on one slope was 0.6 inch but on another 1.3 inches. Consequently, when all readings are combined on one diagram, the scatter of points is wide.

A regression line fitted to the points of the scatter diagram by the method of least squares

TABLE 12.—EROSION MEASURED ALONG THE SLOPE PROFILES

Stake No.	Erosion at each stake in inches													
	1	2	3	4	5	6	7	8	9	10	11	12	13	14
Profile														
A1	1.6*	.7	.7	.7	.7	.5	...	...	...	....	..	..	..	..
A2	.8*	1.7	1.4	1.1	1.1	1.1	1.0	.7	...	....	..	..	..	..
A3	.8*	1.1	1.1	1.0	1.4	1.0	1.1	1.4	.6	..	..	..	..	..
B1	.7*	1.1	1.0	1.4	1.2	1.2	...	...	...	....	..	..	..	..
B2	.3*	.5	.9	.8	.8	.6	.5	.6	...	....	..	..	..	..
C	.3*	.5*	.7	.8	.6	1.0	.8	1.0	.6	....	..	..	..	..
D1	1.3*	.8	.6	.7	.7	.8	.9	.7	.8	....	..	..	..	..
D2	1.3*	.9	1.0	.4	.4	1.0	...	...	...	....	..	..	..	..
E1	1.5*	.8	1.2	1.2	1.8	1.9	2.6	...	...	....	..	..	..	..
F	1.0*	.9*	.7	.7	.6	.4	.8	.8	.9	2.3*	..	..	..	..
G	.3*	.6	.8	.4	.5	.7	.5	1.0	1.4	1.2	..	..	..	..
H	.4*	1.1	1.3	1.2	1.4	1.0	1.0	...	...	....	..	..	..	..
I	.8*	.9*	1.0	.8	.9	.7	1.0	.9	1.0	.7	.6	.9	.8	.6
J	.8*	1.0	.9	.9	.6	.6	...	...	...	....	..	..	..	..
K	.7*	.7*	.8	1.6	1.4	1.6	1.6	1.5	.6	1.3	..	..	..	..
L	.7*	.9	.8	.7	.9	.8	.5	...	...	....	..	..	..	..

* Reading eliminated from regression Figure 27.

slope profile which deviated by 10° or more from the straight segment. These values are nevertheless listed (Fig. 27; Table 12) with the 113 readings of erosion depth that remained. These remaining values were combined into one scatter diagram by the use of a dimensionless parameter: per cent of distance from upper to lower end of the straight slope segment. Most (Croxton and Cowden, 1939, p. 655–657) has the equation

$$Y_c = 0.92 - .00025X.$$

A t-test, to determine the validity of the null hypothesis that the deviation from zero slope, shown by the regression equation, can be attributed to chance sample variations alone

when sampling from a population with zero slope, reveals a probability greater than 0.65. Thus at least 65 times in 100 this great a trend or greater would occur. Lack of significant trend suggests that erosion is uniform along the straight segment of the slopes.

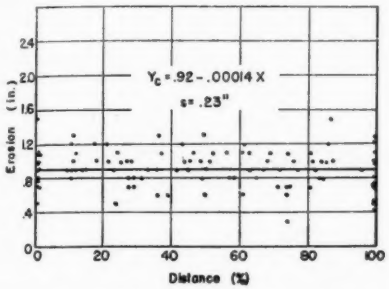

FIGURE 28.—REGRESSION LINE FITTED TO ADJUSTED VALUES OF FIGURE 27

In order to take into account the uniformity of erosion depth on a given slope profile and decrease the scatter about the regression line the mean of erosion for each slope was adjusted by addition or subtraction to equal the mean of all, 0.92 inch. Thus independent, and for this purpose, irrelevant variations in erosion from slope to slope were minimized. For example, to the values of one profile for which the mean depth of erosion is 0.6, a constant, 0.32, was added in order to increase the sample mean to 0.92. An appropriate constant was subtracted from each mean greater than 0.92 and added to each less than 0.92. Figure 28 shows the decreased scatter produced by plotting the adjusted values. In addition to adjusting the means of each slope profile, the data of one profile (Fig. 26, D) were eliminated because the basal segment of this slope had been abnormally steepened by channel undercutting. Because the inclusion of this abnormal profile in the regression analysis of Figure 27 did not produce a significant trend, its elimination here would have little effect on the acceptance of the null hypothesis. The regression line fitted to the data on Figure 28 has the equation

$$Y_c = 0.92 - .00014X.$$

The estimated standard deviation, s, of the regression is decreased by 0.2 inch from the value for the unadjusted regression line in Figure 27. The probability of this great a departure from zero slope by chance sample variations alone is found to be greater than 70 per cent, again sustaining the null hypothesis.

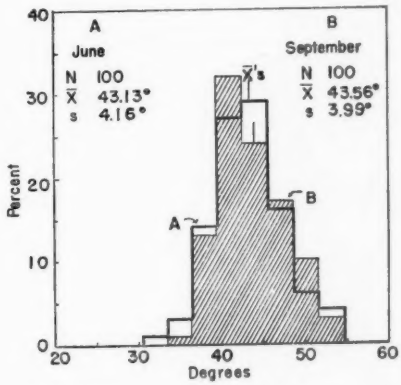

FIGURE 29.—FREQUENCY-DISTRIBUTION HISTOGRAM OF ANGLES BETWEEN STAKES MEASURED IN SEPTEMBER SUPERIMPOSED ON HISTOGRAM OF ANGLES MEASURED IN JUNE

It is possible to check the conclusion suggested by the previous tests because the slope angles between surface points at successive stakes had been measured both at the beginning of the investigation and at the end. Consequently, a lack of significant difference between the means of these two slope-angle samples would support the hypothesis of uniform erosion depth. Again end values deviating 10° or more from the straight profile lines were discarded. One hundred slope angles measured in June and July remained, and the corresponding angles measured in September were similarly selected. Because each angle refers to 1 foot only of the slope profile, any change of slope angle along the straight slope segment would be recorded. Figure 29 (Table 13) shows the frequency-distribution histogram of the angles measured in September superimposed on that of the angles measured in June. The means of the two samples differ by half a degree. Because the September slope-angle measurements were taken at the same profile points as the June–July slope angles, the sample data are paired. Where sample observations are paired in this way the mean of the differences is tested under

the hypothesis that this difference is actually drawn from a population of differences equal to zero. The mean of the differences, $\bar{X}d$, in this case is equal to -0.43 (same value as difference of means in Table 13); the standard deviation of the differences, s_d, is 3.09; the standard error of the mean of differences, $s_{\bar{x}d}$, is 0.309. The statistic, t, equal to $\bar{X}d/s_{\bar{x}d}$, has a value of approximately -1.4. At the 5 per cent level, divided into two tails of 2½ per cent, each, the critical value of t is approximately 1.99 for 99 degrees of freedom. The statistical hypothesis is therefore accepted, and there is no reason to believe that the mean angle of the slope between stakes has changed appreciably. Thus these data suggest uniformity of erosion and parallel slope retreat.

Further information on the uniformity of erosion and resulting constancy of slope angle is afforded by slope data collected by Strahler (1950, p. 680) who measured the maximum slope angles at 154 mid-slope locations by laying a board 20 inches long on the steepest portion of each slope and measuring the slope angle of the board with an Abney hand level, plotting each location on a map of the area. Using the same technique the maximum slope angles were measured at the indicated points during the summer of 1952. The histograms of the samples are superimposed in Figure 30 (Table 13). Here, again, the variates are paired in the two samples. In the 1952 sample, 5 sample points were not relocated, so that 149 pairs are used in the t-test of mean of differences ($\bar{X}_d$) which has a value of -0.21. This mean is not exactly the same as the difference in sample means in Table 13, because the latter uses all 154 variates in the first sample. The standard deviation of the differences (s_d is 3.76; the standard error of the mean ($s_{\bar{x}d}$) is 0.308. The value of t is therefore -0.68; the critical value of t at the 5 per cent point for 148 degrees of freedom is about 1.97. The hypothesis that the mean of the differences is equal to zero is accepted, and we have no reason to doubt that the slopes have been uniformly lowered, without appreciable steepening or flattening.

In summary, three sets of data were used to determine any significant change in the depth of erosion per unit time along the length of straight segments of badland slopes. During the period of observation no significant steepening or decline in angle was apparent, although

TABLE 13.—FREQUENCY DISTRIBUTIONS OF SLOPE ANGLES

	Class mid-values in degrees								Mean grouped data ($\bar{X}$)	Mean raw data ($\bar{X}$)	s	N
	32	35	38	41	44	47	50	53				
June	1	3	14	28	29	15	6	4	43.10	43.13	4.16	100
September	...	1	13	34	22	17	10	3	43.49	43.56	3.99	100

	Class mid-values in degrees												Mean grouped data ($\bar{X}$)	Mean raw data ($\bar{X}$)	s	N
	35.5	37.5	39.5	41.5	43.5	45.5	47.5	49.5	51.5	53.5	55.5	57.5	59.5				
1949	2	1	0	2	6	21	28	40	32	14	6	1	1	49.12	49.06	3.69	154
1952	..	..	3	6	12	19	25	24	40	13	7	..	..	48.82	48.86	3.72	149

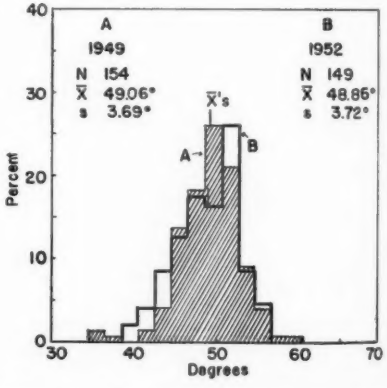

FIGURE 30.—FREQUENCY-DISTRIBUTION HISTOGRAMS OF MAXIMUM-SLOPE ANGLES MEASURED IN 1949 AND 1952

erosion varied from slope to slope. The above evidence sustains the hypothesis that, with an actively degrading stream at its base, the bare, unconsolidated, highly cohesive slopes of badland topography retreat in parallel planes when adjusted to the controlling conditions of their environment.

The effect of rilling and frost heaving on slopes are discussed below, but the importance of these processes does not invalidate the discussion of slope retreat under the action of runoff alone, for during the measurement of erosion depth on the slopes no frost heaving occurred and there was no important rilling.

Channel erosion was also checked by repeated surveying of the main channel. During the year of observation this showed slight aggradation in the lower sections of the channel and degradation in the headwater areas.

Experimental Erosion Measurements and Study of Runoff

Success of the use of wooden dowel rods to measure erosion during a short period of the study suggested the use of simulated rainfall on the slopes to study in more detail the processes of erosion and to measure the amount of erosion produced by measured amounts of precipitation. A 2½-gallon hand pump was used to simulate rainfall. A horizontal circular motion of the pump nozzle delivered an approximately uniform intensity of fine spray to an area of 36 square inches. Investigations were thus limited to areas of this size.

The following technique gave consistent results: The hand pump was filled with water to within 6 inches of the top and 50 full strokes of the pump provided constant initial pressures. When the nozzle was held 18 inches above the surface and moved in a circular motion for 5 minutes about 640 cc were delivered to the area.

Six hundred and fifty cc of water delivered to a 36 square inch area was equivalent to 1 inch of precipitation, a far greater intensity (12 inches per hour) than all but the most severe natural rains. Because the aim of the experiment was to determine the relation between slope angle and erosion, the high intensity of precipitation is not thought to invalidate it. On a slope several feet long a heavy rain would produce cumulatively an equivalent runoff intensity over a small area of the slope base, although this flow would enter the area with considerable sediment entrained.

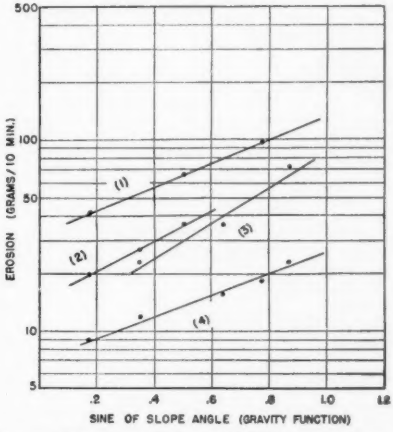

FIGURE 31.—RELATION OF EROSION TO SINE OF SLOPE ANGLE

Eroded material collected after ten minutes of spraying (2 in. of ppt.)

Attempts to measure erosion in the field by spraying the surface upslope from metal sediment traps set in the slope failed because wind deflected the spray. Field trials were discontinued in favor of laboratory studies.

Sheet metal containers 6 inches square were constructed to hold sediment from a composite sample collected at Perth Amboy, and adjustable wooden stand was made to support the containers at the required angles (Pl. 2, fig. 4). The sediment in the container approximated field conditions: size components of the sediment were roughly equally distributed; surface was smooth and level and sealed by clogging of the pores by clay particles after wetting (Hendrickson, 1934).

The container and sediment were placed on the wooden stand, and spray was directed onto the sediment surface for 5 minutes. The eroded sediment and runoff were taken from the collecting pan and weighed.

Figure 31 shows the results of four trials where sediment loss in grams is plotted against sine of slope angle, termed the gravity function

(Strahler, 1952a, p. 928) because it represents that proportion of the acceleration of gravity acting parallel with the slope and producing shear. The regression line representing each experiment reveals clearly that erosion on the slope is well described as an exponential function of the sine of slope angle. A similar relationship results if erosion is plotted directly against slope angle, changing only the constants of the regression equations. The total volume of runoff from the slopes remained essentially consant during each experiment. These results appear to agree with those of Borst and Woodburn (1940) and Duley and Hays (1932) although their values for erosion increase more rapidly with increased slope, probably because of the greater length of the trial plots and the loose plowed surfaces on which the water was sprayed.

The variation in amount of erosion from experiment to experiment is attributed in part to unrecognized variations in water delivered by the spray; experiment 4 was performed on a day noticeably colder than the days the other experiments were performed. The lower temperature may have decreased the pressure sufficiently to cause decreased water delivery and lessening of erosion.

Although many sources of error existed, a consistent relationship within each series suggests that, with better equipment, quantitative determination of the relations between slope angle, amount and intensity of precipitation, soil type, and erosion would not be difficult. The Department of Agriculture made numerous studies of this type, dealing primarily with surfaces representing fallow or cultivated plots and rarely with slopes greater than 20°. A large field remains for further experimentation.

The effect of increased slope angle on the grain size of the eroded sediment was determined by sieving the collected samples. The samples were arbitrarily separated on the 0.5 mm (Wentworth's greater than medium sand) and 2.0 mm (greater than coarse sand) sieves. It was supposed that with increased slope the percentage of larger sizes would increase, but instead the percentage by weight of sediment greater than 2.0 mm varied only slightly from 27 per cent of the total (Table 14). The runoff, therefore, had removed a proportionally equal amount of each grain-size component as the slope steepened.

Although the percentage of each component did not change appreciably, the size of the largest particle transported increased with slope angle. Weight of the largest grain transported in experiments 3 and 4 (Fig. 32) is directly proportional to the sine of slope. Data from experiment 2 is not linear and data from experiment 1 showed no consistent relationship. Deviation from a straight-line relationship may be due to pump variations, but in general the increase of maximum grain size transported with slope is attributed to the more rapid uncovering of the larger sizes on steeper slopes of the originally smoothed plots. Therefore, if by chance the largest grain possible of transport was not uncovered, the relationship would not appear to exist simply because of the absence of the larger particles.

TABLE 14.—PER CENT BY WEIGHT OF ERODED SEDIMENT GREATER THAN 2 MM

Slope angle (degrees)	Experiments 1 and 2	Experiment 3	Experiment 4	Mean of all experiments
10	27.0	29.0	27.0	27.7
20	26.8	31.0	....	28.9
30	26.7	27.5	26.0	26.7
40	22.0	....	18.0	20.0
50	34.8	26.0	26.0	28.9
60	27.5	30.0	26.0	27.8

Erosion was greatest on the steepest slopes, and even on slopes of the lowest angle used (10 per cent), all components of the sediment moved in approximately the same proportion, but more slowly. The size of the largest particles transported on any slope appears to be directly proportional to the gravity function.

Perhaps the most interesting part of the study was the observation of the action of runoff on the slopes of varying inclination. On a 10-degree slope, exposure of the coarser grains, as the fine sediment is carried away, gave a sandy appearance to the surface. On a 30-degree slope the medium-sized particles moving downslope jam between larger grains, forming miniature dams which check the flow of the runoff and pond the water on the slope

until the weight of water and sediment is great enough to burst this tiny dam. When the dam is broken a pulse of water and sediment moves downslope with energy enough to move even the larger grains. The characteristic arcuate ridges of sediment left by check dams on a slope can be recognized. Horton (1945, p. 312–313) discusses surge-flow transport where debris on a slope causes the same checking and temporary ponding of runoff. Large grains on this 30-degree slope are loose on the surface and appear ready to move when the force of runoff is great enough. The large pebbles are undermined. Activity on the 50-degree slope is markedly different. Large pebbles are undermined and roll downslope. The cavity left by the removal of a pebble allows concentration of runoff, and a rill begins headward growth even in the small confines of the experimental container. The check-dam pattern is strongly developed.

Examination of slopes of different inclination after a storm confirms that similar features develop in the field. The lower slopes appear quite sandy and a casual observer would assume that the sediment is all sand and gravel. On steeper slopes the characteristic check-dam patterns develop with evidence of rilling if the slope is long enough. Slopes steeper than 50° appear stripped of the sand and gravel components, exposing an essentially clayey sediment. Spraying water on these slopes in the field develops similar features.

Watching runoff on these slopes impresses one with the importance of microtopography on the runoff. Each grain of sediment assumes importance as it checks and deflects threads of water moving downslope. Formation of check dams causes water threads to move in zig-zag paths downslope. Dye placed on the slope spreads into a fan shape with apex upslope because of interdrainage among the irregular interlacing threads of the water current. Turbulent diffusion of the dye may cause some of this spreading, but individual water drops or threads widely deflect from straight paths downslope.

The large pebbles or small cobbles imbedded in the slope check water on their upslope sides, causing deposition of sediment and partial burial of their upslope surfaces. The desilted water flows around the pebble, undermining it until it rolls downslope.

Obviously, the term sheet erosion or sheet flow does not strictly apply here. Although water covers the entire slope, much is merely a thin film over the spaces within a network of

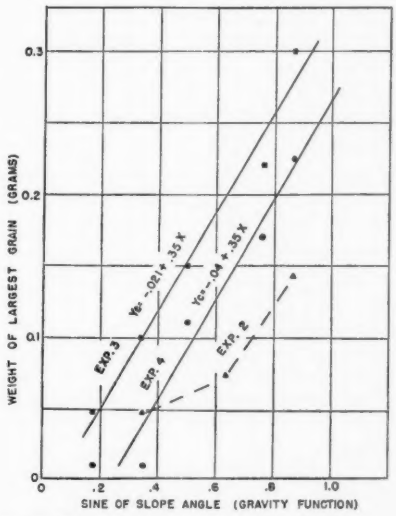

FIGURE 32.—RELATION OF THE LARGEST PARTICLE MOVED ON A SLOPE TO SINE OF SLOPE ANGLE

streamlets flowing around numerous obstacles and deflected from a true downslope course. Nevertheless, in a general sense in the Perth Amboy area, erosion intensity on both convex divides and straight slopes is a function of the slope angle and is caused by surface runoff, whatever the minute variations in its flow.

Studies of erosion depth on the badland slopes at Perth Amboy support the principle that the slopes may retreat in parallel planes. Straight slopes are obviously the dominant form here, as in many other areas of rapid channel dissection, but the reason for maintenance of these straight slopes by runoff is not obvious and is contrary to two major theories of the action of runoff.

Lawson (1932) assumes that rainwash erosion decreases in intensity downslope; he criticizes Chamberlin and Salisbury (1905, p. 59) for stating that it increases downslope. Each theory is based on one of two principles, both of which seem mathematically valid if the

required assumptions are accepted: (1) erosion is decreased downslope because of increasing sediment load in the runoff; (2) erosion is increased downslope by an accompanying increase in runoff discharge, depth, and velocity.

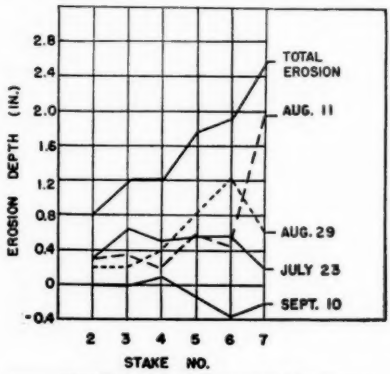

FIGURE 33.—DEPTH OF EROSION MEASURED ON SLOPE PROFILE D DURING THE SUMMER OF 1952

Stakes are about 1 foot apart. Stake 2 is nearest the crest of the slope. Stake 7 is at the base.

The first principle requires the assumption that ample quantities of easily entrained sediment are continually available to the runoff. This will not always be the case, although when a long interstorm period allows the accumulation of much loose weathered material the earliest runoff may be loaded to capacity when it reaches the slope base, and this condition may persist during an entire storm period. Horton (1945, p. 310) quantified the second principle, stating that the velocity of runoff is a power function of the depth of overland flow which increases downslope. He qualifies this statement, however, by showing that this relation does not exist for subdivided or surge flow, the type of runoff that occurs on the steeper slopes at Perth Amboy, as evidenced by the development of minute check-dam features. Subdivided flow is defined as that occurring on plots containing vegetation, where the runoff expends energy against the stalks of the plants and breaks into numerous independent streamlets. This description also fits the runoff on the Perth Amboy slopes where each large surface grain subdivides the runoff. Therefore, on anything but extremely smooth surfaces, either subdivided or surge flow is probably characteristic. Despite increased depth of overland flow downslope the resistance of large surface grains and the temporary halting of the flow by miniature check dams may prevent an appreciable increase of velocity downslope. Because the development of check dams increased with higher slopes, it may also increase with runoff depth and velocity. The tendency to disrupt and confuse the flow may increase to a point where further increase in velocity is prevented and a steady state results. Thus, erosion may be constant on a slope of constant angle as observed in measurements of slope erosion. If velocity remains nearly the same on the entire slope, a straight slope may be expected to remain straight as long as the stream channel removes the debris from the slope base but does not undermine it.

Measuring and comparing the depth of erosion on slopes after each of several periods of heavy precipitation illustrates the action of sheet-wash erosion. Slope D of Figure 26 has a marked steepening at its base produced by channel undercutting. If erosion is dependent on the angle of slope increased erosion should occur on the basal segment of slope D, causing modification of the entire slope profile.

The writer measured progressive exposure of the rods on the slope profiles at Perth Amboy four times. Figure 33 shows the depth of erosion at each stake plotted for the four observations. The uppermost points indicate total erosion depth during the 10 weeks of observation, showing a marked increase in erosion downslope. Stake 2 at the left of the diagram is 1 foot below the crest of the slope. The stakes were installed June 18 and the first measurement of erosion on July 23 indicated only that erosion was greatest above the break in slope. On August 11, however, the great exposure of the basal stake (7) indicated that maximum erosion was occurring on the oversteepened portion of the slope. On August 29 the zone of maximum erosion had shifted upslope as a pulse of erosion moved upward straightening and steepening the slope. On September 10 the greatest erosion was occurring at the upper three stakes, while sediment from upslope partly buried the lower three. Continued observations on this slope would be expected to reveal that further erosion would be essenti-

ally constant, maintaining the restored straight slope. Figure 34 shows the two successive profiles of slope D in June and September. The irregularity has been removed and the slope steepened four degrees.

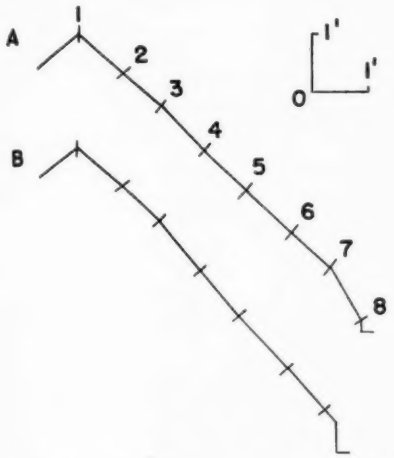

FIGURE 34.—SLOPE PROFILE D IN JUNE AND SEPTEMBER 1952

(A) Profile in June with over-steepened base.
(B) Same slope in September after straightening by erosion.
No significance should be attached to relative vertical spacing of the two profiles.

Figure 35 illustrates erosion on a slope with originally straight profile from crest to base, contrasted with the basal slope steepening of the previous case. Erosion depth for the uppermost stake which was on a sharp-crested divide is not shown, for the retreat of the two adjacent slopes causes an abnormally large value for the lowering of the divide. A geometric construction shows that where the retreating valley-wall slopes are 45° the crest is lowered in the ratio of 1 to $\sqrt{2}$, or 40 per cent faster than the rate of wasting of the valley walls.

Erosion depths in Figure 35 are not uniform along the slope profile in any one short period but are essentially uniform over longer periods. Compare the erosion depths measured on July 23 and August 11. Points of deep erosion measured July 23 are points of shallow erosion measured August 11 except at the lower three stakes. Erosion measured August 29 was less at these lower points, compensating for the earlier two periods of deeper erosion. Total erosion, shown in the upper line, varies between 0.6 and 0.9 inch, reasonably uniform in comparison with the nonuniform erosion or greater erosion at the slope base of the previous case (Fig. 33).

This and other profiles observed at Perth Amboy show that runoff erosion depth on straight slopes varies from point to point during each small unit of time but is essentially uniform over the entire slope length during long periods. Slope irregularities cause erosion where the slope is steepest and decreased erosion where the slope is gentler, thus tending to smooth out the irregularities and restore the straight profile. The slope angle may increase or decrease during this alteration depending on how much the stream channel at the slope base is actively downcutting. Baulig (1939) has stressed the interdependence of all parts of the graded slope profile, preventing the indefinite perpetuation of irregularities assumed by W. Penck (1953). The above studies support Baulig's concept.

If badland erosion is uniform over the length of a straight slope and bears an exponential relationship to the slope angle or gravity function, as the Perth Amboy data suggest, the concepts of a continual downslope increase in the depth, velocity, competence, and eroding force must be replaced by a theory of runoff as subdivided or surge flow in which runoff cannot be directly compared to continuous uniform fluid transport, but is more analogous to surface creep of soil under the action of disturbing forces and gravitational stresses alone. In the runoff at Perth Amboy each surface grain moves intermittently downslope, and its average velocity depends primarily on the angle of the slope on which it rests rather than on distance from top of the slope and slope angle combined. The action of runoff and its velocity at any particular point is seemingly unrelated to the increase in discharge at increasing distance from the top of the slope. On materials of low infiltration capacity the discharge of runoff must increase downslope. There are three possible reasons why the rate of erosions does not also increase: First, if the sediment in suspension and traction moving downslope with the water is not deposited, it increases in

discharge as the water discharge increases, thereby continuously equalling the capacity of the flow for debris transport despite an increase in capacity caused by greater water depth. Second, a rapid increase in tractive bedload movement and suspensional movement near the bed may reduce bed velocity, thus setting up a blocking effect proportional to the increase in depth. A steady state, analogous to the terminal velocity of a falling raindrop, may thus ensue, in which the rate of erosion depends only on the intensity of the downslope component of the gravitational force field. Third, it may be that neither distance from divide nor increased discharge modifies the action of surge and subdivided flow.

Rainwash erosion can be thought of as occupying an intermediate position or transitional stage between surficial soil creep without a fluid medium and transport by relatively deep channel flow.

Seasonal Effects on Erosion; the Rill Cycle

The dominance of erosion by runoff during the summer season is conspicuous but may give the erroneous impression that this is the only process causing slope retreat at Perth Amboy. A study of rill development throughout the year indicates that other processes are active. The slopes quickly alter appearance as the dominant process changes.

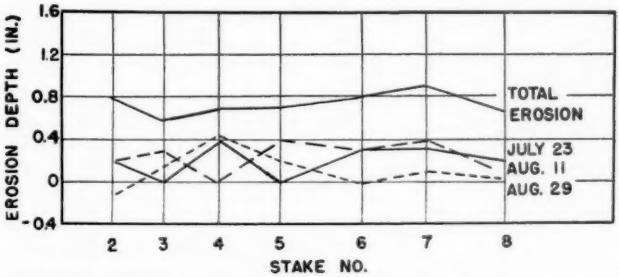

FIGURE 35.—DEPTH OF EROSION MEASURED ON AN INITIALLY STRAIGHT SLOPE DURING THE SUMMER OF 1952
Stake 2 is nearest the crest of the slope.

Rills are the first clear manifestation of the action of runoff concentrated in definite channels. These rill channels do not have a clearly delimited drainage area, but are simple, narrow troughs eroded into the slope by running water and its load of sediment (Pl. 3). The rills form on smooth valley-side slopes between permanent drainage channels, although the combined erosive power of two or three closely spaced rill channels may develop a true permanent drainage basin. Rills are ephemeral features yet play a varied role in the erosion cycle. They aid frost-heaving processes and even alter the slope profile. At Perth Amboy rills are especially well developed not only because of the ease of erosion of the fill but because rapidity of channel degradation at the slope base intensifies the rill cutting. Depth of rills appears to be directly related to rapidity of channel degradation.

PLATE 2.—PERTH AMBOY BADLANDS

FIGURE 1.—GENERAL VIEW OF WEST FRONT OF TERRACE AT PERTH AMBOY
Total relief here is about 40 feet. Intricately dissected terrace front is bordered by alluvial fans

FIGURE 2.—EAST FRONT OF TERRACE AT PERTH AMBOY FROM POINT NEAR MOUTH OF A FIFTH-ORDER STREAM

FIGURE 3.—TYPICAL SMALL SECOND-ORDER DRAINAGE BASIN WITH STEEP STRAIGHT SLOPES
Flat undissected remnants of the upland surface are visible

FIGURE 4.—EQUIPMENT USED FOR RUNOFF EXPERIMENTS
Nozzle of sprayer is tied to tripod to maintain constant distance from sediment surface in container

FIGURE 1

FIGURE 2

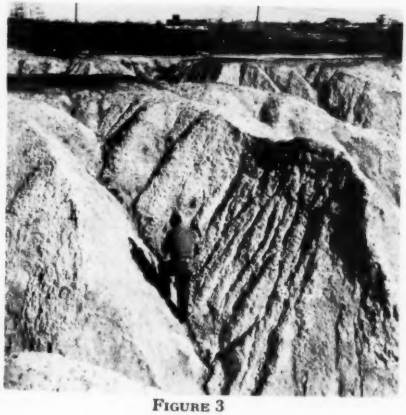

FIGURE 3

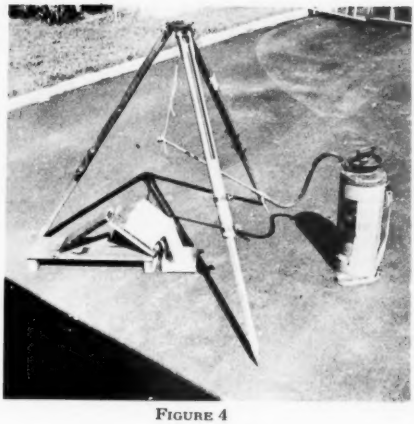

FIGURE 4

PERTH AMBOY BADLANDS

FIGURE 1

FIGURE 2

FIGURE 3

FIGURE 4

RILL CYCLE

A series of photographs from select stations illustrates the role of rills in slope erosion and the seasonal morphological changes at Perth Amboy (Pls. 3, 4). Approximate position of camera and scope of photographs are shown on Plate 1 by arrows and dashed lines. The following summary of conditions during the year was abstracted from field notes:

Spring (Pl. 3, fig. 1; Pl. 4, fig. 1): After the last severe spring frost, rains begin the development of rills on the slopes. These rains cause rapid clearing of drainage channels and initiate renewed degradation after sliding and slumping of much frost-heaved material into the channels during the winter months.

Rainbeat forms small soil pillars on the broader divides. Tributaries begin degradation, and small knickpoints form in their channels as the tributary profile gradation lags behind the rapid degradation of the main channel.

Summer (Pl. 3, fig. 2; Pl. 4, fig. 2): Rills develop complicated networks on slopes and in some basins develop an amphitheater form (Pl. 4, fig. 2). Continued lowering of drainage channels causes deep rill trenching of adjacent slope surfaces. Light rains fill rills with loose, easily eroded material, which is flushed out during the next rain of moderate intensity. The rills extend upslope, but seem to reach a limit at about 1½ feet from the crest of any slope. Figure 2 of Plate 3 shows this rill line where runoff concentration attains sufficient force to cause rill formation. Here the slope may develop a concavity which is due to the sudden increase in erosion rate along this line.

Rills reach maximum development during the summer when they have scarred most slopes. Torrential rains in some cases seem to reduce the number of rills by destroying the narrow intervening divides.

Fall (Pl. 3, fig. 3; Pl. 4, fig. 3): The north-facing slopes show the effects of frost first. Desiccation fractures develop because of evaporation of soil moisture concentrated near the surface by freezing (Anderson, 1946). Downslope sliding of entire layers of loosened material causes long fractures which develop along contours at the heads of gully slopes (Pl. 4, fig. 5). Frost heaving breaks and loosens a surface crust half an inch thick which was formed by surface sealing with fine sediment moving downward and clogging the interstices under the action of rainbeat (Ellison, 1945, p. 418). The dominance of creep, rolling, and sliding accompanying frost heaving over water erosion is obvious in this phase. Rill and gully channels are continuously receiving this material which collects until torrential spring rains flush the channels. While they persist, rills and small gullies act as chutes for rolling and falling debris, in some cases building tiny debris cones into the adjacent drainage channel. Rills decay as the divides break down between them.

Winter (Pl. 3, fig. 4; Pl. 4, fig. 4): On a sunny day when temperature is near freezing it is difficult to climb on south-facing slopes because the surface is saturated with water melted from ice layers, and additional stress causes sliding and mud flowage (Pl. 5, fig. 1). The north-facing slopes on such a day are frozen (Pl. 4, fig. 6) with a heaved surface produced by the growth of needle ice. When these ice needles, up to 3 inches long, melt on warm days, the surface of the slope moves downward and there is a continuous rolling of material into channel bottoms. The ice columns raise both fine material and pebbles. The entire surface heaved above the tops of the wooden rods which had been driven flush into the slopes and were too deeply imbedded to be disturbed. Beneath this layer of banded and needle ice the clay was moist but not frozen. If frost penetrated deeper into the slopes the effects would be greatly increased.

During the winter the entire drainage basin

PLATE 3.—RILL CYCLE

FIGURE 1.—RILLS BEGIN TO DEVELOP ON THE SLOPE AFTER FIRST SPRING RAINS, JUNE 1952

FIGURE 2.—RILLS AT MAXIMUM DEVELOPMENT AT END OF SUMMER, AUGUST 1952
Note rill line

FIGURE 3.—RILLS BEGIN TO DECAY AFTER FIRST FROSTS, DECEMBER 1952

FIGURE 4.—RILLS OBLITERATED FROM SURFACE OF THE SLOPE, MARCH 1953

has the appearance of rapid decay. The rills are eventually completely destroyed (Pl. 3, fig. 4; Pl. 4, fig. 4), and the drainage channels clogged with debris. This spring flushing process may explain high spring-sediment loads in streams draining areas of sediment susceptible to frost heaving. Two types of erosion are active in the rill cycle: (1) rainwash in the spring and summer; (2) creep and flowage induced by frost heaving and thawing (with some runoff from winter rains) during the fall and winter. The rill cycle is a product of the two processes, one forming the rills, the other healing them.

Frost heaving during the winter months at Perth Amboy is an important factor causing slope retreat. The writer obtained no quantitative measurements of its effect but the slope profiles previously studied did not appear significantly altered by it. The lack of significant difference between slope-angle samples measured in 1949 and 1952 (Fig. 30) substantiates this observation. It is possible, however, that frost heaving would reduce slopes steeper than the angle of repose of the heaved material to a lower angle.

Cycle of Development of Erosional Topography

Relation of Stream Profiles to Slopes

Initial channel incision caused the steep valley-side slopes at Perth Amboy. To understand the development of these slopes it is necessary to examine the way a stream channel advances headward into such a terrace. The lengthening channel follows the most direct path toward the maximum source of runoff and extends itself only where the concentrated runoff has sufficient discharge and erosion velocity to scour the ground below the level of the surrounding surface.

The main stream growing back into the terrace at Perth Amboy has three segments (Fig. 36) recognizable in the longitudinal profile: (a) a lower segment concave upward, (b) an upper flat segment, essentially a shallow channel trace on the upland surface, and (c) a convexity separating these two segments. As this convexity advances upchannel lengthening the lower segment, rapid incision occurs, producing the steep valley-side slopes.

Transverse valley profiles taken along the same channel profile illustrate this development (Fig. 36):

Profile 1: Uppermost point on stream profile. Runoff following shallow depressions of the initial surface caused slight degradation separating broadly convex surfaces.

Profile 2: Point just above channel convexity. More rapid degradation and development of true channel with banks indicates nearness of convexity.

Profile 3: Point on convexity, showing point of maximum rate of degradation. Incision is so rapid that valley sides are vertical and little affected by runoff erosion.

Profile 4: Point at lower limit of convexity. Degradation of channel is still rapid, but the effects of runoff and frost heaving have lowered the slopes to near the mean maximum-slope angle characteristic of the region. The upper portions of the slopes are broadly convex where rounding of the intersection between steep slope and flat upper surface occurred, as on left half of the profile. With the reduction of slopes to this characteristic high angle, experimental studies of erosion on slopes assume importance in the understanding of further slope development.

Profile 5: Point well down on up-concave part of profile. Continued channel degradation accompanied by rapid, almost-parallel retreat of the slopes has greatly reduced the upper-slope convexity. Slopes bordering the main channel at and below this point on the longitudinal profile are commonly slightly up-concave because of rilling.

The angle assumed by the steep straight slope under the action of the erosive processes manifests an equilibrium among the steepening and reducing mechanisms. A steeper angle would lessen the effect of rainbeat and the amount of rainfall per unit area on the slope but would increase the component of gravity acting parallel with the slope; a gentler angle would increase intensity of rainbeat and rainfall but would lessen the influence of gravity. More important than an optimum angle for combination of rainbeat and rainfall interception in determining the characteristic slope is rate of downcutting of the adjacent channel. As erosion depth measurements showed, when

the base is over-steepened by rapid-channel cutting, a wave of erosion travels upslope, removing a wedge of material and steepening the slope. On the other hand, if the streamflow failed to remove all the material washed downslope, it would accumulate in the channel and dation of the adjacent channel governs development of the slope. If the channel degradation slows by attainment of grade with respect to a base level at the drainage-basin mouth, and the slopes are no longer vigorously undercut at the base, retreat of the slope will slacken with the

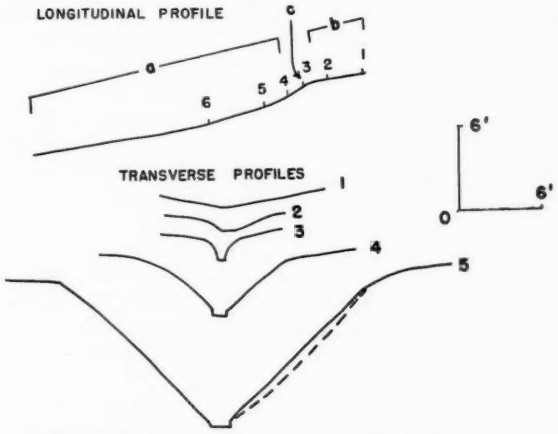

FIGURE 36.—DEVELOPMENT OF VALLEY-SIDE SLOPES

Numbers on the longitudinal profile indicate the positions of the transverse profiles. The dashed line indicates the effect of rills on a slope.

the slope angle might lower gradually. In small drainage basins, however, degrading and aggrading of the stream channel is regulated by the discharge and load from the adjacent slopes (Strahler, 1950). Slope steepening brings more detritus into the channel, causing aggradation, which reduces basal slope undercutting. On the other hand, lowering of slopes brings less detritus into the channel, which can then be scoured more deeply, oversteepening the slopes at the base and initiating a compensatory wave of steepening which travels upslope. With such automatic blocking mechanisms interrelating the slopes with their adjacent channels, it is not surprising that a characteristic slope angle is maintained, but with continued adjustment activities in progress.

The essential slope element (Fig. 36, profile 5) is a straight slope at an angle characteristic of the region bounded at the base by a degrading channel and at the crest by a flat or gently convex upland surface. Under the self-regulating mechanism described above, the rate of degra- result that the upper convexity will become important and will extend downslope, reducing the length of the straight segment. If channel degradation again becomes rapid (*e.g.*, by lowering of base level) the rapid retreat of the steepened slope segments intercepts this upper convexity in a distinct break in slope profile. Strahler (1950, p. 803) noted such composite slope profiles in the Verdugo Hills and applied the same explanation.

Runoff is the dominant process forming the upper slope convexities at Perth Amboy. The action of runoff is confirmed in this instance by the lack of convexity or rounding of the break in slope between upland and valley-side slopes where the upper surface slopes away from the break (Fig. 37a) preventing runoff from reaching it. Some degree of rounding always occurs where runoff flows across this break (Fig. 37b). Also, erosion increases from a minimum on the crest at a convex summit to a maximum on the straight segment (Fig. 26). These observations, although limited to small-scale features, sup-

port Fenneman's (1908) thesis of rounding of hilltops by "unconcentrated wash".

As channel degradation and slope retreat proceed the convex divide area is reduced and disappears when the slopes intersect forming a sharp-crested divide. When the slopes intersect, lowering of the divide by slope retreat may keep pace with channel lowering and the relief may remain constant (Fig. 38). This condition is similar to W. Penck's (1953, p. 147) *gleichförmige Entwicklung* or "uniform development". This explains the observed constancy of the relief ratio above 25 per cent mass removal in the Perth Amboy basins. The ideal case (Fig. 38a) would not exist in nature because degradation in adjacent channels and erosion on adjacent slopes is not exactly equal, causing shifts of the divide and unequal lowering. Over a long period these inequalities might balance, and the uniform lowering be generally preserved over the entire drainage area.

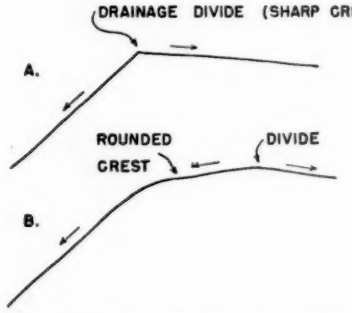

FIGURE 37.—EFFECT OF DIRECTION OF DRAINAGE OF UPLAND SLOPES ON SLOPE-PROFILE FORM

The entire slope erodes uniformly as long as the transporting power of the stream at the slope base is undiminished. When the supply of sediment is too great for transportation by the stream, deposition at the base of the slope occurs. This deposit forms a basal up-concavity which migrates upslope as deposition continues. With basal deposition, waves of slope erosion no longer move upslope from the channel wall possibly slowing the retreat of the straight segment and the planing back of the upper convexity, allowing it to widen and grow downslope to meet the advancing depositional concavity. This would yield the characteristic sigmoid, or concave-convex, slope profile of humid regions of moderate to low relief. The straight segment may be reduced by the encroaching convexity and concavity until it becomes the point of inflection of the concave-convex slope, erosion predominating above and deposition below.

On the longer slopes at and downstream from the location of profile 5 (Fig. 36) on the main channel, the development of closely spaced rills on the valley-side slopes causes a slightly concave-up slope profile illustrated on the right side of profile 5. This effect of rilling may be the reason for the development of the lower concave section of a slope, but at Perth Amboy when the rills have altered the slope profile this way the integration of the rills to form a permanent channel begins. The concentration of the runoff from the many rills forms a hopper-like drainage basin (Pl. 4). Possibly only on strongly rilled slopes will the basal concavity be an erosional rather than a depositional feature.

Available Relief and the Development of Landforms

Because a correlation exists between relative relief and other drainage basin parameters at Perth Amboy and other areas it may be possible to predict some effects of dissection in areas of widely different degrees of available relief but similar in lithology, structure, and climate. Glock (1932, p. 75) defines available relief as the vertical distance from the initial upland surface to the lowest level of channel degradation; it is the total relief available to the stream channels for dissection. It is reasonable to suppose that within one topographic type basins of high relief ratio would also have high available relief so that whatever relationships exist between relief ratio and other morphological elements (maximum slope angles, stream gradients, drainage density, and basin shape) would also exist for available relief.

Glock (1932) compared profiles of areas of high, moderate, and low relief; his main conclusion was that an "upper flat", the undissected upland surface, disappears with increased relief. His discussion of the evolution of an area of high relief agrees with W. Penck's (1953) that in the condition of "uniform development" constant relief may be maintained dur-

ing dissection. Glock states that downcutting of a thick mass maintains a region of high available relief until the lower limit of channel degradation is reached, as illustrated in Figure 38a where the retreating steep slopes intersect in a sharp-crested divide which is lowered at the same rate as the channel.

The writer chose the following as illustrative examples based on observed quantitative relationships between relief ratio and drainage density in mature areas of the fifth order: an area of high available relief with relief ratio greater than 0.15 (Fig. 38a); an area of moderate relief with relief ratio of 0.04 (Fig. 38b); an area of low relief with relief ratio of 0.009 (Fig. 38c). The range in Figure 12 supplied the relief-ratio values, and corresponding drainage-density values were read. This is a reasonable procedure, for in areas of similar lithology drainage density is related to relief ratio (Fig. 13). The values for the length of overland flow (distance water would flow from the divide to a stream channel) are half the reciprocal of drainage density (Horton, 1945, p. 284). Twice the length of overland flow is the average distance between adjacent stream channels, and is a mean value for the spacing of stream channels in any area. The three cross sections of areas of high, low, and moderate relief (Fig. 38) were constructed so that the distance between divide and channel is proportional to the drainage density which is in turn proportional to the relief ratio for each section. It is now possible to compare the three hypothetical areas, remembering that the fundamental difference is available relief; lithology is assumed to be the same in each.

The area of high relief has a relief ratio of 0.15, a drainage density of 20, and a length of overland flow of 0.025 miles. Therefore, the following characterize the area (Fig. 38a):

(1) Degradation of stream channel will be rapid.

(2) Straight slopes will develop early at a steep angle characteristic of the area (Stage 1).

(3) Parallel retreat of the slope will maintain the steep maximum angle during most of the geomorphic evolution of the area (Stages 1–7).

(4) Slopes will quickly intersect, eliminating the "upper flat" (Stage 4).

(5) Local relief will remain constant during much of the evolution; the mature stage dominates during the topographic evolution (Stages 4–6).

(6) With cessation of channel downcutting lateral planation may maintain the characteristic steep angle, but relief will be reduced (Stage 7).

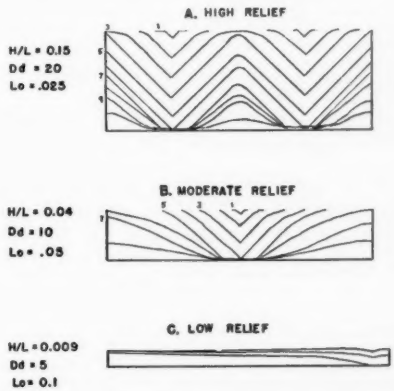

FIGURE 38.—DEVELOPMENT OF TOPOGRAPHY IN AREAS OF HIGH, MODERATE, AND LOW RELIEF
Horizontal and vertical scales: about 1 inch equals 0.025 mile or 132 feet

(7) Slope angles will lower as basal deposition occurs. Strahler (1950, p. 813) compared mean maximum-slope angles of slopes protected at their base with slopes with actively degrading streams at their base and found a significant decrease in angle (Stage 8).

(8) Continued deposition at slope base will result in a concave-convex profile (Stages 9, 10). Erosion at this late stage may approach Lawson's (1932) postulation that runoff would remove lune-shaped segments from the crest of hills. Development of drainage basin form at Perth Amboy is an example of a region of high available relief.

The hypothetical area of moderate available relief (Fig. 38b) has a relief ratio of 0.04, a drainage density of 10, and a length of overland flow of 0.05 miles, differing as follows from areas of high available relief:

(1) Degradation will be less rapid.

(2) The intersection of straight parallel retreating slopes will not quickly eliminate the "upper flat".

(3) The stage of maturity (maximum relief) will be briefer (Stages 4, 5).

(4) Stream channels will be twice as far apart.

Evolution is not markedly different from the region of high relief in early stages, but the

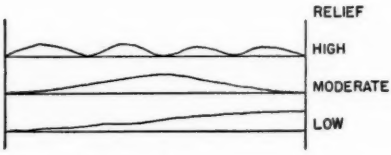

FIGURE 39.—POSSIBLE TOPOGRAPHIC DIFFERENCES, AT A LATE STAGE OF DEVELOPMENT, BETWEEN AREAS OF ORIGINALLY HIGH, MODERATE, AND LOW RELATIVE RELIEF

area is soon one of rounded slopes with decreasing slope angles (Stages 6–9).

The hypothetical area of low available relief has a relief ratio of 0.009, a drainage density of 5.0, and a length of overland flow of 0.1 mile, differing from the others as follows:

(1) Distance between adjacent channels will be four times that of the area of high relief.

(2) Channel degradation is assumed to be slow, and incision will be slight.

(3) Straight slopes never develop, and broad convexities characterize the area. (*Cf.* Fig. 36, profile 2.)

This hypothetical discussion takes into account the effects of increased relief on topographic development within areas of the same lithology. In late stages closer spacing of channels may distinguish areas of originally high relief from areas of originally lower relief. Hypothetical sections of the three areas (Fig. 39) illustrate the expected topography. It may be, however, that integration of the systems would reduce drainage density, as relief declined, and interstream spacing in the later stages, so that no basis of comparison would remain.

This discussion is not intended to set forth any cycle of slope development but rather to show that diverse slope-profile forms are rational parts of sequences in which both parallel and declining slope retreat play parts, depending on the relative relief at the start of denudation and the stage to which reduction of relief has progressed.

Hypsometric Study of Geomorphic Stages of Development

The classic Davisian geomorphic cycles list criteria for delimiting each stage of development of landscape. Many geomorphologists have studied the relative time required or the proportionate mass removed from any basin in each stage. Johnson (1932, p. 488) guessed that the youthful stage takes up 15 per cent of the total time required for the complete cycle. Johnson (1933) also used per cent of total erosion as a basis of stage classification, stating that youth persists until 30–40 per cent of the available mass is removed, on the supposition that the initial surface would at this point be largely destroyed. Strahler (1952b, p. 1130) proposed that the youthful stage persists until the hypsometric integral reduces to about 60 per cent, implying about 40 per cent removal of mass.

Strahler (1952b, p. 1130) states:

"From the standpoint of hypsometric analysis, the development of the drainage basin in a normal fluvial cycle seems to consist of two major stages only; (1) an inequilibrium stage of early development, in which slope transformations are taking place rapidly as the drainage system is expanded and ramified. (2) An equilibrium stage in which a stable hypsometric curve is developed and maintained in a steady state as relief slowly diminishes. The monadnock phase with abnormally low hypsometric integral, when it does occur, can be regarded as transitory, because removal of the monadnock will result in restoration of the curve to the equilibrium form. . . . The hypsometric curve of the equilibrium stage is an expression of the attainment of a steady state in the processes of erosion and transportation within the fluvial system and its contributing slopes."

The writer studied these concepts in a series of second-order basins whose hypsometric curves form a series of increasing mass removal (Figs. 18, 19). Detailed description of these curves has already been presented. To the 11 basin curves plotted in Figure 19 two hypothetical curves were added in accordance with the supposed further reduction of the basins.

The curves illustrating the distribution of mass within each basin (Fig. 19) demonstrate that as erosion continues the following changes occur: (1) The point of maximum erosion migrates toward the head of the basin. The vertical distance between curves is greatest near the mouth of the basins (right side of illustration) in

early stages but is greatest near the basin head in later stages (left side of illustration), beginning with curve 10. (2) The rate of lowering of the main channel decreases as the point of maximum erosion advances upchannel. Vertical distance between curves at right side of

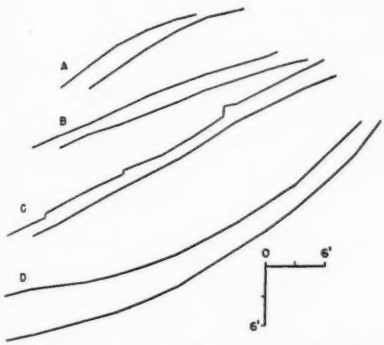

FIGURE 40.—CHANGES IN LONGITUDINAL STREAM PROFILES AT PERTH AMBOY

The profiles were measured on four stream channels ranging from very youthful to fully mature. The lower profile of each pair is a resurvey 1 year after the upper profile was surveyed. Relative vertical spacing of each pair of profiles has no significance in terms of actual vertical lowering.

illustration, or mouth of basin, decreases downward indicating reduced rate of lowering of mouth of basin or reduced degradation of main channel. (3) The profile of the hypsometric curves changes with mass removal from convex-up to essentially straight to concave-up.

Although these hypsometric curves are not stream profiles they seem to reflect the activity of the stream in each case. Channel degradation has not greatly affected Curve 1, for the channels are mere traces on the upland surface. Curve 2 gives the first evidence of channel degradation in the abrupt down bend at the right. Curves 2, 3, 4, 5, and 6 reveal successively that the deeply incised channel is growing headward. At the same time the channel to which these basins are tributary is lowering rapidly and there is no stable base level at the basin mouth. Challinor (1930) stated that a stream not controlled by a fixed base level will have such a convex profile.

In the stage of Curves 7 and 8 the main channel has ceased rapid degradation and the tributaries immediately respond by removing convexities in their channels. Continued adjustment of basin forms brings a concavity to the hypsometric curves. Figure 40 shows that stream-channel profiles follow a similar evolution.

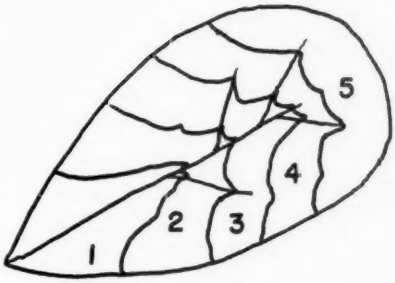

FIGURE 41.—METHOD OF DIVIDING A DRAINAGE BASIN INTO FIVE EQUAL AREAS AND THE SYSTEM OF NUMBERING EACH 20 PER CENT AREA

Comparing erosion in different areas of a basin at successive times further illustrates the progress of erosion. The mass removed from any portion of a basin can be determined by measuring the area above the hypsometric curve within limits of that percentage area class of the basin. The basins were divided into five equal-area classes bounded by the vertical lines for each 20 per cent increase of area. For example, the mass removed in the lower 20 per cent of the basin area was determined by measuring with a planimeter the area remaining above each curve limited by the ordinates for 80 and 100 per cent of basin area. The basins were thus divided into five equal areas (Fig. 41) numbered from lowest to highest. To illustrate the progress of erosion within each 20 per cent unit of basin area, each drainage basin represented by a curve in Figure 19 was replotted as a vertical series of points (Fig. 42). The percentage of total mass removed from each 20 per cent area unit of one basin is a point on the new curve. Five new curves are thus drawn, corresponding to each 20 per cent area, numbered in accordance with Figure 41 where the lowest area, nearest the mouth, is number 1. These curves then show the changes in the relative magnitude of mass removed from

each 20 per cent area during the progress of the erosion cycle.

Comparison of Figure 42 with Figure 19 shows that the shape of each hypsometric curve in Figure 19 depends upon which area begins, shown by the steepening of area unit curve 5. Beyond 40 per cent total mass removed the hypsometric curves (Fig. 19) become increasingly concave from increased erosion at the basin heads.

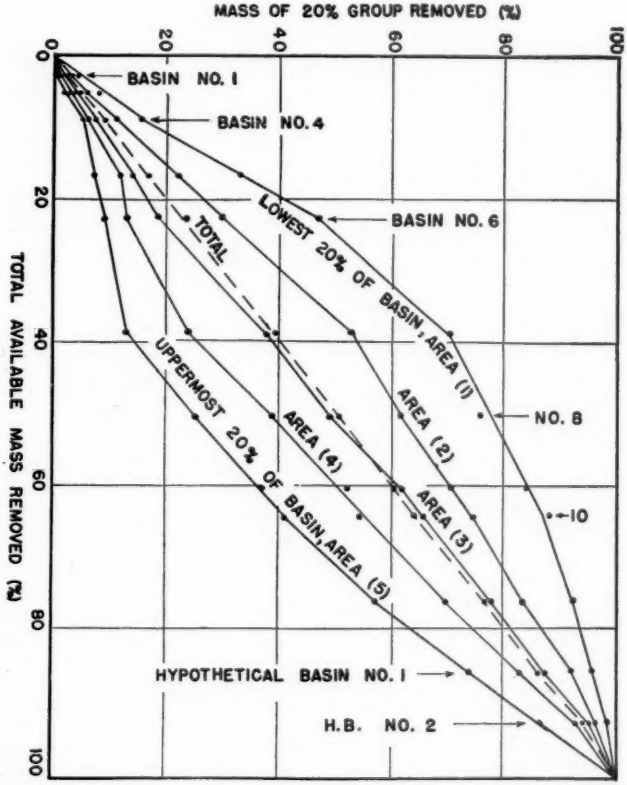

FIGURE 42.—RELATION OF EROSION WITHIN EACH 20 PER CENT AREA OF A BASIN TO TOTAL EROSION DURING A COMPLETE GEOMORPHIC CYCLE

segment is experiencing maximum erosion. Erosion in area unit 1 (Fig. 42) is greatest during the earliest stages of basin development but begins to decrease at about 25 per cent total mass removed (Basin 6) and is markedly decreased at 40 per cent (Basin 7). In Figure 19 hypsometric curve 6 is the last of the series showing a pronounced up-convexity. In Figure 42, at 40 per cent total mass removed, area unit 1 has lost 70 per cent, of its mass, whereas area unit 5 has lost only 13 per cent. Erosion in area unit 5 is minor until 40 per cent total mass removed (Basin 7), when an increase in erosion

A comparison of curves in Figure 42 shows that erosion is greatest at first near the basin mouth (area unit 1) but dominant later in area unit 5. Erosion in area unit 1 decreases after removal of 25 per cent of the total mass. This is the same percentage at which the relief ratio becomes constant, for the relief ratio may reach a fixed value when the mouth of the stream has lowered to local base level. Erosion progresses upchannel into the higher area units causing modification of the other basin characteristics until later in the cycle.

Beyond 40 per cent total available mass re-

moved, all curves of Figure 42 converge toward 100 per cent mass removal or peneplanation. This suggests that in this sequence there is no sudden change to an equilibrium stage in distribution of erosion but rather a zone of transition between 25 and 40 per cent of mass removal.

Strahler's selection of hypsometric integral of 40 per cent as the beginning of the equilibrium stage agrees roughly with the curve inflections in Figure 42, although the fortuitous occurrence of a basin at 40 per cent total available mass removed may give the misleading impression that abrupt changes in erosion occur at this point. It is safer to say that major changes occurred between 30 and 40 per cent.

Strahler's equilibrium stage includes both maturity and old age stages of the Davisian cycle. Observations of basin-form parameters suggest subdividing the equilibrium stage into two parts. Therefore the equilibrium stage will have two phases, one in which the mean values for relief ratio, gradient, and basin shape are constant or essentially constant, and a later phase when these values decrease. The phase of constant values would vary in duration; it would be shorter in areas of moderate available relief and absent in areas of low relief. Maturity and old age are thus recognizable in the constant and decreasing phase respectively, within the equilibrium stage of hypsometric development.

Comparative Studies in Badland Regions of the West

Topographic Forms and Erosion Processes

At Perth Amboy rainbeat and surface runoff were the dominant erosion processes active in topography development during the summer. The writer assumed that in similar badland areas in the western United States runoff erosion would also be dominant, but field observations in the Badlands National Monument, South Dakota suggested that it was not.

The presence of two distinct topographic forms in the South Dakota area is obvious (Pl. 5, fig. 2). Steep sharp-crested slopes with a mean maximum slope angle of 44° develop on the Brule formation. The underlying upper Chadron formation, where exposed by the retreat of the steep-sloped Brule, develops the rounded, rolling topography in the lower parts of the photograph. The mean maximum slope angle of the Chadron slopes is 33°. Poorly consolidated clay, sandstone, limestone, and nodular layers compose both formations, but the portion of the Chadron exposed is essentially homogeneous. Both formations contain the clay minerals illite and montmorillonite (Van Houten, 1953).

Smith (In press) attributes the difference in angles to the more resistant layers in the Brule formation or to a larger percentage of calcareous cement in the Brule clays, 10 to 20 per cent, as against 4 per cent for the Chadron (Wanless, 1922). In any case the surface of the two formations is distinctly different (Pl. 5, figs. 3, 4). The surface of a slope underlain by the Chadron in the dry summer period is a loose mass of clay aggregates. A surface layer of 1 to 2 inches can be scooped up by hand. Walking over such a surface breaks down the aggregates and starts the rolling and sliding of loose material downslope. The Brule surfaces are very different under similar conditions (Pl. 5, fig. 4). Despite desiccation the surface is so hard that a hammer is required to break it up. Three faint rill channels are visible in the photograph, but in most places rills are scarce on Chadron surfaces. Figure 5 in Plate 5 shows an upper slope of strongly rilled Brule; on the slope below the contact with the underlying upper Chadron the rill channels decrease sharply in number and clarity. The lack of cement in the Chadron may allow swelling of the clay minerals to produce the loose crumbly surface, a process Smith (In press) called disaggregation.

The rapidity of breakdown of the Chadron clay and the looseness of the surface might suggest more rapid erosion of these slopes, but the overlying Brule must retreat to expose the Chadron. Where the upper Chadron is free of overlying Brule it forms a rolling topography extending some distance from the base of the retreating Brule slopes (Pl. 5, fig. 2). Although softer, the Chadron is the more enduring of the two formations. When canteens of water were emptied on both types of slopes, runoff occurred almost immediately on the Brule but the Chadron completely absorbed the water, suggesting that the Brule retreats rapidly under runoff while the Chadron, with great infiltration capacity, is a more resistant rock removed

slowly by creep of surface particles and subsurface flow.

The writer used a 5-gallon hand pump, adjusted to fine spray, to spray the slopes of both formations. On the Brule, runoff always occurred before 1 gallon was sprayed, quickly concentrating into rill channels and flowing rapidly away. Four and one half gallons was sprayed on a Chadron slope before runoff occurred (Pl. 5, fig. 6). By then the surface was a sticky mud; the individual aggregates had absorbed water and slumped downslope until they were in contact with the next lower aggregate.

Water was next poured on the two slopes near their crests. On the Brule slope runoff was rapid; on the Chadron the water rapidly disappeared between the aggregates, flowed in subsurface channels, and reappeared at the base of the slope to continue as surface flow across the pediment. Figure 1 in Plate 6 shows the course followed by water poured on the crest of a small residual. Three elements are visible in the photograph: an upper light-colored layer of resistant clay (probably basal Brule), a darker Chadron slope, and the basal pediment surface. The water followed a rill channel across the Brule but at the Chadron contact it disappeared to follow a subsurface channel (emerging at one point on the surface) and finally reappeared at the base of the slope. The remaining water was quickly absorbed by the pediment surface. Figure 2 in Plate 6 shows water issuing from a subsurface channel at the slope base during another trial. This process may be very effective in miniature pediment

---

PLATE 4.—RILL CYCLE

THE COMBINED EROSIVE POWER OF THE NUMEROUS RILL CHANNELS HAS ERODED A PERMANENT DRAINAGE BASIN

FIGURE 1.—SPRING

FIGURE 2.—SUMMER; RILLS AT MAXIMUM DEPTH

FIGURE 3.—FALL

FIGURE 4.—WINTER; ONLY MAJOR DIVIDES REMAIN

FIGURE 5.—BEGINNING OF DECAY OF RILLS BY BREAKUP OF SURFACE CRUST

Note fractures, paralleling the divide, due to downward creep of the disturbed surface

FIGURE 6.—NEEDLE ICE AT BASE OF SLOPE

Ice columns, about 3 inches long, allow downslope movement of heaved material upon melting

PLATE 5.—BADLAND SLOPES AT PERTH AMBOY AND BADLANDS NATIONAL MONUMENT, SOUTH DAKOTA

FIGURE 1.—SMALL MUDFLOWS CAUSED BY THE MELTING OF THE FROZEN SOIL SURFACE AT PERTH AMBOY

FIGURE 2.—TYPICAL BRULE AND CHADRON FORMATION TOPOGRAPHY IN THE BADLANDS NATIONAL MONUMENT, SOUTH DAKOTA

Contact between the two formations, just above the center of the photograph, separates the steep slopes developing in the Brule formation from the gentle, rolling topography developing on the Chadron formation.

FIGURE 3.—CLOSE-UP OF LOOSE MOSAIC OF AGGREGATES FORMING THE SURFACE OF SLOPES FORMED ON THE CHADRON FORMATION

FIGURE 4.—CLOSE-UP OF SURFACE OF SLOPE DEVELOPING ON THE BRULE FORMATION

Surface is compact, and three faint rill channels are present.

FIGURE 5.—DECREASE IN CLARITY AND NUMBER OF RILL CHANNELS BELOW THE CONTACT BETWEEN THE BRULE AND CHADRON FORMATIONS

FIGURE 6.—SURFACE OF THE CHADRON FORMATION AFTER BEING SPRAYED WITH 4½ GALLONS OF WATER

Surface is saturated, but no runoff has occurred

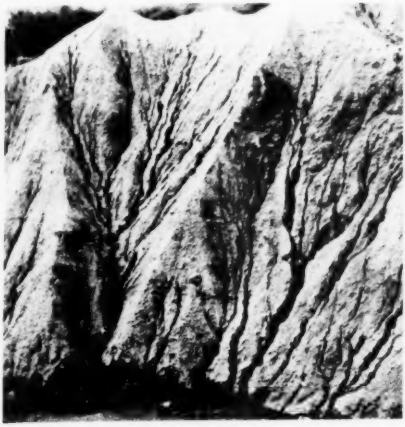

FIGURE 1

FIGURE 2

FIGURE 3

FIGURE 4

FIGURE 5

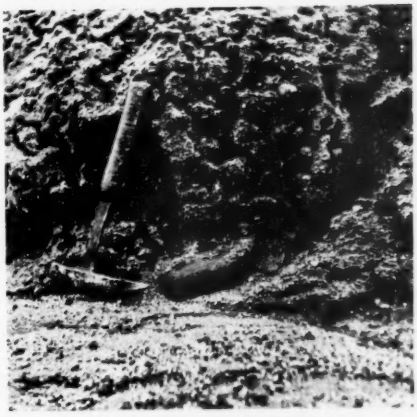

FIGURE 6

RILL CYCLE

FIGURE 1

FIGURE 2

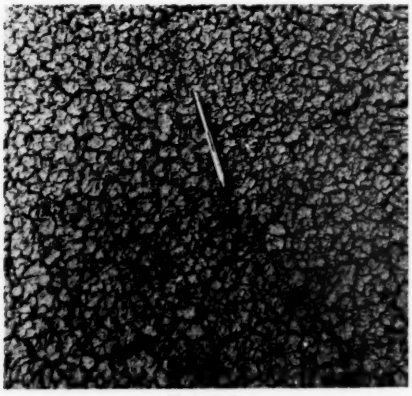

FIGURE 3

FIGURE 4

FIGURE 5

FIGURE 6

BADLAND SLOPES AT PERTH AMBOY AND BADLANDS NATIONAL MONUMENT, SOUTH DAKOTA

FIGURE 1

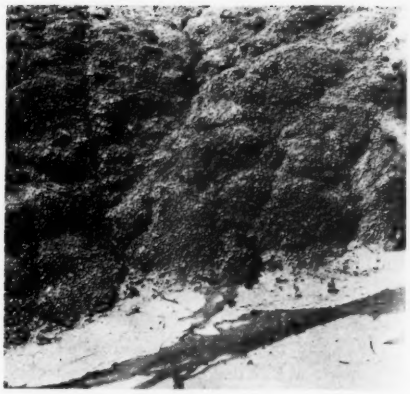

FIGURE 2

FIGURE 3

FIGURE 4

FIGURE 5

FIGURE 6

BADLAND SLOPES AND DRAINAGE CHANNELS, SOUTH DAKOTA AND ARIZONA

formation in this area. Smith (In press) discussed a similar process, suggesting that the water fanning out from the base of a rill results in basal sapping of the slope, causing it to retreat. The large number of miniature natural bridges occurring in drainage channels cut into the Chadron testifies that subsurface flow is of major importance.

To determine the effects of the different processes on the slopes, the writer measured slope angles on small buttes and other residuals composed of essentially homogeneous material. Length of slope was the criterion of age of the residuals, for obviously their slopes would be shortened by continuous slope retreat and lowering of the divide. The slopes studied were short and could be expected to show changes if any occurred during their evolution. On the Brule residuals slopes longer than 5.6 feet had a mean maximum slope angle of 44.3°; slopes less than 4 feet had a mean angle of 44.0°; slopes shorter than 3 feet had a mean of 45.0°. Retreat of these slopes is essentially parallel under the action of surface runoff.

The Chadron slopes on the other hand, showed a decrease in angle with decrease in slope length:

Length of Slope	Mean Maximum Slope Angles
less than 12′	29.9°
less than 6′	30.1°
less than 4′	27.5°
less than 2′	20.8°
less than ½′	11.6°

The action of creep evidently lowers the slope angle, producing a broad convexity of divide, for without a rapidly retreating straight slope this upper convexity is preserved. Perhaps here the hilltop slope results from dominant rainbeat and creep, following Gilbert's hypothesis (1909). This study, coupled with that at Perth Amboy, suggests that convex slopes may result from the combined action of runoff and creep where basal slope steepening is not active.

In certain respects the differences between the Brule and Chadron topography illustrate form differences between humid and arid regions. The typically arid-landscape forms of sharp divides and steep slopes developing on the Brule formation are in sharp contrast to the rounded topographic forms with gentler slopes developing on the Chadron. The disaggregation of the Chadron forms a mulch analogous to vegetation and deep soil horizons in humid regions, in that all reduce runoff by aiding infiltration. Thus, humid and arid topographic types may be part of a continuous series, each component dependent on the importance of surface runoff and rate of infiltration. Certainly arid forms develop in humid regions where runoff is unusually rapid, as at Perth Amboy, or the Copper Basin at Ducktown, Tennessee, or in volcanic ash deposits.

Similar comparisons and measurements were made in badlands developing on homogeneous clays of the Chinle formation near Cameron,

---

PLATE 6.—BADLAND SLOPES AND DRAINAGE CHANNELS, SOUTH DAKOTA AND ARIZONA

FIGURE 1.—WATER POURED ON THE BRULE FORMATION NEAR DIVIDE FLOWS DOWNSLOPE IN RILL CHANNEL UNTIL RUNOFF CROSSED THE CONTACT BETWEEN THE UPPER LIGHT-COLORED BRULE AND THE LOWER DARKER CHADRON

Water disappears into a subsurface channel below the contact, reappears at the surface to the left of the hat and finally at the slope base where it flows onto the pediment surface.

FIGURE 2.—WATER POURED ONTO THE SURFACE OF THE CHADRON FORMATION FOLLOWS SUBSURFACE CHANNELS TO THE BASE OF THE SLOPE WHERE IT REAPPEARS ON THE PEDIMENT SURFACE

FIGURE 3.—RETREAT OF STEEP BADLAND SLOPES BY SLUMPING IN BADLANDS FORMED ON THE CHINLE FORMATION NEAR CAMERON, ARIZONA

FIGURE 4.—VIEW DOWN STREAM CHANNEL AT POINT WHERE UPPER PRAIRIE SLOPES AWAY FROM THE TOPOGRAPHIC BREAK

Note narrow badlands zone between the Upper and Lower Prairie

FIGURE 5.—VIEW DOWN STREAM CHANNEL WHERE UPPER PRAIRIE SLOPES TOWARD WALL

Compare with figure 4 above, and with figure 43

FIGURE 6.—TYPICAL BADLAND STREAM CHANNEL

Gradient is very steep, and downcutting is so rapid that the valley is very narrow. Board wedged between the valley walls is 3 feet long.

Arizona. The presence of montmorillonite (Gregory, 1950, p. 69) causes swelling and contraction with alternate wetting and drying of the surface and the formation of a loose surface composed of aggregates. Numerous sinks characterize the area, and many minor drainage lines are interrupted or poorly developed, testifying to the paucity of surface runoff. Spraying and pouring of water on the Chinle surface provided results similar to those obtained on the Chadron slopes. Where long straight slopes had developed because of rapid channel degradation, the slopes showed forms produced by slumping and sliding of the surface layers (Pl. 6, fig. 3). The mean maximum angle measured along the base of slopes bordering on pediments was about 32°.

Similar measurements were made in near-by areas where the Chinle is more sandy, better cemented, and less susceptible to swelling and the formation of aggregates; the slopes had a mean maximum slope angle of 36.5°. When these slopes were sprayed, runoff occurred in half the time required on the less well-cemented Chinle. With these figures in mind it appears that, in general, as time required to initiate runoff increases the slope angle decreases, or as infiltration rates increase slope angles decrease. Paulsen (1940, p. 440) found that infiltration increases with decrease in mean land slope. Field work in Wyoming (Hadley and Schumm, In preparation) indicates that infiltration rates are related to the mean relief ratio for each lithologic unit studied.

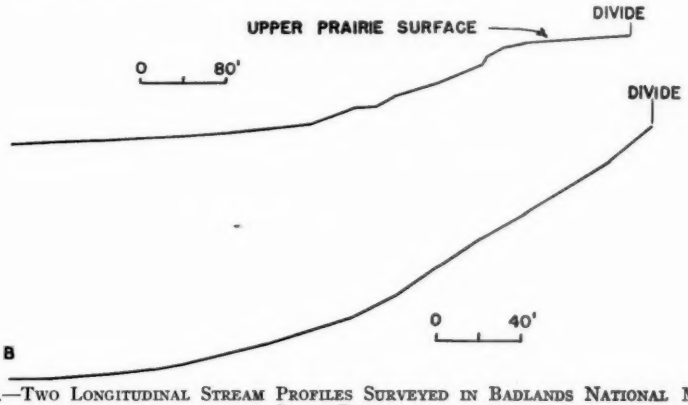

FIGURE 43.—TWO LONGITUDINAL STREAM PROFILES SURVEYED IN BADLANDS NATIONAL MONUMENT, SOUTH DAKOTA
Vertical and horizontal scales are the same.

Influence of Regional Upland Slope on Topography

One other factor influencing the development of youthful topography, especially the escarpment scenery in some of the National Parks and Monuments, is the relative direction of regional slope of the upland surface. At Perth Amboy the upper terrace surface sloped toward the terrace front, supplying additional discharge to the heads of insequent drainage lines. The streams grew rapidly headward and the entire surface was soon drained by channels sloping in the direction of the original upper slope. In the Badlands National Monument the badland topography is limited to a narrow zone between the Upper Prairie, or upland, and the Lower Prairie bordering the White River, because most of the upland runoff is directed away from the badlands by the northward regional slope away from the scarp. Here the badland channels cannot advance rapidly over the lip of the upper surface, so that a sharp break is maintained. The badland areas encroach upon the upper surface as a retreating scarp, known locally as The Wall (Pl. 6, fig. 4). If the Upper Prairie sloped toward the badlands, the badland area would rapidly extend at the expense of the grazing land of the Upper Prairie, destroying the scarp and the unique scenic value of the region. Figure 43 shows two longitudinal stream profiles surveyed

across the scarp of the badlands. The upper profile, A, was surveyed where the upper surface for a short distance along the wall slopes toward the advancing badland streams; the lower profile, B, is typical of the general plan where the upper surface drains away from the badlands. Profile A resembles the typical profile at Perth Amboy (Fig. 36) where the stream is cutting into the upper surface above the convexity typical of that development (Pl. 6, fig. 5). Figures 4 and 6 of Plate 6 show the area where the lower profile of Figure 43 was obtained.

The striking scenery of Bryce Canyon National Park and Cedar Breaks National Monument is also accentuated by the slope of the upland away from the break between badland and upland surface. The main effect of such an arrangement of slopes is an increase in the relief ratio in the badlands with an attendant increase in steepness of stream profiles and slope angles. An upland slope toward the break reduces the relief ratio by increasing the length of the basin.

Summary and Conclusions

The drainage system at Perth Amboy conforms to Horton's laws of drainage composition; further, the mean drainage areas of streams of each order also form a geometric progression. Within an area of homogeneous lithology and simple structure the scale of the drainage-network elements is determined by a characteristic value for the minimum area required for channel maintenance. Relationships between channel lengths, drainage-basin area, and stream-order number are dependent on this constant of channel maintenance, which is in turn dependent on relative relief, lithology, and climate. The constant of channel maintenance is valuable as a measure of texture and decreases with increasing erodibility. Other characteristics of the drainage network which vary with relative relief are: drainage density, maximum valley-side slope angles, stream-channel gradient, drainage-basin shape, rate of sediment loss, and drainage pattern. Hadley and Schumm (In preparation) found relief ratio related to the infiltration rate of the soil on a lithologic unit and infiltration rates to texture of the topography. This suggests that infiltration rates are one of the most important factors influencing topographic development.

The mass-removal sequence of drainage basins strongly supports Strahler's concept of an open system in a steady state as related to drainage-basin development. At Perth Amboy the equilibrium stage begins at 25 per cent of mass removal as indicated by the constancy of drainage-basin parameters beyond this stage.

A comparison of young and mature angles of junction shows a significant difference suggesting that the angles change during the geomorphic cycle. During the reduction of a landmass of high relief much erosion may occur by lateral shifting of tributaries toward main channels.

Experimental studies and field observations reveal that erosion and the development of slope profiles may not conform to certain widely assumed concepts of the action of runoff as a function of depth and distance from a divide. Because runoff occurs as subdivided and surge flow, runoff erosion is more analogous to creep than to transport by fluid flow in channels.

Parallel and declining slope retreat may both be important in the evolution of erosional topography, depending on the available relief and perhaps on infiltration rates of the soil.

At Perth Amboy slopes are initiated by channel degradation and maintained by runoff and creep induced by frost heaving. Convex divides may be formed either by runoff or by rainbeat and creep. Rills follow a definite cycle of destruction and reappearance under the action of frost heaving and runoff.

Two types of topography appearing in the Badlands National Monument resemble arid and humid landscapes, the first with sharp-crested, steep, straight slopes bordered by pediments, the second with more gentle slopes and convex summits. The topographic differences are explained by the differences of infiltration rates of the two formations on which they form. This distinction may apply generally to differences between arid and humid topography. Vegetation and thick-soil horizons aid infiltration which promotes creep and the development of the rounded humid-cycle landforms characterized by declining slope retreat in later stages. In arid regions sparse vegetation and meager soils aid rapid runoff and the formation of steep, parallel retreating slopes and pediments.

Much work must be done before a workable theory of erosional landform development can be projected from detailed field examination and measurements of topographic characteristics and geomorphic processes, but there is no alternative to an empirical quantitative approach if these relationships are to be clarified in realistic terms.

References Cited

Anderson, H. W., 1946, The effect of freezing on soil evaporation from a bare soil: Am. Geophys. Union Trans. v. 27, p. 863–870

Baulig, H., 1939, Sur les "Gradins de Piedmont": Jour. Geomorphology, v. 2, p. 281–304

Borst, A. L., and Woodburn, R., 1940, Rain simulator studies of the effect of slope on erosion and runoff: Soil Conserv. Service Tech. Pub. 36

Burmister, D. M., 1952, Soil mechanics, v. 1: N. Y., Columbia Univ. Press, 153 p.

Challinor, J., 1930, The curve of stream erosion: Geol. Mag., v. 67, p. 61–67

Chamberlin, T. C., and Salisbury, R. D., 1905, Geology, v. 1, 2d ed.: N. Y., H. Holt & Co., 684 p.

Croxton, F. E., and Cowden, D. J., 1939, Applied general statistics: N. Y., Prentice Hall, 944 p.

Davis, W. M., 1909, Geographical essays: N. Y., Ginn & Co., 777 p.

Duley, F. L., and Hays, O. E., 1932, The effect of degree of slope on runoff and soil erosion: Jour. Agr. Research, v. 45, p. 349–360

Ellison, W. D., 1945, Some effects of raindrops and surface-flow on soil erosion and infiltration: Am. Geophys. Union Trans., v. 26, p. 415–429

Fenneman, N. M., 1908, Some features of erosion by unconcentrated wash: Jour. Geology, v. 6, p. 746–754

—— 1922, Physiographic provinces and sections in western Oklahoma and adjacent parts of Texas: U. S. Geol. Survey Bull. 730, p. 115–134

Gilbert, G. K., 1909, The convexity of hilltops: Jour. Geology, v. 17, p. 344–350

Glock, W. S., 1931, The development of drainage systems: a synoptic view: Geog. Rev., v. 21, p. 475–482

—— 1932, Available relief as a factor of control in the profile of a landform: Jour. Geology, v. 40, p. 74–83

Gregory, H. E., 1950, Geology and geography of the Zion Park region, Utah and Arizona: U. S. Geol. Survey Prof. Paper 220, 200 p.

Hadley, R. F., and Schumm, S. A., (In preparation) Studies of erosion and drainage basin characteristics in the Cheyenne River Basin: U. S. Geol Survey Water-Supply Paper

Hendrickson, B. H., 1934, The choking of pore-space in the soil and its relation to runoff and erosion: Am. Geophys. Union Trans., v. 15, p. 500–505

Horton, R. E., 1945, Erosional development of streams and their drainage basins; hydrophysical approach to quantitative morphology: Geol. Soc. America Bull., v. 56, p. 275–370

Hursh, C. R., 1948, Local climate in the Copper Basin of Tennessee as modified by the removal of vegetation: U. S. Dept. Agriculture Circ. 774, 38 p.

Johnson, D., 1932, Streams and their significance: Jour. Geology, v. 40, p. 481–497

—— 1933, Available relief and texture of topography: a discussion: Jour. Geology, v. 41, p. 293–305

Krumbein, W. C., and Pettijohn, F. J., 1938, Manual of sedimentary petrography: N. Y., Appleton-Century Co., 549 p.

Langbein, W. B., *et al.*, 1947, Topographic characteristics of drainage basins: U. S. Geol. Survey Water-Supply Paper 968c, p. 99–114

Lawson, A. C., 1932, Rain-wash in humid regions: Geol. Soc. America Bull., v. 43, p. 703–724

Leopold, L. B., and Maddock, T., Jr., 1953, The hydraulic geometry of stream channels and some physiographic implications: U. S. Geol. Survey Prof. Paper 252, 57 p.

Leopold, L. B., and Miller, J. P., in press, Channel characteristics and drainage patterns of ephemeral streams: U. S. Geol. Survey Water-Supply Paper

Paulsen, C. G., 1940, Hurricane floods of Sept. 1938: U. S. Geol. Survey Water-Supply Paper 867, 562 p.

Penck, W., 1953, Morphological analysis of landforms (translated by Czeck and Boswell): London, MacMillan and Co., Ltd., 429 p.

Schumm, S. A., 1955, The relation of drainage basin relief to sediment loss: Internat. Union Geodesy and Geophys., 10th General Assembly (Rome), Trans., v. 1, p. 216–219

Segerstrom, K., 1950, Erosional studies at Paricutin, State of Michoacan, Mexico: U. S. Geol. Survey Bull. 965 A, 164 p.

Smith, K. G., In press, Erosional processes and landforms in Badlands National Monument, South Dakota: Geol. Soc. America Bull.

Strahler, A. N., 1950, Equilibrium theory of erosional slopes approached by frequency distribution analysis: Am. Jour. Sci., v. 248, p. 673–696, 800–814

—— 1952a, Dynamic basis of geomorphology: Geol. Soc. America Bull., v. 63, p. 923–938

—— 1952b, Hypsometric (area-altitude) analysis of erosional topography: Geol. Soc. America Bull., v. 63, p. 1117–1142

—— 1953, Revisions of Horton's quantitative factors in erosional terrain: Paper read before Hydrology Section of Am. Geophys. Union, Washington, D. C., May 1953

U. S. Weather Bureau, 1929–1948; Climatological data for the U. S. by sections: v. 16–35

Van Houten, F. B., 1953, Clay minerals in sedimentary rocks and derived soils: Am. Jour. Sci., v. 251, p. 61–82

Wanless, H., 1922, Lithology of the White River sediments: Am. Philos. Soc. Proc., v. 61, p. 184–203

Wolman, M. G., 1955, The natural channel of Brandywine Creek Pennsylvania: U. S. Geol. Survey Prof. Paper 271, 56 p.

Yarnell, D. L., 1935, Rainfall intensity-frequency data: U. S. Dept. Agriculture Misc. Pub. 204, 67 p.

Building 25, Federal Center, Denver, Colorado

Manuscript Received by the Secretary of the Society March 24, 1955

Project NR 389-042, Technical Report No. 8

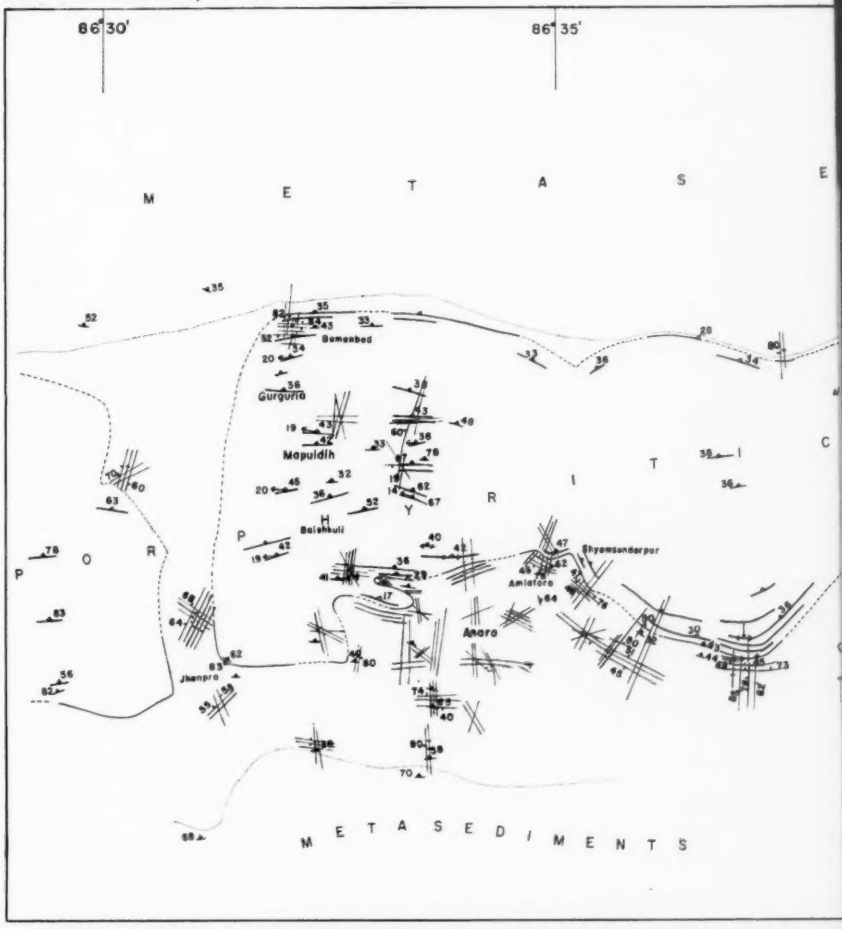

STRUCTURE MAP SHOWING FOLIATION, LINEATION, AI

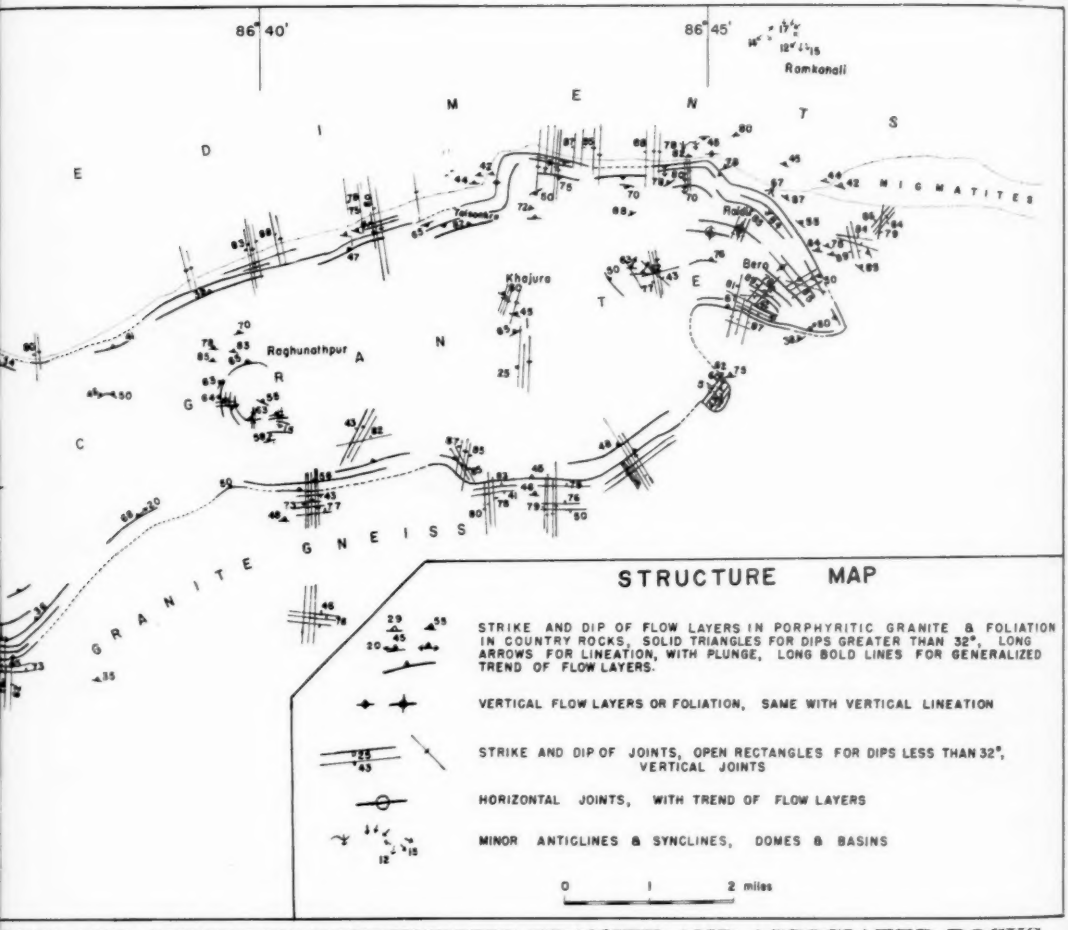
86° 40'
86° 45'
Ramkanali
MENTS
EDI
NIGMATITES
Raidih
Bero
Khajura
Raghunathpur
GRANITE GNEISS
STRUCTURE MAP
STRIKE AND DIP OF FLOW LAYERS IN PORPHYRITIC GRANITE & FOLIATION IN COUNTRY ROCKS, SOLID TRIANGLES FOR DIPS GREATER THAN 32°, LONG ARROWS FOR LINEATION, WITH PLUNGE, LONG BOLD LINES FOR GENERALIZED TREND OF FLOW LAYERS.
VERTICAL FLOW LAYERS OR FOLIATION, SAME WITH VERTICAL LINEATION
STRIKE AND DIP OF JOINTS, OPEN RECTANGLES FOR DIPS LESS THAN 32°, VERTICAL JOINTS
HORIZONTAL JOINTS, WITH TREND OF FLOW LAYERS
MINOR ANTICLINES & SYNCLINES, DOMES & BASINS
0 1 2 miles

TION, AND JOINTS IN PORPHYRITIC GRANITE AND ASSOCIATED ROCKS

BULLETIN OF THE GEOLOGICAL SOCIETY OF AMERICA
VOL. 67, PP. 647–670, 36 FIGS., 1 PL. MAY 1956

STRUCTURES OF THE PORPHYRITIC GRANITE AND ASSOCIATED METAMORPHIC ROCKS OF EAST MANBHUM, BIHAR, INDIA

BY S. SEN

ABSTRACT

Porphyritic granite, associated with metamorphic rocks and migmatites in East Manbhum (23°27′45″–23°35′ N. Lat.; 86°30′–86°49′ E. Long.), India, crops out as a lenticular body showing well-developed planar banding of alternating feldspar phenocrysts and a finer-grained assemblage of quartz, feldspar, and accessories. Arrangement of phenocrysts within the banding may be random, or they may show perceptible lineation. Lineation, foliation, and joints are primary. Regional distribution of flow layers suggests an inclined lens, with two secondary domes, one at Raghunathpur and the other at Bero. Lineation, generally within a few degrees from the horizontal, parallels *b*, except in the two domes where it parallels *a*.

The porphyritic granite is concordant for the greater length except toward the eastern margin of the exposure. North-northeast of Raghunathpur, it is discordant with the structural trends of the country rocks. There are a few small-scale discordances where the granite boundary takes sharp turns, leaving the schistose alignments of the country rocks abutting against the boundary. Spatial distribution of foliation, lineation, and joints of the porphyritic granite is independent of that of the metamorphic and migmatitic country rocks. Wall rocks have been mylonitized, and three joint systems developed. Distribution and concentration of joints prove that the effect of tension was comparatively greater close to the contact. Compression diminishes more slowly and is effective over a greater distance.

Lineation in the country rocks may be parallel to both *a* and *b*. It is chiefly of two types produced by (1) microfolds of different dimensions, or by (2) alignment of elongated minerals such as quartz or sillimanite. Biotite fabric of the metamorphic rocks is not indicative of their tectonic trend as the mineral is a result of neocrystallization. Quartz-axes diagrams show peripheral *ac* girdles with maxima I, II, and V, and occasionally an $ac \wedge bc$ diagonal girdle. The orientation in the metamorphic rocks, especially as they belong to a high grade of regional metamorphism, presumably originated in solid flow by translation, chiefly along megascopic *s* planes. Fabric of migmatites, ultramigmatitic granite gneiss, and two types of quartz in leptynites (granulites) are very similar to that of the metasediments, and their orientation is ascribed to mimetic retention of tectonitic orientation during metasomatic recrystallization.

Country rocks show simultaneous fabric reconstitution near the porphyritic granite. Along the granite contact the fabric is symmetrical about the bisectrices of the shear joints caused by intrusion of porphyritic granite. The intrusion also produced minor secondary folds or intensification of folding. Quartz fabric of the porphyritic granite is independent, with regard to its pattern and relation to geographic coordinates, of the country rock fabric.

CONTENTS

TEXT

	Page
Introduction	648
Acknowledgments	649
Structures of the porphyritic granite	649
General statement	649
Structures of the late fluid (plastic) stage	650
Flow layers	650
Lineation	651
Form of the intrusive	651
Structures of late solid stage (joints)	651
Structures of the country rocks	654

	Page
Structures of the wall rocks	656
Mineral orientation in metasediments, migmatites, and granite gneiss	659
General statement	659
Biotite fabric of metamorphic rocks and migmatites	659
Quartz fabric of metamorphic rocks	660
Quartz fabric of migmatites and granite gneiss	660
Mineral orientation of wall rocks	662
Mineral orientation of the porphyritic granite	664
Origin of the structural features	665
Foliation, lineation, and joints in the granite	665
Mineral fabric of the granite	666
Megascopic fabric of the wall rocks	667
Mineral fabric of metasediments, migmatites, and granite gneiss	667
Mineral fabric of the wall rocks	668
Summary and conclusions	669
References cited	669

ILLUSTRATIONS

Figure		Page
1.	Sketch of porphyritic granite vein in granite gneiss	649
2.	Minor disordance between porphyritic granite and granite gneiss	649
3.	Xenoliths in porphyritic granite	650
4.	Porphyritic granite intrusive	652
5.	Block diagram showing relation of joints, flow layers, and lineation in porphyritic granite	653
6.	Equal-area projection of joints of system 2 in porphyritic granite	653
7.	Joint planes of system 2 in porphyritic granite	653
8.	Structure map of granite southwest of Bamanbad	654
9.	Structure map of Raghunathpur and its environs	655
10.	Stereogram structure section	656
11.	Structure map of granite about 1½ miles northwest of Anara railroad station	657
12.	Elongate feldspar phenocrysts in laminated porphyritic granite	657
13.	Sketch map showing structure of country rocks	658
14.	Minor structures in wall rocks northeast of granite pluton	658
15.	Frequency distribution of joints of systems 1 and 2 in country rocks	658
16.	Equal-area projection of joints of system 1 in wall rocks	659
17.	Relation of joints of systems 1, 2, and 3 in wall rocks	659
18.	Biotite fabric of biotite schist	661
19.	Biotite fabric of ultramigmatite	661
20.	Synoptic quartz-axes diagram	661
21.	Quartz fabric of sillimanite schist	661
22.	Quartz fabric of sillimanite schist	662
23.	Quartz fabric of sillimanite schist	662
24.	Quartz fabric of quartzite	662
25.	Quartz fabric of quartz-sillimanite schist	662
26.	Quartz fabric of an ultramigmatite	663
27.	Quartz fabric of leptynitic granite gneiss	663
28.	Selective quartz fabric of granulitic quartz	663
29.	Quartz fabric of leptynitic granite gneiss	663
30.	Quartz fabric of sillimanite schist	665
31.	Quartz fabric of mylonitized granite gneiss	665
32.	Quartz fabric of porphyritic granite from south of Mapuidih	665
33.	Quartz fabric of porphyritic granite from southwest of Raghunathpur	665
34.	Quartz fabric of porphyritic granite from Bero	666
35.	Quartz fabric of porphyritic granite from Khajura	666
36.	Relation of incomplete girdle in Figure 31 to conjectured vector field	669

Plate		Facing page
1.	Structure map showing foliation, lineation, and joints in porphyritic granite and associated rocks	647

Introduction

In the area studied, in the province of Bihar, India (86°30′–86°49′ E. Long. and 23°27′45″–23°35′ N. Lat.), the porphyritic granite crops out as an elongated, lenticular body. It is associated with granite gneiss, migmatites, and metamorphic rocks in the following stratigraphic sequence:

(4) Porphyritic granite

(3) Granite gneiss, migmatites, composite gneisses

(2) Norites, pyroxene granulites, amphibolites

(1) Metasediments, including calc-silicate granulites and amphibolites underlain by sillimanite-almandine gneisses, quartzites, and magnetite quartzites

Mineral assemblages in the metamorphic rocks and in the granite resemble the charnockite-khondalite association of South India (Sen, 1953). Where unaffected by granite or granitization, the metasediments and metamorphosed norite dikes show high-grade metamorphic assemblages of sillimanite-almandine-(graphite), quartz-magnetite, diopside-calcite-plagioclase, and hypersthene-diopside-plagioclase. These rocks, variously influenced by granitization, show transitions through migmatites and composite gneisses into granite gneisses that range in composition from diorite and granodiorite to alaskite and kalialaskite. Leptynite, a common variety of granite gneiss, has alternating paper-thin bands of flattened quartz and even-grained, xenomorphic, quartz-feldspar assemblage. It resembles the *granulites* of German

authors. The granite gneiss is similar to the Chotanagpur granite gneiss (Dunn, 1929; Dunn and Dey, 1942). The two may prove to be continuous. The porphyritic granite shows distinctive features and is an easily separable structural unit. It extends for about 27 miles from

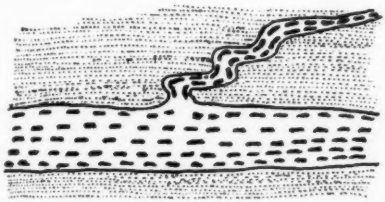

FIGURE 1.—SKETCH OF A PORPHYRITIC GRANITE VEIN IN GRANITE GNEISS

Vein foliation parallels its walls and sends a sinuous offshoot into the country rocks.

west of the area mapped to east of Bero (Pl. 1), but is covered for about a mile by granite gneiss and migmatites. There are innumerable veins and lenses of porphyritic granite within this granite gneiss and migmatite cover. Although most of these veins are parallel to their foliation, some cut across the foliation at various angles (Fig. 1).

ACKNOWLEDGMENTS

The paper is condensed from a thesis accepted for D.Sc. degree of the Calcutta University, 1952. I wish to thank Dr. P. K. Ghosh of the Geological Survey of India for his help at the start of the study. I wish also to thank Profs. W. H. Bucher, Ernst Cloos, H. W. Fairbairn, and Arie Poldervaart for reading the manuscript and suggesting improvement in presentation.

STRUCTURES OF THE PORPHYRITIC GRANITE

General Statement

The porphyritic granite shows well-developed planar banding (foliation) of alternating layers of large microcline phenocrysts and fine-grained quartz, microcline, oligoclase, biotite, and accessories. The planar nature of the structure is evident in exposures along joint faces and stream cuts. Besides small rises which give good three-dimensional views of structural elements, some excellent sections are available both near the wall-rock contact and toward the interior of the granite pluton.

Foliation of the granite near the boundary wall everywhere parallels the contact—even

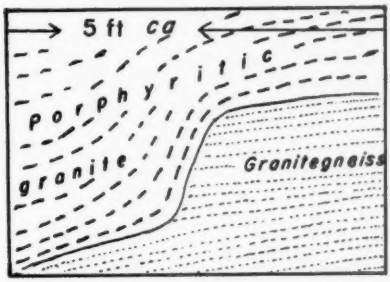

FIGURE 2.—MINOR DISCORDANCE BETWEEN PORPHYRITIC GRANITE AND GRANITE GNEISS

About 1 mile east-northeast of Adra (*see* Fig. 11a).

near considerable changes in the trend of the contact. There is no continuity of the structural trends of the granite and its wall rocks; however, the structures of the granite generally are conformable with those of the schistose and gneissose country rocks. Minor discordances appear where the granite boundary swerves sharply leaving the country rocks abutting against the wall (Fig. 2). Where the granite pluton tapers down and ends east of Bero, it exhibits a spectacular discordance with the country rocks (Pl. 1).

The porphyritic granite contains many inclusions of country rocks; the smaller inclusions have been drawn out into discoid shapes, with their flattest surfaces parallel to the foliation. Bands in the granite wrap around inclusions even where trend of the layers changes (Fig. 3a). Although in some instances the feldspar layers may not show perfect wrapping, they are nevertheless twisted and rotated away from the inclusion. Some fragments of xenoliths are torn from bigger xenoliths and rotated (Fig. 3b).

Pegmatites and pegmatoid rocks of different dimensions are common. They may run parallel to the foliation or the joint planes or cut across them. The pegmatites are composed of coarse-grained feldspar and quartz or of feldspar alone, with occasional tourmaline or mica grains. Some pegmatites merge into the feldspar bands of

the granite. Thus southwest of Bamanbad (Pl. 1) a few pegmatites parallel the flow layers. One vein arising out of a feldspar foliation band swerves, bifurcates, and cuts across the layers in sinuous trends (Fig. 8). A thick, lenticular pegmatite follows the joint plane and is encircled by thin mafic bands which continue northward for a short distance. Another lenticular pegmatite is likewise encircled by a thin mafic rim which continues northward and southward. North of Shyamsundarpur (Pl. 1), about half a mile north of the southern wall, there is a large number of pegmatite veins, some of which follow planes of different joint sets, a few cut the joints at random. Some of these pegmatites contain tourmaline crystals up to 6 inches long.

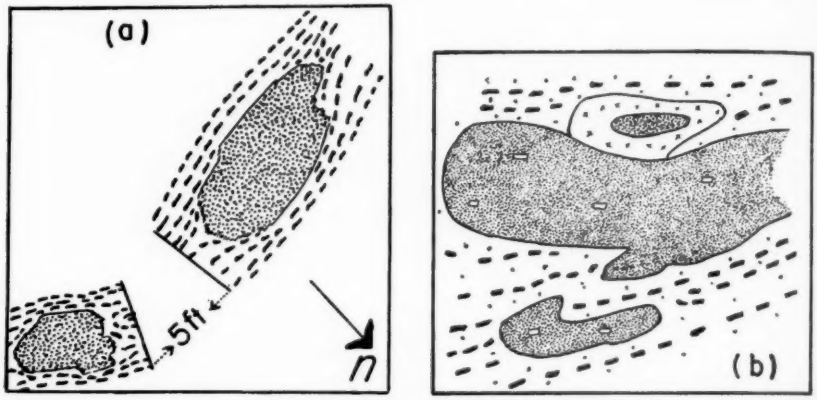

FIGURE 3.—XENOLITHS IN PORPHYRITIC GRANITE

a—Folded flow layers with included mafic xenoliths.

b—Flow layers wrapping mafic inclusion. There are a few automorphic feldspar phenocrysts in the inclusion.

Merging of pegmatites with the feldspar bands of the granite indicates that they emanated from the granite, and since they cut across both the foliation and the joints the structures formed before complete solidification of the granite.

Partially or completely granitized pyroxene granulites and amphibolites, bordering large inclusions of these rocks within the granite, contain feldspar porphyroblasts in random arrangement. Such occurrences, results of granitization *in situ*, support the conclusion that a similar process could not have been responsible for foliation in the main porphyritic granite pluton.

Foliation, lineation, and joints of the porphyritic granite bear no spatial relation to the regional deformation structures. This independence, proved further by the major and minor discordances, points to its intrusive emplacement. The structures were not impressed after complete solidification of the granite. Microscopic examination of the granite shows no evidence of postcrystalline deformation, especially in relation to microcline and quartz. The major structures in the granite are evidently paracrystalline or precrystalline in age, younger than the regional structures. Their relation to the pegmatites suggests formation before the rock was fully solid. Assuming the structures are primary, the foliation could have been produced only by movements of an essentially fluid body with considerable intratelluric solid phases. Thus foliation in the granite will be referred to as flow layers (Balk, 1937). Upon complete solidification, toward the late solid stage, continuation of movement resulted in yielding by rupture, producing joints. Primary structures thus belong to two stages (Balk, 1937; E. Cloos, 1937), the late fluid (plastic) stage (flow layers and flow lines), and the late solid stage (joints).

Structures of the Late Fluid (plastic) Stage

Flow layers.—Flow layers are parallel to the bounding walls of the porphyritic granite. They

are also parallel with the structural alignments of the country rocks where the granite pluton appears conformable with the regional trends (Pl. 1).

In places feldspar phenocrysts in the flow layers show parallelism of their longest axes. This lineation may be parallel or subparallel to the strike, or may be close to the direction of dip of the flow layers. Occasionally the phenocrysts are arranged at random, although the flow layers are perfectly developed. Along restricted, local zones the flow layers may be irregular while there is a well-developed lineation (*e.g.*, in Bero, Raidi, and Raghunathpur).

The strike of the flow layers ranges from N. 80° E.–N. 80° W. There is a similar variation in the trend of the wall. Near the northern contact west of Talsankra the flow layers dip about 36° N.; near the southern contact the dip ranges from 20° to 60°. Near Talsankra, 5 miles from the eastern end of the pluton, the dip steepens, becomes vertical, and finally reverses direction with angles of 83°–65° S. The flow layers then bend parallel to the boundary and dip at steep angles toward the center of the pluton near and south of Bero where the body terminates in a two-pronged lens.

In the center of the granite pluton the flow layers are more or less parallel to the trends of the southern and the northern walls. Local variations in the strike of the flow layers are particularly noticeable near inclusions or roof pendants (Pl. 1).

South to south-southwest of Raghunathpur a series of peaks arranged in a crescent partially encircles the village Nanduara (Fig. 9). About a quarter of a mile west is another small rise. North of the westernmost rise (Δ 856), the flow layers strike N. 80° E. and dip 70° N. Southward the dip steepens gradually to 85° N. The three northernmost peaks are encircled by flow layers that dip about 65° N., and the two southernmost peaks are encircled by flow layers that range in dip northward from 42° to 58° to vertical (Fig. 9).

Lineation.—Toward the center of the granite pluton the trend of the lineation varies only slightly from the strike of the flow layers. In the west near the break in exposure of the granite (Pl. 1) the lineation plunges 18°–20° W. Along the eastern end of the pluton around Bero and Raidi steep lineation is parallel to the dip direction of the flow layers. Similar lineation occurs in the peaks south-southwest of Raghunathpur.

In correlating primary lineation with Sander's axes of movement, Hans Cloos (1936, p. 87; 1928, p. 247, Fig. 6) suggests that lineation is generally parallel to the direction of magmatic flow, hence parallel to *a*, especially in marginal zones or narrow cylindrical bodies, while in the central regions of the pluton the lineation may be normal to the direction of major movement (flow) and hence parallel to *b*. In the area studied the horizontal to low-plunging lineation parallels *b* and is found to be the axis of girdling of quartz and biotite fabrics. The lineation in Bero and Raghunathpur is parallel to *a* and is associated with secondary domes mentioned later.

Form of the Intrusive

The porphyritic granite pluton resembles an inclined, moderately dipping lens, which bifurcates near the eastern edge (Figs. 4a, 10). The lens dips north, and its shape resembles that of a highly drawn-out dome whose axes plunge gently east and west. The eastern portion of the lens has been twisted so that the dip along the northern wall changes from outward to inward. Here the intrusive resembles an elongated, steep-walled, elliptical funnel open toward the west (Fig. 10; Pl. 1). Lineation parallel to *a*, sometimes developed at the expense of the flow layers, suggests differential and forceful movement along this narrow zone.

Peaks south-southwest of Raghunathpur are encircled by domes of flow layers (Balk, 1937, p. 56). The northern dome (Fig. 9) is partially constricted in the middle, elongated north-south, and about three-fourths of a mile long. It is a steep-walled, asymmetric, elliptical dome. The southern half is an incomplete, inclined cylinder. The elliptical southern dome, less than half a mile long, is elongate east-west and has a low-dipping, subhorizontal (5°S.) roof (Figs. 4b, 4c, 9).

Structures of the Late Solid Stage (Joints)

Primary joints have been grouped by Hans Cloos (1922, p. 2–4; Balk, 1937, p. 27–42) into the following types:

(1) Cross joints, *Q*, formed at right angles to tension, thus at right angles to the direction of flow and to flow lines. Lineation parallels direction of flow.

There are three major joint systems in the porphyritic granite, and a fourth minor one. One joint system, consisting of two sets, strikes roughly parallel to the strike of the flow layers.

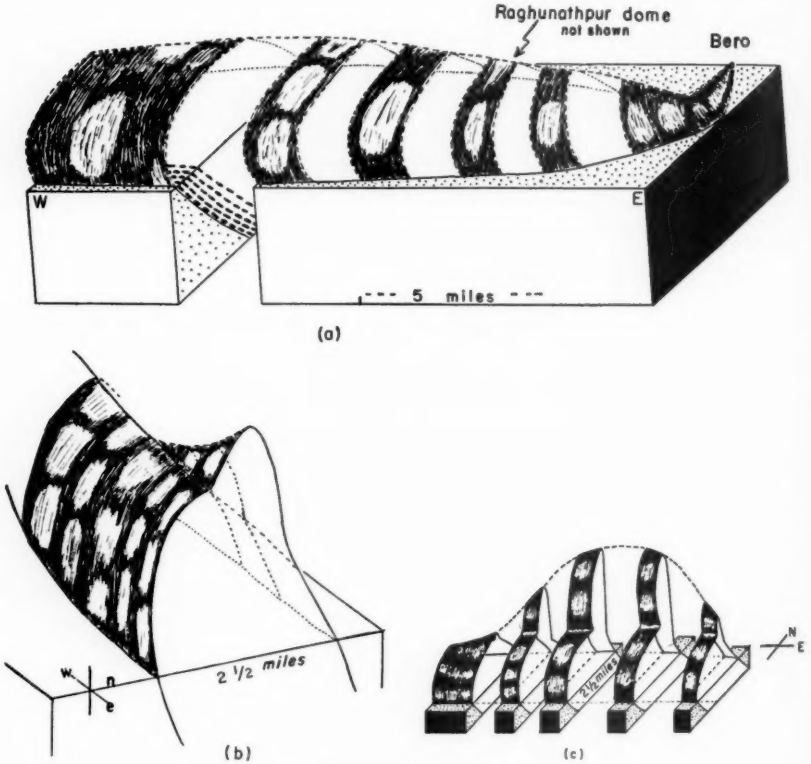

FIGURE 4.—PORPHYRITIC GRANITE INTRUSIVE
a—Form of intrusive.
b—Raghunathpur dome, looking west.
c—Raghunathpur dome, looking north.

(2) Longitudinal joints, *S*, dip steeply and strike parallel to flow lines.

(3) Primary flat-lying joints, *L*, embrace flow lines; well-formed sheetlike intrusions with subhorizontal roofs facilitate their formation.

(4) Diagonal joints dip steeply and are diagonal to the dip of the flow layers.

Cloos described tension joints formed at right angles to tension as *Q* joints, which are described with reference to flow lines and are at right angles to them. As lineation may develop at right angles to the direction of flow, caution must be exercised in describing a joint system as *Q* joints.

The planes of one of these sets are approximately normal to the planes of the flow layers. Those of the second set are disposed diagonally with respect to the flow layers. The joints of the second system strike roughly at right angles to the strike of the flow layers, and are at right angles to the low-plunging lineation. The third system consists of two intersecting sets which are diagonal to the strike of the flow layers or direction of the low-plunging lineation. The planes of the fourth system parallel the planes of the flow layers. All the systems are not necessarily found together.

The average direction of strike of the joints

of system 1 (representing the mode determined from the frequency distribution of the measured strikes) is roughly parallel to the strike of the flow layers. The maximum range is 20° (*i.e.*, ±10°). The joints are perfectly parallel to the low-plunging lineation where such lineation is evident. One set of planes of this system is horizontal or dips at low angles away from the dip of the flow layers. The planes are thus at right angles to the layers. These planes containing the lineation are parallel to *bc*, (in terms of the axes of movement picture[1]), and are therefore typical cross joints (planes normal to tension). These joints are less common than the second set of this system. The second set consists of two intersecting groups of planes, one dipping at low to moderate angles (20°–40°) in the same direction as the dip of the flow layers, the second dipping at steep angles (up to 90°) in the opposite direction. The acute bisectrix of this conjugate set of planes lies roughly on the flow layers. Where the flow layers are vertical or nearly so, some fairly well formed horizontal or subhorizontal joints occur. These are *bc* joints. The fractures of both sets of this system of *bc* and *ab* ∧ *bc* diagonal joints are often filled with quartz and pegmatite veins. Figure 5 shows the relation of the joint sets in system 1 to other structural elements.

Joints of system 2 far exceed the others in concentration and occur alone in zones especially near the granite-country rock contact. It consists of narrow cracks, occasionally filled with vein minerals, and in places continuing into the wall rocks as open tension cracks. The planes of this system are closely spaced as a rule, at times only a fraction of an inch apart. The vertical or steeply dipping planes cut the low-plunging lineation at right angles and are thus at right angles to the flow layers. Equal-area projection of several planes of this system (756 joints) shows concentration of poles around 90°–270° within a range of ±12°, and with slight scattering along all points of the compass (Fig. 7). Similar variation is shown in trend of the lineation and strike of the flow layers, indicating that the joints maintain a right-angle relation to these structures. The joints are well developed in most of the exposures mapped in detail. In places the joints of system 2 appear to be displaced along joints of the first system—*e.g.*, near Gurguria and near Chapari, about 2 miles west-northwest of Baishkuli (Fig. 7).

The two intersecting planes of system 3 do not always occur together. One or both may occur with joints of other systems. They are rarer than the other joints. These planes are

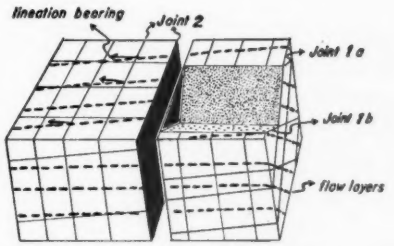

FIGURE 5.—BLOCK DIAGRAM SHOWING RELATION OF JOINTS, FLOW LAYERS, AND LINEATION IN PORPHYRITIC GRANITE

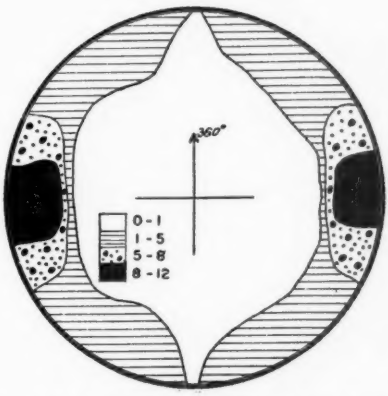

FIGURE 6.—EQUAL-AREA PROJECTION OF JOINTS OF SYSTEM 2 IN PORPHYRITIC GRANITE

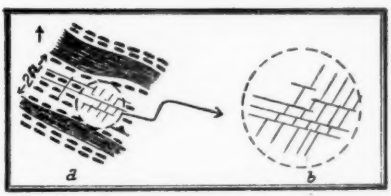

FIGURE 7.—JOINT PLANES OF SYSTEM 2 IN PORPHYRITIC GRANITE
a—Displaced along planes of system 1.
b—Magnified view of enclosed area in *a*.

[1] Sander's terminology for fabric axes, recognized megascopically, is here applied to describe the primary flowage structures of the porphyritic granite; *ab* for important *s* plane (flow layers), and *a*, in analogy to tectonic flow, for the direction of maximum *magmatic transport*.

often closely spaced, sometimes a few inches apart, and they generally extend 15–20 feet. All types of angular relations with the flow layers are observed. Strike of the layers may coincide with either the acute or the obtuse bisectrices of the conjugate planes. The joint planes may intersect at 90°. Rarely the strike of the layers may not coincide with any of the bisectrices.

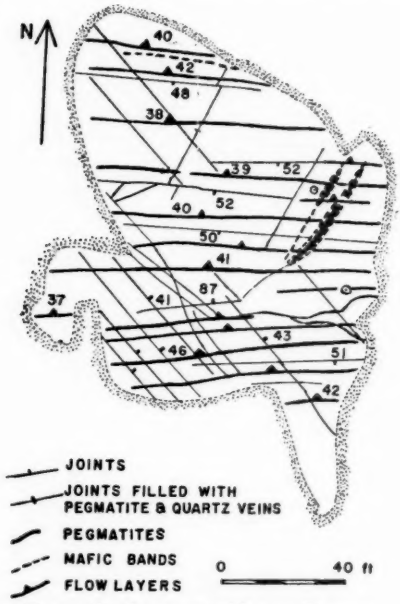

FIGURE 8.—STRUCTURE MAP OF GRANITE SOUTHWEST OF BAMANBAD

Where the first two or all three joint systems occur together, fractures of the first system are invariably filled with vein minerals, while a few joints of the second system may remain unfilled, and fractures of the third system are usually unfilled. The third system of joints appears to be younger than the other two.

Jointing is very well developed in the vicinity of Bamanbad (Fig. 8; Pl. 1). The strike of one conjugate member of the third joint system ranges from N. 50° W. to N. 35° W. The second group of this diagonal system, striking N. 65° E., is comparatively sparse. Strike of the flow layers ranges from N. 82° E. to N. 80° W., and the layers dip northward at moderately steep (44°±) angles. Joints of the first system, which strike parallel or subparallel to the strike of the flow layers, dip at moderate angles (50°) away from the dip of the flow layers. Many of these fractures are filled with pegmatite and quartz veins. One set of joints of system 2 strikes N. 5° W. to N. 20° E. Its planes are in places displaced along planes of system 1.

About 1½ miles northwest of Anara, and approximately 500 yards from the southern contact of the porphyritic granite, the flow layers strike between N. 84° W. and N. 76° W. and dip 36°–40° N. (Fig. 11). A closely spaced joint system, a few inches to a fraction of an inch apart, consists of narrow, parallel, unfilled cracks which strike N. 7° E. and dip steeply, often up to 90°. Frequently a few planes of this second joint system extend from one end of the exposure to the other. One joint set of the first system, with planes 1–2 feet apart, strikes N. 86° W.–N. 80° W. and parallels the strike of the flow layers. A third system of narrower cracks strikes N. 15° W.– N. 10° W. and dips at moderately steep angles west-southwest. Relative concentration of the three joint systems is: system 1, 38 per cent; system 2, 50 per cent; system 3, 12 per cent.

In places along the boundary the porphyritic granite has the appearance of a sheared rock. Feldspar phenocrysts are slightly granulated along the margin, and the rock is sheeted. Occasionally the granite seems to have been dragged while plastic, and the feldspar phenocrysts distorted and drawn out like dough (Fig. 12).

STRUCTURES OF THE COUNTRY ROCKS

The country rocks dip northward at angles ranging from 30° to 90°. Variations in dip of the rocks sometimes yield broad warps and folds, the axes of which are subparallel to the regional strike of foliation. These folds are of different dimensions down to minute puckers. They define a conspicuous regional lineation which is nearly parallel to the regional foliation strike and hence parallel to *b*. Regional structure consists of close isoclinal folds, in which the fold axes are horizontal or plunge at low angles east or west (Fig. 13a, b). Along a narrow zone near the northern boundary of the area the meta-

sediments dip 40°–45° S., then dip northward at moderate angles. The south-dipping narrow zone is a limb of a knee fold whose north limb dips below the calc-silicate rocks and amphibolites (Fig. 13b). Northward the folds change from nearly closed folds on horizontal or low-plunging axes to open folds of moderately low-dipping anticlines and synclines which plunge both ways and are arranged *en echelon*. Where the structures flatten out, individual pitching anticlines and synclines embrace small domes and basins (Pl. 1).

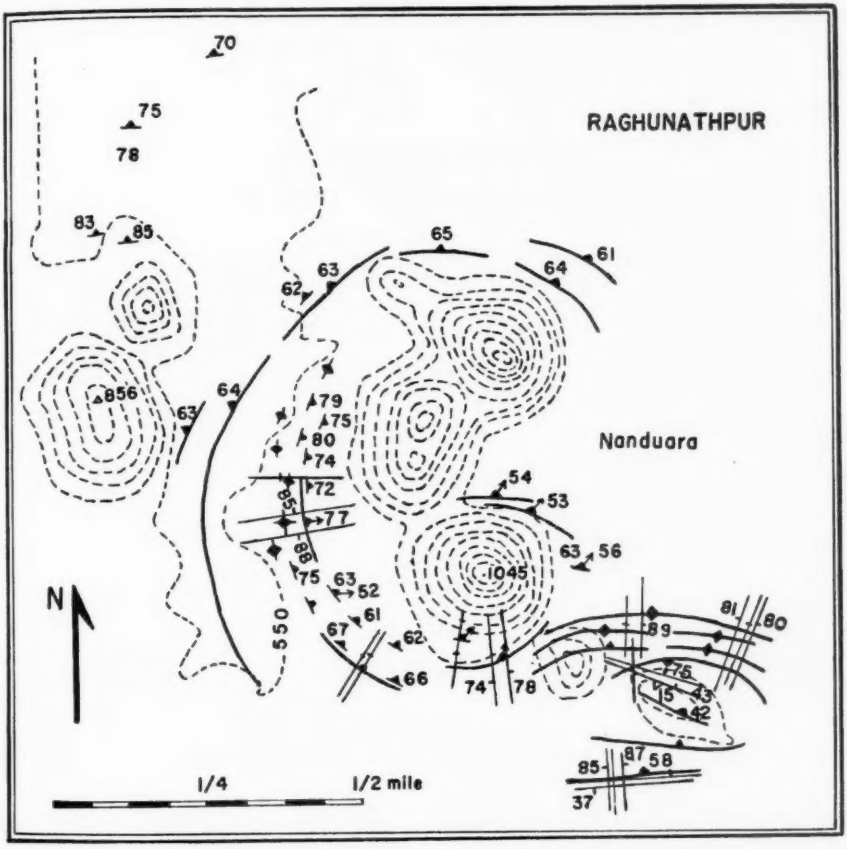

FIGURE 9.—STRUCTURE MAP OF RAGHUNATHPUR AND ITS ENVIRONS

Both metasediments and granite gneiss show several types of well-formed lineation (E. Cloos, 1946). Sometimes lineation produced by microfolds occurs with mineral lineation produced by parallel arrangement of elongated quartz or sillimanite, and the two are then invariably parallel. The microfolds are often visible only on polished *ac* planes of the megascopic fabric. Closely spaced vertical joints also give rise to a nearly vertical lineation. This type is not very common. Microfolds and mineral lineation, when associated with microfolds, are always parallel or subparallel to the strike of foliation, parallel to the major fold axes, and hence parallel to *b*. Lineation parallel to the dip of foliation, not so extensively developed, is always the mineral-lineation type and parallels *a*. Over large areas of north-dipping metasediments, where folding is not evident, lineation

indicates the direction of plunge of the fold axes.

the dip of the granite gneiss changes from vertical to 45° N. (Fig. 14).

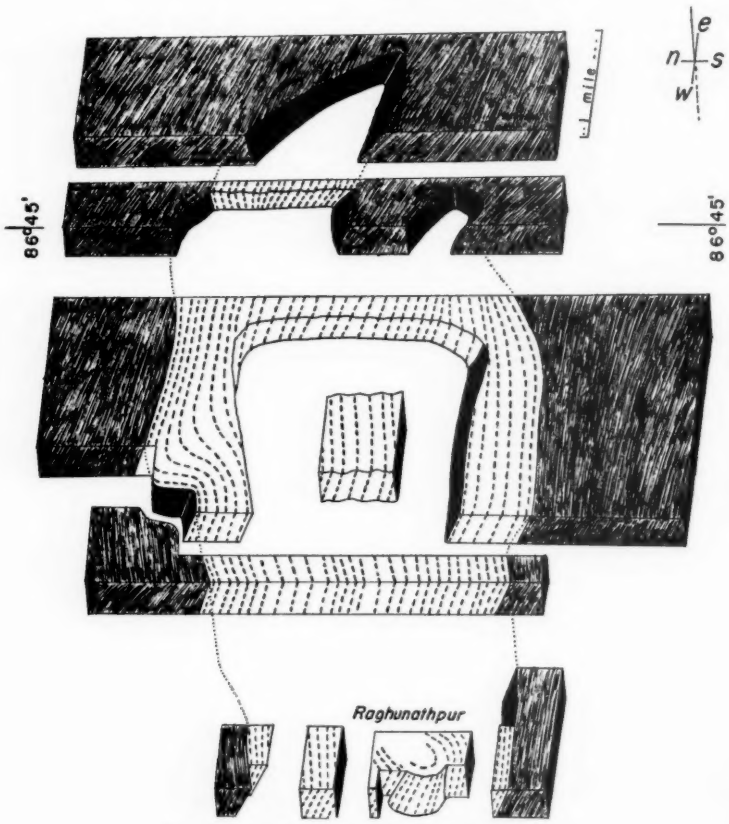

FIGURE 10.—STEREOGRAM STRUCTURE SECTION

STRUCTURES OF THE WALL ROCKS

Near the porphyritic granite pluton, where the trends are conformable to the granite, the country rocks show an intensification of their original structures with steep minute folds parallel to regional fold axes and small thrusts along planes nearly parallel to original megascopic *s* (foliation) planes.

Near the contact, north-northwest of Raghunathpur, the flow layers of the granite dip 52° N., and the granite gneiss with similar structural trend dips 75°–80° S. This is a good example of major discordance. The granite gneiss is closely folded in a syncline which has almost vertical limbs. About 300 yards away

Secondary folds, with axes at right angles to the regional fold axes, occur within the granite gneiss and metasediments close to the granite contact, especially where the contact is discordant. Where the granite boundary sweeps southeast, about 1¼ miles north-northwest of Raidi, the schistose micaceous quartzites have been folded into successive anticlines and synclines which gradually die out toward the east (Pl. 1). The axes of these folds plunge about 78° S.

Granite gneiss has been crushed along the granite contact, and mylonites occur along most of the contact and some distance within the gneiss. Three major joint systems are developed in the wall rocks. One system strikes at right

angles to the wall; a second parallels the contact; and the third is diagonal to the contact. Measurement of more than 5000 joints in the country rocks shows the relative importance of the joint systems and reveals their relation to the trend of the contact and their proximity to the granite. The writer measured all joints at stations, 8–10 feet square, scattered all over the area. Concentration of joint systems 1 and 2, expressed per unit areas of 3 feet square, was then plotted against the distance from the contact of the porphyritic granite (Fig. 15). The joints used in the plot were measured south of the pluton; as the main rock type within 2–2½ miles from the contact is granite gneiss or migmatite, difference in lithology was not a factor. The diagram shows a decrease in frequency of both joint systems with increasing distance from the granite contact, and also a gradual change in the relative abundance of the two systems. About 1½ miles from the wall, joints of system 2 become more abundant than those of system 1.

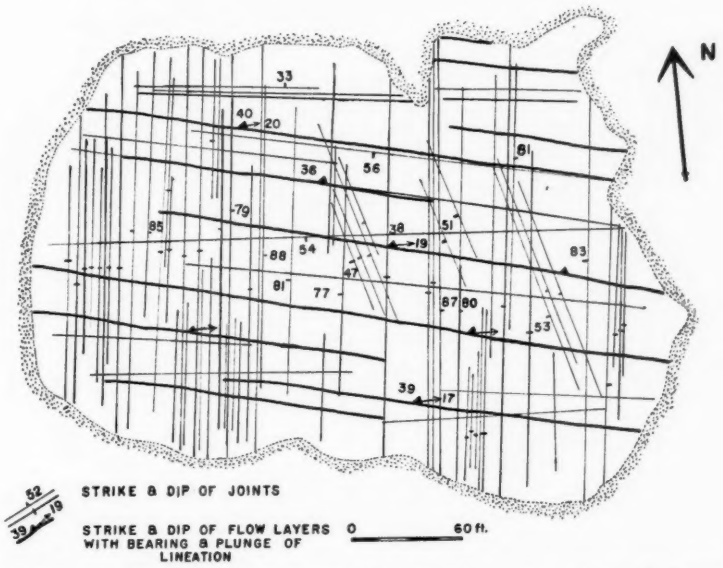

FIGURE 11.—STRUCTURE MAP OF GRANITE ABOUT 1½ MILES NORTHWEST OF ANARA RAILROAD STATION

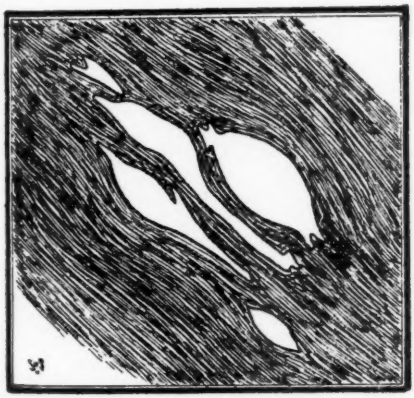

FIGURE 12.—ELONGATE FELDSPAR PHENOCRYSTS IN LAMINATED PORPHYRITIC GRANITE
Two and one-half miles east-southeast of Shyamsundarpur (*see* Pl. 1).

At places joints of system 1 continue from the tension joints (system 2) of the porphyritic granite and have steep or vertical dips. These are mostly unfilled, uneven fractures which are sometimes only a fraction of an inch apart. Spacing ranges from a few inches near the contact to about 10–12 inches at distance. Near the granite contact the planes are well formed even in incompetent rocks such as

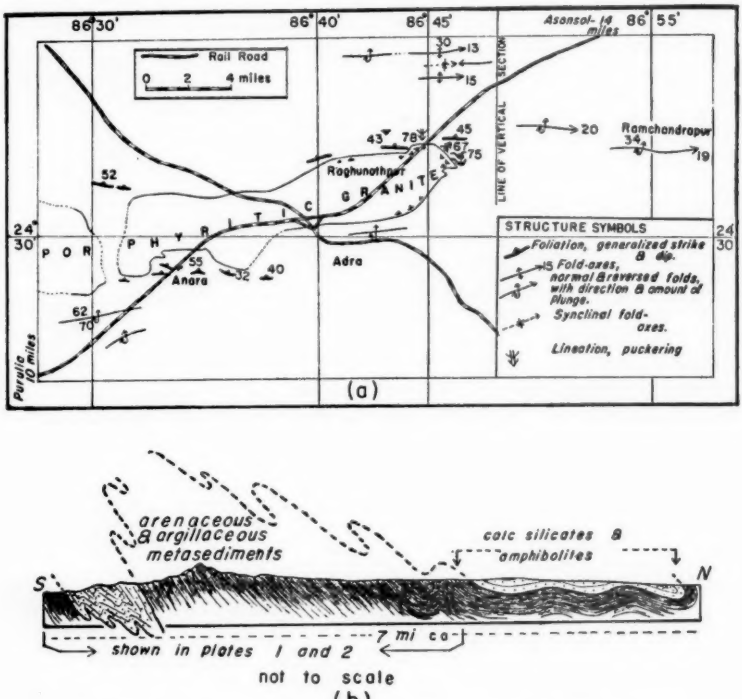

FIGURE 13.—SKETCH MAP SHOWING STRUCTURE OF COUNTRY ROCKS
a—Regional fold axes and microfold axes.
b—North-south structure section along line shown in Figure 13a.

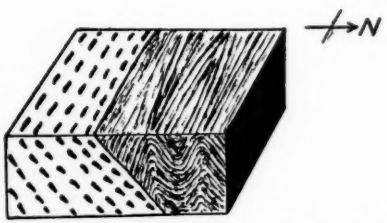

FIGURE 14.—MINOR STRUCTURES IN WALL ROCKS NORTHEAST OF GRANITE PLUTON

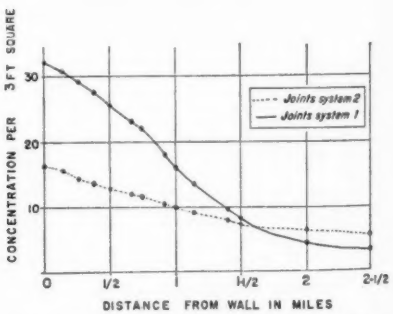

FIGURE 15.—FREQUENCY DISTRIBUTION OF JOINTS OF SYSTEMS 1 AND 2 IN COUNTRY ROCKS
Plotted against the distance from the wall of the porphyritic granite.

metamorphosed argillites. With increasing distance from the contact the planes become irregular.

Equal-area projection of some 2500 joint planes of system 1 (Fig. 16) shows that the poles are concentrated along a zone within 65°–105°. The strike thus ranges from N. 65° W.–N. 15° E. Variation in the strike of the joints is similar to the variation in the trend of the wall; the joints are always at right angles to the contact.

Although the frequency of joints of system 2 near the contact is lower than those of system 1,

they may locally outnumber all other joints. Their planes are more clear cut than the planes of system 1. The second system consists of a group of two intersecting planes which occur together in the majority of joints measured. The planes strike parallel to the wall and dip 65°–75° N. or 50°–68° S. North-dipping planes predominate. The obtuse angle of intersection of these joints faces the wall (Fig. 17), the acute bisectrix is in a plane that deviates slightly from the vertical.

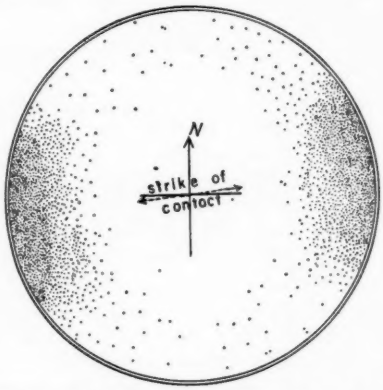

FIGURE 16.—EQUAL-AREA PROJECTION OF JOINTS OF SYSTEM 1 IN WALL ROCKS

Modal direction of the trend of contact shown as a double arrow.

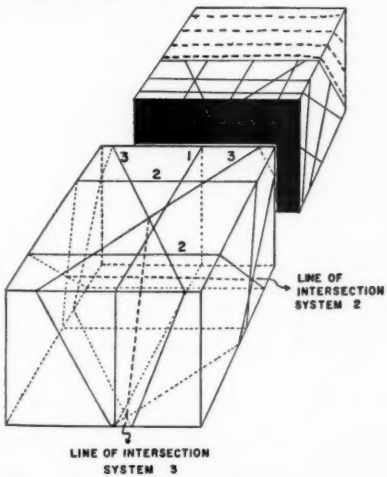

FIGURE 17.—RELATION OF JOINTS OF SYSTEMS 1, 2, AND 3 IN WALL ROCKS

The third system consists of intersecting diagonal planes, with axis of intersection nearly vertical. In some places the obtuse bisectrix of these joints faces the wall; in others, the acute bisectrix is toward the wall.

MINERAL ORIENTATION IN METASEDIMENTS, MIGMATITES, AND GRANITE GNEISS

General Statement

Influence of the porphyritic granite on the quartz and biotite fabrics of the country rocks was studied in specimens from different distances from the wall (Knopf, 1933; Knopf and Ingerson, 1938; Ingerson, 1936; Fairbairn, 1949; Sander, 1930). To get an idea of regional fabric of the metamorphic and migmatitic rocks, six specimens were collected from an area out of the zone of direct influence of emplacement of the granite. Quartz fabric of three more specimens successively nearer the granite, one of them within a few yards of the pluton, were also studied (Sen, 1949a; 1949b).

The lineation near the strike of the foliation and parallel to the regional fold axes has been taken as the *b* axis. This is also the girdling axis in quartz and biotite diagrams. Where lineation nearly parallels the dip of foliation it is at right angles to the axis of girdling for quartz diagrams. Thus the regional direction of the girdling axis remains constant.

Biotite Fabric of Metamorphic Rocks and Migmatites

The poles of 200 cleavage planes of biotite in a sample of biotite schist were measured on a section parallel to the megascopic *ac* plane (Fig. 18). The specimen grades from slightly biotitized pyroxene amphibolite and pyroxene granulite to a biotite schist in contact with a pegmatoid granite vein that cuts the schistosity. There is a concentration of the poles around *c*, the flakes parallel to *ab*, with a spread suggesting an incomplete peripheral *ac* girdle around *b*. There is also a slight spread on *bc*. Biotite formed at the expense of hornblende and pyroxene and has, in the words of Fairbairn (1949, p. 142), "no petrofabric past". The diagram of 100 biotite cleavage poles on *ac* megascopic fabric plane of an ultramigmatite,

near granite in composition, shows a partial peripheral *ac* girdle with a slight tendency to spread on *bc* (Fig. 19). Though the existing *ab* planes exerted a control on orientation, it seems that the fortuitous spread of the poles resulted from neocrystallization, chiefly around borders of hornblendes and pyroxenes.

Quartz Fabric of Metamorphic Rocks

Two hundred quartz axes were plotted (Fig. 21) from a thin section of a sillimanite gneiss occurring near the foot of a small rise west-northwest of Ramchandrapur peak (Fig. 13a). The section was not quite parallel to the *ac* plane of the megascopic fabric. The plane of section could be obtained by rotating the *ac* plane about 18° on *a*, clockwise, looking toward the direction of dip, and then about 5° on *c* again clockwise. The *ac* plane is indicated on the diagram. The specimen shows well-developed lineation in an equally well-formed *s* (foliation) plane. The bearing of the lineation is close to the direction of dip of the foliation. This was taken as parallel to *a* with reference to the regional fold axes. Lineation is produced by arrangement of sillimanite needles and elongated quartz crystals. The diagram shows a thick *ac* girdle, extending an average of 40° on both sides of *ac*, with no strong tendency to form a point maximum. The maximum concentration is 6 per cent per 1 per cent area. The small maxima near *c* are roughly equivalent to maximum V of synoptic diagram (Fig. 20). There is a second, intermediate between V and II, and a third less important one on *a* (maximum I).

Figure 22 shows 80 quartz axes of a specimen of quartz-sillimanite schist from the eastern edge of Ramchandrapur hill. The rock shows a faint lineation, and the foliation dips 72° N. 30° E. Lineation, near the strike of foliation, pitches 20° and was chosen as the *b* axis. The section prepared nearly on the *bc* plane is parallel to the strike of the foliation. The diagram was rotated through 70° to the right to get the *ac* plane projection on the positive[2] side of *b* (Fig. 23). There is a well-formed peripheral *ac* girdle. The girdle seems more clearly defined as only 80 grains were measured. A direction nearly parallel to the strike of foliation (parallel to lineation in this diagram and at right angles to lineation in Figure 21) is always the axis of girdling. In Figures 22 and 23 the maximum concentration does not exceed 8 per cent in 1 per cent area, and the distribution is uniform along the girdle. Three small zones show a concentration exceeding 4 per cent, one on *a* (maximum I), the other two close to *a*.

Figure 24 is a quartz-axes diagram of a quartzite from west-northwest of Ramchandrapur (*Cf.* Fig. 21). This quartzite is very coarse-grained, and only 60 grains were oriented. The diagram shows a high order of preferred orientation, which may not indicate the true fabric, as only a few axes were measured. The specimen is well foliated with a lineation almost parallel to the dip direction of the foliation. It also shows well-formed joints parallel to *ac*, with modal strike parallel to lineation, which was taken to be parallel to *a*. Fabric shows a nearly peripheral *ac* girdle, and the quartz axes spread to form a second girdle almost half complete intermediate between *ac* and *bc*.

Figure 25, an *ac* fabric of 100 quartz axes of a quartz-sillimanite gneiss from the eastern edge of Ramchandrapur hill (*Cf.* Fig. 22), shows two girdles; the diagonal *ac* $\wedge$ *bc* girdle is more prominent, the peripheral *ac* girdle is only half complete. There is a maxima, concentration exceeding 5 per cent per 1 per cent area, near *a* (maximum I), and a small zone with a similar concentration near *c* (maximum V).

Quartz Fabric of Migmatites and Granite Gneiss

Quartz axes fabric of an ultramigmatite (Fig. 26), almost granite in composition, is similar to the first two quartz-axes diagrams (Figs. 21, 22). It shows a distinct peripheral *ac* girdle with maximum concentration not exceeding 6 per cent per 1 per cent area. The maxima are equivalent to maxima I and V of the synoptic diagram (Fig. 20). The *ac* fabric of 200 quartz axes of a leptynitic granite gneiss (Fig. 27), about 2 miles from the southern wall of the porphyritic granite again shows well-formed peripheral *ac* girdle. A selective diagram (Fig. 28) of 80 quartz axes of flat granulitic

[2] Left-hand side of the *b* axis (western end), looking along direction of regional dip direction, has been taken in all diagrams as the positive end of the microfabric.

quartz from the same slice is similar to the composite diagram. The latter has one chief maximum on *c* (maximum V) and a minor one on *a* (maximum I). The selective diagram has a third maximum, one pair of the two possible pairs of maximum II. Maximum I is more prominent in the selective diagram.

From a regional study of the granulites of Finnish Lapland, Sahama (1936) found that the quartz grains have typically heterogeneous fabric. The granulitic quartz crystals show strong perferred orientation, while postdeformational crystallization in the higher grades of metamorphism has obliterated any preferred orientation in the fine-grained quartz. In the granulites of Rosswein, Saxony (Sander, 1930), the quartz fabric is homogeneous as in the present diagrams.

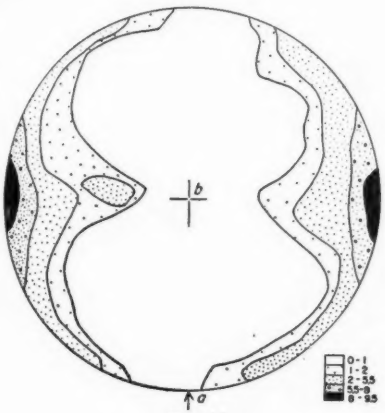

FIG. 18

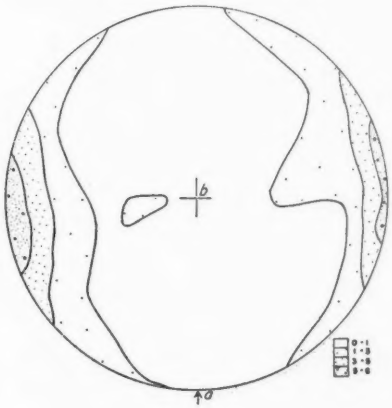

FIG. 19

FIGURE 18.—BIOTITE FABRIC OF BIOTITE SCHIST
FIGURE 19.—BIOTITE FABRIC OF ULTRAMIGMATITE

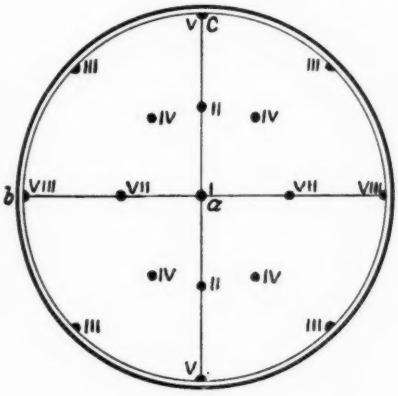

FIG. 20

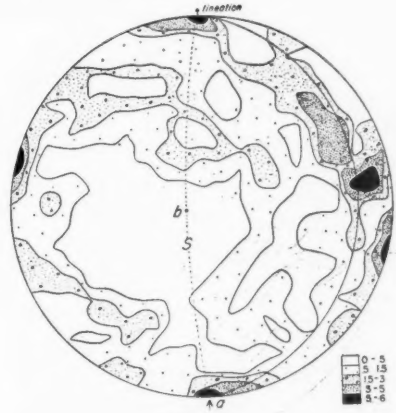

FIG. 21

FIGURE 20.—SYNOPTIC QUARTZ-AXES DIAGRAM
Fairbairn, 1949, Figure 9-3.
FIGURE 21.—QUARTZ FABRIC OF SILLIMANITE SCHIST
From foot of a small rise west-northwest of Ranchandrapur.

MINERAL ORIENTATION OF THE WALL ROCKS

The *ac* quartz-axes fabric of 300 axes of a fine-grained leptynitic granite gneiss (Fig. 29), of higher concentration (4–5.5 per cent) are close to maxima III, V, and II, none exactly peripheral.

FIG. 22

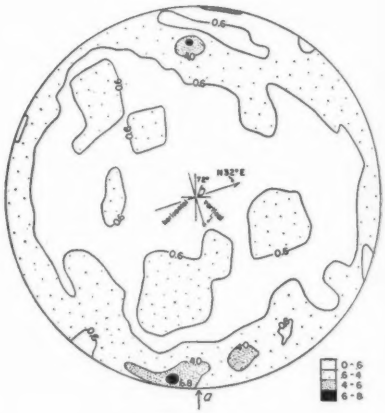

FIG. 23

FIGURE 22.—QUARTZ FABRIC OF SILLIMANITE SCHIST
From east-edge of Ranchandrapur hill.
FIGURE 23.—QUARTZ FABRIC OF SILLIMANITE SCHIST
Figure 22 rotated on *ac*.

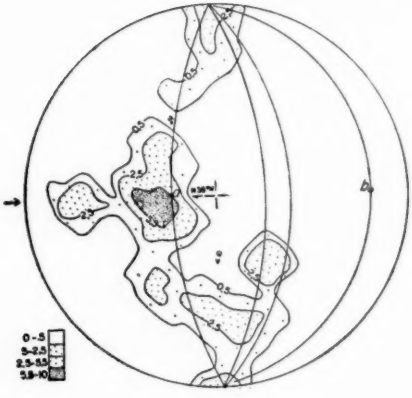

FIG. 24

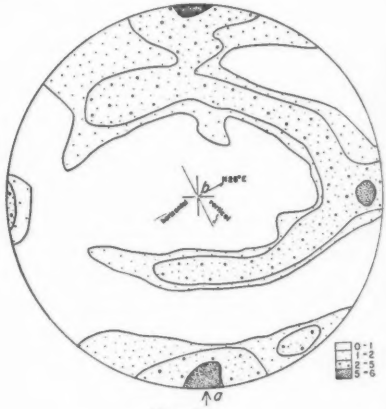

FIG. 25

FIGURE 24.—QUARTZ FABRIC OF QUARTZITE
West-northwest of Ranchandrapur (*Cf.* Fig. 21).
FIGURE 25.—QUARTZ FABRIC OF QUARTZ-SILLIMANITE SCHIST
From east edge of Ranchandrapur hill.

three-fourths of a mile from the southern contact of the porphyritic granite, exhibits poor orientation; the 1 per cent contour shows a complete peripheral *ac* girdle, with maximum concentration of 5.5 per cent. Four small zones

Figure 30, quartz-axes fabric on *ac* plane of 200 quartz axes of a sillimanite schist also shows poor orientation with a very broad *ac* girdle; but the zones of maximum concentration give an almost complete *ab* girdle. There is a

slight spread indicating a tendency for a *bc* girdle. It is not clear whether the orientation of the specimen, occurring farther from the porphyritic granite than the preceding specimen (Fig. 29), was directly affected by the intrusion and whether the *ab* girdle is to be ascribed to this. Such *ab* girdles have been reported from Finnish quartzites by Hietanen (1938). The pattern with two, almost three, cross girdles is similar to diagram k of Fairbairn (1949, Fig. 2-1).

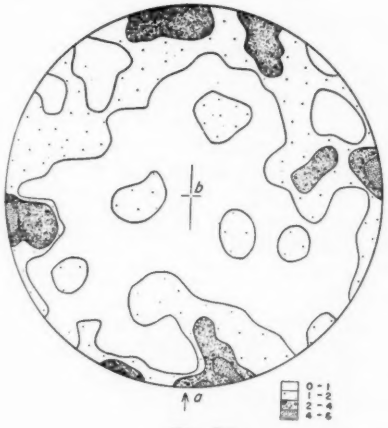

FIG. 26

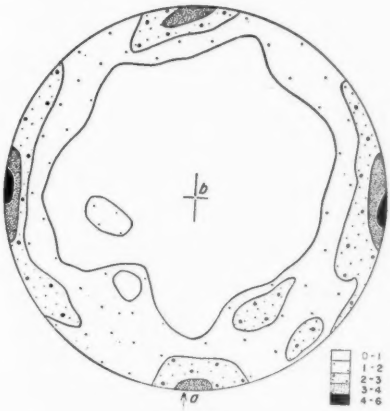

FIG. 27

FIGURE 26.—QUARTZ FABRIC OF ULTRAMIGMATITE
FIGURE 27.—QUARTZ FABRIC OF LEPTYNITIC GRANITE GNEISS
Two miles from southern wall of granite.

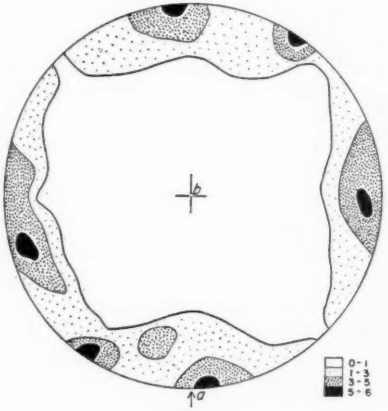

FIG. 28

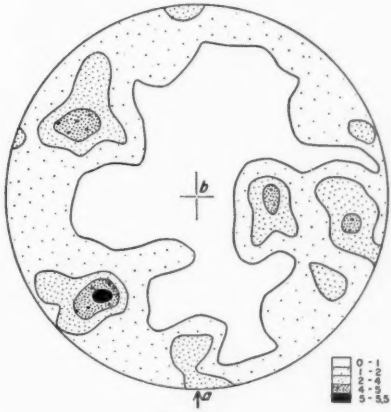

FIG. 29

FIGURE 28.—SELECTIVE QUARTZ FABRIC OF GRANULITIC QUARTZ
From same slice as in Figure 27.
FIGURE 29.—QUARTZ FABRIC OF LEPTYNITIC GRANITE GNEISS
Three-fourths of a mile south of granite contact.

A quartz-axes diagram was prepared of a granite gneiss occurring about 100 yards from the porphyritic granite contact. On the *ac* fabric of the granite gneiss (Fig. 31) modal directions of intersecting shear joints of system

2 and of joints of system 1 have been plotted. The planes of system 1 are nearly parallel to *ac* (010), and the conjugate planes of system 2 are intermediate between *ab* and *bc* (h0l). This diagram of 150 quartz axes shows a good preferred orientation, with a thick girdle about half complete. The quartz axes are concentrated around a comparatively small zone. The incomplete girdle, diagonal with respect to the megascopic fabric axes, is around an axis coincident with the direction of acute bisectrix of the conjugate planes. When the modal strike of conjugate planes of the shear joints of system 3 are plotted on the *ac* fabric, the obtuse bisectrix of these planes nearly coincides with *b* of the megascopic fabric and lies on a plane intermediate between *ab* and *bc*. This plane contains the acute bisectrix of the first intersecting system. The fabric shows monoclinic symmetry with reference to the bisectrices of the conjugate planes of system 2. The obtuse bisectrix is centered about the scattering of the quartz axes and contains the maximum (Sen, 1949a; 1949b).

Mineral Orientation of the Porphyritic Granite

Quartz-axes diagrams of the porphyritic granite were prepared from four widely spaced specimens along the length of the exposure, one from the west end between Baishkuli and Mapuidih, one from near the southernmost rise of the peaks south-southwest of Raghunathpur, one from Khajura, and the fourth from Bero (Pl. 1). Figure 32 is the *bc* quartz-axes fabric of the specimen from south of Mapuidih. Flow layers at this locality dip 32° N. 18° W.; there are two systems of perfectly developed joints, one with modal strike N. 45° E. and dip about 65° SE., and the other with modal strike N. 70° W. dipping about 63° S.-SW. Acute bisectrix of these planes (acute angle 43°) is nearly coincident with the strike of the flow layers. Fabric shows a moderately high degree of preferred orientation with a maximum concentration of 14 per cent per 1 per cent area, and an incomplete girdle which is diagonal if the strike direction is chosen as the *b* axis. A few yards away well-formed feldspar lineation makes an angle of 18° with the horizontal (strike) in the plane of foliation (pitch of lineation). This lineation interposed on Figure 32 becomes the axis of the incomplete girdle. There is also a tendency for another girdle in the spread of the axes diagonally between *ab* and *bc*. The maximum is close to maximum II of the synoptic diagram.

On a rise south-southwest of Raghunathpur the flow layers strike N. 89° W. and dip 46° N. There is also a system of well-developed vertical joints striking N. 28° E. Near Bero lineation plunges 65° N., and the foliation dips 78° N. 21° W.

The quartz-axes fabric of a specimen from a rise near Raghunathpur (Fig. 33) shows a thick peripheral *ac* girdle and a better-developed small-circle girdle (35° from the center). Girdling axis for both is slightly off the strike of foliation. There is also an incomplete peripheral *bc* girdle. Maximum concentration is 7 per cent. There are small zones with concentration 3 per cent upward close to maxima V, II, and VI. The distribution of the axes is rather uniform throughout the girdle.

A slice of the granite from Bero, inclined about 23° from the *ac* plane and easily referred on the *ab* plane to the well-formed *a* lineation, shows good orientation and a peripheral *ac* girdle, with a maximum axes concentration of 13 per cent per 1 per cent area (Fig. 34). Two zones could be described as maxima, both are peripheral and intermediate between maxima II and I, close to *a*. The fabric is symmetrical about *ab*. Zones of maximum concentrations show an incomplete small-circle girdle parallel to *ab* (18°–20° from *ab*) and symmetrically disposed about *ab*. The axis of major girdling is at right angles to lineation; the small-circle girdle is about *c*.

The quartz-axes diagram (Fig. 35) of the granite from Khajura (Pl. 1) does not show preferred orientation and is almost isotropic, though there is a good cluster on *c*.

The quartz fabric of the porphyritic granite differs from those of the country rocks not only in their patterns and the presence in some of small-circle *ab* girdles but also in the geographic coordinates of the symmetry planes of fabric and of girdling axes.

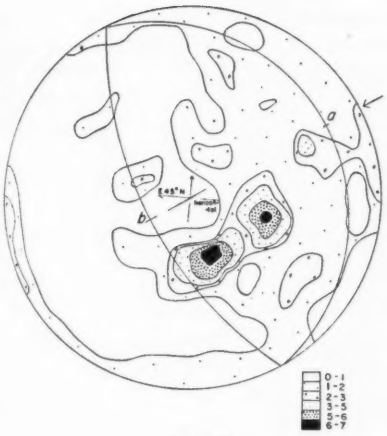

FIG. 30

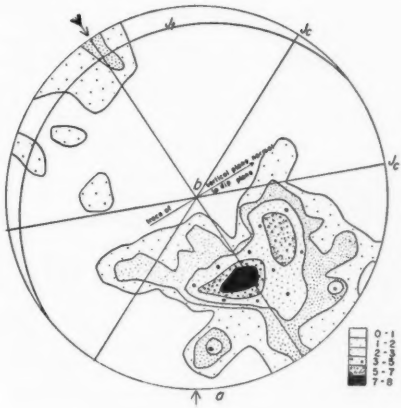

FIG. 31

FIGURE 30.—QUARTZ FABRIC OF SILLIMANITE SCHIST
FIGURE 31.—QUARTZ FABRIC OF MYLONITIZED GRANITE GNEISS
South of Jhanpra, 100 yards from the granite contact.

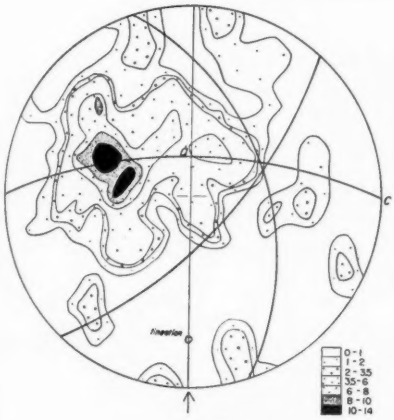

FIG. 32

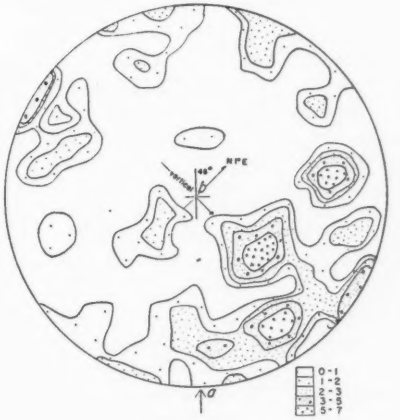

FIG. 33

FIGURE 32.—QUARTZ FABRIC OF PORPHYRITIC GRANITE FROM SOUTH OF MAPUIDIH
FIGURE 33.—QUARTZ FABRIC OF PORPHYRITIC GRANITE FROM SOUTHWEST OF RAGHUNATHPUR

ORIGIN OF STRUCTURAL FEATURES

Foliation, Lineation, and Joints in the Granite

All evidences adduced (*cf.* Sen, 1948), especially the independence in spatial distribution from the regional diastrophic structures, point to a primary origin for the internal structures of the porphyritic granite. Foliation of the porphyritic granite shows evidence of a fluxion structure, originating before complete solidification. The pattern of the flow layers does not conform to that of a dome or an arch (Balk, 1937). The eastern end of the granite lens and a small area surrounding the rises of Raghunathpur have moved up differentially relative to the main body. Movement in the fluxion stage resulted in development of well-formed lineation parallel to the direction of

movement, an unequivocal example of flow lines.

The *b* lineation, as every primary lineation in magmatic rocks, is by implication also a "flow line" as it is thought always to be parallel

ment of the granite. Joints of system 2 near the boundary indicate elongation at right angles to the contact (effecting similar joints in the wall rocks), which may have been caused by volume increase by continued emplacement

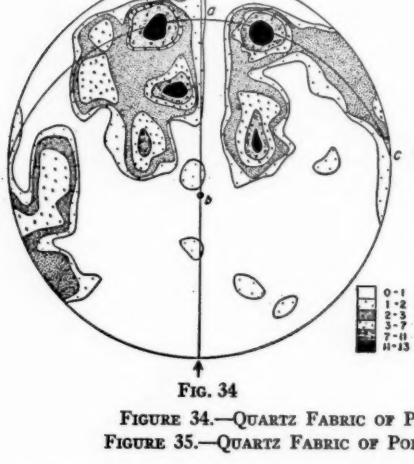

FIG. 34

FIG. 35

FIGURE 34.—QUARTZ FABRIC OF PORPHYRITIC GRANITE FROM BERO
FIGURE 35.—QUARTZ FABRIC OF PORPHYRITIC GRANITE FROM KHAJURA

to the direction of local flow—"of maximum motion at the individual locality" (E. Cloos, 1946, p. 25). It is suggested that here the *b* lineation, which occurs as the regional lineation in the porphyritic granite, formed at right angles to the direction of flow with no implication of local flow and hence no subsidiary stretching in the direction of lineation. Such lineation could develop in response to laminar flow, within certain velocity limits, by interplanar slips, where rotational motion at right angles to flow direction would orient elongated forms parallel to the axis of rotation. Thus they would offer the least resistance to flow (Jeffery, 1922; Taylor, 1923). In the porphyritic granite, subsidiary elongation parallel to length of the pluton occurred only in the late solid stage, toward the closing stages of emplacement. Structures of the intervening plastic stage also indicate plastic drag upward and not sideways.

Joints of systems 2 and 3 postdate those of the first. The first system contains a group of *bc* tension planes and some diagonal joints formed during the last phase of upward movements. Normally, tension would be more effective along the walls. Joints prove continuation of emplacement beyond solidification, and a few structures are referred to the plastic stage when viscosity reached its maximum.

Mineral Fabric of the Granite

Three quartz-axes fabrics of the porphyritic granite show (1) prominent peripheral *ac* girdle, *b* axis nearly horizontal, parallel to lineation in some examples and at right angles to the lineation in others, (2) small-circle girdle around the same *b* axis, (3) partial small-circle girdle on *c*, and (4) tendency for partial peripheral girdle around *a*. The fabric shows a predominant rotation around *b* and subsidiary rotation around *c* and *a*, a complicated picture of movement associated with the two dome structures. Since the granite shows structural independence from associated metamorphic rocks, the mineral orientation is to be ascribed to viscous flow. Such complicated rotations, as shown by the quartz axes, could be more easily conceived in viscous flow than in solid flow. Though both

ab and *bc* girdles are known from metamorphic rocks, *bc* girdles seem to be common in thrust zones (Balk, 1952). Occurrence of more than one girdle in tectonites would normally indicate more than one period of deformation.

Megascopic Fabric of the Wall Rocks

In the wall rocks (1) joints of system 1 decrease in proportion to joints of system 2 with increased distance from the contact; (2) joints of systems 2 and 3 may proxy for each other, generally one or the other occurring with system 1, but the third system may occur exclusive of all others; (3) the obtuse angle of intersection of the joints of system 2 faces the wall, their line of intersection being horizontal; and (4) in system 3, either the obtuse or the acute angle of intersection faces the wall, the line of intersection lying in a more or less vertical plane (Fig. 17).

The second system consists of oblique shear joints formed by expansion of the porphyritic granite pluton. These diagonal planes lie intermediate between *ab* and *bc*. In such squeezing the direction of maximum relief would lie in a vertical plane (roughly at right angles to the wall), while *b* would lie in a horizontal plane, at right angles to the direction of compression—*i.e.*, roughly parallel to the wall. The line of intersection of these planes, parallel to their strikes, is the *b* direction. In terms of these axes of movement the first joint system would represent *ac* planes. Its presence indicates elongation parallel to *b*. Extensive development of these planes near the wall shows that there was considerable elongation parallel to the walls. In concluding stages of emplacement expansion of the intrusive, with incidental tension along the wall, caused compression radially in all directions (Sen 1949a). Tension was most effective near the wall. Compression was so effective that 1½ miles from the wall the oblique shear joints outnumber the tension joints (Fig. 15).

During the final phase of emplacement and solidification, closely spaced *ac* joints developed at right angles to the walls and caused greater elongation parallel to the contact. Presumably, the joints of system 3 formed at this stage, with their line of intersection more or less vertical. Squeezing continued with incidental maximum elongation parallel to the walls. Thus the third system of joints comprises conjugate shear planes, with a change in spatial position of the direction of maximum elongation and of the planes of maximum deformation.

Without going into detailed discussion of the deformation hypotheses (Becker, 1893; Bucher, 1920; 1921; Leith, 1937; Griggs, 1935; 1936), it may be noted that the two types of angular relations found in joints of the area studied may have two explanations; where the acute angles of the conjugate planes face the wall deformation may have taken place by fracturing without prerupture flow, or there may have been considerable solid flow making the angles obtuse (Fairbairn, 1949; Griggs, 1936).

Possible explanation of spatial position of joints of the second system, relative to inferred compression, is that the planes formed or their orientation was determined before commencement of rupture and antedate those of the first system. First system joints continued to form after completion of the second system, when the joints of the third system began to appear. Joints of system 2 in the country rocks formed during the last phase of upward emplacement of the granite when, helped by heat of the ascending granite and its hyperfusibles, deformation in the walls took place by flow, which resulted in shear planes with their obtuse angle of intersection facing compression. A slightly younger tension caused formation of the *ac* joints. The flow deformation stopped abruptly, and typical mylonites were produced in the wall rocks. Expansion parallel to the wall now gained the upper hand, and the third system of shear planes was formed.

Mineral Fabric of the Metasediments, Migmatites, and Granite Gneiss

The features common to quartz fabrics of the four metamorphic rocks are a more or less well-defined peripheral *ac* girdle and in places an $ac \wedge bc$ diagonal girdle. There are no prominent maxima, and the axes are about equally dispersed throughout the girdles. Positions of small zones which could be described as maxima lie close to maxima I, II, and V of the synoptic diagram (Fig. 20). The *b* axis, always nearly parallel to regional strike of foliation and

parallel to the regional fold axes, is the tectonic axis of Sander.

No definite evidence supports any of the proposed explanations for an *ac* girdle. Microfolding as well as grain rotation around *b* might have been responsible for the girdles. Lack of strong maxima may be regarded as evidence for rotation, though it is in no way unequivocal. Since the metamorphic rocks belong to high-grade granulite and amphibolite facies (Sen, 1951; 1953) and occur in association with typical granulites having similar quartz-axes fabric, the *ac* girdle and poorly developed maxima I, II, and V may also be ascribed to flattening accomplished by translation on (h0l) slip planes (Sander, 1930; *see* Knopf and Ingerson, 1938; Fairbairn, 1949; Turner, 1948).

The *a* lineation resulted from maximum tectonic transport in that direction; in specimens showing this lineation an *ac* girdle is developed. The microfolds indicate some external rotation around *b*. Also a subsidiary transport parallel to *b* is shown by the abundance of *ac* joints. Thus the *ac* girdle may have resulted from (1) transport along *a* with incidental grain rotation around *b*, accentuated at times by microfolds developed parallel to *b*, or (2) slip on (h0l) planes, intersecting on *b*. If the last mechanism were responsible, there should have been more pronounced maxima developed, and more than one *s* planes visible. Orientation might also have been caused by fracturing of quartz grains during commencement of deformation, the seed crystals being oriented by the suggested mechanism during sustained deformation. All evidence of such rupturing would be completely healed by paratectonic recrystallization. Needle axes of such seed crystals would then parallel horizontal edges (*m*:*r*, *m*:*z*, *r*:*c*, *z*:*c*, and *m*:*c*), so that the *c* crystallographic axis would be at right angles to the needle axes, and their bounding planes parallel to *m* ($10\bar{1}0$), *r* ($10\bar{1}1$, *z* $01\bar{1}1$), or *c* (0001). At the first stage of deformation the needle axes would be rotated parallel to *b* and, in the rotation toward *b*, would lie in intermediate positions giving "axes maxima (having) orientation different from those known to occur" (Fairbairn, 1949, p. 122). Sustained deformation would rotate all the needle axes parallel to *b*. Further deformation, with forward movement parallel to *a* by rolling the needle axes about *b*, will give an *ac* girdle with maxima I, II, and V.

In progressive metamorphism such rotation of grains is difficult to visualize in view of evident paratectonic recrystallization. Under conditions of high-grade metamorphism, deformation must have been accomplished by postelastic flowage. A rotation similar to that pictured above may be effected indirectly by translation gliding along preferred planes in preferred directions on variously oriented quartz seed crystals (Fairbairn, 1949). The probable explanation is that initiation of the orientation was by forward rolling toward *a* by rotation on *b*, accentuated by microfolding parallel to *b*. This resulted in continuing orientation by translation toward *a* controlled by a single set of *s* planes, the megascopic *ab* plane.

Fabrics of migmatites, ultramigmatites, and granite gneiss, including two generations of quartz in the granulites, are similar to the fabric of the metasediments. The granulitic quartz appears to be the product of late recrystallization by metasomatism in the metamorphite-granite gneiss transition. This quartz wholly or partially encloses and replaces other minerals of the assemblage. Orientation of the granulitic quartz is posttectonitic and can only be ascribed to mimetic retention of original tectonitic orientation during replacement by metasomatism.

Mineral Fabric of the Wall Rocks

In specimens successively closer to the granite wall a gradual change is noticed in the quartz fabric. Original girdles break down and finally disappear. The first stage is marked by a complete shattering of the girdle (Fig. 29), although a major proportion of the axes retain original orientation, a peripheral *ac* girdle. Finally near the contact an almost S-tectonite fabric is obtained, symmetrical about the vector systems generated by the intrusion.

Relation of quartz fabric to shear joints on the walls is apparent, and the fabric is symmetrical about the inferred directions of stress incidental to intrusion of porphyritic granite. In the quartz fabric of the granite-gneiss speci-

men in contact with the granite (Fig. 31), the maximum lies on this direction of compression and shows an incomplete girdle on the same plane around an axis coincident with the acute bisectrix of the shear joints and close to *c* of megascopic fabric (Fig. 36). Compression would

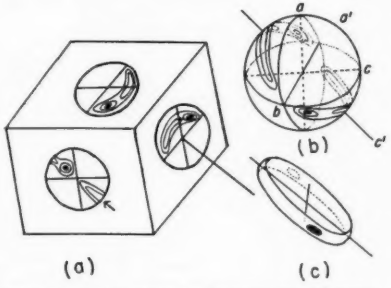

FIGURE 36.—RELATION OF INCOMPLETE GIRDLE IN FIGURE 31 TO CONJECTURED VECTOR FIELD
Caused by intrusion and the axes of tectonic transport.

induce maximum tectonic transport in the direction indicated by interplanar slips and small-scale thrusts. The resultant transport, controlled by the *ab* planes which lie at right angles to the direction of compression, would be up the dip of foliation and near megascopic *a*. The girdle would thus be an $a'b'$ girdle relative to axes of tectonic transport ($b' = b$) in response to the inferred stress, appearing as the $ab \wedge bc$ diagonal girdle relative to the axes of megascopic fabric. In view of extensive occurrence of cataclastic structures along the wall, the fabric may well be explained by the rupture hypothesis (Griggs and Bell, 1938). Thus, catastrophic impact of intrusion may have ground the quartz crystals into elongate needles with needle axes parallel to $r{:}z$ (or $z{:}z$; and $r{:}r$?) and bounded by *m* (or *a*?) needle surfaces, as suggested by the maximum (Fairbairn, 1949). But the needles were probably multifaced and had well-developed unit rhombohedrons, *r* or *z*, the possible directions of best cleavage in quartz (Fairbairn, 1939b; 1949). Deformation rotated the fractured crystals so that they came to lie on the megascopic *ab* plane with the needle axes gathered toward *a* (of megascopic fabric), the resultant direction of maximum transport.

SUMMARY AND CONCLUSION

Structurally the granite gneiss belongs to the same unit as the metasediments and associated rocks. It shows imperceptible gradation from all types of metasedimentary rocks, which often renders exact delimitation of a boundary difficult. Petrographic evidence (Sen, 1951), some of which is not published, points to metasomatic origin of the rock. The best evidence in favor of such an origin is the structural identity of the two groups of rocks. In several places the metasediments can be traced laterally along strike into the granite gneiss, where the lithologic boundary cuts the common structure trends (Pl. 1). The granite gneiss retains every detail of the broader structural alignments as well as internal space-lattice orientation of quartz, characteristic of the metasediments. The granitization, evidently posttectonic, was effected *in situ*.

In the porphyritic granite, though petrographic characters would indicate origin by transformation (Sen, 1951), both megascopic and microscopic fabric are independent of regional structures. Forceful emplacement of the granite is proved by (1) structural discordance, (2) wall-rock joints correlative in distribution in respect to distance from the contact, and (3) mylonites and interplanar slips and thrusts in wall rocks. The porphyritic granite was not intruded as a completely liquid body. Presence of solid phases of large proportion is well established. In view of petrographic evidences suggesting metasomatic derivation, a partly synkinematic granitization with sufficient interstitial liquid to give required mobility to the granite would explain all the features.

REFERENCES CITED

Balk, Robert, 1937, Structural behavior of igneous rocks: Geol. Soc. America Mem. 5, 155 p.

—— 1952, Fabric of quartzites near thrust faults: Jour. Geology, v. 60, p. 415–435.

Becker, G. F., 1893, Finite homogeneous strain, flow and rupture in rocks: Geol. Soc. America Bull., v. 4, p. 13–90.

Bucher, W. H., 1920, 1921, The mechanical interpretation of joints: Jour. Geology, v. 28, p. 707–730; v. 29, p. 1–28.

Cloos, Hans, 1922, Über Ausbau und Anwendung der granit-tektonischen Methode: Pr. Geol. L. A. Abh. N. F., v. 89, p. 93–102.

Cloos, Hans, 1928, Bau und Bewengung der Gebirge in Nordamarika, Skandinavien und Mitteleuropa: Fortschr. d. Geol. u. Pal., v. 7, Heft 21, p. 241–327.

—— 1936, Einführung in die Geologie, ein Lehrbuch der inneren Dynamik: Berlin, Borntraeger, 503 p.

Cloos, Ernst, 1937, The application of recent structural methods in the interpretation of crystalline rocks of Maryland: Md. Geol. Survey, v. 13, p. 25–108.

—— 1946, Lineation, a critical review and annotated bibliography: Geol. Soc. America Mem. 18, 122 p.

Dunn, J. A., 1929, The geology of North Singhbhum including parts of Ranchi and Manbhum districts: Geol. Survey India Mem., v. 54, 166 p.

Dunn, J. A., and Dey, A. K., 1942, The geology and petrology of eastern Singhbhum and surrounding areas: Geol. Survey India Mem., v. 69, p. 281–456.

Fairbairn, H. W., 1939a, Hypotheses of quartz orientation in tectonites: Geol. Soc. America Bull., v. 50, p. 1475–1492.

—— 1939b, Correlation of quartz deformation with its crystal structure: Am. Mineralogist, v. 24, p. 357–368.

—— 1949, Structural petrology of deformed rocks: Cambridge, Mass., Addison Wesley, 344 p.

Griggs, D., 1935, The strain ellipsoid as a theory of rupture: Am. Jour. Sci., 5th ser., v. 30, p. 121–137.

—— 1936, Deformation of rocks under high confining pressure: Jour. Geology, v. 44, p. 541–577.

Griggs, D., and Bell, J., 1938, Experiments bearing upon the orientation of quartz in deformed rocks: Geol. Soc. America Bull., v. 49, p. 1723–1746.

Hietanen, A., 1938, On the petrology of the Finnish quartzites: Comm. Geol. Finlande Bull., v. 21, no. 122, 118 p.

Ingerson, E., 1936, Fabric analysis of a coarsely crystalline polymetamorphic tectonite: Am. Jour. Sci., 5th ser. v. 31, p. 161–187.

Jeffery, G. B., 1922, The motion of ellipsoidal particles immersed in a viscous fluid: Royal Soc. London Proc., v. 102A, 161 p.

Knopf, E. B., 1933, Petrotectonics: Am. Jour. Sci., 5th ser., v. 25, p. 435–470.

Knopf, E. B., and Ingerson, E., 1938, Structural petrology: Geol. Soc. America Mem. 6, 270 p.

Leith, A., 1937, The strain ellipsoid: Am. Jour. Sci., 5th ser., v. 33, p. 360–368.

Sahama, T. G., 1936, Die Regelung von quarz und Glimmer in den gesteinen der FinnishLapplandischen Granulitformation: Comm. Geol. Finlande Bull., v. 113, p. 1–110.

Sander, B., 1930, Gefügekunde der Gesteine: Vienna, Springer, 352 p.

Sen, S., 1948, A note on the magmatectonics of the porphyritic granite in Manbhum: Quart. Jour. Geol. Min. Metall. Soc. India, v. 20, no. 2, p. 57–60.

—— 1949a, Structural petrology of the wall rocks of the porphyritic granite, Manbhum: Quart. Jour. Geol. Min. Metall. Soc. India, v. 21, no. 2, p. 51–58.

—— 1949b, Some examples of quartz grain orientation in tectonites and nontectonites: Curr. Sci., v. 18, p. 328–330.

—— 1951, Mineralogical and structural evolution of metamorphites in east Manbhum (abstract): Proc. Indian Sci. Cong., pt. 3, p. 116–117.

—— 1953, Origin of charnockitic assemblages of East Manbhum, Bihar: Am. Jour. Sci., v. 251, p. 388–392.

Taylor, G. I., 1923, The motion of ellipsoidal particles in a viscous fluid: Royal Soc. London Proc., v. 103A, p. 58–61.

Turner, F. J., 1948, Mineralogical and structural evolution of metamorphic rocks: Geol. Soc. America Mem. 30, 342 p.

Department of Geology, Calcutta University, Calcutta, India

Manuscript Received by the Secretary of the Society, April 20, 1955

Short Note

BULLETIN OF THE GEOLOGICAL SOCIETY OF AMERICA
VOL. 67, PP. 671–674, 1 FIG., 1 PL. MAY 1956

UNUSUAL "POTHOLE"

BY CHARLES G. HIGGINS

C. K. Wentworth (1924) described a bowl-shaped "pothole" enlarged by rotation-in-place of a single cobble in the Potomac River. Nearly 30 years later, the following similar but more spectacular case was discovered 0.8 mile upstream from the mouth of Stockhoff Creek on the California coast, 4 miles northwest of Fort Ross, and 70 miles north-northwest of San Francisco.

In March 1953 Harvey Moss and Newell Winsted, 15-year-old students at Stillwater Cove Boys' School, found a discuslike sandstone cobble, 6 inches in diameter and 2½ inches thick (Pl. 1, figs. 1, 2), lying broken side up in a bowl-shaped depression, 1 foot in diameter and 4½ inches deep (Fig. 1; Pl. 1, fig. 5), cut neatly into the nearly level floor of a shallow "cave" at the edge of Stockhoff Creek (Pl. 1, fig. 4). This "cave" is formed by huge sandstone boulders which locally obstruct the valley and cause a series of waterfalls.

Two weeks later, at the suggestion of John Allan, an instructor at the school, the boys replaced the discus with a subrounded sandstone cobble of approximately the same size (Pl. 1, fig. 3).

Shortly after this, during a flood following a hard rainstorm in early April, Mr. Allan and Paul Rudy, Jr., son of the school's director, climbed to the site and found water spilling down a shallow chute (Pl. 1, fig. 6) and free-falling 2½ feet onto the upstream edge of the new cobble in the bowl. The cobble was not turning, but they believed the creek had fallen from its highest flood stage and that, with higher water and greater velocity, the waterfall would have struck the cobble on the edge toward the back of the "cave," turning it anticlockwise and escaping over the lowest part of the bowl's rim, toward the back of the "cave." A few days later, when the creek was even lower, a group of boys climbed to the site and found the waterfall still pouring into the bowl, though the cobble was not turning.

However, the new cobble must have been rotated at some time during this flood, for, when the writer saw it in mid-May, 1953, one side was well started toward the smooth discus shape of the original cobble and the other side had been slightly modified as well. It turned easily in the bowl and, although of softer sandstone than the original, had already modified the bowl so that the original did not quite fit, nor turn so smoothly as it did when first found.

There can be little doubt that this abrasion was produced by rotation of the new cobble in the bowl. Probably this was caused by impact of the waterfall during flood stage. It therefore seems safe to conclude that the original discus-shaped cobble and the bowl itself were formed in the same manner.

Both abraded sides of the original sandstone discus have the curvature of a sphere of 4-inch radius. Except for small pits and cavities, the surfaces are remarkably smooth, bevelling hard chert pebbles, the largest of which is 10 mm long.

As shown by the dashed line in Figure 1, concave curvature of the bowl's bottom matches that of the discus, but the bowl flares somewhat on the sides, probably because of nutational wobbling of the cobble during rapid rotation at times just before being flipped over in the bowl. On the downstream side, concave curvature breaks sharply into convex curvature that may be the remnant surface of an initial depression in which the cobble began to rotate.

The occurrence is similar to Wentworth's

(1924) in that a rotating cobble deepened and modified a pre-existing bedrock depression. The Stockhoff Creek sandstone cobble is remarkably symmetrical because its rotation under the waterfall appears to have been, at most times, around a single axis, rather than around various axes as was the case with Wentworth's amphibolite cobble, which rotated in a high-water eddy. The differences between the two similar occurrences suggest that rotation-in-place of cobbles and boulders may occur under a fairly wide variety of circumstances and may even be a fairly common, though unnoticed, mechanism of abrasion in high-velocity streams.

One characteristic of both Wentworth's and the present cobble is the preservation of older broken or faceted surfaces despite an extreme degree of recent rounding and smoothing (Pl. 1, fig. 2). Another characteristic is the absence of differential erosion on the recent surfaces. These distinctive features should serve to identify the origin of any cobble that has been shaped by rotation-in-place, even after it has been dislodged from its "pothole." The only danger is that such cobbles and their abraded bowls may easily be mistaken for man-made artifacts.

Previous writers have long debated the role of coarse material in pothole erosion. Brögger and Reusch (1874) reported boulder-size "grinders" from the "giant's kettles" at Christiana, and it has been a recurrent popular notion that some potholes, especially those supposed to be of glacial moulin origin, are bored by single rotating boulders. (For a recent example, *see* Streiff-Becker, 1951, Fig. 3.) Alexander's (1932) hydraulic experiments led him to question the efficacy of coarse material in deep pothole grinding, but Ängeby (1952) reported grinders up to 0.5 m diameter from a recent deep pothole in Sweden.

To avoid lengthy discussion, we may conclude simply that, regardless of the part played by coarse material in abrasion of deep potholes and kettles, shallow potholelike depressions can be formed by single large rotating cobbles in somewhat the manner suggested by some previous writers. Such depressions may even be fairly common, although perhaps not so perfect and obvious as those reported by Wentworth and the present writer. However, because

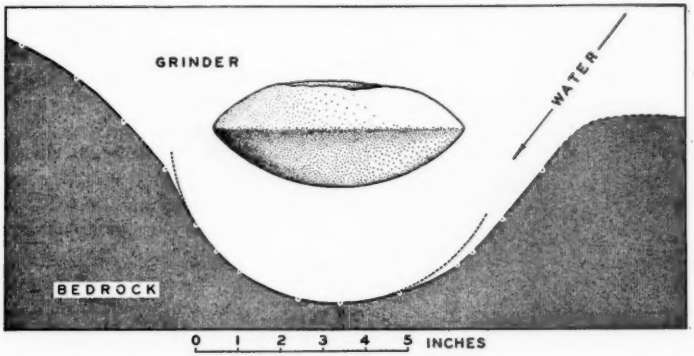

FIGURE 1.—CROSS SECTION OF "POTHOLE" WITH ORIGINAL GRINDER
Dashed line has same curvature as grinder

PLATE 1.—"POTHOLE", GRINDERS, AND SURROUNDINGS

FIGURE 1.—Original grinder
FIGURE 2.—Original grinder, showing older broken surface
FIGURE 3.—Replacement grinder in "pothole"
FIGURE 4.—"Cave" in which "pothole" formed
FIGURE 5.—"Pothole" without grinder
FIGURE 6.—Close-up of "cave"

POTHOLE, GRINDERS, AND SURROUNDINGS

of expendibility of the grinders and the fact that they can work only where the stream current is nearly or completely toolless, these depressions must always be shallow, with widely flaring sides—quite unlike the familiar deep, steep-sided, eddy-hole potholes and giant's kettles.

References Cited

Alexander, H. S., 1932, Pothole erosion: Jour. Geology, v. 40, p. 305–337.

Ängeby, Olof, 1952, Recent, subglacial and lateroglacial pothole-erosion (evorsion): Lund Studies in Geography, ser. A, no. 3, p. 14–24

Brögger, W. C., and Reusch, H. H., 1874, Giant's kettles at Christiana: Geol Soc. London Quart. Jour., v. 30, p. 758–771.

Streiff-Becker, R., 1951, Potholes and glacier mills: Jour. Glaciology, v. 1, p. 488–490

Wentworth, C. K., 1924, Note on a cobble of peculiar shape: Jour. Geology, v. 32, p. 524–528.

Department of Geological Sciences, University of California, Davis, California

Manuscript Received by the Secretary of the Society, January 3, 1956

BULLETIN OF THE GEOLOGICAL SOCIETY OF AMERICA
VOL. 67, PP. 675–678, 1 PL. MAY 1956

CARBON-14 DATE FOR A MARINE TERRACE AT SANTA CRUZ, CALIFORNIA

BY WILLIAM C. BRADLEY

Introduction

The central California coast in the vicinity of Santa Cruz (Fig. 1) is indented by five prominent and several indistinct marine terraces. These terraces have been described by Lawson (1893), Wilson (1907), Branner *et al.* (1909), Rode (1930), Page and Holmes (1945), Alexander (1953), and others. The lowest prominent terrace contains an old wave-cut platform whose shoreline angle (the junction between the platform and the sea cliff) is now approximately 100 feet above sea level. Although subsequent warping has destroyed the original horizontality of the shoreline angle (Wilson, 1907, p. 14; Rode, 1930, p. 33; Alexander, 1953, p. 12–16), for convenience this terrace is here referred to as the 100-foot marine terrace; it is the same as Lawson's (1893, p. 140) 96-foot terrace, Wilson's (1907, p. 16) 112-foot terrace, Branner *et al.*'s (1909, p. 6) 100-foot terrace, Rode's (1930, p. 33) and Alexander's (1953, p. 12) first terrace, and Page and Holmes' (1945) 90-foot terrace. Mollusk shells associated with this 100-foot marine terrace were used for the carbon-14 dating.

Acknowledgments

A study of the marine terraces in the Santa Cruz area was made under the supervision of Professor A. D. Howard of Stanford University; the writer is grateful to him for help and encouragement throughout the study. The carbon-14 dating of the mollusk shells was made possible by a grant from the Shell Fund for Fundamental Research at Stanford University, and the analysis itself was made at the Lamont Geological Observatory of Columbia University.

The 100-foot Marine Terrace

Figure 2 is a generalized cross section of the 100-foot marine terrace at Santa Cruz. The wave-cut platform, eroded into the Miocene Monterey formation, slopes seaward at an angle of 1° or less and is slightly concave upward; the concavity is most pronounced within half a mile of the former sea cliff. A sheet of marine deposits, generally 5 to 15 feet thick, overlies the platform and is overlain in turn by a wedge of nonmarine detritus near the old sea cliff. The marine deposits have been interpreted as beach deposits which were prograded seaward across the platform during a period of slow emergence (Bradley, 1955).

When the wave-cut platform was under water, rock-boring mollusks pitted its surface in the same fashion that mollusks pit the modern platform. Their holes are well exposed at the top of the present sea cliff, where the platform is only about 25 feet above sea level and waves have stripped the unconsolidated terrace deposits back from the edge (Pl. 1, fig. 2). Along West Cliff Drive in Santa Cruz, approximately 1½ miles from the old sea cliff, mollusk shells still occupy some of the holes; a number of these shells were collected from the edge of the sea cliff (Fig. 2) near the intersection of West Cliff Drive and Columbia Street and were determined by carbon-14 analysis at the Lamont Geological Observatory to be older than 39,000 years (Broecker and Kulp, 1956).

Discussion

Because the mollusks pitted the wave-cut platform, they cannot be older than the date at which erosion of the platform ceased. If it is assumed that platform erosion was halted by emergence, then the mollusks can be no older than the time when emergence began. Emergence is believed to have taken place relatively slowly (Bradley, 1955), and inasmuch as the mollusks that were dated lived 1½ miles from the sea cliff, where they remained under water for a longer period of time than those nearer the cliff, it is conceivable that these mollusks are somewhat younger than the beginning of emergence. It is therefore concluded, on the

basis of the carbon-14 analysis, that the emergence which ultimately led to the formation of the 100-foot marine terrace began at some time prior to 39,000 years ago.

Other recent work suggests that this date is reasonable. Kulp *et al.* (1952, p. 411) reported that the lowest marine terrace on the Palos Verdes Hills in southern California is more than 30,000 years old. Rubin and Suess (1955, p. 482) have reported slightly elevated shore lines in Australia which are also more than 30,000 years old. Recent studies in southern California have led W. S. Broecker (Personal communication) to the tentative conclusion that there have been no stands of the sea higher than the present in at least the last 30,000 years, and possibly not since the third interglacial interval. The dating of the 100-foot

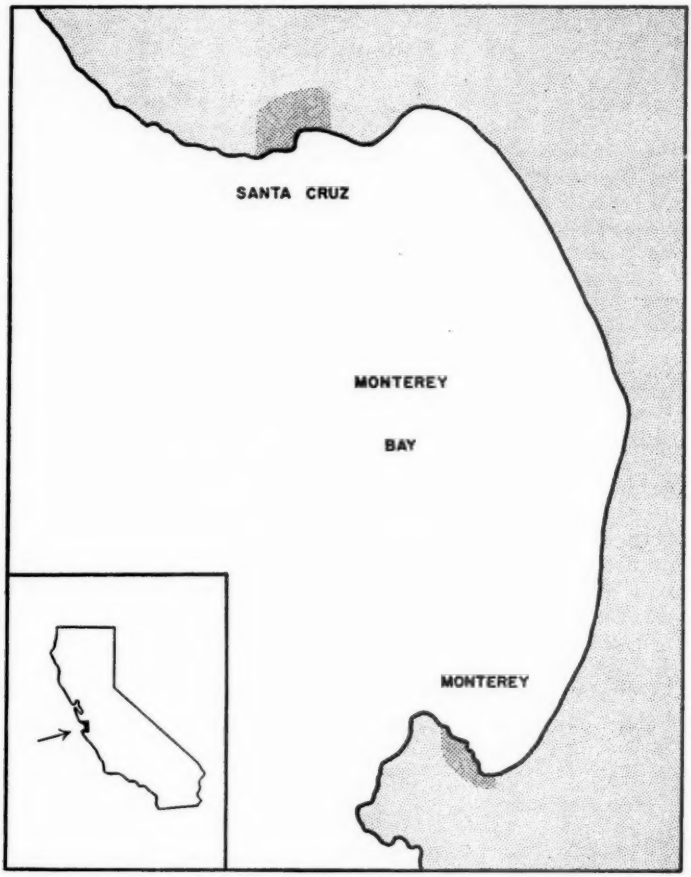

FIGURE 1.—LOCATION MAP OF SANTA CRUZ, CALIFORNIA

PLATE 1.—ROCK-BORING MOLLUSK HOLES IN THE WAVE-CUT PLATFORM OF THE 100-FOOT MARINE TERRACE AT SANTA CRUZ, CALIFORNIA

FIGURE 1.—Close-up of the holes

FIGURE 2.—The platform and mollusk holes (lower part of the picture) exposed by stripping back of the terrace deposits; deposits are 15 feet thick

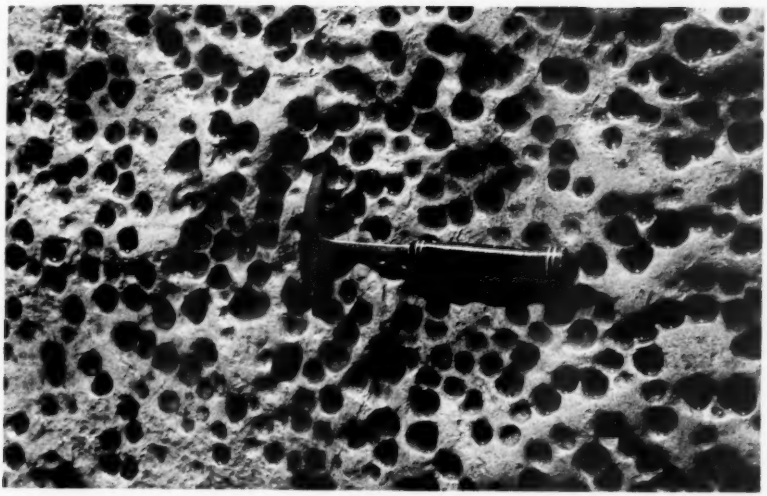

FIGURE 1

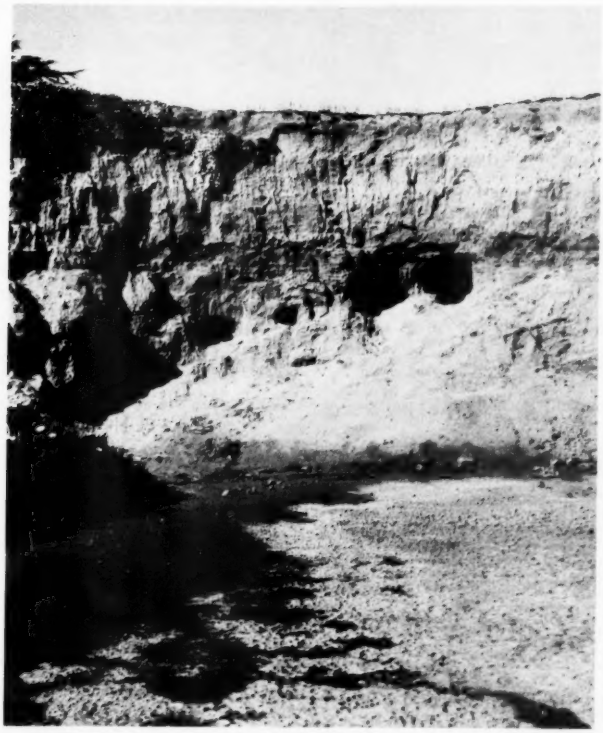

FIGURE 2

ROCK-BORING MOLLUSK HOLES IN THE WAVE-CUT PLATFORM OF THE 100-FOOT MARINE TERRACE AT SANTA CRUZ, CALIFORNIA

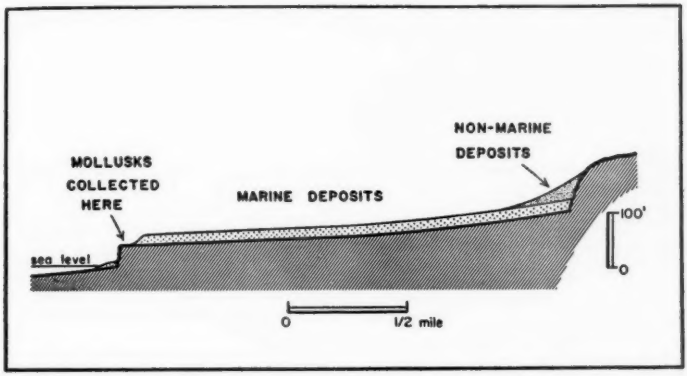

FIGURE 2.—GENERALIZED CROSS SECTION OF THE 100-FOOT MARINE TERRACE AT SANTA CRUZ, CALIFORNIA

marine terrace at Santa Cruz supports this conclusion. If the conclusion is correct, sea level has been lower than at present for a relatively long period of time, and shore lines produced during this interval of lower sea level should now lie submerged on the continental shelf. Such submerged features are known; for example, Fairbridge (1952, p. 348) reported that submerged marine terraces are common features on continental shelves, Stearns (1945) and Emery *et al.* (1954) have recorded submerged terraces bordering some of the Pacific islands, and Upson (1949, p. 107–108) and Emery (Personal communication) have reported terraces on the southern California shelf.

References Cited

Alexander, C. S., 1953, The marine and stream terraces of the Capitola-Watsonville area: Univ. Calif. Pub. Geog., v. 10, p. 1–44

Bradley, W. C., 1955, Marine terraces and their deposits in the vicinity of Santa Cruz, California (Abstract): Geol. Soc. America Bull., v. 66, p. 1645

Branner, J. C., Newsom, J. F., and Arnold, Ralph, 1909, Santa Cruz folio: U. S. Geol. Survey Geol. Atlas, Folio 163, 11 p.

Broecker, W. S., and Kulp, J. L., 1956, Lamont radiocarbon measurements III: Sci., v. 123 (in press)

Emery, K. O., Tracey, J. I., and Ladd, H. S., 1954, Geology of Bikini and nearby atolls: U. S. Geol. Survey Prof. Paper 260-A, 265 p.

Fairbridge, R. W., 1952, Marine erosion: 7th Pacific Sci. Cong., Pacific Sci. Assoc. Proc., v. 3, p. 347–358

Kulp, J. L., *et al.*, 1952, Lamont natural radiocarbon measurements, II: Sci., v. 116, p. 409–414

Lawson, A. C., 1893, The post-Pliocene diastrophism of the coast of southern California: Univ. Calif. Dept. Geol. Sci. Bull., v. 1, p. 115–160

Page, B. M., and Holmes, C. N., 1945, Geology of the bituminous sandstone deposits near Santa Cruz, Santa Cruz County, California: U. S. Geol. Survey Oil and Gas Inv., Prelim. Map 27.

Rode, Karl, 1930, Geomorphogenie des Ben Lomond (Kalifornien), eine Studie über Terrassenbildung durch marine Abrasion: Zeitschr. Geomorph., v. 5, p. 16–78

Rubin, Meyer, and Suess, H. E., 1955, U. S. Geological Survey radiocarbon dates II: Sci., v. 121, p. 481–488

Stearns, H. T., 1945, Eustatic shore lines in the Pacific: Geol. Soc. America Bull., v. 56, p. 1071–1078

Upson, J. E., 1949, Late Pleistocene and Recent changes of sea level along the coast of Santa Barbara County, California: Am. Jour. Sci., v. 247, p. 94–115

Wilson, M. E., 1907, Shore topography near Davenport, Santa Cruz County: California Phys. Geog. Club Bull., v. 1, p. 11–17

UNIVERSITY OF COLORADO, BOULDER, COLO.

MANUSCRIPT RECEIVED BY THE SECRETARY OF THE SOCIETY, JANUARY 26, 1956

BULLETIN OF THE GEOLOGICAL SOCIETY OF AMERICA
VOL. 67, PP. 679-682, 1 PL. MAY 1956

TYPES OF *BATHYURISCUS HOWELLI* VAR. *LODENSIS* CLARK

BY ALEXANDER STOYANOW

The status of *Bathyuriscus howelli* var. *lodensis* Clark from the Middle Cambrian of southern California, as presented in the literature, has been discussed recently by Stoyanow and Susuki (1955, p. 467) as follows:

"A trilobite of the *Anoria-Glossopleura* group but with eight thoracic segments, collected from the Middle Cambrian strata in Bristol Mountains, southern California, was described as *Bathyuriscus howelli* var. *lodensis* by Clark (1921, p. 6) but was not figured. Later Resser (1928, p. 10, Pl. 3, fig. 9) illustrated Clark's type advancing it to the status of species, *Dolichometopus? lodensis* (Clark), and also mentioned eight thoracic segments. However, in a more recent paper Resser (1935, p. 29, 34) placed this species, as *Glossopleura lodensis* (Clark), with other species possessing only seven thoracic segments, as also did Mason (1935, p. 109, Pl. 15, fig. 11) while describing, as *Anoria lodensis*, a plesiotype of Clark's species collected in Marble Mountains. Like *Anoria*, Clark's species has a macropleural fifth thoracic segment. The illustrations of Resser and Mason do not allow the figuring of the number of thoracic segments (eight as by Clark, or seven as by Resser and Mason) in either of the two types with any degree of assurance. Clark's holotype was not available at the time of this writing, but Mason's plesiotype, preserved in the Los Angeles Museum, has been examined by the writers through the kindness of Dr. G. P. Kanakoff. It has seven thoracic segments with the fifth segment macropleural as in *Anoria*."

Clark's rock specimen, USNM 78400, illustrated by Resser (1928, Pl. 3, fig. 9), shows two trilobites without individual numbers—a smaller trilobite in the lower part of his illustration, which he selected (Resser, 1928, p. 14; 1935, p. 34) as holotype of Clark's species, and which alone, in accordance with Resser's designation, was regarded as the holotype by Stoyanow and Susuki (1955); and another, much larger trilobite in the upper part of the same illustration. This larger trilobite was at first identified by Resser (1928, p. 10, 14) as *Dolichometopus productus* (Hall and Whitfield) but later designated as *Glossopleura mohavensis* Resser (1935, p. 34). These two trilobites are two different species and possibly may belong in two different genera.

Clark's brief reference to his *Bathyuriscus howelli* var. *lodensis* reads:

"This species is probably new, but the cephalons of all the specimens were crushed so that the original characters could not be accurately determined. It is referred to *B. howelli* as it has *eight thoracic segments* (italics mine) and seems to correspond to this species excepting in the fifth segment, which is broader than any of the others and terminates in a long spine that curves well back toward the pygidium. It is therefore called *B. howelli* var. *lodensis*."

In this statement is a direct reference to the presence of eight thoracic segments, in complete agreement with Clark's upper example as in Resser's Figure 9 (Resser, 1928, Pl. 3). For some reason Resser omitted mention of the eighth segment, albeit it is plainly visible in his illustration (Pl. 1, fig. 1). As to the macropleural segments, the figure shows both the fifth and the sixth segments enlarged, and the sixth possibly even more so.

Regarding the smaller trilobite, with questionable number of thoracic segments, the lower illustration of Resser's Figure 9, which he finally designated as the holotype of his *Glossopleura lodensis* (Clark), it should be noted that this type cannot be placed under *Glossopleura* Poulsen (1927, p. 268) since according to Poulsen's generic definition the absence of the macropleural development in the fifth thoracic segment is one of the cardinal characteristics of *Glossopleura* by which it is distinguished from *Anoria* Walcott. This trilobite is congeneric, and to all evidence conspecific, with the topotype-plesiotype, which has the fifth thoracic segment macropleural, described and illustrated by Mason (1935, p. 109, Pl. 15, fig. 11) as *Anoria lodensis* (Clark). The topotype has only seven thoracic segments as mentioned by Mason and as checked by Stoyanow and Susuki. Originally Mason (1935, p. 109, 118) placed it in *Anoria* Walcott, but following Resser's publication of 1935 he moved it to *Glossopleura*, notwithstanding the macropleural fifth segment in the thorax (Mason, 1935, p. 117). Both Clark's and Mason's examples have a long and narrow macropleural thoracic segment, clearly marked from the

rest, and similar facial sutures with strongly curved, nearly semicircular, palpebral lobes, the latter feature regarded by Mason as a distinction from *Anoria tontoensis* (Walcott, 1916, p. 373, Pl. 51, figs. 1c, 1d; 1924, p. 54, Pl. 9, fig. 2; 1925, p. 68, Pl. 18, fig. 20).

In Mason's topotype the entire axial part of the thorax is destroyed, but Clark, Resser, and Mason did not mention an axial tuberculation in Clark's type selected by Resser as holotype of Clark's species, and indeed Resser's illustration of this smaller specimen shows an untuberculated thorax (Pl. 1, fig. 1); the absence of this characteristic would further remove this species from *Anoria* Walcott and probably has served as a determining factor in Resser's placing it, as well as Clark's larger specimen, in *Glossopleura*.

Dr. G. Arthur Cooper very kindly examined Clark's specimen, USNM 78400. Although the cephalon of the smaller specimen is somewhat offset and crushed, a "lip" of what might have been the eighth (that is the first thoracic) segment is in evidence. In the larger trilobite, with eight thoracic segments, it is difficult to decide which segment is the larger, the fifth, or the sixth. Actually the fifth seems a little larger (measured in the direction of long axis), but the segmental spine is decidedly smaller than that of the sixth segment. Doctor Cooper was unable to find an ornamentation on any part of either trilobite. He mentioned, however, as the illustration shows, that the axial crest in the larger trilobite has been stripped off (Cooper, Personal communication).

Subsequently Doctor Cooper sent me a rubber cast of Clark's specimen (Pl. 1, fig. 2). I think the "lip" in the smaller trilobite is a thickening and a furrow which developed in the posterior margin of the posterolateral limbs. Similar swelling and groove have been illustrated by Walcott (1918, Pl. 14, fig. 1, right side; Pl. 16, fig. 3, right side) for *Olenoides* (*"Neolenus"*) (Pl. 1, fig. 3). Such a development is also observable in the right side of Mason's example, and I have seen it in several cranidia of the *Anoria-Glossopleura* material from the Grand Canyon. If this interpretation is correct, Resser was right in assuming seven thoracic segments in the example which he selected as holotype of Clark's species. This, however, would disagree with the fundamental part of Clark's diagnosis. It is interesting that Mason (1935, p. 110) refuted the presence of the eighth segment in the smaller trilobite in believing that the thickened anterior edge of the pygidium of the holotype was mistaken for an eighth segment. This species differs from *Glossopleura* by the macropleural development and from *Anoria* by the lack of axial tuberculation. Whether it may be placed in *Sonoraspis* will depend on the verification of the number of thoracic segments in better-preserved topotypes.

The larger specimen illustrated by Resser is described here.

Sonoraspis mohavensis (Resser)

(Pl. 1, fig. 1)

Bathyuriscus howelli var. *lodensis* Clark (part), 1921, Univ. Calif., Dept. Geol. Sci. Bull., v. 13, p. 6

Dolichometopus productus (Hall and Whitfield) Resser, 1928, Smithsonian Misc. Coll., v. 81, no. 2, p. 10 and 14, Pl. 3, fig. 9 (upper part only)

Glossopleura mohavensis Resser, 1935, Smithsonian Misc. Coll., v. 93, no. 5, p. 34. (Specimen illustrated in the upper part of Resser's Figure 9 of Plate 3, publication of 1928, assigned here as holotype of this species)

This species, in agreement with other described species of *Sonoraspis* Stoyanow, differs from *Anoria* (Walcott) and *Glossopleura* Poulsen by the presence of eight segments in the thorax. It is distinguished from other species of the first genus by the macropleural development in the thorax—the fifth segment as in Clark's text, the sixth segment as in Resser's illustration. Of importance is the fact that

Plate 1.—INTERPRETATION OF THE NUMBER OF THORACIC SEGMENTS IN CLARK'S TYPES

Figure 1.—Reproduction of Resser's photographic illustration taken from Clark's original, USNM 78400 Note eight thoracic segments in the upper specimen; GS—genal spine; MP—the fifth and the sixth macropleural segments.

Figure 2.—Rubber cast of *Glossopleura lodensis* (Clark) by Resser's designation, USNM 78400, the lower specimen of Figure 1

A—groove between two salients below the posterolateral furrow.

Figure 3.—Walcott's illustration of *Olenoides serratus* (Rominger), USNM 58591

PLF—posterolateral furrow; A—groove between two salients below.

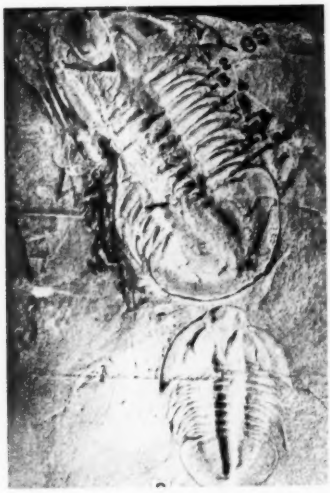

FIGURE 1

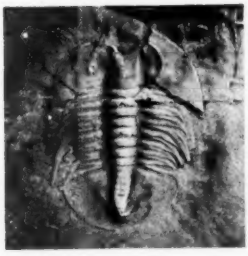

FIGURE 2

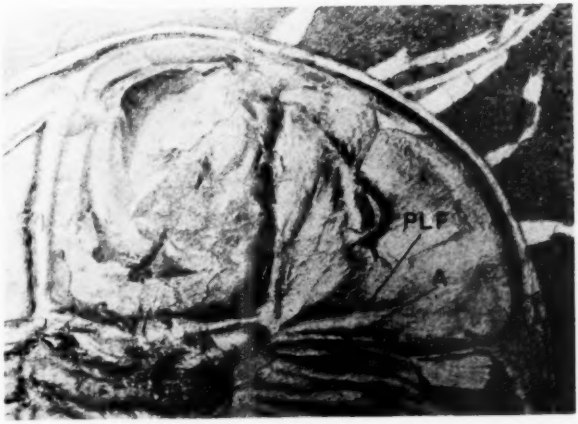

FIGURE 3

INTERPRETATION OF THE NUMBER OF THORACIC SEGMENTS IN CLARK'S TYPES

according to the mentioned illustration the pleurae of the longer-sp ned macropleural segment overlap the two last po erior thoracic segments exactly as in *Anoria*. The left part of the cephalon is not preserved in Clark's type, but the *Anoria*-like course of the facial suture visible in its right part is as in *S. torresi* Stoyanow (1952, p. 53, Pl. 14, fig. 3) and in *S. californica* Stoyanow and Susuki (1955, p. 468, Pl. 1, figs. 1, 2). The axial part of the thorax does not seem to be satisfactorily preserved in the type, but, since Clark, Resser, and Mason do not mention the presence of axial tubercles, it may be presumed that, as in *S. torresi*, the thoracic axis of this species is untuberculated, unlike the thoracic segments of *S. gomezi* Stoyanow (1952, p. 54, Pl. 14, figs. 5, 6) and *S. californica* which bear the axial tubercles.

Type: Holotype, U S N M 78400, larger specimen only

Occurrence: Middle Cambrian, Bristol Mountains, southern California

References Cited

Clark, C. W., 1921, Lower and Middle Cambrian formations of the Mohave Desert: Univ. Calif. Dept. Geol. Sci. Bull., v. 13, p. 1–7

Mason, John F., 1935, Fauna of the Cambrian Cadiz formation, Marble Mountains, California: Southern Calif. Acad. Sci. Bull., v. 34, pt. 2, p. 97–119, Pl. 15

Poulsen, Chr., 1927, The Cambrian, Ozarkian, and Canadian faunas of northwest Greenland: Meddelelser om Grønland, v. 70, p. 233–343, Pls. 14–21

Resser, Charles E., 1928, Cambrian fossils from the Mohave Desert: Smithson. Misc. Coll., v. 81, no. 2, p. 1–14, Pls. 1–3

—— 1935, Nomenclature of some Cambrian trilobites: Smithson. Misc. Coll., v. 93, no. 5, p. 1–46

Stoyanow, Alexander, 1952, The original collection of Cambrian trilobites from Sonora *in* Cambrian stratigraphy and paleontology near Caborca, northwestern Sonora, Mexico: Smithson. Misc. Coll., v. 119, no. 1, p. 49–59, Pl. 14

Stoyanow, Alexander, and Susuki, Takeo, 1955, Discovery of Sonoraspis in southern California: Geol. Soc. America Bull., v. 66, p. 467–470, Pls. 1–2

Walcott, Charles D., 1916, Cambrian geology and paleontology. Cambrian trilobites: Smithson. Misc. Coll., v. 64, no. 5, p. 303–456, Pls. 45–67

—— 1918, Cambrian geology and paleontology. Appendages of trilobites: Smithson. Misc. Coll., v. 67, no. 4, p. 115–216, Pls. 14–42

—— 1924, Cambrian geology and paleontology. Cambrian and lower Ozarkian trilobites: Smithson. Misc. Coll., v. 75, no. 2, p. 53–60, Pls. 9–14

—— 1925, Cambrian geology and paleontology. Cambrian and Ozarkian trilobites: Smithson. Misc. Coll., v. 75, no. 3, p. 61–146, Pls. 15–24

University of Arizona, Tuscon, Ariz., and University of California, Los Angeles, Calif.

Manuscript Received by the Secretary of the Society, November 30, 1955